EXPERIMENTAL STUDIES AND ANALYSIS OF COMPACTED FILLS OVER A SOFT SUBSOIL

A THESIS

Presented to

The Faculty of the Division of Graduate Studies

by

Somboon Intraprasart

In Partial Fulfillment

of the Requirements for the Degree

Doctor of Philosophy

in the School of Civil Engineering

Georgia Institute of Technology

December, 1978

EXPERIMENTAL STUDIES AND ANALYSIS OF

COMPACTED FILLS OVER A SOFT SUBSOIL

Approved:

R. D. Barksdale, Chairman

G. F. Sowers

B. B. Mazanti

C. O. Pollard

Date approved by Chairman: Nov 27, 1978

ACKNOWLEDGMENTS

The author wishes to express his deep gratitude to Dr. R. D. Barksdale, his major professor, for guidance and encouragement throughout the whole project. Special thanks go to Professor G. F. Sowers, Dr. B. B. Mazanti, and Dr. C. O. Pollard for their help as advisors and serving as members of the Reading Committee. Thanks are also extended to Dr. Q. L. Robnett for being on the Examining Committee.

The help of Mr. Ben Reevse, machinist, Mr. John Pinson, electronic technician, and Mr. Larry Westbrooks, assistant machinist, was sincerely appreciated.

The financial support of the project from the School of Civil Engineering is gratefully acknowledged.

Finally, he wishes to express many thanks to his wife, Karuna, for her patience, encouragement and understanding throughout the course of his study at Georgia Tech.

TABLE OF CONTENTS

LIST OF TABLES

LIST OF ILLUSTRATIONS

Figure Page

Figure Page

Figure Page

SUMMARY

The high cost of the development of marginal land and areas with poor subsoils can, in some instances, be reduced considerably by the use of controlled, compacted fills rather than other more costly foundation stabilization or support techniques. At the present time, the beneficial effects of placing compacted structural fill over a weak foundation soil are not completely understood and have not been fully investigated.

In this study, the beneficial effects of compacted fills in reducing the stress and settlement in the soft subsoil were investigated experimentally utilizing 1.5 foot diameter footing load tests. A soft subsoil using micaceous clayey silt (ML) was constructed in a test pit 8 feet wide, 12 feet long, and 7 feet deep. Three different fill materials which consisted of sandy clay, river sand, and crushed stone were used. Measurements of settlement, stress, and strain within the fill-subsoil systems and the surface settlement of the footing were made. The effects of varying fill thickness in reducing the stress and the settlement of the soft subsoil were also investigated.

The effectiveness of compacted fills in reducing the settlement of the soft layers beneath the fills was determined by comparing the measured settlements of the soft layers

beneath the fills with that of the soft soil of the same stratum in a homogeneous condition. The test results indicated that sandy clay and sand fills placed over the soft subsoil were effective in reducing the settlement of the soft subsoil and that the amount of settlement reduction depended on the thickness of the compacted fills. Replacing only portions of the soft subsoil with lightly compacted crushed stone was effective in reducing the surface settlement, but the beneficial effect of reducing the settlement in the soft layers depended on the replacement width.

The measured vertical stresses beneath compacted sandy clay and sand fills using three different thicknesses were found to be less than the measured vertical stresses in the homogeneous layer of the same soft soil, thus indicating the beneficial effect in reducing the vertical stresses. The measured vertical stresses were predicted using a linear finite element method for a vertical stress distribution of two-layer systems loaded with a rigid footing. The modular ratios were estimated from the results of triaxial shear tests. Good comparison between the measured and predicted stresses was obtained, especially for stresses in the soft layers.

The measured settlements were predicted using the layer-strain method and effective moduli from cyclic triaxial shear tests. The predicted settlements compared favorably with the measured values.

CHAPTER I

INTRODUCTION

Although fill has been placed for many years, it is not until relatively recently that carefully controlled structural fill has been used for supporting the foundations of residential, commercial, and industrial structures. Many early fills were merely wasted material, often mixtures of various types, dumped without compaction and selection of suitable material for the fill. Structures established on such fills usually experience severe total and differential settlement and cracking. In contrast to the uncontrolled fills often used in the past, most fills today are carefully controlled with respect to soil type and field density. This fill is placed on natural ground from which portions of weak and compressible materials may first be removed. Structural fill, which is a well-constructed earth fill using quality control with regard to both material type and compaction, often provides a better foundation base for structures than natural deposits, and are widely used in developing residential subdivisions and industrial areas.

At present, the development of marginal lands including areas of poor subsoils with high ground water table is increasing rapidly under the impetus of rapid urban growth.

Often cost associated with the development of such areas are higher than necessary because of a general lack of knowledge of the design and performance of structures built on these poor subsoils. Consequently, buildings constructed in these areas are often supported on pile or pier foundations which go through the unsuitable soils rather than using considerably less expensive foundation schemes. The problems of construction on marginal sites, the risk involved and the design approach as well as the need for innovative ideas in developing marginal land have been fully described by Sowers [111]. Mitchell [77] discussed various special methods and techniques of site improvement when the existing soil conditions at a proposed site are inadequate for support of a proposed structure.

The high cost of the development of the marginal areas and the areas with poor subsoils can, in some instances, be reduced considerably by the use of structural fill rather than other more costly foundation stabilization or support techniques. At the present time the beneficial effects of placing a structural fill over a soft subsoil are not completely understood and have not been fully investigated.

The main purpose of this study is to examine experimentally the probable effectiveness of two compacted structural fills in reducing settlement of the foundation and the stresses transmitted to the underlying soft subsoils. The settlement of the fill layer is often small when placed under carefully controlled conditions. Meyerhof [74] has published data

indicating that well-compacted sand and gravel fills show settlements of only about one-half per cent of their height. In practice, settlement rather than bearing capacity of such two-layer systems usually governs the foundation design. Methods which have been verified are not presently available for designing structural fills over soft subsoils.

The main portion of this study consists of conducting three test series of large scale footing load tests in a test pit 8 feet wide, 12 feet long and 7 feet deep using a circular concrete footing 18 inches in diameter. The load tests were conducted for the following subsurface conditions:

1. A uniform single layer of soft micaceous clayey silt (ML),
2. Compacted sandy, silty clay fill (CH) over the soft soil, and
3. Compacted sand fill over the soft soil.

In addition, load tests on footings resting on lightly compacted crushed stone replacing a portion of the soft soil beneath the footing foundation were also conducted during Test Series I and III.

The settlement of the footing and the soft subsoil as well as the strain distribution within the soil mass is measured for all test series using Bison strain sensors. The stress distribution beneath the test foundation in a single soil layer and two-layer systems is measured in all test series using specially designed stress cells which incorporate the latest design criteria.

By using different types of fill materials and varying the fill thicknesses, the beneficial effects of compacted structural fill in reducing the settlement of the soft subsoil and the stresses due to the foundation load is evaluated. From this study, proposed recommendations are made for the design of compacted cohesive and granular structural fills over soft subsoils.

CHAPTER II

LITERATURE REVIEW

Introduction

The design of a structural fill constructed over a soft foundation involves predicting settlements of shallow foundations located within the fill and the bearing capacity of the fill-subsoil system. Settlement predictions require a knowledge of the stresses transmitted by the foundation system through the fill into the underlying subsoils. To analyze this problem, the following factors must be known:

1. The foundation configuration and fill thicknesses;
2. The magnitude and distribution of the applied foundation loads;
3. The load-deformation characteristics and the strength of the fill materials; and,
4. The load-deformation characteristics and the strength of the soft-subsoils.

Exact solutions which take into account all the foregoing factors in the analysis are not presently available, and approximate theories and methods must be presently used.

The literature review is divided into four parts which are related to this study:

1. Stress and strain distribution in soil;
2. Settlement analysis;

3. Analysis of ultimate bearing capacity; and,
4. Finite element methods.

Stress and Strain Distribution in Soil

Stress Distribution

Single Layer. The best known theoretical solution for the distribution of stresses in ideal elastic material was derived by Boussinesq [17]. The solution was for a point load acting on the surface of a homogeneous, isotropic, semi-infinite elastic medium, and was subsequently extended by integration to give the stress distribution produced by a uniformly distributed load acting on the surface. A very complete set of tables for determining stress, strain, and deflection patterns beneath a uniform circular load have been presented by Alvin and Uhley [2]. Although no real soils satisfy the assumptions of the Boussinesq's theory, it has remained as a convenient standard of comparison for measured stress distribution in soils, particularly for vertical stresses. Westergaard's theory [132], which assumes a homogeneous, elastic mass reinforced with thin strips so that no lateral strains occur, has also been used to calculate stresses and displacements.

To account for measured deviation from the theories found by early investigators, approaches were developed to consider real soil properties such as non-homogeneity, (e.g., modulus of elasticity varying with depth) [45, 48] and anisotropy (e.g., horizontal modulus of elasticity differing

from vertical modulus) [8, 45, 59].

Layered Systems. Both theoretical analyses and field measurements indicate that the stresses and displacements developed in layered soil systems, where there are large differences in the properties of the layers, can be considerably less than would be developed in a homogeneous system. The layered system in which the properties of each layer, particularly the modulus of elasticity, are different, has been studied by several investigations. Burmister [25] was the first to solve the problem of a two-layer system using the elastic theory. The general assumptions employed in the analysis have been reviewed by Barksdale and Leonards [12]. Whiffin and Lister [133] have presented a summary of the various theories both for two-layer and three-layer systems. Solutions are available in tabular and chart forms for two-layer systems [44] as a function of the modular ratio, E_1/E_2, the ratio of footing radius to fill thickness, and Poisson's ratio as parameters. A few solutions for stresses in three-layer elastic systems subjected to uniform, circular surface loading have been presented in tabular and chart form by Acum and Fox [1], Jones [56], and Peattie [83]. But, due to the many parameters in the solution, interpolation is quite involved and time consuming.

A system of compacted fill over a soft subsoil in which the stiffness of the fill layer is usually greater than that of the underlying soft subsoil may be treated as a two-layered

system. The stress and deformation of this system are greatly dependent upon the fill thickness and modular ratio of the layers, E_1/E_2, where E_1 and E_2 are the moduli of the compacted fill and subsoil, respectively. According to the elastic solutions of the two-layer system, significant beneficial effects of placing a stiff layer over soft soils are obtained by reducing vertical stresses in the subsoil under the center of a uniformly loaded footing to less than that predicted by Boussinesq's theory.

Several crude methods for determination of the stress distribution in a two-layer system have been proposed [60, 86, 135]. When the stiffness of the load-bearing stratum exceeding that of the underlying softsoil by more than ten times, the stresses can be calculated by assuming the upper stiff layer to be increased in thickness by 15% and using the Boussinesq's theory [86].

Using the solutions of layered system by Burmister [25], Kezdi [60] prepared a figure in which the thickness of the stiff layer is increased according to the modular ratio of the two layer system. Once the substitute layer is known, the stresses are calculated as if the foundation were resting on a homogeneous soil mass. This method applies only if the upper layer possesses some tensile strength.

For the case of an upper granular layer which is incapable of carrying tension, Kezdi [60] suggests that the thickness of the stiff layer be increased according to the following

relationship:

$$h' = h\sqrt{\frac{E_1\delta_2}{E_1\delta_2}} \qquad (1)$$

where h' = thickness of the substitute layer

h = thickness of the stiff layer

E_1 = modulus of elasticity of the stiff layer

E_2 = modulus of elasticity of the soft layer

δ_1 = density of the stiff layer

δ_2 = density of the soft layer

When the load is applied on the surface of a rigid soil stratum underlain by a deposit of medium to high or very high compressibility, Zeevaert [135] suggests that a corrected Boussinesq stress distribution may be used. The method is to use the Westergaard stress solution in the rigid stratum. In the underlying compressible soil, the Boussinesq solution is corrected by the proportion of the Westergaard to the Boussinesq interface stresses. The corrected stress distribution in the soft layer is found below the interface to be slightly greater than the Westergaard solution. This method, however, makes no distinction between granular and cohesive stiff layers which may not have the same ability to spread the load.

The existing theoretical solutions for predicting the stress distribution within the fill-subsoil system assume that

the foundation is flexible and uniformly loaded. The foundations of most structures founded on structural fills are relatively rigid, and theoretical solutions are not available to predict the stress distribution under this condition. The problem can be solved, however, using a finite element method.

Because the properties of real soils are not truly homogeneous, isotropic, elastic and linear, attempts have been made in the past by several investigators to verify the stress distribution theory or to determine the behavior of real soils under loads.

Tests on Single Layer System. A number of investigations of stresses and deflections in single layer systems have been done using laboratory models or prototype pavements. The most extensive series of tests carried out on uniform soil mass under flexible load were those reported by the Waterways Experiment Station (W.E.S.) [126, 127]. The W.E.S. work in 1951 [126] involved measuring stresses and deflections within a carefully prepared homogeneous clay silt test section subjected to a uniform circular load on the surface. Their experiments indicated that the distribution of vertical stress resulting from the applied surface loading corresponded very closely to that determined using Boussinesq's theory. The W.E.S. work on a uniform sand under flexible loads, summarized by Turnbull, et. al., [124], suggested that the stress patterns measured were in good general agreement with those predicted by Boussinesq's theory, except in the regions close to the

load where the measured stresses were greater than the predicted values. The results, however, are not as good as for the clayey silt. The surface deflection basin could not be predicted using Boussinesq's theory which assumes constant modulus of deformation.

Morgan and Holden [80] performed model tests on a uniform sand compacted in a tank having dimensions 6 feet by 6 feet by 4 feet 8 inches. The surface was loaded by a 10-inch diameter flexible membrane to a maximum pressure of 30 psi, and deflections were recorded under both initial and repeated applications of the load. Stresses in both vertical and horizontal directions were measured using miniature earth pressure cells. They found that measured vertical and radial stresses in the sand were greater than those predicted by the Boussinesq theory, the discrepancy being greatest for the radial stresses, and that better agreement was obtained for stress prediction by assuming that the material was anisotropic using $E_h/E_v = 0.6$ in the solution.

As reported by Morgan and Holden [80], Allwood [5] had carried out stress distribution studies in sand similar to those reported by W.E.S. Measured stresses did not agree well with those predicted by either the Boussinesq or Frochlich theories.

Brown and Pell [23] conducted stress measurements in a medium plastic clay (L.L. = 41%; P.L. = 18%) under flexible loads using diaphram pressure cells 2-1/2 inches in diameter

and 0.43 inch thick. The soil was compacted in six inch layers in a test pit 8 feet by 8 feet by 5 feet deep to give an average dry density of 121 pcf. The stress measurement results show generally good agreement with Boussinesq theory, particularly vertical stress and major principal stress. Horizontal stresses tend to be higher than the theoretical values. Most of the stress measurements in single layers were carried out in either compacted sand or clay which possessed relatively low compressibility and high shear strength to simulate the subgrade conditions for pavement systems.

Few measurements of the stress distribution in uniform soils which have low shear strength and high compressibility have been reported in the literature. To verify the reliability of predicted undrained stresses and deformations by a finite element method, Das and Gangopadhyay [34] conducted a small size footing load test on a normally consolidated kaolin clay contained in a tank having two compartments, each size 35 inches by 27.6 inches by 47.2 inches. In one compartment, a bed of kaolin was prepared in layers by consolidating the sediment obtained from a slurry. In between successive layers diaphragm type pressure cells and pore pressure cells were placed at predetermined locations and orientations. The miniature cells provided with resistance strain guages were made of anodized aluminum and designed for a pressure range of 0 to 15 psi. The system was designed to permit

drainage from both the top and bottom of the soil. The other compartment of the tank was filled with water and the two were interconnected at the bottom. A flexible circular footing 7.3 inches in diameter was used for loading the soil surface. Das and Gangopadhyay found that the measured vertical stress along the load axis could be favorably predicted using the stresses computed from the elastic analysis of Poulos [88]. The measured horizontal stresses, however, were greater than those predicted by elastic theory. Good agreement was obtained when the computed horizontal stresses were adjusted in such a way that the shear strength of the soil was not exceeded. They found that a nonlinear finite element analysis using a bilinear elastic, plastic model with a Poisson ratio of 0.45 gave a good prediction of the measured vertical and horizontal undrained stresses. The results of this investigation suggest that the nonlinear properties of the kaolin clay have insignificant effects on the stress distribtuion and that the vertical stresses in nonlinear soils can be predicted by using linear elastic theories.

In summary, the measured vertical stresses in single clay layers were in good agreement with those predicted by Boussinesq theory. The measured horizontal stresses were generally greater than computed from elastic theories. The measured stresses in sand were generally greater than those predicted by Boussinesq theory and the results were not conclusive.

Tests on Two-Layer Systems. A few experimental investigations have been conducted to determine the effects of layered systems on the stress and deformation. Investigations of pressures and deformations in two-layer systems have been made on a clayey second layer by McMahan and Yoder [72] and by Brown and Pell [22], on a micaceous silt layer by Sowers and Vesic [115], and on a granular layer by Trollope, et. al. [123].

The study conducted by McMahan and Yoder [72] consisted of two series of field stress measurement tests in an 8 foot by 8 foot model. Rigid plates varying in diameter from 7 to 18 inches were loaded in increments. After each increment of load stress readings were taken over a period of approximately 5 minutes. Loads were applied at the surface of the clay layer and also at the surface of two layer structures; however, for the two layer system pressure measurements (vertical direct stress) were only obtained in the clay layer. For the tests on the two layer structures, four, eight, and twelve inches of the compacted clay were replaced by the same thickness of crushed stone. Results of these tests were compared with the stresses calculated by different theories. The data for tests at the surface of the uniform clay layer indicate that the measured stresses and those computed according to Boussinesq theory follow the same general pattern; however, the measured stresses are somewhat larger, particularly at the shallow depths. In tests at the surface of the crushed stone over the clay layer, a slight reduction in stress was

obtained at the interface as compared with the measured stresses at the same depth in the uniform clay layer test with no crushed stone. The measured stresses at intermediate depths were higher than they were for the homogeneous condition. Comparison between measured stresses and those computed according to Burmister's theory for a two-layer system assuming a modular ratio of the crushed stone and clay to be 10 indicated the computed values to be lower than those measured.

An experimental investigation of the stresses, strains, and deflections in a two-layer system subjected to dynamic loads were conducted by Brown and Pell [22]. The soil used for the second layer was an inorganic clay of medium plasticity. The stiff layer consisted of a well graded crushed stone with maximum particle size of 3/8 inch. The system was tested under dynamic loads using flexible loading. Stress and strain cells were employed throughout the compacted clay layer to measure both vertical and radial stresses and strains. The results of the stress measurements indicated that the measured values can be predicted adequately by using Boussinesq theory. The modular ratio E_1/E_2 of the two layers, however, was close to unity. Of interest are the high values of E for the lower layer ranging from 9,100 psi to 25,000 psi as compared to the crushed stone layer of 13,500 psi. The low modulus of the granular material prevented them from a rigorous examination on the applicability of two layer theory.

An extensive experimental investigation in connection with the performance of pavement systems were conducted by Sowers and Vesic [115] to determine the distribution of stresses within the subgrade and the relative load spreading ability of different base course materials. For all tests the subgrade soil was a compacted micaceous sandy silt. Four types of bases were studied: 1) well graded silty sand, 2) soil-bound macadam, 3) soil cement, and 4) sand asphalt; tests were made with base course thickness of 6 and 8 inches. Pressures were measured by different locations within the subgrade with pressure cells 4 to 6 inches in diameter. The results of the measured stresses for the silty sand and soil-bound macadam bases showed stress patterns close to those computed by the Boussinesq theory, and the results for the sand asphalt base were comparable to or slightly higher than the computed values. It was concluded that the load spreading ability of these bases was no better than that of a homogeneous soil even though the ratio of the modulus of elasticity obtained by triaxial and plate load tests was from 8 to 9. The observed disagreement with the two-layer theory was explained by the lack of tensile strength of the upper layer. The test results for the soil cement base indicated the measured stresses being less than those by the Boussinesq theory and comparable to the stresses computed by the two-layer theory with the modular ratio of 100. The stress reduction obtained for the soil cement base was attributed to the high

tensile strength of the soil cement. Burmister [26] and Schiffman [96] have challenged the validity of these test results because of the change in conditions which results from the introduction of instruments for the measurement of stresses.

The purpose of the investigation by Trollope, et. al. [123] was to evaluate the ability of upper layers to transmit stresses to a deep granular subgrade. The materials in the upper layer were concrete, soil cement and a sand-filler asphalt mix whereas the subgrade was a poorly graded sand which has been dried to remove free moisture. Vertical stresses at various positions in the subgrade resulting from a uniform surface load were recorded by earth pressure cells. The test results for the concrete and soil cement layers were compared with the stresses determined by Burmister's two-layer theory. Agreement between measured and computed vertical stresses were extremely good. The measured stresses for the sand-filler-asphalt layer were very close to those computed using the Boussinesq theory. This test result agrees with the findings of Sowers and Vesic [115].

In summary, the stress distribution within a two-layer system depends upon the ability of the upper layer to spread the loads. If the upper layer has high tensile strength such as soil cement or concrete, the stresses in the lower layer are comparable to those indicated by Burmister's theory. The stresses in the lower layer are closer to those computed

by Boussinesq's theory when granular materials are used for the upper layers.

The inability of granular layers to reduce stresses in the lower subgrade to less than that indicated by Boussinesq theory can be contributed to the large surface pressure applied in the prototype pavement tests, which is on the order of 2 to 3 times greater than normal foundation pressures of structures founded on structural fill. At a high stress level, the effectiveness of the granular layer in reducing the stresses in the subgrade, which could be detected at a lower stress level, has probably been overcome. It is therefore appropriate to conduct footing load test on granular fills using applied footing pressure comparable to those which would be expected under a typical foundation loading.

Strain Distribution

The strain distribution beneath a footing over a uniform soil which is assumed to be homogeneous, isotropic, linearly elastic and semi-infinite can be computed using the solutions given by Ahlvin and Ulery [2] for a case of uniform loading. For loading on a rigid circular area the stress and strain at any point in the elastic medium can be obtained using closed-form solutions given by Gerrard and Harrison [46].

Conventional settlement calculations assume that the distribution of vertical strain under the center of a footing over a uniform soil layer is proportional to the distribution of the increase in vertical stress due to the applied loading.

This means that the greatest strain would occur immediately under the footing. The elastic solutions by Ahlvin and Ulery [2] indicate that the maximum strain does not occur immediately beneath the loading, where the vertical stress is greatest, and equal to the applied footing load, q, but rather at a depth (z/R) = 0.6 to 0.7 for Poisson's ratio of 0.4 and 0.5, respectively, where the Boussinesq increase in vertical stress is only about 0.8 q. According to the Boussinesq's rigid displacement theory [46], the stress increase immediately beneath the footing at the load axis is only 0.5 q and reaches its maximum value of 0.56 q at a depth (z/R) = 0.55. The strain distribution under the center of the load is similar to that computed for a flexible load area but reaches its peak value at a depth (z/R) = 0.9 and 1.0 for Poisson's ratio of 0.4 and 0.5, respectively, where the stress increase is only about 0.5 q.

Measurements of vertical strain within the soil mass, particularly under the center of the footing, to verify the existing settlement theories have received very little attention in the past. The most complete vertical strain measurement along the load axis beneath a rigid circular footing in homogeneous sand was first conducted by Eggestad [42]. The sand used for the model tests was a medium fine fluvial sand compacted in a steel container having a diameter of 44.5 inches and a height of 20 inches. The interior of the tank was lined with a thick rubber membrane to reduce friction.

The deformation recorders were a type of variable inductance gages consisting principally of a coil and an iron core. The movement of the core inside the coil changed the impedance of the coil. The variation of the impediance of the coil was recorded by a direct-reading measuring bridge. All gages were calibrated showing the accuracy on the order of $\pm$0.01 mm to 0.03 mm. Five gages were placed along the load axis for vertical deformation. Six gages were positioned at different depths off the center line to measure the lateral deformation. A perspex plate 2 cm thick and 20 cm in diameter which had no effect on the impedance of the coil was used to apply the load on the surface. Four different tests were performed by varying the sand relative density from 34% to 85%. The results of the tests showed that in all cases the maximum strain did not occur immediately beneath the plate and that a depth to maximum vertical strain was about 1.5 times the radius of the loading plate for both loose and dense sand.

Eggestad also reported the results of a similar model study by Bond [16] with depths to maximum vertical strain at (z/R) = 0.8 for dense and 1.4 for loose sand. Morgan and Holden [80] using a uniformly loaded circular area on the surface of a medium sand with a relative density of 67% report maximum strain at (z/R) = 1.2. The strain distribution, however, was obtained from predicted values using the results of the triaxial tests. No attempt was made to measure the strain directly because of the presence of the stress cells

along the center line close to the footing.

Schmertmann [98] reports the results of a finite element study of the axisymmetric strain distribution under a circular concrete footing resting on the surface of homogeneous sand. Both nonlinear stress-strain behavior and soil properties dependent on effective stress were incorporated in the finite element formulation. The results show that the depth to the greatest vertical strain increases as footing pressure increases from about 0.72 to 1.2 times the footing radius. Schmertmann, et. al. [99] later presented the results of an additional study using finite element methods and small model footing load tests in sand. The finite element study was performed using the nonlinear behavior of sand to determine the effects of parameter variations. The results of this parametric study indicate that the strain distributions for plain strain and axisymmetric conditions differed significantly and that increasing the magnitude of the footing pressure increased the peak value of strain distribution.

The model tests in medium sand were conducted using a rigid rectangular footing with B = 6 inches and different L/B ratios. The sand layer was pluvially placed in a 4 foot diameter and 4 foot high steel tank. The strains were measured by embedding horizontal aluminum disks attached to a vertical tube at different depths. The tube extended above the footing and the movement of the tube was monitored using a cathetometer to sight the top edge. The test results indi-

cate that the maximum strain under a rigid rectangular footing does not occur immediately beneath the center of footing but the peak values depend on the magnitude of the applied footing pressures. The results of the finite element study agree well with the model test results.

Measurements of vertical strain distribution so far have been done exclusively in uniform sand using small model tests. Tests have not been performed on other types of soils, such as silt or clay using a large size footing. The reason is probably a lack of strain sensing devices which are relatively efficient, easy to install and capable of measuring strain in any direction conveniently. These problems can now be overcome by using the Bison strain sensors [104]. In addition, the lack of testing facilities and the labor involved often preclude the use of large scale model tests.

For a two-layer system of a stiff layer over a softer layer, theoretical solutions in tabular form are available for stress and strain distribution along the center line of a circular area uniformly loaded and at the interface for different E_1/E_2 and H/R ratios [44].

Few measurements of vertical and horizontal strains beneath a loaded area over a two-layer system have been made in the past. The most comprehensive ones are the work conducted at the University of Nottingham by Brown and Pell [22]. The two-layer system consisted of crushed stone compacted over clay subgrade. Strain cells were placed in both upper

and lower layers to measure vertical strains with depth and radius and radial strains with radius. Dynamic loading was applied using a flexible membrane 6 and 9 inches in diameter. The results were compared with those computed using elastic thoery soltuions for layer systems [25]. The comparison with elastic theory shows that vertical strains under the load are much lower than theoretical predictions for the two-layer system, while at greater radii the agreement was very good.

Settlement Analysis

Methods of predicting the structure-related settlement are reviewed. The analysis of other possible causes of the settlement is beyond the scope of this study. Detailed descriptions of other causes of foundation settlements, such as environmental settlement have been given by Sowers [112].

Elastic Methods

The initial or distortion settlement of a foundation on clay is normally predicted using elastic methods [106, 108] which assume that the modulus of elasticity, E, is constant with depth. Procedures which are more frequently used in practice have been tabulated by Lambe [65]. For soil deposits having the modulus of elasticity increase linearly with depth, elastic settlement of a foundation uniformly loaded can be estimated using the solutions given by Brown and Gibson [19] for an elastic semi-inifinite soil mass and Gibson, et. al., [48] for the soil deposits underlain by a rigid stratum. Computation of distortion settlement of a rigid foundation on

non-homogeneous soil mass whose E depends on the state of stress is difficult [30], and theoretical solutions are not available at the present time. Carrier and Christian [29] have solved this problem using a finite element method.

Structural fills are normally composed of two soil layers with different properties. The distortion settlement of a flexible foundation rested on the surface of this two-layer system can be predicted using the solutions given by Burmister [25] and Gerrard [44] for constant modulus in each layer. If a rigid foundation is used and the modulus of the soils increases with confining pressure, the problems become very complicated, but can be solved using a finite element method [78].

Elastic methods have been used to predict long term settlement of structures founded on both cohesive and cohesionless soils [13, 35, 38, 43].

DeJong and Harris [38] report settlement observations of two multistory buildings on overconsolidated clay till. Analysis of the foundation settlements by elastic methods shows good agreement between measured and calculated values during construction period. They observed that long term settlement for a period of 6 years accounted for only 20% of the total settlement.

Egorov, et. al. [43] applied an elastic method to predict total settlement of the foundation for several multi-story buildings. The foundation soils mostly consisted of

sandy clay, clayey sand and sand. They concluded that the order of the maximum settlement could be predicted reliably using the elastic method.

The elastic method proposed by Davis and Poulos [36] for settlement under three-dimensional conditions has been used successfully to predict initial and consolidation settlements of foundations on compressible clayey soils [78, 87].

D'Appolonia, et. al. [31], Lambe and Whitman [64] and Schmertmann [98] advocate the use of elastic methods to predict the settlement of structure on sand. The methods of obtaining the modulus of elasticity, however, are different. While D'Appolonia, et. al. [31] and Schmertmann [98] suggest that E should be determined from in situ testing, such as standard penetration tests or static cone penetration tests, Lambe and Whitman [64] recommends to use the second loading of stress-strain data from triaxial tests. Schmertmann method has been found to give reasonable estimates of settlement of footing on sand [57].

Barksdale, et. al. [13] performed settlement analyses of a test foundation and an air craft hangar founded on the Piedmont residual soils, using an elastic method and effective modulus obtained from slow, cyclic triaxial tests on undisturbed samples. Good agreement was obtained between the calculated and observed settlements. Martin [71] applied the Schmertmann method [98] to predict settlements of several buildings founded in the Piedmont residual soils. The Menard

pressuremeter was used to obtain E at different depths below the foundations. He presented several case records where a reasonably good agreement between the observed and calculated settlements was obtained.

Janbu [55] proposed to base settlement calculations on the tangent modulus for materials ranging from rock to plastic clays. The tangent modulus which is obtained from the arithmatic plots of pressure vs. strain curves depends on stress conditions and stress history and can be considered to represent a resistance against deformation. No case study on the application of this method is available.

Consolidation Methods

For structures founded on normally consolidated clays, prediction of long-term settlement can be made with reasonable accuracy using the results of conventional consolidation tests and the Terzaghi theory [105, 106]. If the clays are not normally consolidated, Skempton and Bjerrum [108] proposed correction factors to account for three-dimensional effect with the factors being functions of the pore pressure parameter A (which depends primarily on the stress history and sensitivity of the clay) and the geometry of the problem. For most clays, the effect of the correction factor is to reduce the computed consolidation settlement below values that are based on the assumption of one-dimensional consolidation, with the amount of reduction increasing with increasing overconsolidation ratio. For normally consolidated clay, the

amount of reduction is very little.

To obtain a fairly reliable estimate of preconsolidation pressure, P_c, using conventional consolidation tests, Brumund, et. al. [27] suggest that for medium to soft saturated clays, a load increment of one may be used, but for very sensitive clays and soft plastic clays with high liquidity index, the load increment ratio should be reduced to less than one in the vicinity of the estimated P_c.

Leonards [69] proposes a method to estimate consolidation settlements of shallow foundations on overconsolidated clay for the case where the maximum stress in the clay stratum due to overburden plus net increase in pressure due to the foundation load is less than the preconsolidation pressure. Detailed procedure is described to determine the recompression index, C_r, to be used in the settlement calculation. The method is rational but needs field verifications to substantiate the reliability of the method. If the final pressure due to the foundation pressure and the overburden exceeds the preconsolidation pressure, Raymond and Wahl [92] suggest a method which takes into account the influence of P_c in the settlement calculation.

Stress Path Methods

Lambe [62, 63] proposed a method of estimating magnitude of settlement that is based on the use of stress paths. This method consists of selecting representative specimens of soil that will be affected by the proposed construction and imposing

on them in the laboratory the stress changes (stress paths) that will occur as a result of construction. The measured vertical strain during these tests are assumed to be equal to those that will occur in the field, and they are used as the basis of estimating the sum of both immediate and consolidation settlements. The elastic method proposed by Davis and Poulos [36] is also a stress path method which simulates the field conditions in the laboratory.

The use of Lambe's stress path method [62] has been shown to result in smaller (and more reliable) predictions of settlements for structures on overconsolidated clay [63, 107]. Few data available for normally consolidated clay [105] indicate that the stress path method gave closer estimates to the measured settlements than the one-dimensional consolidation method.

Pile [87] used four different methods to predict the settlements of a large footing (3.75 foot square) tested at a depth 9.5 feet below the ground surface on overconsolidated, saturated silty clays. The measured and predicted settlements for each method are summarized in Table 1.

It was concluded that Lambe method greatly overpredicted the settlements for all three pressure increments and that Terzaghi method considerably overpredicted the settlement at low footing pressure but gave a good estimate at higher footing pressures. Davis and Poulos method gave the closest estimates to the measured values.

Table 1. Measured and Predicted Settlements of Large Footing Load Tests on 3.75 Foot Square Footing (Pile [87]).

Methods	Settlement, inches		
	Footing Pressure, psf		
	1700	3400	4900
Measured	.11	.43	.87
Terzaghi [121]	.35	.64	.88
Skempton and Bjerrum [108]	.31	.63	.97
Davis and Poulos [36]	.21	.45	.74
Lambe [62]	.36	.76	1.37

Field Test Methods

Methods of settlement prediction which are based on the results of field tests are often used for foundations rested on cohesionless soils because of the difficulty in obtaining undisturbed samples for laboratory testing. Some of these methods are based on the use of 1) plate load tests [121], 2) standard penetration tests [75, 82, 121] and, 3) static cone penetration tests [37, 75, 98]. An extensive review of field test methods for estimating settlement in cohesionless soils with their advantages and limitations has been given by Sutherland [117] and recently by Jorden [57]. Sutherland [117] concluded that there was no

evidence to suggest that anyone of the existing methods would in all situations give an accurate prediction of settlement although some of the methods consistently gave more correct predictions than others. He suggested that the Meyerhoff [75] procedure should give a reasonably good estimate of the maximum probable settlement. Jorden [57] has even indicated that a reasonable prediction of settlement would be obtained by averaging the results from the methods by Schmertmann [98], Meyerhoff [75], Peck and Bazara [85], Alpan [6], and Parry [82] where this is possible.

Rate of Settlement

The rate of consolidation settlement is usually predicted using the Terzaghi one-dimensional consolidation theory and the data from consolidation tests. There are a number of consolidation theories which are available for use to predict the rate of consolidation settlement [9, 15, 45, 73]. Scott [100] has pointed out that the mathematics involved are too complicated for practical use. Barden and Berry [10] suggested that the best approach was to use the Terzaghi model for preliminary computations and to make qualitative modifications to account for the influence of actual conditions which violate the assumptions of the Terzaghi theory. According to Leonards [68], the errors associated with incorrect evaluation of soil properties are generally far greater than those arising from using one-dimensional theory.

Sample Disturbance

The prediction of initial settlement of a foundation on clay requires the determination of the value of the undrained modulus, E_u, which is usually obtained from laboratory compression tests. Sample disturbance is known to affect considerably the value obtained [14, 91, 106]. Simon [106] suggests that samples are reconsolidated under a stress system equal to that existing in the field. A simpler method to account for the sample disturbance is to isotropically reconsolidate the samples to a stress equal to 1/2 or 2/3 of the in situ vertical stress [91].

The effects of sample disturbance on the prediction of consolidation settlement has been recognized for many years [95, 97, 119] and methods have been suggested to correct laboratory stress-strain relationships for such disturbance. According to Schmertmann [97], sample disturbance will lead to underpredict the settlement of a foundation on normally consolidated clays. For overconsolidated clays, the results are opposite [107]. Methods have also been suggested to correct sample disturbance for this type of soils [67, 112].

Bearing Capacity Analysis

The theories for the ultimate bearing capacity of homogeneous foundations on clay or sand have largely been accepted by the profession as sufficiently reliable. These theories have been accompanied by numerous small scale model studies and some field verifications. Since several of

these solutions have received wide spread circulation in the usual soil mechanics literature, the detail of the work will not be reviewed. The theoretical solutions have been summarized by Vesic [128], and Terzaghi and Peck [122].

Of practical interest is the recognition of the importance of soil compressibility effect on the ultimate bearing capacity. Terzaghi [120] recognized this shortcoming and proposed arbitrary modifications to his general bearing capacity equation to cover cases involving loose sands or soft clays, by pointing out that the full shear strength of such soil would not be mobilized simultaneously through the plastic zone. These modifications consisted of reducing the cohesion and angle of shearing resistance to take into account progressive failure (local shear failure). Vesic [130] has shown that the greatest shortcoming of available theories lies in the assumption of soil imcompressibility and proposed a method to reduce the general bearing capacity by using a compressibility factor. His approach gives similar results to those of Terzaghi [120].

The research on the ultimate bearing capacity of two-layer systems has received a great deal of attention within the last ten years. There are several solutions for a stiff stratum over a softer stratum, which are now available in the soil mechanics literature. For a stiff clay layer over a softer clay layer, solutions have been given by Button [28], Reddy and Srinivasan [93], Brown and Meyerhof [18]. When

the soils involved possess both cohesion and friction, the bearing capacity of the two-layer system may be determined using the solutions given by Tcheng [118], Yamaguchi [134], Meyerhof [76], and Vesic [130]. Some of the theoretical solutions have been verified using small scale model tests [76. 130]. The whole concept of using small scale experiments to verify proposed bearing capacity theories is regarded with considerable skepticism by many prominent foundation engineers. The scale effect on the ultimate bearing capacity of soils has been considered by Vesic [130] who found a decrease in values of bearing capacity factors with increase in size for all soils. To verify the theories, a large scale footing load test is, therefore, preferrable to small scale tests.

Finite Element Method

A more sophisticated way of assessing the stress distribution, settlement, and bearing capacity of soils, is by means of the finite element method of analysis. While the method is very powerful, it is still based on certain soils parameters such as E and ν, and, therefore, has the same shortcomings in accuracy as in any other method. The main advantage of the method is that it can take into account the nonlinearity of the stress-strain relationship of the soil as well as the effect of stress-dependency on the soil properties.

The effects of nonlinearity of soils on stress and

strain distributions in a homogeneous layer has been studied by Huang [53]. He assumed nonlinear behavior of clays and sands, and analyzed their effect on the distribution of stresses and displacements in a homogeneous semi-infinite solid using the finite element method. Huang found the nonlinear behavior to have a large effect on vertical and radial displacements, an intermediate effect on radial and tangential stresses, and a very small effect on vertical and shear stresses.

Das and Gangopadhyay [34] compared the load-deformation behavior and undrained stress distribution behavior obtained from finite element analysis with the results of instrumented model footing tests. A bilinear elastic-plastic model was used in the nonlinear analysis with material properties obtained from the triaxial stress-strain curves. The small scale footing load tests were conducted on consolidated sediments of kaolin placed in a tank. Both radial and vertical stresses as well as pore pressure were measured. A comparison between the predicted and measured load-deformation curves showed good agreement. A good prediction was obtained using the measured undrained stresses and $\nu = 0.45$. The measured vertical stresses compared well with the computed values from the elastic analysis of Poulos [88]. The computed radial stresses using Poulos' method had to be adjusted not to exceed the shear strength of the soil. The adjusted radial stresses showed good agreement with the mea-

sured. The results of this investigation confirms the finding of Huang [53] that the nonlinear behavior has only a small effect on the distribution of vertical stresses calculated using linear elastic theory, but does effect horizontal stresses. Lee and Idriss [67] also considered the effects of nonlinearity on the stress distribution in earth dam embankments. They concluded that a linear elastic theory could be used to compute the stresses but that deformation was greatly affected by nonlinearity.

The settlement and bearing capacity of shallow foundations on a single or two-layer system can be predicted using nonlinear methods. Duncan and Chang [41] applied a hyperbolic model to represent the stress-strain behavior, and predicted the settlement of a strip footing on sand and clay. Good agreement between the measured and computed load-settlement curves was observed. D'Appolonia and Lambe [32] used a bilinearly elastic model to predict the initial settlement of a footing on clay. In the analysis, the effects of anisotropy in the shear strength were included. A comparison showed good agreement between observed and measured settlements.

The consolidation settlement of oil storage tanks supported on clay was predicted using a nonlinear method by Domaschuk and Valliappan [40]. The nonlinearity was modeled by assigning bulk and shear moduli to each element compatible with the soil type and the prevailing state of stress. Iso-

tropic compression tests and constant mean normal triaxial compression tests were used to obtain the bulk and shear moduli, respectively. A comparison of the measured settlement with that obtained using the finite element method considering the base of the tank to be rigid showed good agreement.

Desai and Reese [39] used the finite element method which incorporated the nonlinear characteristics of the clays to predict the experimental load-settlement behavior of a rigid circular plate on the clay layers for the case of one and two-layer systems having stiff over soft layers. The computed and measured valued were found to show excellent agreement for the major portion of the load-settlement curves in both cases.

Mitchell and Gardner [78] performed theoretical analysis of load-bearing fills over soft subsoils by utilizing a nonlinear finite element method. The analysis was done to study the behavior of a 7-foot thick sand fill overlying a 26-foot thick layer of soft clay loaded by a concrete footing having a 4-foot radius founded at a depth of 3 feet below the surface of the sand. Nonlinear material properties dependent on strain and confining pressure were used in the computer program. The analysis was made for the cases of a homogeneous clay and a sand layer over clay. The vertical and shear stresses at a depth of 4.5 feet beneath the base of the footing were compared. The theoretical study indicated

that the sand layer has beneficial effects in reducing stresses in the clay.

The results of Mitchell and Gardner, however, contradict the findings of Sowers and Vesic [115], McMahon and Yonder [72], and Seed, et. al.[101] who have shown that stresses in two-layer systems consisting of a layer of compacted granular material overlying a compressible soil are very similar to those in a homogeneous layer. Mitchell and Gardner expressed the need to compare the finite element solutions with directly measured values of stresses and deformations from any actual load-bearing fill.

CHAPTER III

STATEMENT OF THE PROBLEM

Analysis of the compacted fill problem to determine the stress transmitted to the soft subsoils is usually resorted to either approximate load distribution methods or two-layer elastic theory. The approximate methods involve uncertainties in that no distinction is made between granular or cohesive fills.

Analysis of the problem using conventional two-layer elastic theory [25] involves the following assumptions:

1. Linear elastic behavior
2. Constant modulus of elasticity
3. Modulus of elasticity equal in compression and in tension
4. Uniform circular loading

Nonlinear properties of soils have been found experimentally and theoretically to have negligible effects on the vertical stress distribution in the soil media [34, 51, 67, 81]. From these results, deviation from linear elasticity in the first assumption should not induce a large error in the computation of stresses imposed by normal working loads.

The use of compacted cohesive fills on saturated clay subsoils should approximately satisfy the second assumption. The modulus of granular materials, however, is strongly

dependent on confining pressure and hence not constant. Using granular fills therefore does not satisfy the second assumption.

The assumption of equal modulus in tension and in compression is not always satisfied [3, 4]. Use of the two-layer elastic theory predicts tension at the base of the upper layer. Compacted granular fills, however, are incapable of carrying tension above initial compressive stress level. For cohesive soils, Ajaz and Parry [3] and Al-Hussiani and Townsend [4] have found that the modulus of compacted clay in tension may be 2 to 3 times greater than that in compression. This difference in modulus would tend to be another source of error if the two-layer theory is applied.

Since reinforced concrete footings are more closely rigid than flexible, the assumption of condition four is not satisfied.

Because of these considerations, it should not be expected that two-layer elastic theory will correctly predict stresses imposed by fill supported foundations in all cases.

From the results of several previous investigations, it is now well recognized that the distribution of vertical stress in a uniform soil layer, resulting from the applied surface load corresponds reasonably close to Boussinesq theory. The actual distribution of stresses within a two-layer system subjected to a surface loading, however, has yet to be completely defined by measurement.

Attempts have been made in the past to measure the change in stresses within the stiff-over-softer layer system. Because of the many difficulties involved in measuring stress as discussed in Appendix A, accuracies greater than ±20 percent cannot be expected [21, 54].

Approach

When a footing is loaded on the surface of a compacted fill, the deformation or settlement of the soft layer is dependent on the magnitude of stresses transmitted to it through the compacted layer. To determine the beneficial effect of the compacted fill in reducing the subsoil stresses, the deformation of the soft layer under the fill can be measured and compared with the deformation of same stratum of a homogeneous layer case. This method would eliminate comparing stresses if compressibility characteristics of the soils is the same. Figure 1a shows a typical footing resting on the surface of a homogeneous, isotropic, semi-infinite, linearly elastic medium before and after load P is applied. Point B is located at a depth H below the base of the footing. The application of load P causes the footing to settle to A_1. The total settlement of the footing under load P is w_0. The settlement of Point B which moves to B_1 is w_1.

The depth H between A and B in Figure 1a is now replaced with a stiff layer as shown in Figure 1b. When the same load P is applied, the total settlement of the footing is equal to w_0' and the settlement of the softer layer

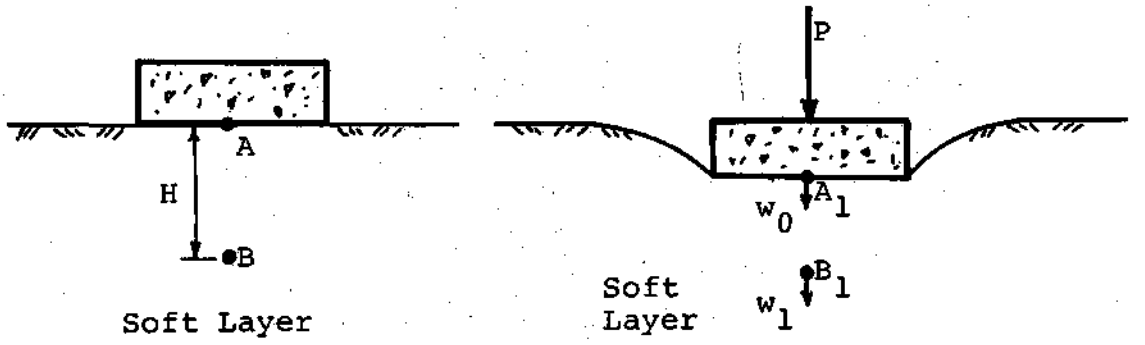

a) Homogeneous Layer

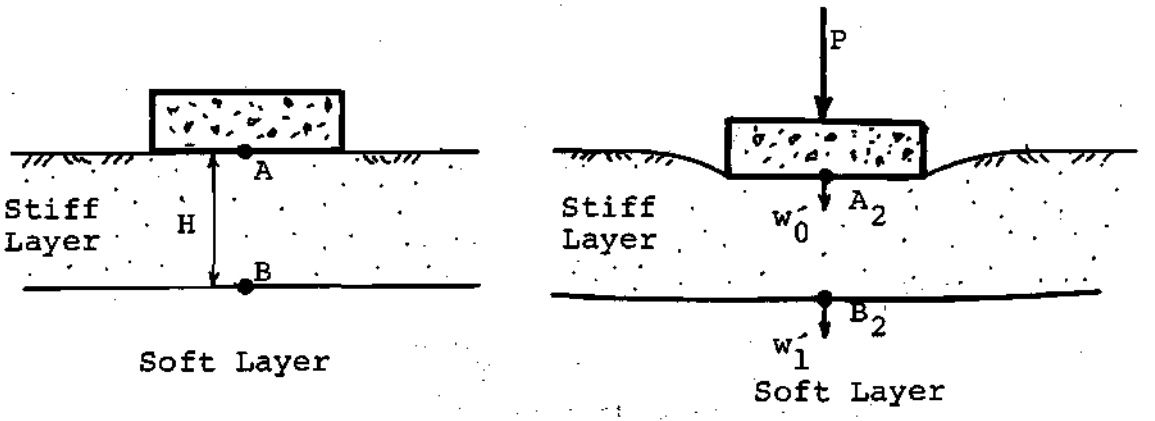

b) Two-Layer

Figure 1. Determination of Beneficial Effect of Structural Fill.

beneath the stiff layer at Point B is w_1'.

If the settlement of Point B under the same load P for both cases is equal, i.e., $w_1 = w_1'$, it indicates that the stiff layer has no beneficial effect whatsoever in reducing the stress and hence the deformation in the softer layer. The presence of the stiff layer merely reduces the deformation between Point A and B causing the total settlement w_0 to be less than w_0'.

If the settlement of the soft layer below Point B_1 is greater than that of Point B_2, i.e., $w_1 > w_1'$, a stress reduction occurs in the softer layer. The beneficial effect of the stiff layer in reducing the stress and deformation in the softer layer is attained.

If the soils satisfy all assumptions of two-layer linear elastic theory, the presence of a stiff layer over a softer layer will certainly cause a stress reduction in the softer layer to less than that indicated by Boussinesq theory. However, real soils do not meet all of the assumptions as discussed earlier; therefore, carefully instrumented experiments must be used to establish stress distribution in layered soils.

If the thickness H of the stiff layer increases or decreases, the beneficial effect should, based on linear elastic theory, vary. In this study the effects were investigated of varying the thickness of the stiff layer as well as the use of different materials on the deformation and stress

distribution within the softer layer.

Method of Investigation

As indicated in Chapter I, three test series were conducted in this study. To measure the deformation between Point A and B in Figure 1, Bison strain sensors (Appendix B) were placed at predetermined locations during construction of the layer systems. For the purpose of comparison and obtaining limited vertical stresses diaphragm stress cells were used for stress measurement. Strains within the soil layers were measured in all test series using the strain sensors as described in Chapter V.

In Test Series I, a homogeneous soil layer was constructed in the test pit and loaded on the surface with a rigid, circular footing 18 inches in diameter. Measurement of the deformations of the soft layer below Point B in Figure 1a was done at depths equal to 1/2D, 1D, and 1-1/2D where D is the diameter of the footing.

For Test Series II and III, three two-layer systems having compacted fill thickness H = 1/2D, 1D and 1-1/2D were constructed for each test series using sandy clay and sand, respectively.

It is also of interest to investigate the effects of replacing only portions of the softer layer beneath the footing area with crushed stone on the deformation and stress distribution of the soft layers. The stone replacements having a diameter equal to 1D and 2D were used, and the experiments

were carried out in Tests Series I and III.

Care was taken in these experiments to construct the soft layers with essentially the same compressibility and strength characteristics for all three test series. After each test series, the soft layers were removed and recompacted to the same density and moisture content.

The final objective of this study was to confirm the postulated method of evaluating the beneficial effects of structural fills. The results of the experiments were analyzed and proposed recommendations based on the test results were made for the design of structural load-bearing fills.

CHAPTER IV

EQUIPMENT AND INSTRUMENTATION

Equipment

To investigate the beneficial effects of structural fills in reducing the settlement within the soft layer using the proposed procedure, large scale footing load tests were conducted on a homogeneous layer of soft soil and two-layer systems of compacted structural fills over the soft subsoils. The following equipment and instruments were used in this study.

Test Pit

The concrete test pit which was located in the Annex adjacent to the Geotechnical/Material Laboratory was 8 feet wide, 12 feet long and 7 feet deep. A steel loading frame having a load capacity of approximately 30 tons was attached to the pit with a heavy beam from one end to the other in the north-south direction. A hydraulic jack mounted on a carriage riding on the beam could be easily positioned to apply load along the centerline of the pit. The beam was removable to provide room during soil compaction in the test pit. A 1.5 ton overhead service crane was used to remove the beam and transfer soils from the storage area to the pit.

Loading System

A rigid, circular concrete footing 18 inches in

diameter and 6 inches thick without reinforcing steel was used as the foundation to transmit the loads to the soil layers. The footing was loaded using an Enerpac hydraulic ram having a capacity of 20 tons and a 20 ton capacity Simplex Model RP5 hydraulic pump.

The footing load tests performed in this study required relatively constant applied loads to be maintained on the footing for a specific length of time because both immediate and long-term settlements of the footing were measured. A constant applied load was also desired when stress cell readings were taken. For this situation, a loading system using dead weights would be ideal but it was not feasible because of a large magnitude of load required. Because the soil layers constructed in the test pit were relatively compressible, large pressure drops during testing were expected. To minimize the pressure drop and load fluctuation within the loading system, a Greer accumulator having a 2,000 psi capacity was pressurized with dry nitrogen and connected to the loading system between the ram and the pump. A reservoir of hydraulic fluid was provided for the pump during testing. To measure the loads imposed on the footing accurately, a model S/N FLU-255P2-0210 single bridge Universal Flat Load Cell with a two millivolt per volt output and an accuracy of 0.03% on loading and a capacity of 25 kips was used. This load cell was manufactured by Strainsert Company, Bryn Mawr, Pennsylvania. The output of the load cell was monitored on

a model 120C Strain Indicator, made by BLH Electronic Inc., Waltham, Massachusetts. The calibration of the load cell was performed using a 20 ton capacity Tinius-Olson Testing Machine with the entire loading system in the testing machine. A Test Gage pressure gage made by Ashcroft, Inc., which had a knife edge needle and mirror and a capacity of 500 psi was also calibrated and used to double check the applied loads. The footing load test setup is shown in Figure 2. Figure 3 is a view of the footing load test in progress.

The performance of the load system in maintaining constant loads imposed upon the test footing was found to be satisfactory particularly for footing pressures up to approximately 8000 psf. Above this range small fluctuation of the load occurred as the capacity of the accumulator was approached. A large temperature variation also caused load fluctuation because of expansion and contraction of the dry nitrogen contained in the accumulator. This load fluctuation was corrected manually by frequently checking the pressure gage and load cell readings.

Stress Cells

The stress cells used in this study were essentially of deflecting diaphragm type having one active diaphragm, the strain of which were measured using etched foil electrical resistance JB type diaphragm strain gage manufactured by Micro-Measurement, Inc., Romulus, Michigan. This strain gage which had a gage designation of EA-06-11CJC-120 was especially

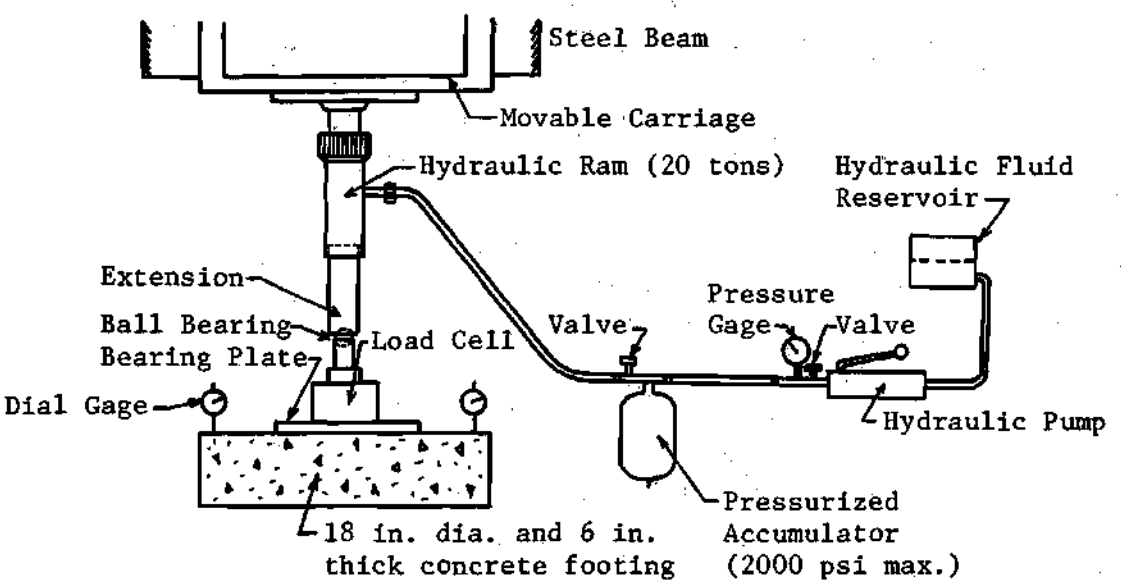

Figure 2. Loading System Setup.

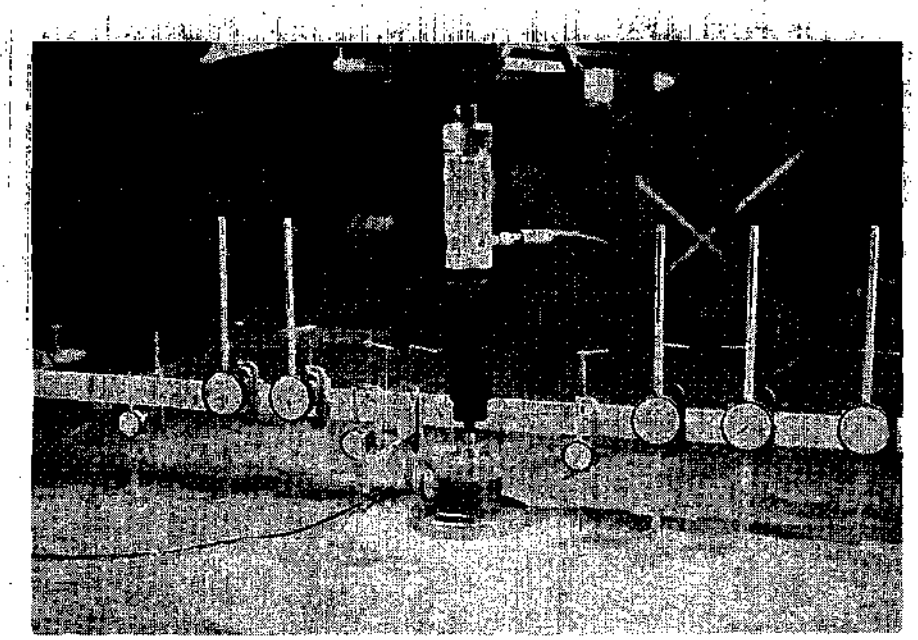

Figure 3. Footing Load Test in Progress.

designed for diaphragm pressure transducers. The cells were made of grade 2024 T-3 aluminum and were 2 inches in diameter and 0.3 inch thick. Figure 4 shows a schematic drawing of the stress cell.

In the design of the stress cell, the following criteria were considered:

1. The diaphragm diameter should be at least 50 times that of the largest soil particle [58].
2. The diaphragm area should be less than 45 percent of the total area of the cell face [84].
3. The thickness to diameter ratio of the cell should be less than 0.1 [7].
4. The central deflection of the diaphragm under pressure should be less than 1/2000 of its diameter [125].
5. The flexibility factor, the ratio of soil stiffness to diaphragm stiffness should be less than 2 [7].

The stress cells were designed to meet the above criteria as much as possible. The sensitivity of the cells depends largely on the diaphragm thickness, thinner diaphragm having increased sensitivity at the expense of a more limited linear range and possible excessive diaphragm deflection. Cells having diaphragm thicknesses of 0.030 inch were designed for a maximum pressure of 10 psi, 0.05 inch for 75 psi and 0.075 inch for 200 psi. The strain outputs of the stress cells were monitored using a model 120C Strain Indicator, made by BLH Electronics, Inc., in conjunction with

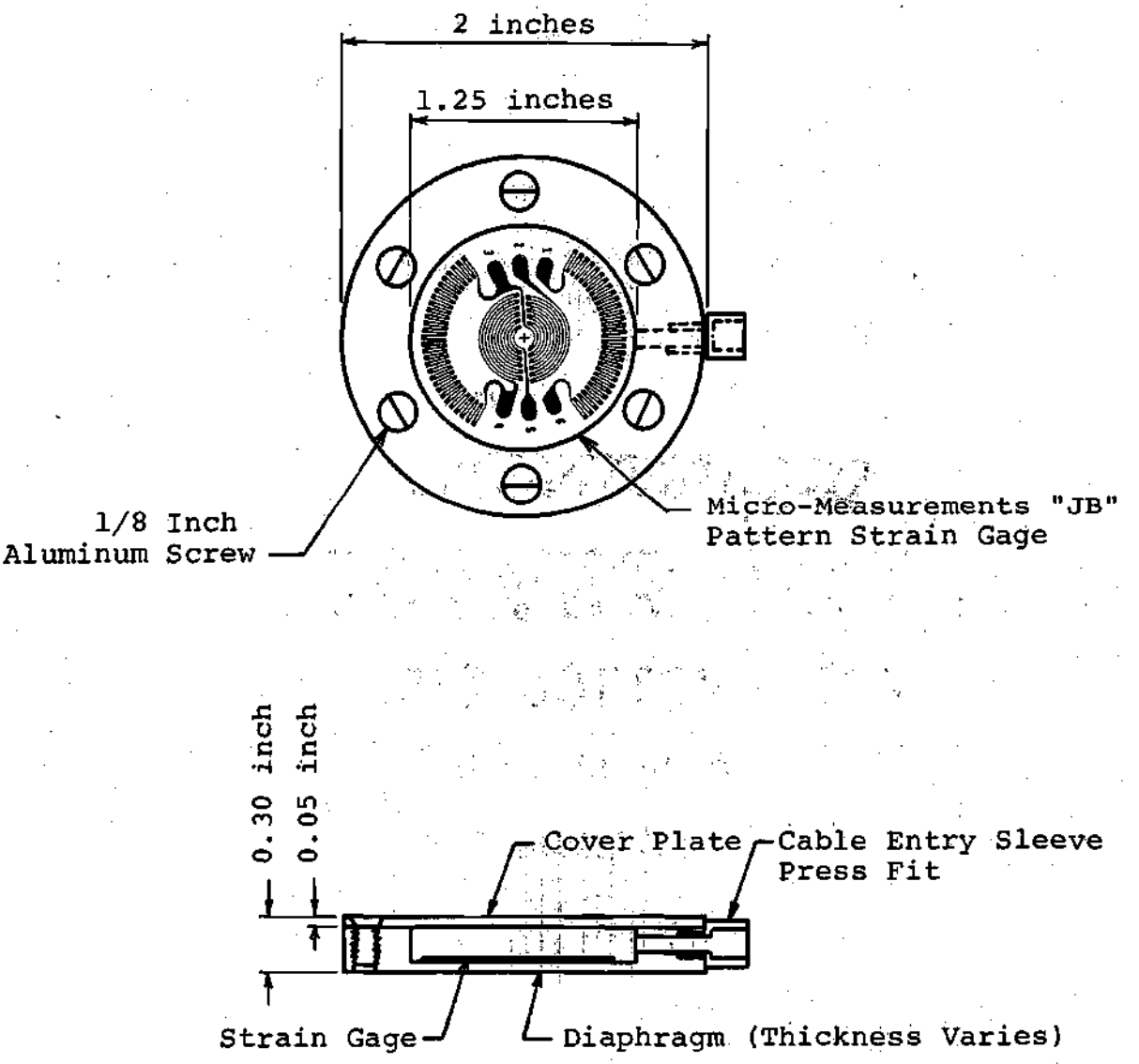

Figure 4. Stress Cell Details.

two 20 channel switching and balancing units also manufactured by BLH Electronics, Inc. The calibration relationship for hydrostatic and soil calibrations in micaceous clayey silt and sandy clay was found to be linear within the design stress range. In sand, the relationship was found to be slightly non-linear. Typical calibration curves are given in Appendix A. Based on the soil calibration in micaceous clayey silt, the sensitivity of the stress cells having a diaphragm thickness of 0.05 inch was 0.05 psi per change of one microinch per inch of strain output and 0.14 psi per change of one microinch per inch for a diaphragm thickness of 0.075 inch. A detailed description of stress cells design, construction, and calibration procedure as well as discussions on stress measuring in soils is given in Appendix A.

Twenty-two cells were employed to measure the vertical stresses in the homogeneous micaceous clayey silt (Test Series I). Because these cells which were made of aluminum were not anodized to prevent corrosion, sixteen of the cells ceased functioning when they were recovered from the test pit after a period of approximately two months, Three of the remaining six cells becames erratic and could not be used. Only three still remained functioning properly. The failure of the cells was due mainly to corrosion which penetrated through the diaphragm.

Twenty-five more stress cells were made to be used in

Test Series II and III. These cells which were also made of aluminum were clear-anodized and several improvements were made on the production of the cells. These improvements included spraying the cell body with corrosion resistant paint, adding cable sleeves, and coating the strain gages with heavy duty Micro-Measurement M-Coat-C, a rubber based water proofing agent. All of the new cells functioned properly in Test Series II and III.

Strain Sensors

The development of inductance strain sensors [104] makes it possible to measure a change in length between any two points in the soil mass. To measure the settlements of the soft layers as well as the vertical and horizontal strains, Bison strain sensors, manufactured by Bison Instrument, Inc., were placed in the soil mass at predetermined locations during the construction of the soil layers.

The sensors are disc-shaped coils of insulated wire with diameters of either one inch, two inches or four inches, and are coated with waterproof plastic. The coils are operated in pairs, the two being situated in the soils either face to face or edge to edge, with up to four diameters distance between them. The separation of any two coils is related to the electro-magnetic coupling between the two. When an electric current is passed through one coil, a flux field is formed in its vicinity which induces a current in the second coil. Should the spacing between the sensors

change, the amplitude of the induced current is changed. The Model 4101A Instrument Unit manufactured by Bison Instrument, Inc., was used to input current to one coil and measure the amplitude of the induction. Change in amplitude readings can be directly related to displacements between a coil pair by a simple calibration procedure. Movement of up to ±0.001 inch could be monitored with two-inch coils. Appendix B gives the complete descriptions and calibration procedure for the sensors.

Tensile Properties of Compacted Sandy Clay

Beam bending tests were performed on the compacted sandy clay to determine the tensile stress-strain characteristics of the stiff layer used in Test Series II. The tests were conducted on block samples cut from the compacted layers in the test pit and also on samples prepared in the laboratory. The size of the beam was 20 inches long and 3 inch by 3 inch in cross section. The tensile and compressive strains in bending were measured using specially designed miniature inductance coils. A complete description of the beam bending equipment, test procedure, and instrumentation is given in Appendix C.

Instrumentation

Settlement and Surface Deflection Measurements

Four soil test dial gages having an accuracy of 0.001 inch were used to measure the settlement of the footing. These gages were placed close to the edge of the footing opposite to each other in the north-south and east-west

directions so that any footing tilting could be detected. The average readings of the four gages were used as the settlement values for the applied loads. To minimize the effects of temperature variation these gages were mounted on a wooden beam which was attached to the top of the walls of the test pit. Six more dial gages were employed to measure the deflections of the soil surface. The dial gage locations are shown in Figure 3.

Deformation and Strain Measurements

Test Series I: Homogeneous Micaceous Clayey Silt Layer. This test series consisted of conducting footing load tests on a homogeneous layer of soft soil and stone replacements. Figure 5 shows the layout of the strain sensors which were placed on a vertical plane along the east-west cross-section at the center of the test pit. A total of 45 Bison strain sensors were used. Along the center line of the footing the sensors were located in such a way that the settlements of a point at a depth of 1/2D, 1D, and 1-1/2D could be determined. The column of sensors along the load axis was extended all the way to the bottom of the test pit. The purpose of the complete strain coil stack was to determine the vertical strain distribution and to provide a means of checking the performance of strain sensors in measuring the soil deformation. This was done by summing up the deformations between each pair of coils from beneath the footing of the test pit. The total deformations obtained

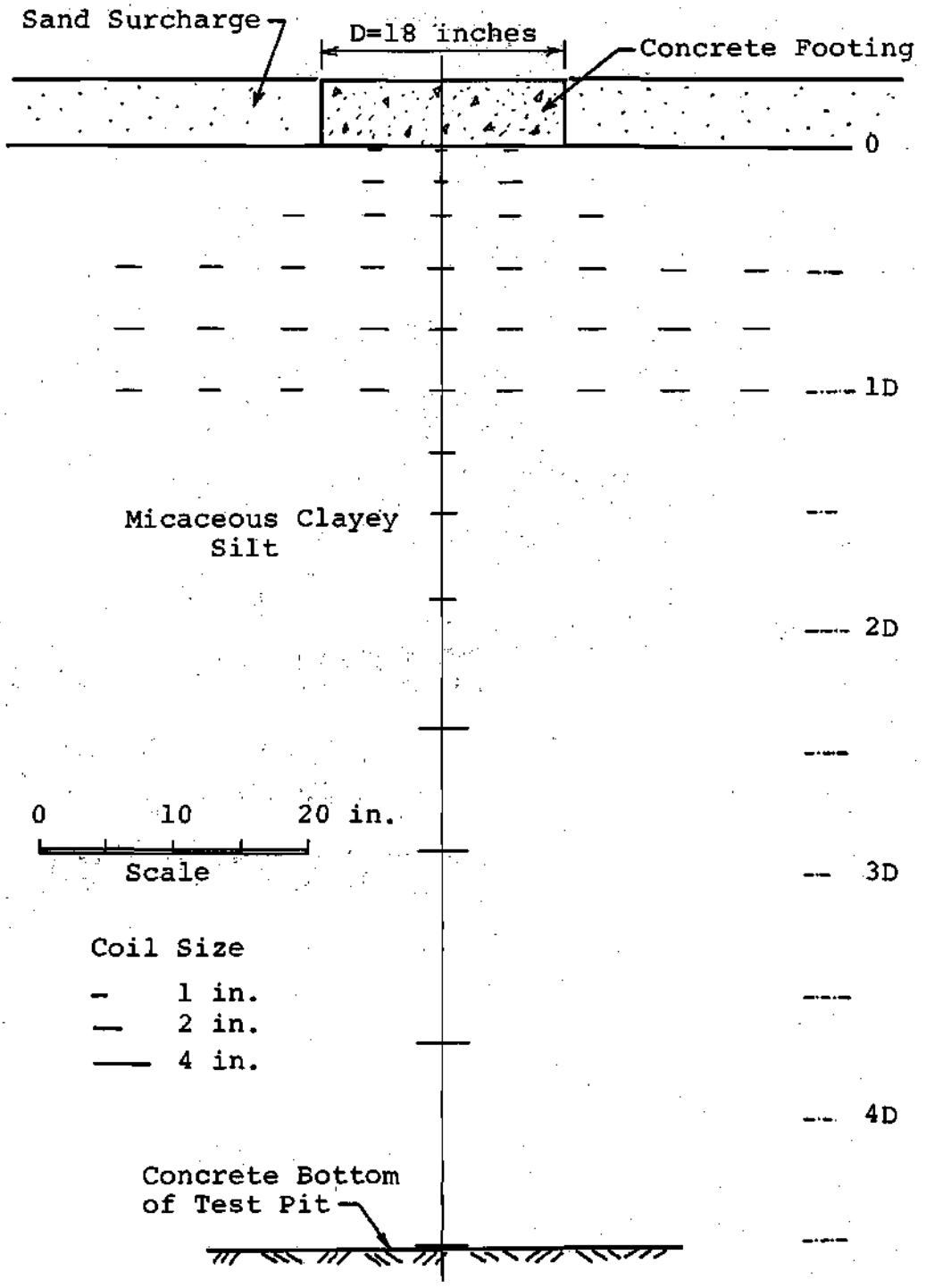

Figure 5. Strain Sensor Layout. Test Series I - Single Layer.

for an applied load should approximately equal the total settlement of the top of the rigid concrete footing. The results of these comparisons are given in Chapter VII. Several strain sensors were placed off the load axis in order to measure the deformations in vertical as well as radial directions.

Sensor placements were done during construction of the soil layers. To insure accurate locations of the sensors, small nylon strings tied to thin wooden strips vertically epoxied to the test pit walls on both axes of the pit were used to establish the center line axis of the footing. A small plumb bob was used to locate the center line on the soil surface. The locations of coils and stress cells off the center line were then measured off radially from the established reference point along the center line axis. Pre-cut recesses having the same diameter of the coil were made for each coil on the soil surface. A small hand level was used to level each coil. Even though small tilting has little effect on the sensors performance [103, 104], best results are obtained if each pair of sensors is parallel. The strain coils were then covered with the same soil as that removed and carefully compacted to the same density as the surrounding area. Small trenches were also provided for the cables. All of the coils were carefully labeled and tagged for identification.

Test Series II and III: Structural Fills Over Soft

Layers. Test Series II and III were conducted on stiff over soft layered systems using compacted sandy clay and Chattahooche River sand as the stiff layers, respectively.

In each test series, three footing load tests were conducted for three different thicknesses of the compacted fills used. Detailed construction procedures are given in Chapter V. Figure 6 shows the layout of the strain sensors for Test No. 1 for Test Series II and III which were conducted on the compacted structural fills having a thickness equal to 1/2D. Eleven coils were placed at the interface in an attempt to measure any lateral deformation at the bottom of the stiff layers. The coils placed along the center line were extended to a depth of 4D where any movement in the soil as a result of surface loads was considered negligible. In addition, several coils were placed off the load axis in the softer layer for measuring vertical and radial strains.

The strain sensor layouts for Test No. 2 and 3 of Test Series II and III in which the thickness of the compacted layers were 1D and 1-1/2D, respectively, are shown in Figures 7 and 8. For Test No. 2, strain sensors were extended to the bottom of the test pit. Vertical coils in the stiff layer were installed at a spacing of approximately 2.25 diameters of the coil. Even though the coils spacing was as much as four coil diameters apart, it was found that at this coil spacing a sensitivity of about 0.0015 to 0.002 inch per change in amplitude was obtained. Greater spacing

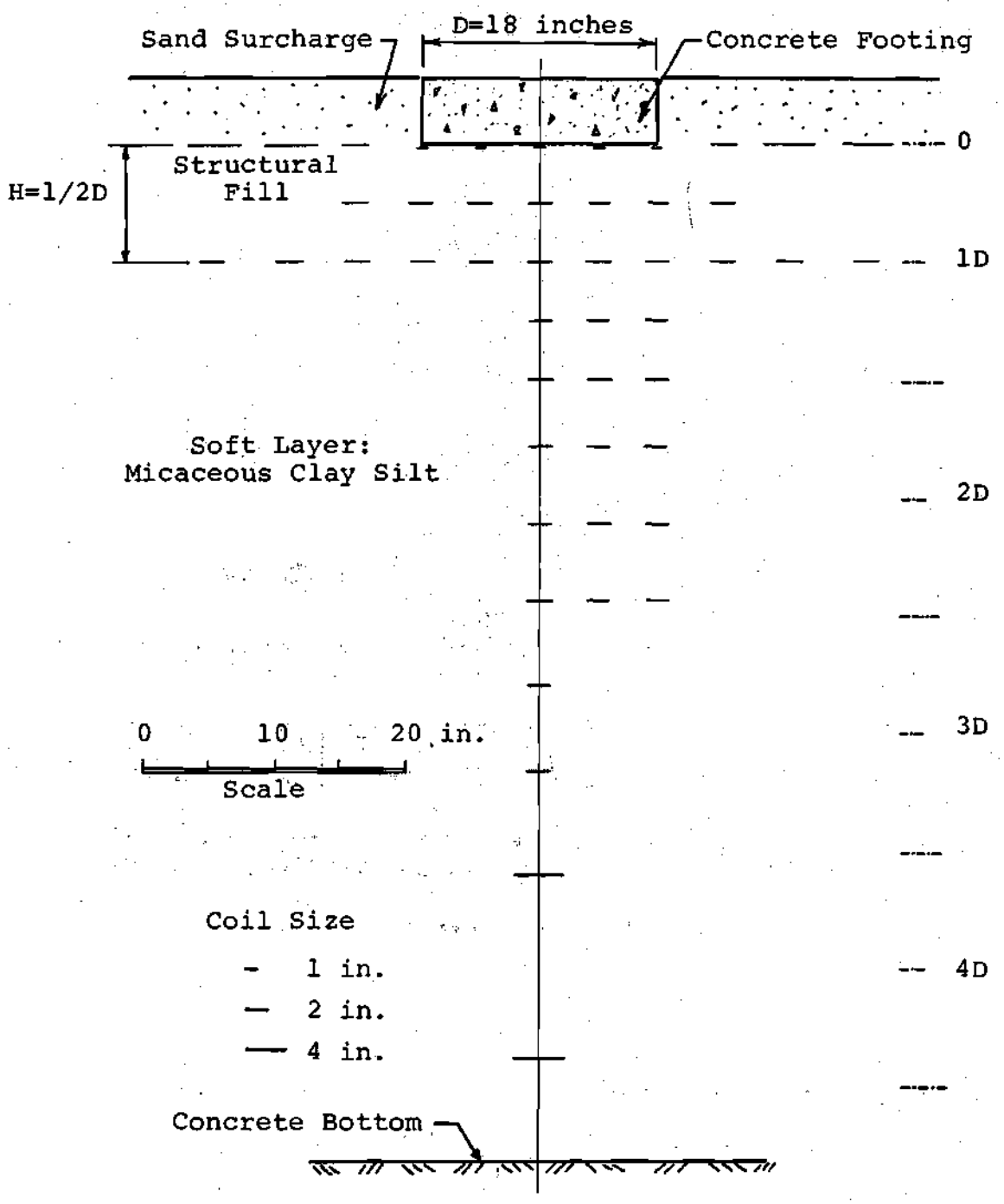

Figure 6. Layout of Strain Sensors for Test 1 (H=1/2D), Test Series II and III.

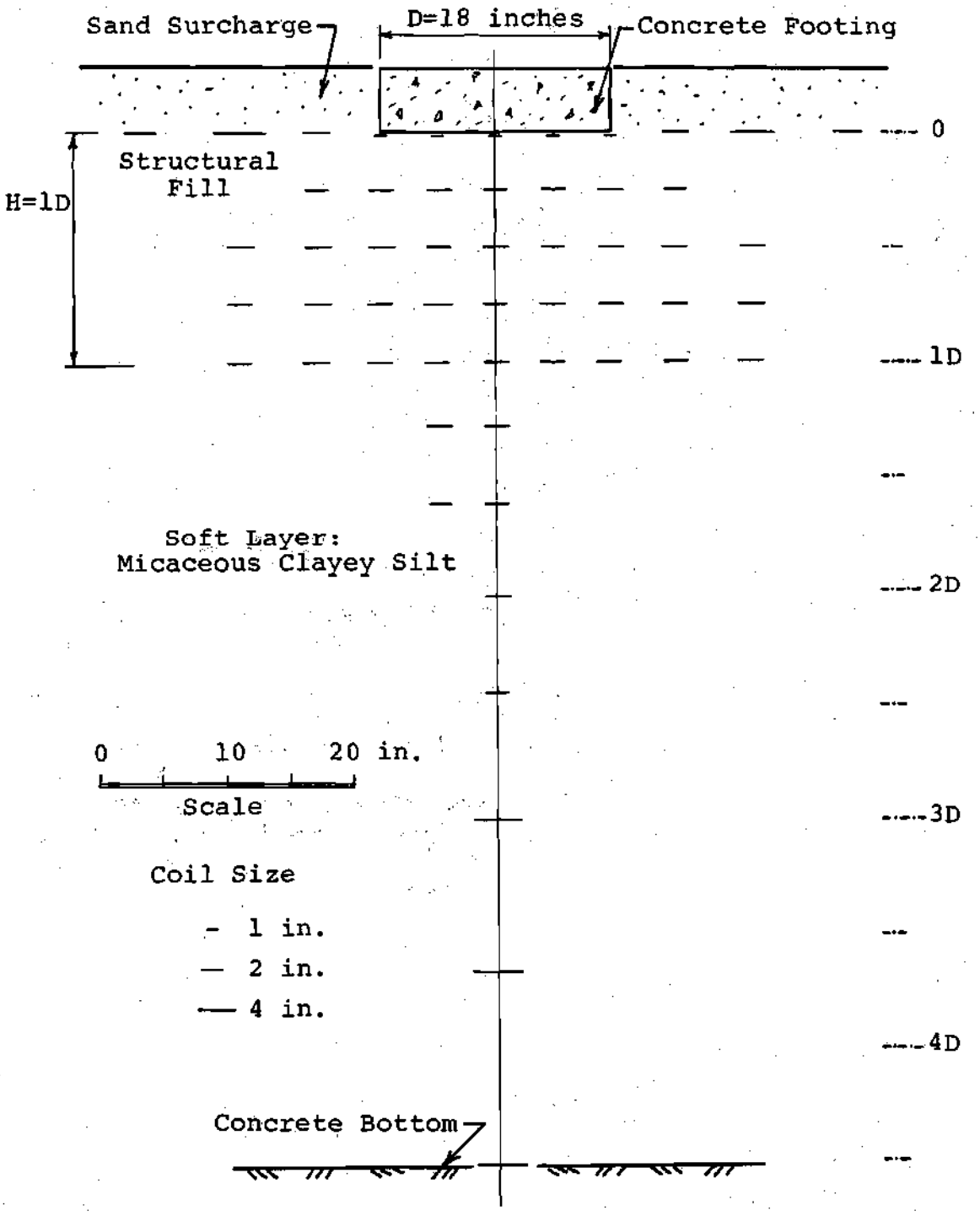

Figure 7. Layout of Strain Sensors for Test 1 (H=1D), Test Series II and III.

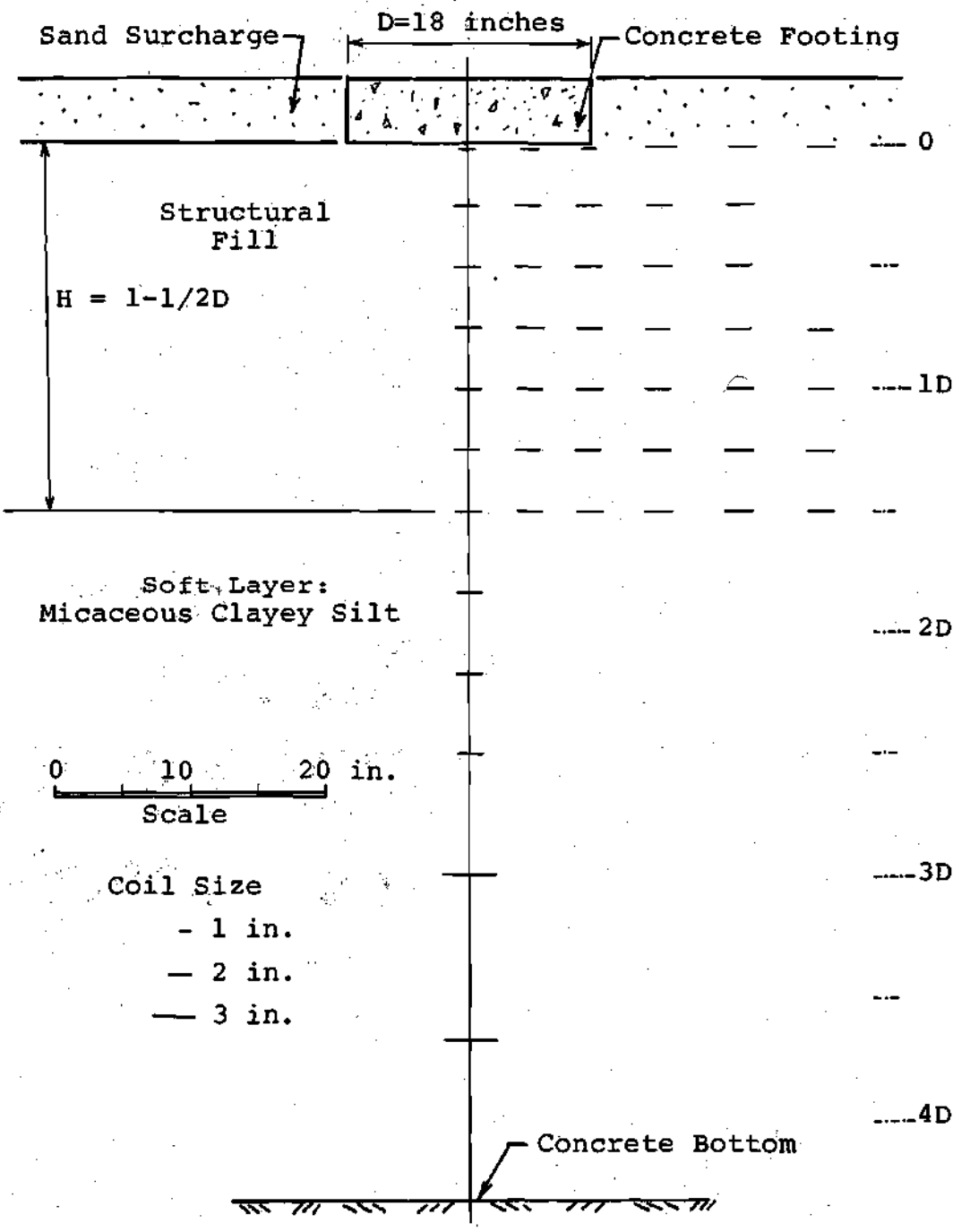

Figure 8. Layout of Strain Sensors for Test 3 (H=1-1/2D), Test Series II and III.

would reduce the sensitivity of the output, and small changes in spacing might not be measurable. Thirty sensors were installed radially in the stiff layer in an attempt to measure vertical as well as radial strains off the center line axis. Small strain sensors 1 inches in diameter were placed flush with the soil surface at the base of the footing.

Figure 8 shows the sensor layout for Test No. 3 in which the fill thickness was equal to 1-1/2D. A total of 44 strain sensors were used in this test. All of the sensors were installed during fill placement using the procedure previously described.

The strain sensors were found to be rugged and affected very little by variation in temperature, and their performance was satisfactory. None of the sensors malfunctioned during the tests. The effects of placement and subsequent rotational misalignment during soil compaction have been found to cause only slight inaccuracies in measurements [104]. Ledbetter [66] has used this type of strain sensors in conjunction with other types of strain cells to measure strains in an airport pavement. He found that the strains measured using the various methods were compatible and complemented each other. The results of this study confirm the reliability of using this type of electrical sensors to obtain movements within the soil mass.

Stress Measurements

Test Series I: Homogeneous Micaceous Clayey Silt Layer. The stress cell layout is shown in Figure 9. To measure the vertical stress distribution with depth beneath the footing, six stress cells were placed at a 4 inch offset from the center line of the footing. This distance is two diameters of the coil, which is the minimum distance required for a metal object to be close to the coil without interfering with the measurements. Vertical stress profiles on a horizontal plane were also measured at different depths below the footing by placing stress cells at depths equal to 1/2D, 1D and 2D. Radial and tangential stresses were not measured in this study.

Installations of the cells were made during fill placement using the same procedure as for Bison strain coils. As suggested by Brown [21], the cells were installed with the diaphragm up in pre-cut recesses in the soil surface.

Test Series II and III: Stiff Over Soft Layer. Figure 10 shows the cell layout for Test No. 1 (H = 1/2D). A total of 21 stress cells were employed in this test. Two cells were placed in the compacted layer, the closest one to the footing being about 3/4 inch below. To measure the interface stresses, stress cells were placed flush with the softer layer surface. When sand was used as the compacted structural fill, these cells were first covered with sand which had been sieved through a No. 30 sieve to insure that the largest particle in contact with the cell diaphragm was less

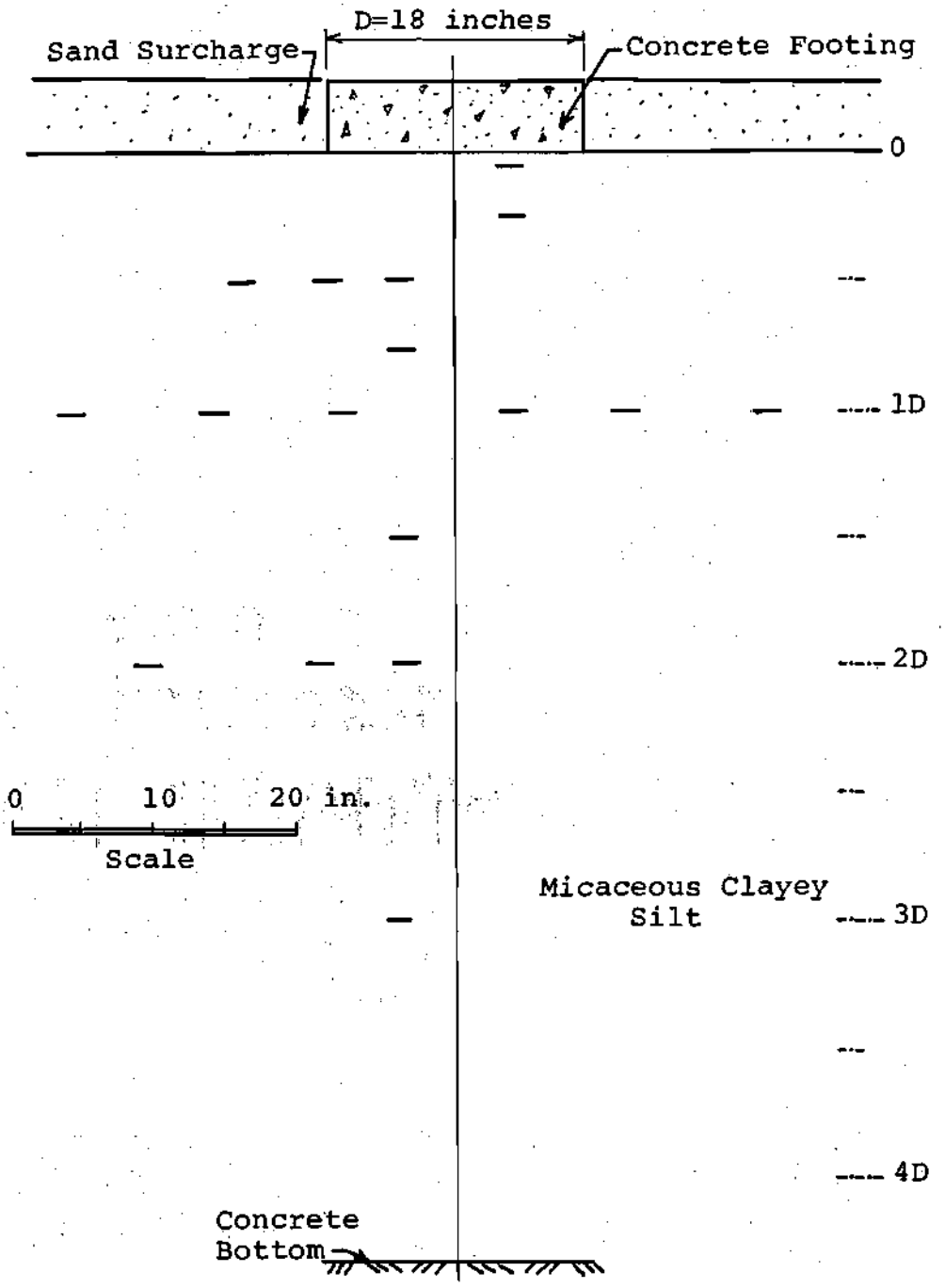

Figure 9. Stress Cell Layout for Test Series I: Homogeneous Fill Layer.

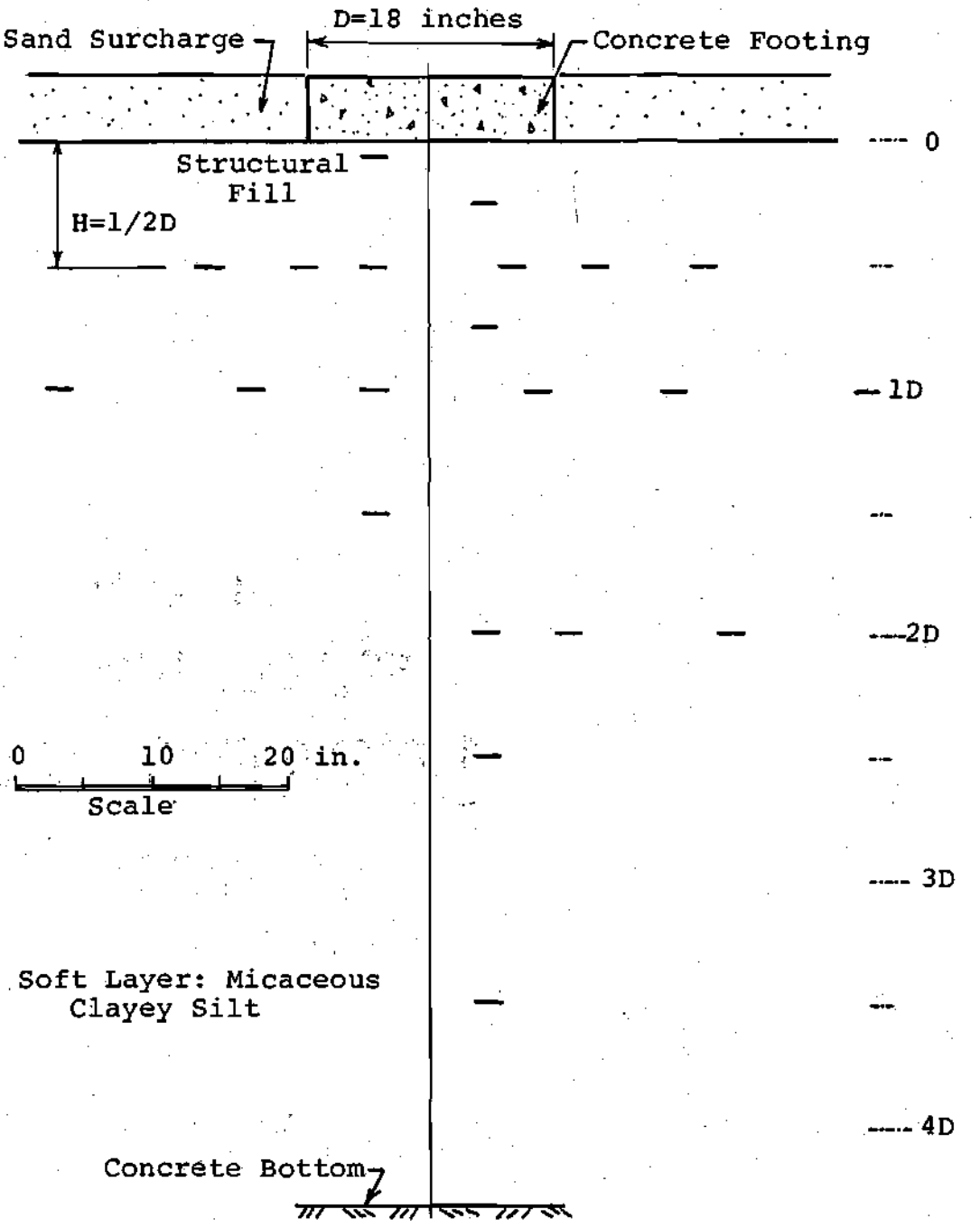

Figure 10. Stress Cell Layout for Test 1 of Test Series II and III: H = 1/2D.

than fifty times the cell diaphragm diameter. All cells embedded in the sand were installed in a similar manner.

The stress cell layouts for Tests No. 2 and 3 of Test Series II and III are shown in Figures 11 and 12. A total of 18 and 21 cells were used in Test No. 2 and 3. Eight stress cells were installed at the interface between the stiff and softer layers. Three cells were used to measure vertical stresses on a horizontal plane in the stiff layer at a depth of 1/2D and three in the softer layer at a depth of 2D. Seven cells were offset 4 inches from the center line vertically to define the vertical stress profile with depth for the two-layer system.

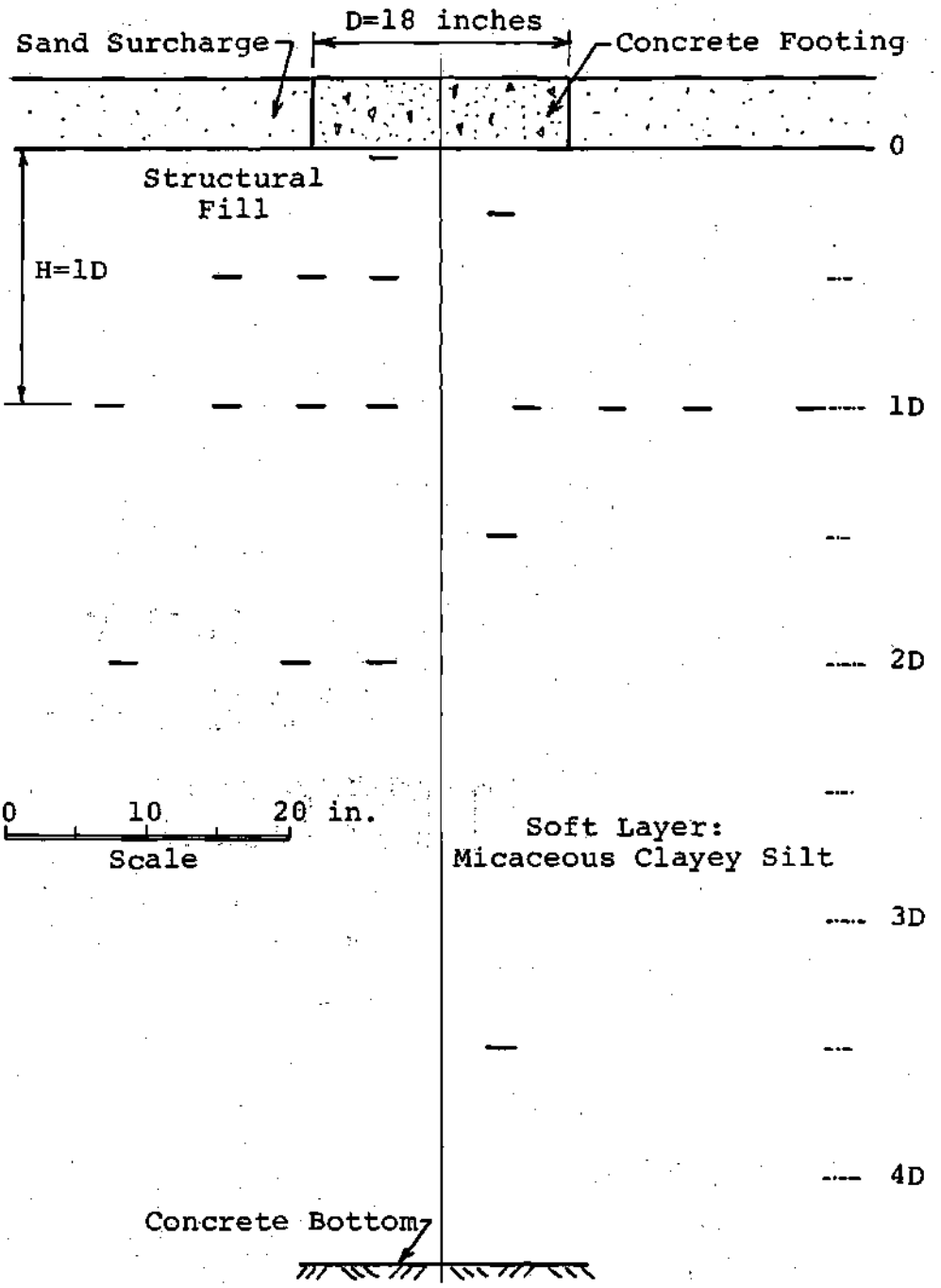

Figure 11. Stress Cell Layout for Test 2 of Test Series II and III: H = 1D.

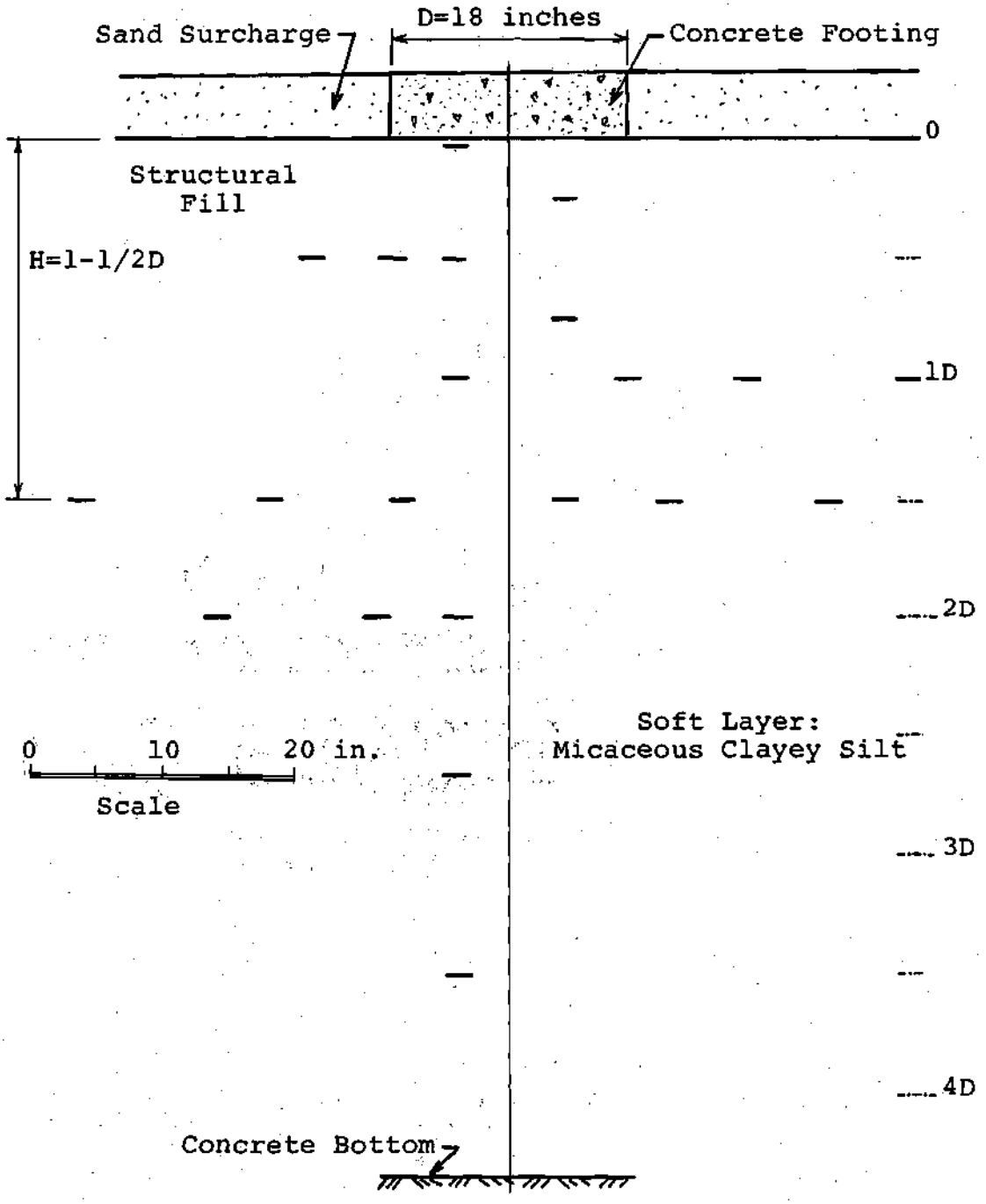

Figure 12. Stress Cell Layout for Test 3 of Test Series II and III: H = 1-1/2D.

CHAPTER V

SOIL CONSTRUCTION AND TESTING PROCEDURE

Materials

The soil used for construction of the homogeneous layer of soft soil in Test Series I was obtained from a MARTA construction site at Mitchell Street in Atlanta. The soil was classified using standard ASTM procedures and laboratory testing as red micaceous clayey silt (ML) which was obtained from the upper zone of the Piedmont region. The grain size distribution of the soil is shown in Figure 13. The compaction curve for Standard Proctor is shown in Figure 14. The results of laboratory test are shown in Table 2. This soil was reused for construction of the soft layers in Test Series II and III.

The material which was used for construction of structural fills in Test Series II was also obtained from the same MARTA construction site. About four percent by weight of commercially available bentonite was added to the soil to increase its plasticity. Table 2 shows the relevant properties of the soil after mixing with bentonite. Using laboratory testing the soil was classified as micaceous sandy clay (CH). The grain size distribution is shown in Figure 13. The Standard Proctor compaction curve is shown in Figure 14.

Table 2. Soil Properties.

Soft Soil Layer

Micaceous clayey silt	
Plastic Limit (ASTM D424-59)	32
Liquid Limit (ASTM D423-66)	43
Plasticity Index (ASTM D424-59)	11
Unified Classification (ASTM D2487-75)	ML
Percent passing No. 200 Sieve (ASTM D422-63)	65
Maximum dry density (ASTM D698-70)	100 pcf
Optimum moisture content	20%

Fill

a. Sandy clay mixed with 4% Bentonite

Plastic Limit (ASTM D424-59)	33
Liquid Limit (ASTM D423-66)	58
Plasticity Index (ASTM D424-59)	25
Unified Classification (ASTM D2487-75)	CH
Percent passing No. 200 Sieve (ASTM D422-63)	67
Maximum dry density (ASTM D698-70)	102 pcf
Optimum moisture content	20%

b. Medium Sand

Maximum dry density (ASTM D2049-69)	103 pcf
Minimum dry density (ASTM D2049-69)	80 pcf
Void Ratio:	
Maximum	1.15
Minimum	0.63
Porosity:	
Maximum	53.5%
Minimum	36.5%

c. Crushed Stone

Maximum size	3/4"
Percent passing No. 200 Sieve	5
Bulk Specific Gravity	2.65
L. A. Abrasion	56%
Aggregate Description	Granitic Gneiss

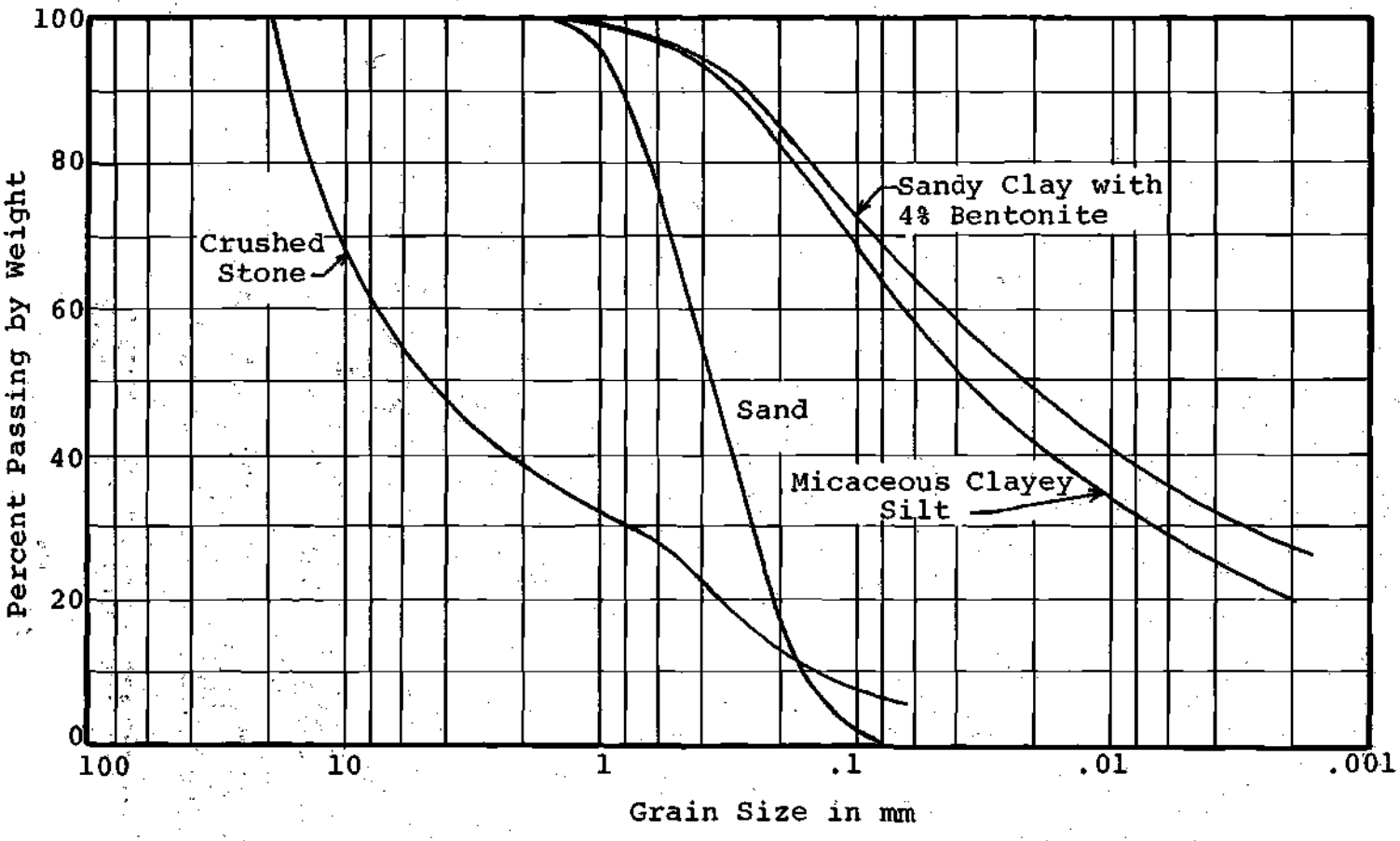

Figure 13. Grain Size Distribution Curves.

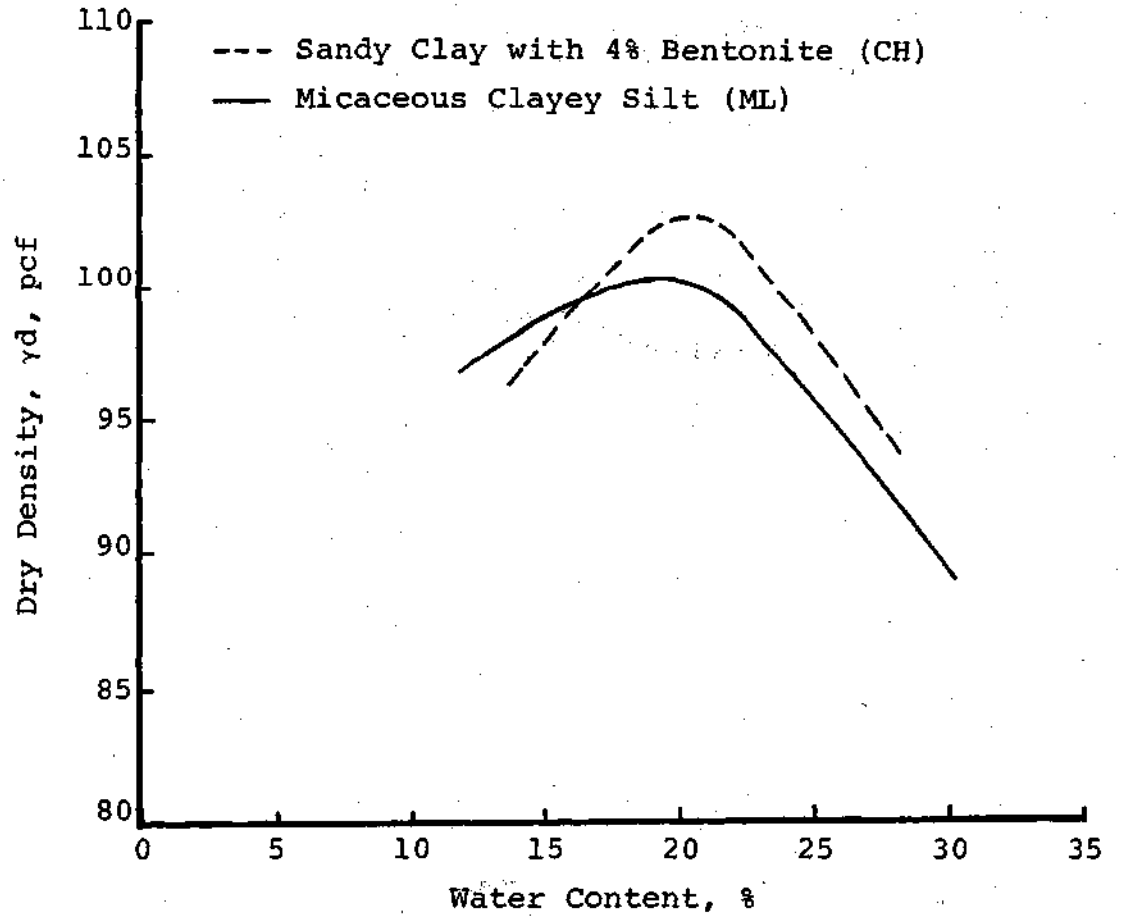

Figure 14. Standard Proctor Compaction Test Results for Micaceous Clayey Silt and Sandy Clay (ASTM D698-70).

A medium sand originating from the Chattahooche River near Atlanta was used for construction of the structural fills in Test Series III. This sand which was used in a previous research project [129] was stockpiled north of the test pit area. A grain size distribution curve of the sand is shown in Figure 13. The sand was composed primarily of subangular quartz particles with mica particles. The maximum and minimum dry densities of the sand as determined by standard procedures are shown in Table 2. These values agree with those found by Vesic [129].

The stone replacement footings were constructed using the crushed stone, known as crusher run, which was obtained from Vulcan Materials Company Quarry in Norcross, Georgia. The stone was sieved through 3/4 inch sieve to keep the maximum size within 3/4 inch. A grain size distribution curve is shown in Figure 13. The amount of fines was approximately 5 percent. Other properties of the stone are given in Table 2.

Test Series I - Homogeneous Layer

Construction

Since a soil layer of relatively low strength and high compressibility was desired to simulate the soft subsoil conditions often encountered in the field, preliminary tests which included consolidation and triaxial shear tests were performed on laboratory remolded samples to determine the deformation behavior and strength at different dry densities

and moisture contents. After several trials, it was decided that the soft soil layer to be constructed in the test pit should be compacted at a dry unit weight of 84 pcf using a moisture content of 31 to 32 percent. The corresponding degree of saturation was 84 percent. The soil used in the experiment should have as close as possible to uniform properties throughout the soil layer. The existing moisture content of the soil stockpiled in the bin north of the test pit area was between 15 to 17 percent. To bring the moisture content up to the desired value, the soil was blended in a 150 pound batch using a 300 pound capacity Lancaster mixer. The mixer uses scraping blades and a heavy roller to mix the soil in a circular steel container having a diameter of 2.5 feet and a height of 1 foot. Prior to adjusting the moisture of each batch, the existing moisture content of the soil was determined using a Speedy moisture tester which was calibrated for this type of soil using a standard oven procedure. After blending the moisture content of the soil from each batch was determined using the standard oven method. A total of 380 batches of soil were required to fill up the pit during soil compaction. Figure 15 shows the frequency distribution of moisture content determined from each batch. An average value of 31.4 percent was obtained for all the batches. During the mixing operation, any stones and organic materials were removed from the soil.

To obtain uniform density of the fill, soil construction

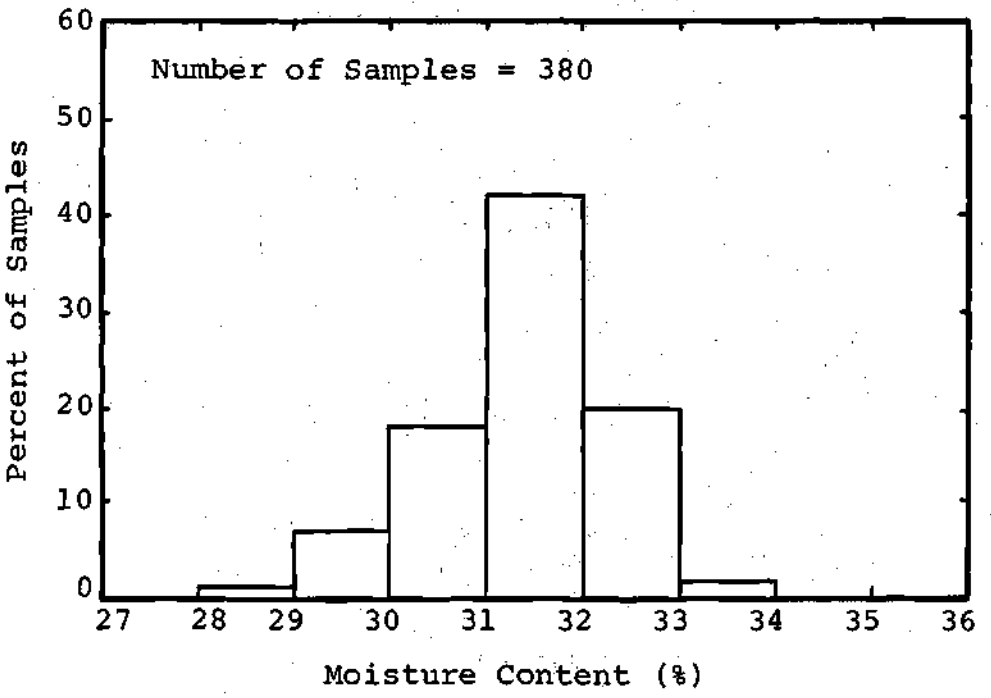

Figure 15. Results of Moisture Content Determinations on Homogeneous Layer Fill - Test Series I.

was done in layers of 4 inches compacted thickness. The soil was stockpiled and kept covered after blending until the amount was enough for one compacted lift. A wooden template was used to divide the test pit area into six equal squares. Each square was then filled with the processed soil which was weighed according to the predetermined amount. A concrete hopper and a 1,000 pound capacity overhead crane were used to transfer the soil from the stockpile area into the test pit. When every square was filled, the loose soil was leveled and the template removed. A small vibratory compactor (Jay Tamper, Model J-12) was used to compact the soil. This vibratory compactor employs a fourteen inch-square steel plate for compaction. The steel plate is actuated by an eccentric wheel powered by a small gasoline engine. During operation the fifty-pound weight of the machine rests on the steel vibrating plate or partially on two rubber wheels. Prior to compaction, the loose soil was initially densified by simply stepping in regular patterns around the test pit. It was found that only two complete passes of the vibratory compactor were required to obtain the required density. The surface of each compacted lift was scarified to insure continuity between layers. Subsequent layers were constructed following the same procedures.

To insure that the soil layers were compacted to the desired density, three to four in-place density tests were taken on every eight inches of compacted soil. The soil was

sampled using a four-inch diameter, thin-walled, steel tube having a volume of one-thirtieth of a cubic foot. The steel tube was first lubricated both inside and outside with silicone grease and gently pushed into the soil layer. Light tapping on the top of the tube with a hammer was required to completely fill the tube. The soil sample was weighed for immediate density determinations. In addition to the density tests, the compacted thickness of each layer was checked by measuring the depths before and after compaction from nylon strings tied to the wooden strips epoxied to the test pit walls. A nuclear soil density meter was also used to check the density, but the results were not consistent and its use was discontinued. It was possible that the unit might not have been working properly.

The results of soil density tests at different depths are shown in Figure 16. Variation of only ± 2 pcf from the desired unit weight of 110 pcf was observed. The fill was constructed to within six inches of the top of the pit. The soil surface was then covered with two polyethelene sheets to prevent moisture loss. A total of approximately seven weeks were required to complete the fill construction. Two more weeks were allowed for the compacted soil to settle under its own weight prior to commencing the footing load tests.

During construction of the soil layers, strain sensors and stress cells were installed according to predetermined

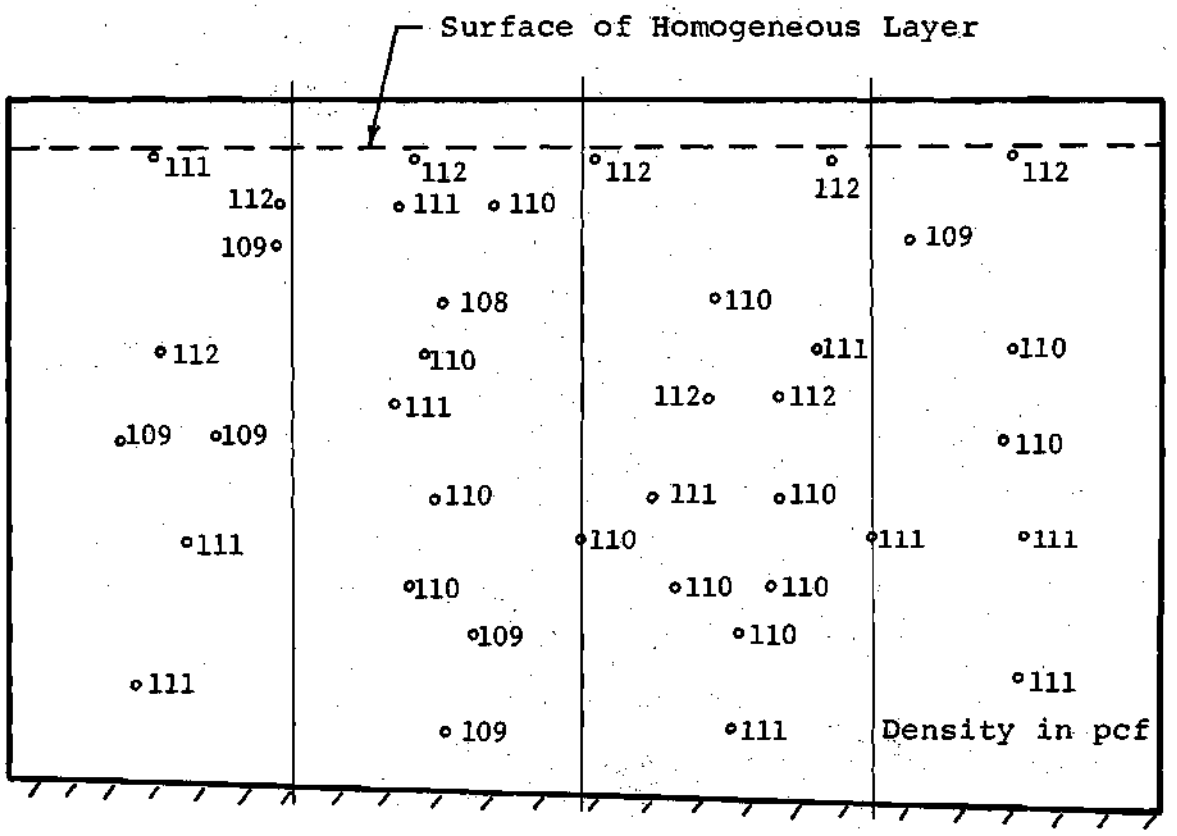

Figure 16. Cross-Section of Test Pit Showing Results of Density Tests on Homogeneous Fill Layer - Test Series I.

locations and depths following the procedures previously described in Chapter IV. All the strain sensors and stress cells were checked to see if they functioned properly prior to compacting the next layer.

Footing Load Tests

Three different footing load tests were performed in this test series. Figure 17 shows the test area and the sequence in which they were conducted. Test 1 was for the footing load test on a single-layer system. After this test was completed, Test 2 was then conducted and followed by Test 3, both of which were performed on stone replacements.

Test 1 was conducted at the center of the pit area. The area of the soil to receive the footing was initially leveled and smoothed and a thin layer of standard uniform Ottawa sand was spread over the surface to fill any small holes or voids that might exist between the bottom of the footing and the soil surface. The exact location of the footing was checked as the final step before starting the test. Since building foundation footings do not rest directly on the soil surface, the whole test pit area was backfilled with 6 inches of coarse sand to provide a surcharge of approximately 50 psf above the bottom of the footing.

The load system used for conducting the tests has been fully described in Chapter IV. Before applying the first load increment, all the instrumentation was checked to see if it was functioning correctly. The initial readings of all

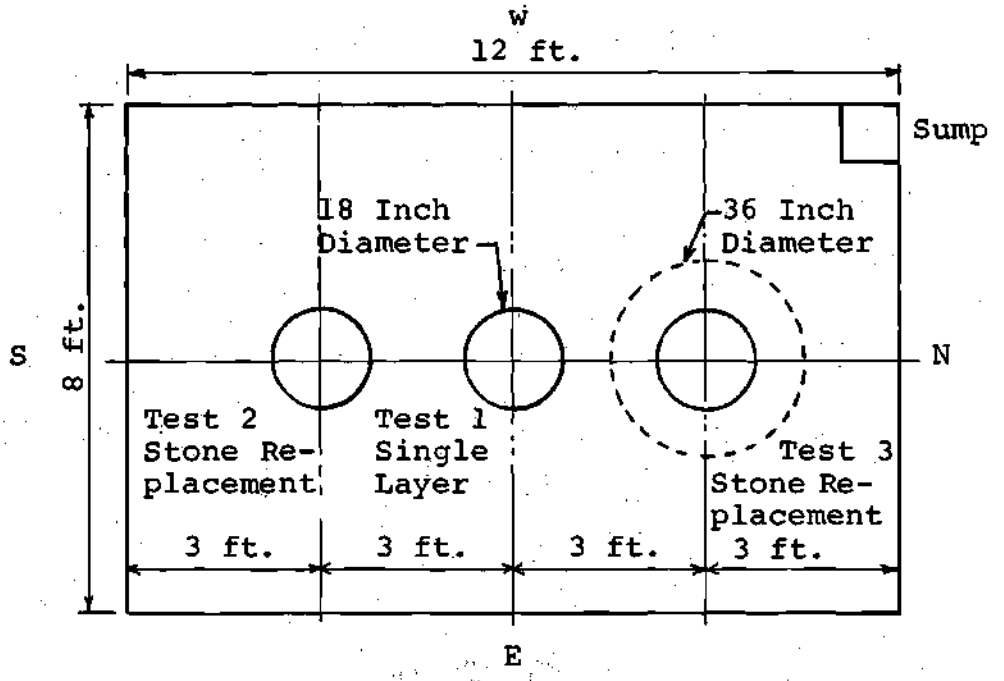

a) Plan of Test Pit

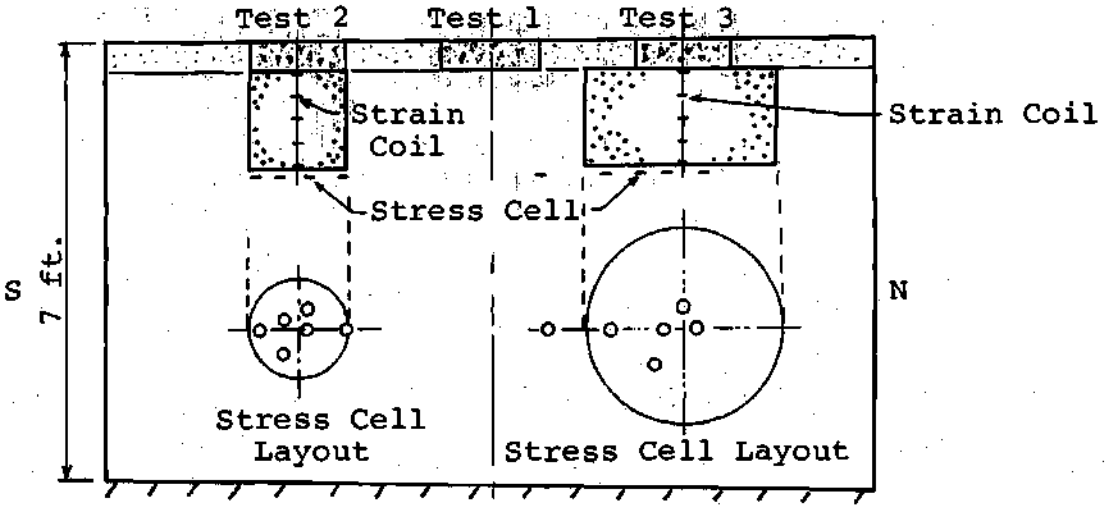

b) Cross-Section of Test Pit

Figure 17. Sequence of Footing Load Tests for Test Series I - Homogeneous Layer.

strain sensors were taken. The stress cells were all set initially to a common reading by adjusting the resistors on the switching and balancing boxes. The dial gages on the footing and on the soil surface were set to zero. Loads were applied in increments and the footing settlement versus time was recorded for each load increment. Since both immediate and consolidation settlements were desired, Taylor's square root method was used as a guide to determine the end of primary consolidation for each load increment. Because the soil was partially saturated, most of the settlement occurred immediately, and a period of two to three days was required for completion of the primary consolidation. The plot of settlement versus time for each load increment is shown in Figure 18. Approximately 80 to 85 percent of the total settlement occurred within a period of one to two hours.

Before the next load increment was added, final readings of the strain sensors were taken. Approximately one hour and a half was required to finish the readings. The readings of stress cells were first taken five minutes after applying the loads. Subsequent readings were made periodically with time to determine the effects of temperature variations and sustained loading. The air temperature was noted for each reading. All of the cell readings were rezeroed prior to adding the next load increment.

It was found that the stress cell readings were almost constant after applying the footing load for about two hours

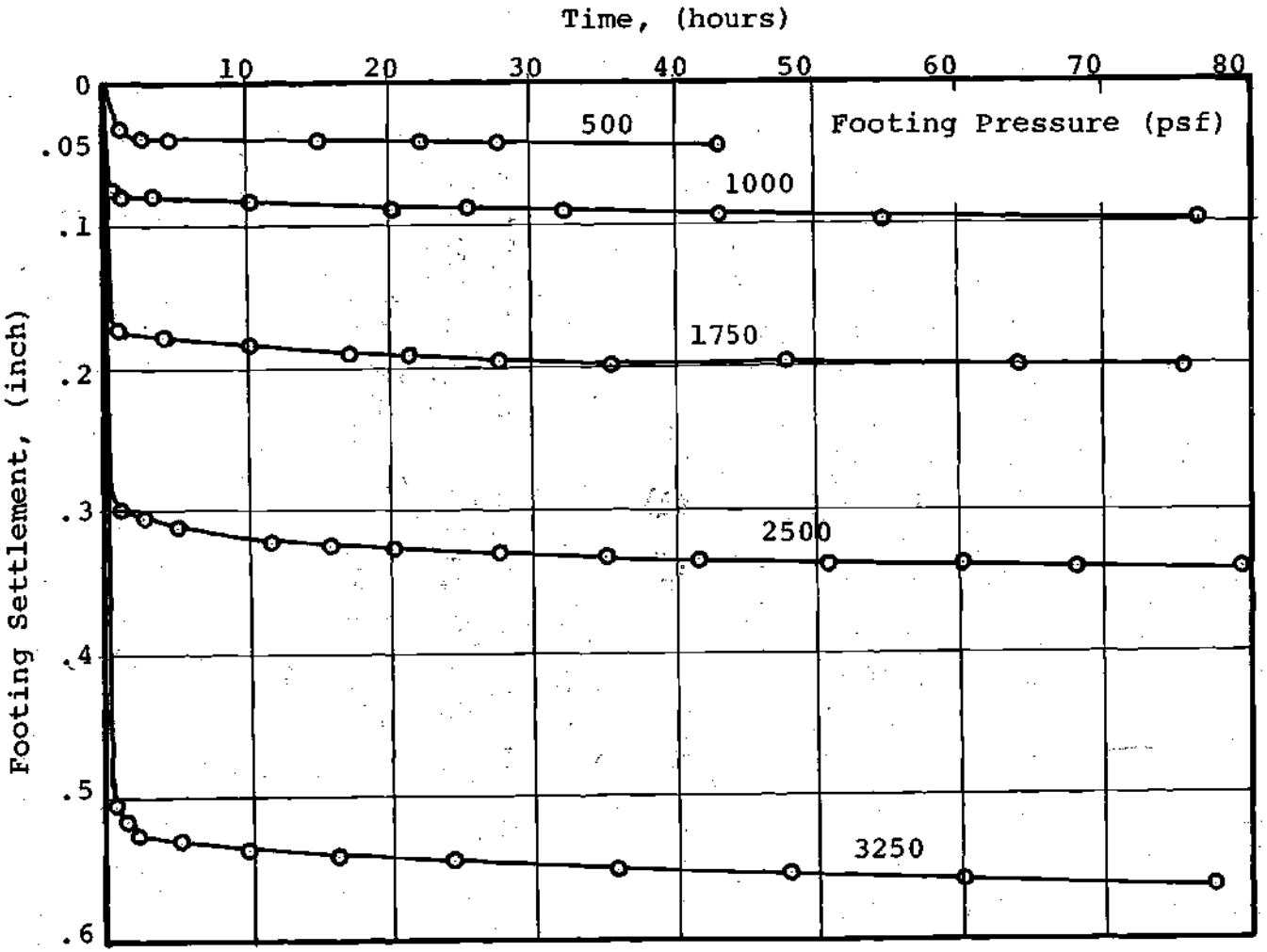

Figure 18. Footing Settlement vs. Time for Test Series I - Homogeneous Layer.

when the test pit temperature was relatively constant. A large fluctuation in temperature affected the performance of the balancing and switching units by changing the impedance in the units causing a decrease in reading with an increase in temperature. Because of the temperature effects, cell readings at two hours after applying the loads were used as measured stress values.

After completion of Test 1, Test 2 was conducted on a stone replacement footing having a diameter equal to that of the footing and a depth of 1D. The area for Test 2 indicated in Figure 17 was carefully cut to produce a circular hole 1D in diameter and 1D deep. Six stress cells were embedded at a depth of approximately 1/2 inch below the bottom of the hole. A thin layer of sand was spread in the bottom prior to backfilling the hole with crushed stone having a maximum size of 3/4 inch. To minimize soil-moisture migration, the stone was compacted at a moisture content of approximately 6 percent. Only slight tamping was performed during compaction to simulate the actual field condition in which a high degree of compaction cannot be obtained. The replacement footing was compacted in layers having a dry unit weight of 122 pcf. Strain sensors were placed along the center line axis inside the stone as shown in Figure 17b. A thin sand layer was spread over the stone footing's surface before placing the concrete footing. Load tests were conducted in increments in a similar manner to Test 1. Both immediate and

long-term settlements were measured.

In Test 3, the diameter of the stone replacement was increased to 2D with the depth kept constant at 1D. The instrumentation layout is shown in Figure 17b. The fill construction procedure closely followed that for Test 2. Stress cells and strain sensors readings were taken in the same manner as previously described.

Penetration Tests

After all three footing load tests were completed, standard penetration and static cone tests were conducted to evaluate the homogeneity of the fill. One soil test boring using the method specified by ASTM Specification D-1586-58T was made to obtain the standard penetration resistance of the soil. The test was conducted in the south-west corner of the test pit where the soil was relatively undisturbed from footing load tests. A trailer mounted Simco drill rig was used in testing. The split spoon sampler was initially seated six inches into the undisturbed fill and then driven an additional one foot using a 140 pound hammer falling thirty inches. The number of hammer blows required to penetrate the soil the last twelve inches was recorded and is designated as the "Standard Penetration Resistance." The results of the test boring at different depths are given in Figure 19. A penetration value of two blows per foot was obtained throughout the soil profile. Other test borings were made in three areas using a dynamic cone penetrometer

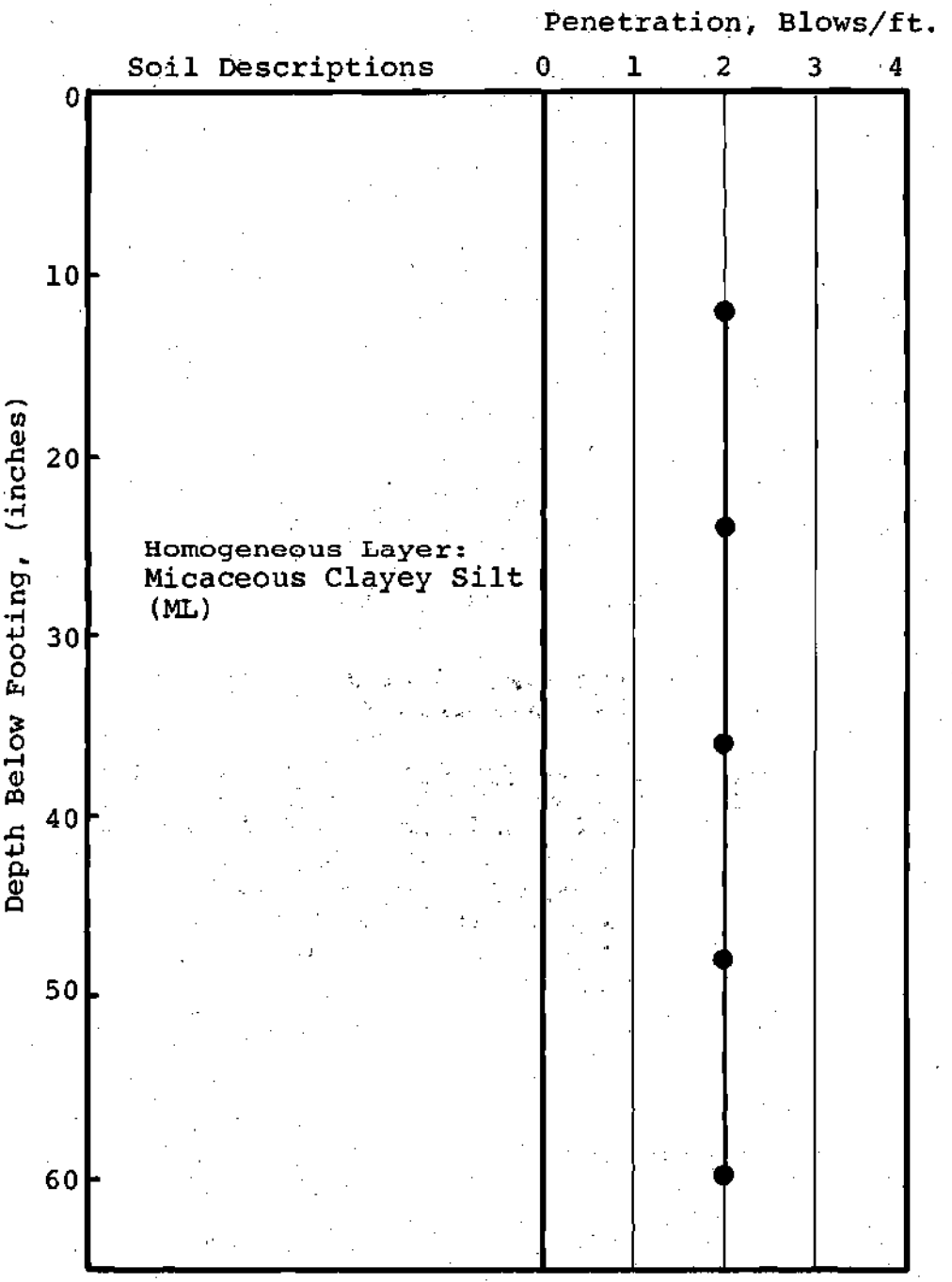

Figure 19. Results of Standard Penetration Test (ASTM D-1586-58T) - Test Series I.

[113]. The test was carried out by first augering to the test depth. The cone point was then seated two inches into the botoom of the hole. The cone point was further driven 1-3/4 inches using a 15 pound ring weight hammer falling 20 inches. The number of blows was then recorded. The test was carried out in intervals of 4.5 inches down to the bottom of the test pit.

The cone penetrometer was also used to check the consistency of the soil profile by first seating the cone point two inches at the test depth and then measuring the depth of penetration under two blows of the ring hammer. In this way, a greater detail of the soil consistency could be made with depths. The test results are shown in Figure 20.

A static cone penetrometer similar to a Dutch cone was developed for use in this study. The penetrometer was designed to measure both point resistance and skin friction. A load cell was developed to measure the loads applied to the rod. To perform static cone penetration tests, both the point and the friction sleeve were pushed down together to the desired depth of testing. The cone point was first advanced and the point resistance recorded using a Sanborn recorder. Next, the friction sleeve was pushed to complete the test. Tests were conducted in a 2.5 inch interval with depth using the hydraulic system of the Simco drill rig. The rate of penetration used was approximately 2 cm/sec. Four tests were performed in undisturbed areas along the west section of the

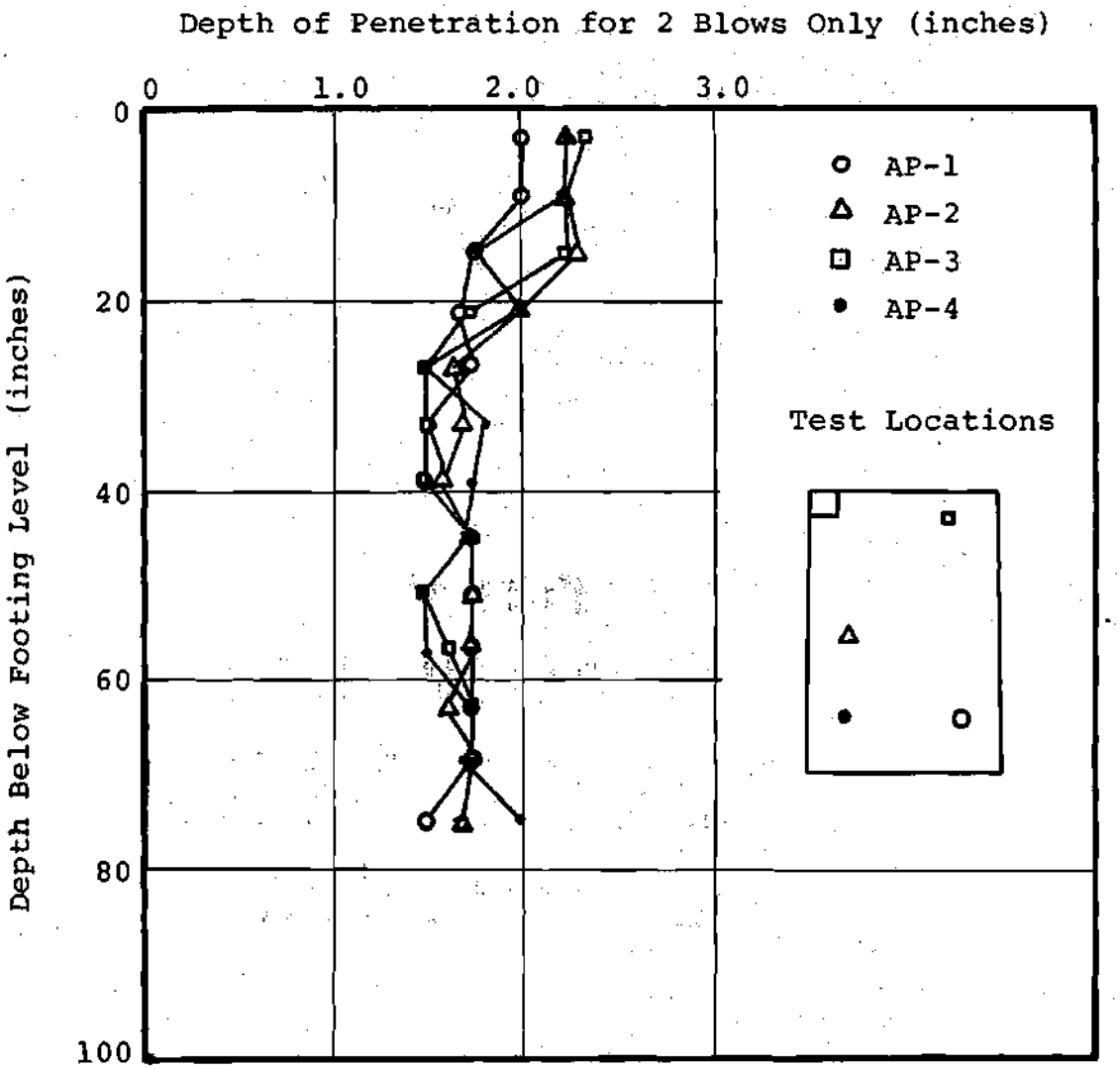

Figure 20. Results of Dynamic Cone Penetrometer Tests for Test Series I - Homogeneous Layer.

test pit. Average readings of the test results are shown in Figure 21. These results indicate that the consistency of the soil profile was relatively uniform except at a depth close to the footing level where the soil was slightly softer than that at greater depths. These static cone penetration tests show similar results to those obtained using the dynamic cone penetrometer (Figure 20).

A series of undisturbed samples of the homogeneous soil fill were taken for laboratory testing. The samples were secured by driving thin-walled Shelby tubes into the undisturbed soil using a portable drop hammer. Each fill soil sample, still encased in the tubing, was carefully removed from the test pit by digging around it, and sealed on each end with paraffin. The soil samples were kept in the moisture room for further testing in the laboratory.

Soil Excavation

After completion of Test Series I and the in situ testing, the soil was excavated from the test pit to a depth of five and one-half feet below the footing level. This soil was stockpiled in a temporary bin constructed next to the test pit. The exposed areas on top of the bin were covered with two layers of polyethelene sheets to prevent excessive moisture loss. During excavation, care was taken not to damage the strain sensors and stress cells. The recovered instrument was later inspected for possible damage and to see if they were still functioning properly.

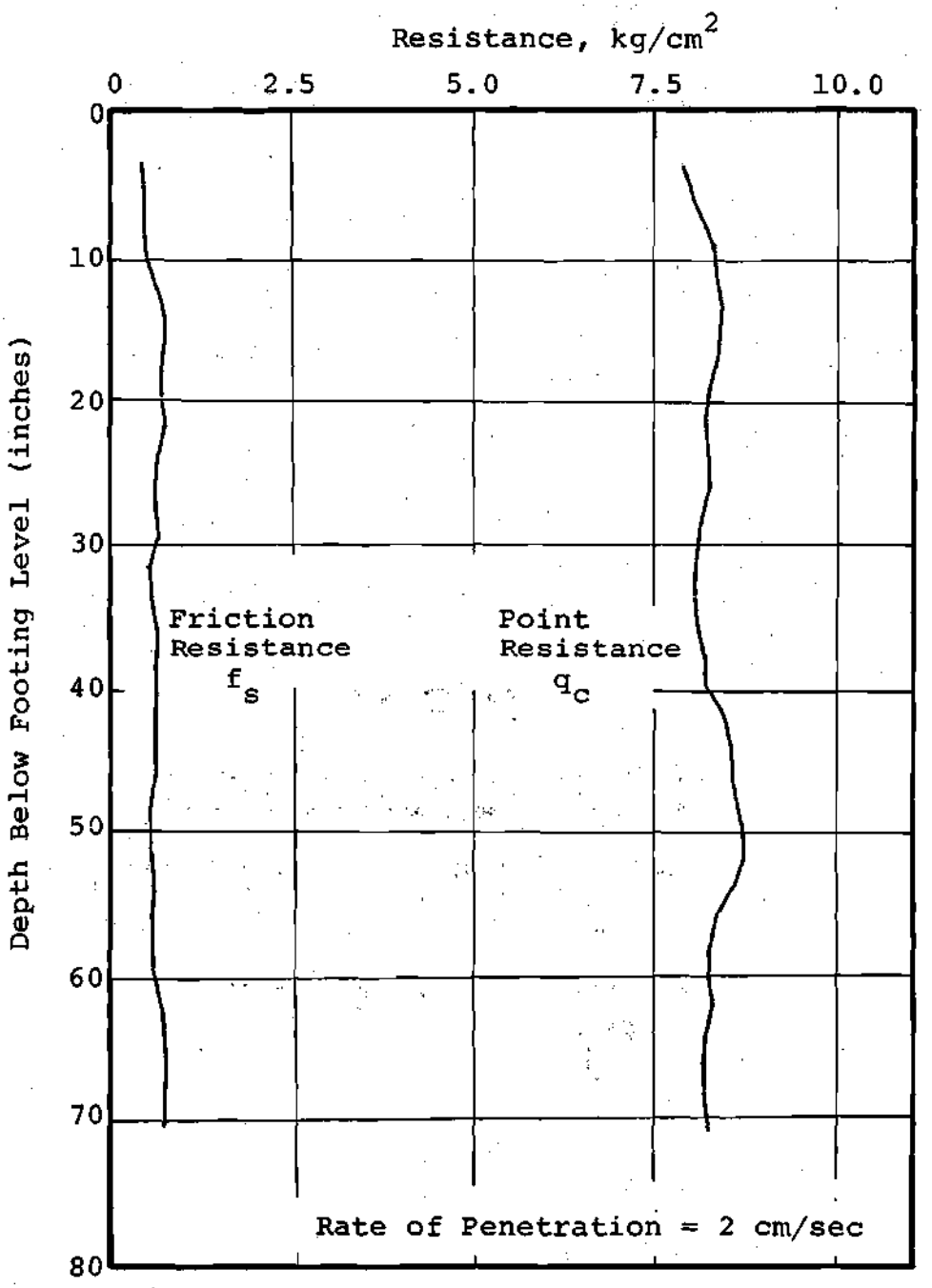

Figure 21. Results of Static Cone Penetration Test for Test Series I - Homogeneous Layer.

Test Series II - Clay Fill Over Soft Subsoil

Test Series II consisted of conducting three footing load tests on compacted sandy silty clay fill over the soft subsoil. The testing sequence and locations are shown in Figure 22.

Construction of Soft Layer

To obtain the same strength and compressibility properties as in Test Series I, the construction of the soft layer followed closely the procedure previously described for Test Series I. The soil stockpiled in the temporary bin was first blended using the soil mixer to breakup large lumps prior to compaction in the test pit. Each batch of soil was checked for possible moisture loss during stockpiling using the Speedy moisture tester, and more water was added if necessary. Soil density tests were also conducted to insure proper compaction and obtain the required density. Test results are given in Table 3. Variations of $\pm$2.5 pcf for density and $\pm$1.5 percent for moisture content were observed. The strain sensors and stress cells were installed as shown in Figures 6, 7, 8, 10, 11, and 12. The soft soil layer was constructed up to nine inches below the footing level of Test Series I.

Construction of Structural Fill

In this test series, compacted sandy clay was used as the fill layers. During processing of the soil through the mixer, commercially available bentonite was added to the

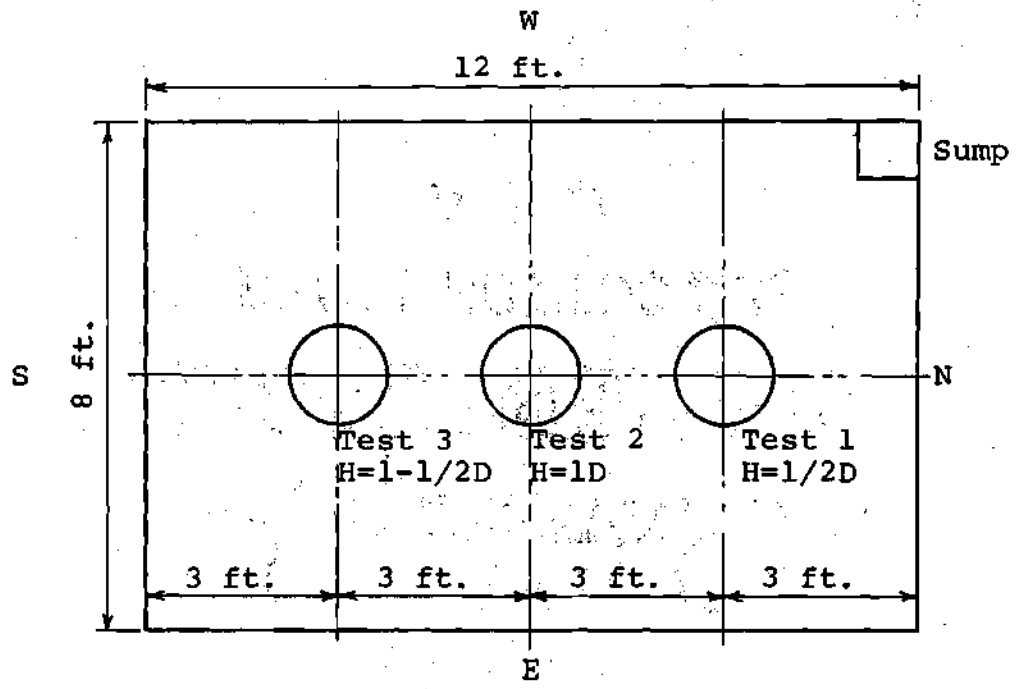

a) Plan of Test Pit for Test Series II and III

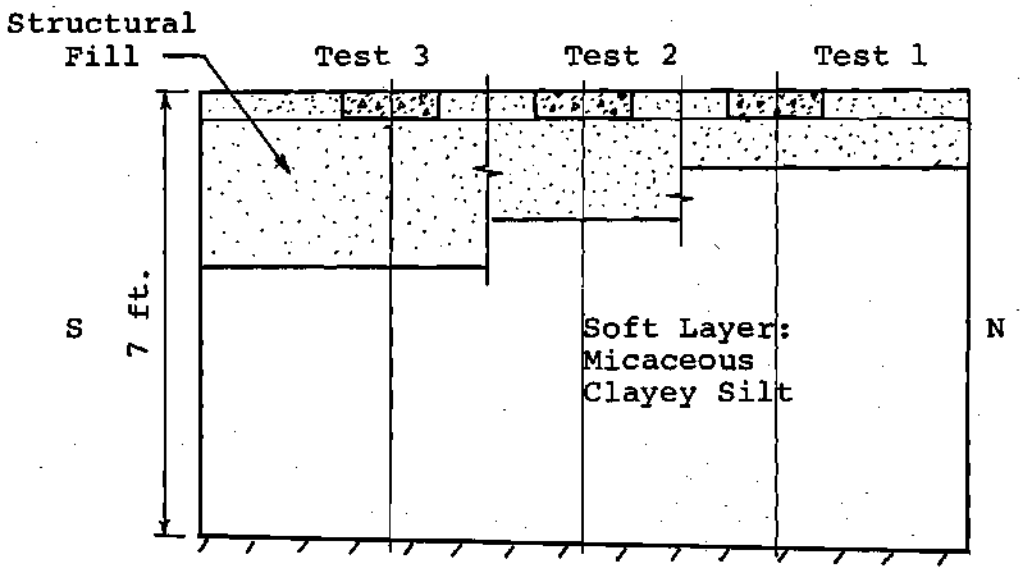

b) Cross-Section of Test Pit for Test Series II and III

Figure 22. Sequence of Footing Load Tests for Test Series II and III.

Table 3. Results of In-Place Density Tests of the Soft Layer - Test Series II.

Depth Below Footing Level (inches)	Density (pcf)	Moisture Content (%)
9	112.0	30.5
13	111.8	31.0
17	112.3	29.8
21	111.5	30.6
25	110.4	31.2
29	111.8	30.7
33	112.8	31.1
37	110.0	30.0
41	112.0	29.9
45	111.5	30.8
49	112.0	31.5
53	111.0	30.4
57	112.0	30.1
60	112.0	29.7
64	113.0	29.8

Table 4. Results of In-Place Density Tests of Compacted Sandy Clay - Test Series II.

Test No.	Depth Below Footing Level (inches)	Density (pcf)	Moisture Content (%)	Percent Compaction
Test 1 (H=1/2D)	0-4.5	122.0	22.0	97.0
	4.5-9	119.5	22.3	95.0
Test 2 (H=1D)	0-4.5	123.3	22.3	97.8
	4.5-9	123.0	22.2	97.0
	9-13.5	122.0	22.1	97.0
	13.5-18	119.5	22.0	95.0
Test 3 (H=1-1/2D)	0-5	122.0	22.0	97.0
	5-10	120.0	21.9	95.5
	10-15	120.5	22.2	95.6
	15-20	120.0	22.1	95.0
	20-25	119.0	21.8	94.8

mixer (4 percent by weight) in order to increase the plasticity of the soil. Soil layers having a three-inch final thickness were compacted to obtain a dry density equivalent to 95 percent of the standard proctor maximum dry density (ASTM-D698-70). The soil layers were compacted at a moisture content of approximately 22 percent or 2 percent higher than the optimum moisture content to reduce the effect of moisture migration from the soft layer. In place density tests as previously described were made to insure proper compaction. Typical test results are given in Table 4. A total of eight passes of the Jay-Tamper compactor was usually required. Because of the presence of the soft subgrade, adequate compaction could not be obtained for the first soil layer. Pumping action was observed in the first lift but disappeared in subsequent lifts. After the second layer no problems in compaction were encountered.

Test 1 was conducted on the structural fill having a fill thickness equal to one-half diameter of the footing. After the footing load test had been conducted, the whole pit area was overexcavated to a depth of 1D. A compacted layer having a thickness of 1D was constructed and Test 2 was carried out. When this test was completed, the pit area was again overexcavated to a depth of 1-1/2D and the stiff layer was constructed to the footing level where the thickness of the compacted fill equaled 1-1/2D. Test 3 was performed in this last section.

After each footing load test was performed, field tests were conducted using the portable cone penetrometer to obtain the consistency profile of the fill materials and the soft layer. The test results are given in Appendix E. The standard penetration and static cone penetration tests were not performed in this Test Series. Undisturbed samples of the structural fill and soft layer were taken using thin-walled Shelby tube. Three block samples were also cut from the fills which were immediately covered with paraffin and stored in the moisture room.

After all testing was completed, the softer layer was excavated to a depth of 5.5 feet below the footing level and stockpiled in the temporary bin. All stress cells and strain sensors were recovered and inspected for damage.

Test Series II - Sand Fill Over Soft Subsoil

Compacted sand was used as the structural fill in this Test Series. The sequence of construction followed that of Test Series II. The soft subsoil layer was constructed in the same manner used in Test Series II. The moisture content of the soil was checked throughout the blending process. The compaction was done in four-inch layers. In-place density tests were made periodically to insure that the required density was obtained. The results of density tests are given in Table 5. Variation of $\pm$2.5 pcf was obtained. The variation of moisture content was within $\pm$1.5 percent. The stress cells and strain sensors were installed during construction

Table 5. Results of In-Place Density Tests of the Soft Layer - Test Series III.

Depth Below Footing Level (inches)	Density (pcf)	Moisture Content (%)
9	110.0	30.5
13	111.5	31.0
17	110.0	30.6
21	112.0	30.5
25	111.0	30.8
29	112.0	30.5
33	112.5	31.0
37	111.0	31.8
41	112.0	31.0
45	111.5	30.5
49	112.0	32.2
53	112.5	30.5
57	111.5	30.1
60	112.0	31.5
64	112.5	30.7

Table 6. Results of In-Place Density Tests of Compacted Sand Using Sand Cone Method - Test Series III.

Test No.	Depth Below Footing Level (inches)	γ_d (pcf)	w (%)	D_r (%)
Test 1 (H=1/2D)	0-4.5	99.4	7.6	89
	4.5-9	97.2	10.3	78
Test 2 (H=1D)	0-4.5	99.5	6.8	88
	4.5-9	101.0	6.6	93
	9-13.5	100.0	7.5	90
	13.5-18	98.5	8.2	82
Test 3 (H=1-1/2D0	0-4.5	99.0	8.8	86
	4.5-9	99.5	9.3	88
	9-13.5	100.2	9.0	90
	13.5-18	100.7	7.4	90.5
	18-22.5	99.3	9.5	86
	22.5-27	97.5	11.0	80

using the same layouts for Test Series II. The construction of the soft soil layer was terminated at a depth equal to 1/2D below the footing level.

A medium sand obtained from the Chattahoochee River was compacted in four-inch layers up to the footing level as shown in Figure 22b. Difficulty similar to clay layers was also encountered in compacting the first layer to obtain the desired density. After the second layer, compaction progressed without difficulty. To minimize soil moisutre migration between layers, the sand was compacted wet having a moisture content of 7 to 8 percent rather than dry. The density of the sand was checked during compaction using sand cone method. The density test results for fills using different thicknesses are given in Table 6. An average relative density of 89 percent was obtained except near the bottom of the fill where the density was slightly lower. The sequence of the footing load tests was the same as that of Test Series II. The sand layers were compacted in the same manner including placing out the strain sensors and stress cells (Figures 6, 7, 8, 10, 11 and 12). Test 1 was conducted for a fill thickness of 1/2D, Test 2 for 1D and Test 3 for 1-1/2D. The footing load test procedure was the same as that previously described.

Stone Replacement Pads

After the completion of Test 1, the sand layer was removed from the testing area to expose the soft soil sur-

face. A crushed stone replacement pad was constructed having a diameter of 2D and a thickness of 1/2D. The stone was lightly compacted to a dry density of 122 pcf. The settlement of the footing as well as the stresses and strains in the soft layer beneath the stone pad were measured using stress cells and strain coils which remained in the soft layer. In addition, seven stress cells were placed in the soft layer approximately 1/2 inch below the interface.

After the first stone pad was completed, a second pad was constructed in the same excavation with the dry density being increased from 122 pcf to 129 pcf. Only vertical stresses were measured in this test.

Undisturbed samples of the soft subsoil were taken for laboratory testing. Since the sand was compacted moist, in-place samples could be taken by driving a 6-1/2-inch long Shelby tube into the sand layer. The triaxial shear tests were immediately performed on the extruded samples. Penetration resistance test was also conducted in both sand fills and soft soil layer for all three test sections. The results are given in Appendix E.

Laboratory Tests

Triaxial Shear Tests

The triaxial shear tests were performed for the purpose of determining shear strength parameters as well as the modulus of elasticity of the materials. The specimens were

trimmed from undisturbed sample of micaceous clayey silt and sandy clay. Both undisturbed and remolded laboratory samples of compacted sand were used. The specimens tested were 2.8 inches in diameter and approximately 6 inches high and were tested in drained conditions, using controlled strain loading. The consolidated-drained (CD) test was used to simulate the footing load test conditions. Because the long-term settlements of the footing were measured, the shearing of soil in the test pit occurred over a long period of time. Since the soil was partially saturated, any pore pressure build-up under applied footing loads would consist mostly of pore air pressure which would dissipate in a relatively short period of time. The specimens of micaceous clayey silt from the homogeneous layer in Test Series I and the soft layers of Test Series II and III were tested at a strain rate of 0.02 in/min. This strain rate was found to be sufficiently slow to allow the dissipation of pore air or pore water pressures which developed during the test. This strain rate was also used for the undisturbed specimens of sandy clay. For sand and crushed stone, a strain rate of 0.04 in/min. was used.

To determine the modulus of elasticity of the soil, cyclic compression tests were performed on all soil samples. The procedure involved first isotropically consolidating the soil specimens. The specimens were then loaded up to a deviator stress corresponding to approximately 25 to 30

percent of the stress that would be required to cause failure and then unloaded to zero stress level. Reloading was applied until the specimens failed or developed strains greater than 15 percent. Barksdale, et. al. [13] have shown that the effective reload modulus of undisturbed samples of micaceous sandy silt can be sufficiently defined by the slope of the stress-strain curve after only one cycle. Solderman and Kim [110] have shown similar results for a clay till. For sand, Lambe and Whitman [64] also suggest obtaining the modulus value from the stress-strain curve obtained from the second cycle of loading.

The soil specimens were tested in a triaxial chamber which had rotating loading piston to minimize the effect of friction load on the soil specimens. A Wykeham Farrance Model T57 Load Machine with rate of feed adjustable from 0.000025 to 0.3 in/min. was employed to load the test samples. A 500 pound capacity proving ring which was calibrated using the Tinius-Olson Testing Machine was mounted on the top of the load frame to monitor the applied loads. The axial deformations of the specimens were measured by a Soil Test gage (capable of measuring deformation to 0.001 inch) mounted on top of the triaxial chamber. The remolded samples of crushed stone which were 6 inches in diameter and 12 inches high and compacted in a steel mold of the same size were tested in a large triaxial chamber designed for testing pavement aggregates [115]. The 20 ton capacity Tinius Olsen Testing

Machine was used to load the specimens and the deformation was measured using a Soil Test dial gage.

The results of triaxial shear tests are shown in Figure 23 through 32. The stress-strain curves shown were plotted from the second cycle of loading.

Figure 23 shows the test results of consolidated-drained tests of soil samples obtained from the soft layer of each test series. The stress strain characteristics of each sample are nearly the same even though some small variations do occur. These test results indicate that strength of the soft layer of all three test series were almost the same as they were recompacted. The results of field tests using a portable penetrometer (Appendix E) also indicate comparable subgrade strength as intended during construction of the soft subgrade. Since the stress-strain curves do not indicate a definite peak of failure but gradually increase with increasing strains as the samples failed by bulging in the middle, the average deviator stresses at 5 per cent strains for each confining pressure were used to plot the Mohr envelope in Figure 24. The envelope is slightly curved with low strength at unconfined compression tests and indicates both friction and cohesion for micaceous clayey silt.

The results of the triaxial shear tests on undisturbed samples of sandy clay obtained from Test Series II are given in Figures 25 and 26. The stress-strain curves of the test

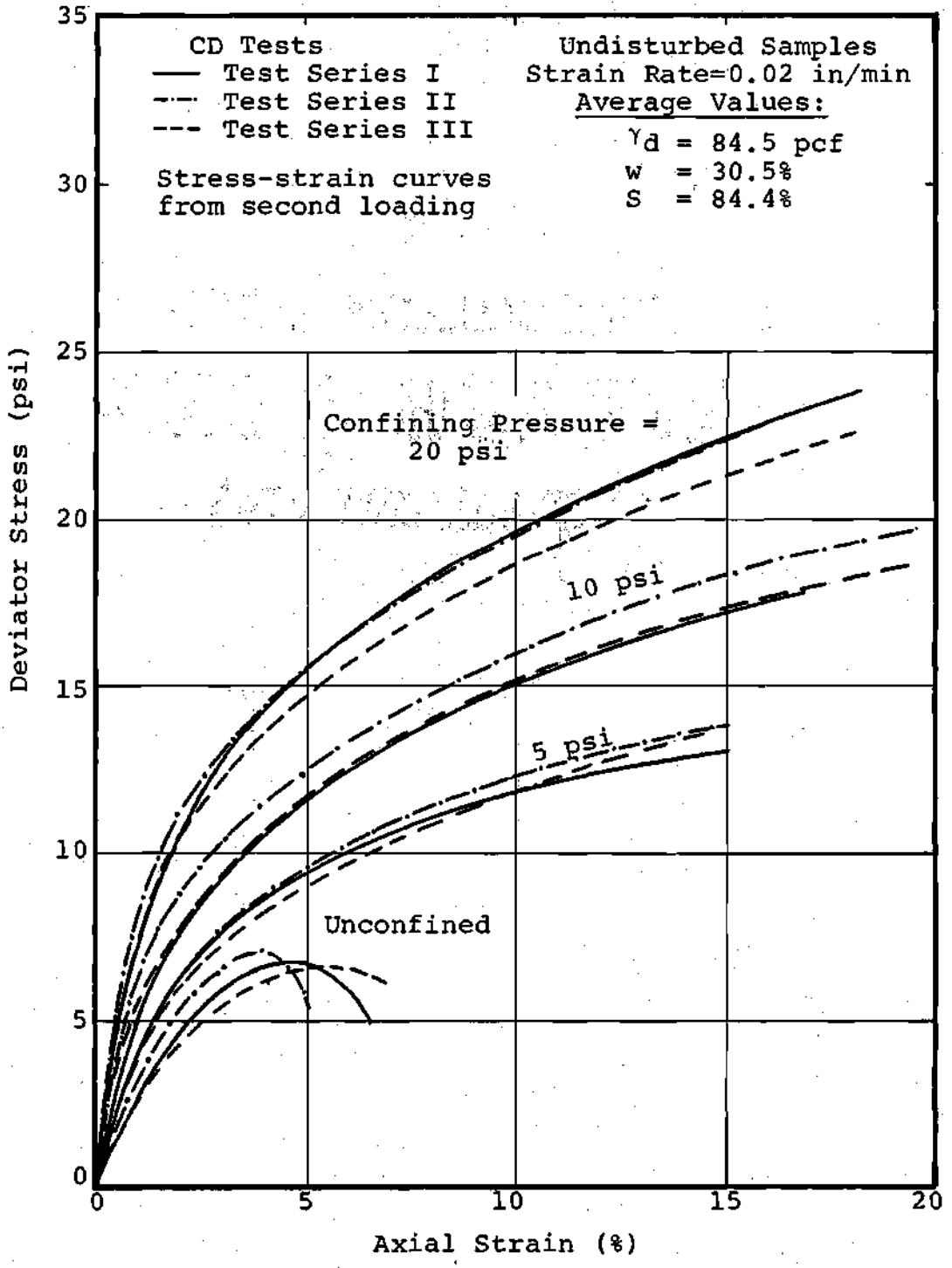

Figure 23. Triaxial Test Results of Micaceous Clayey Silt From Test Series I, II and III Soft Layers.

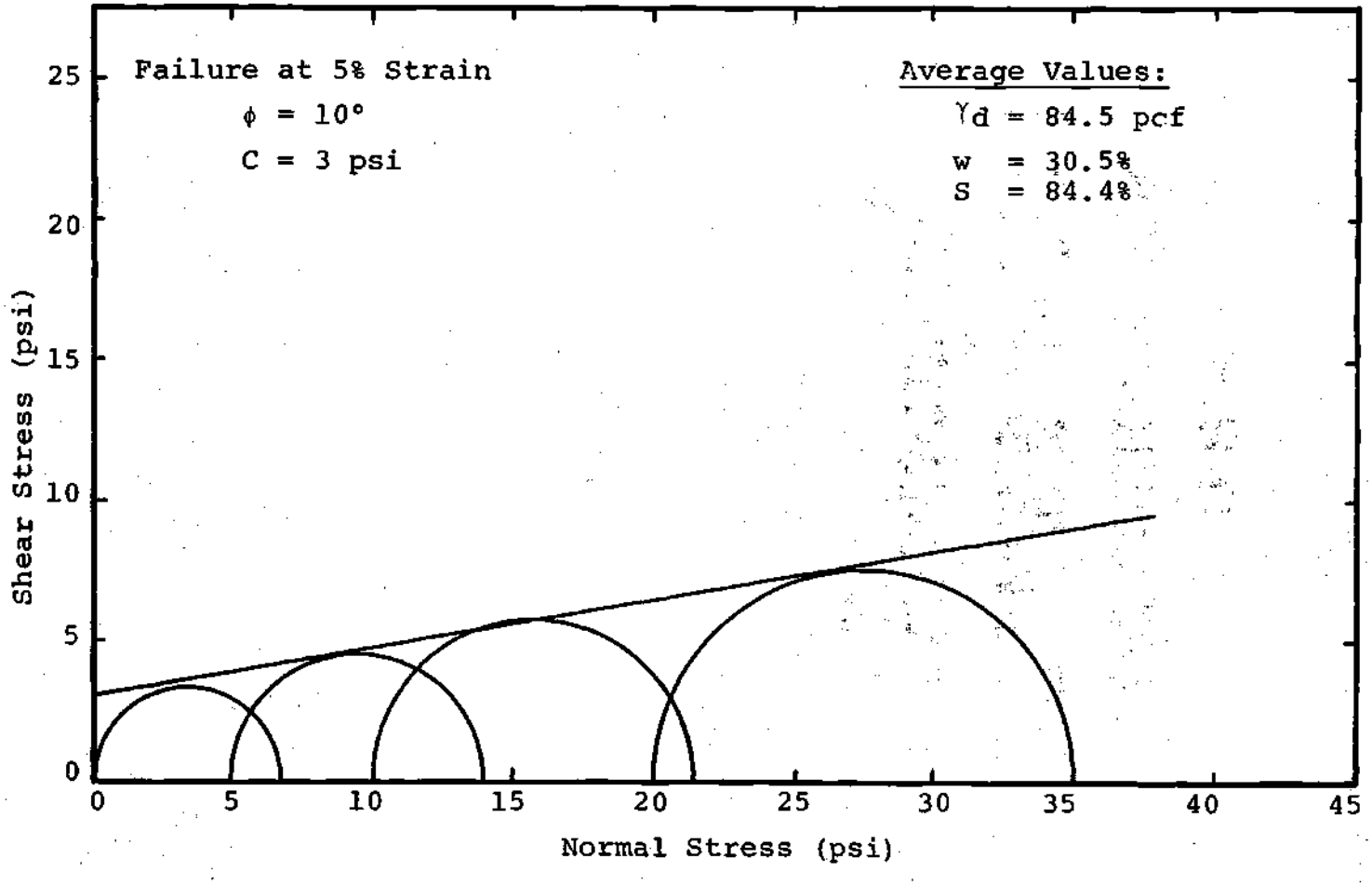

Figure 24. Average Mohr Envelope for Micaceous Clayey Silt from Soft Layers of Test Series I, II, and III.

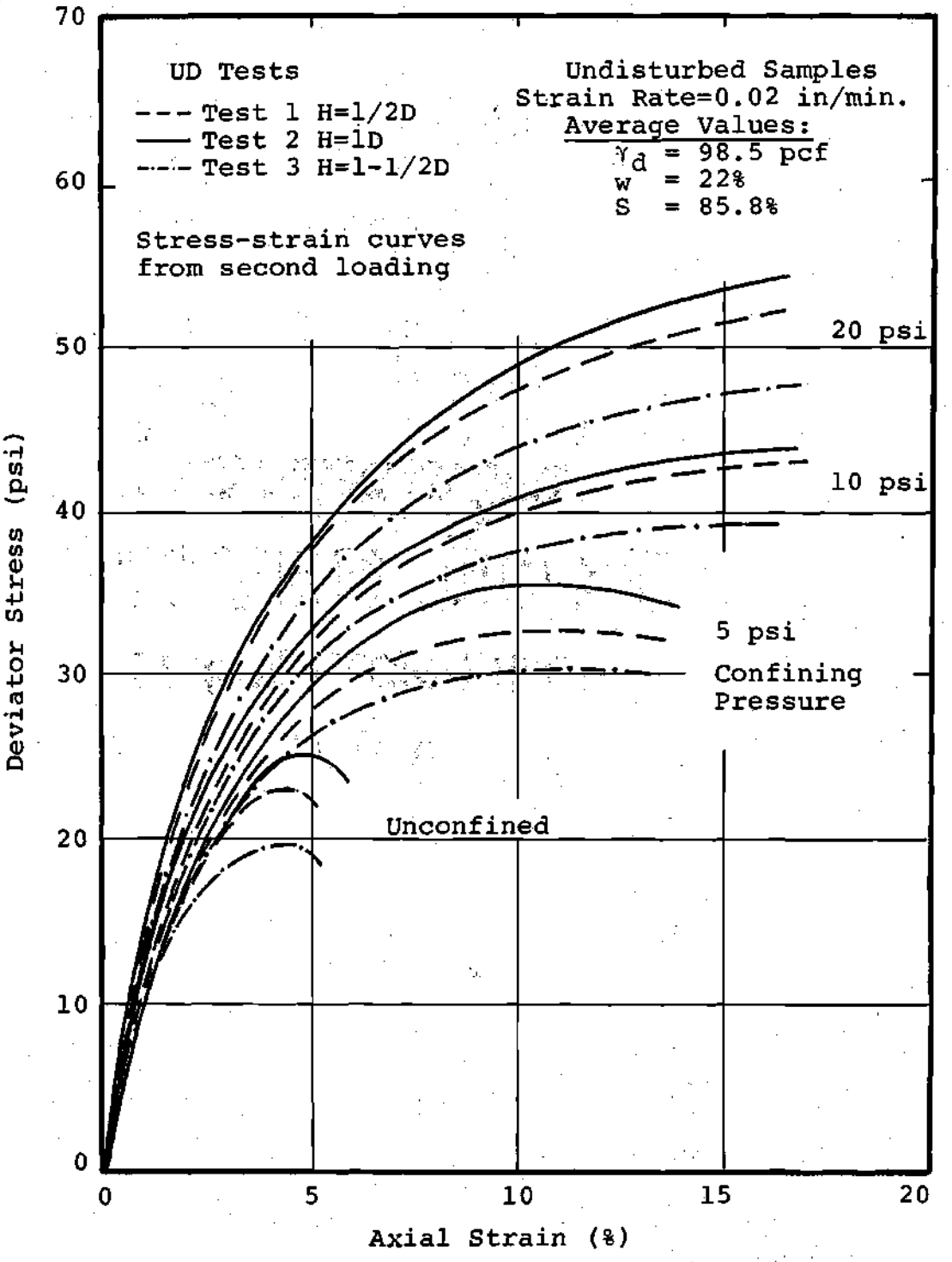

Figure 25. Triaxial Test Results of Compacted Sandy Clay from Test Series I.

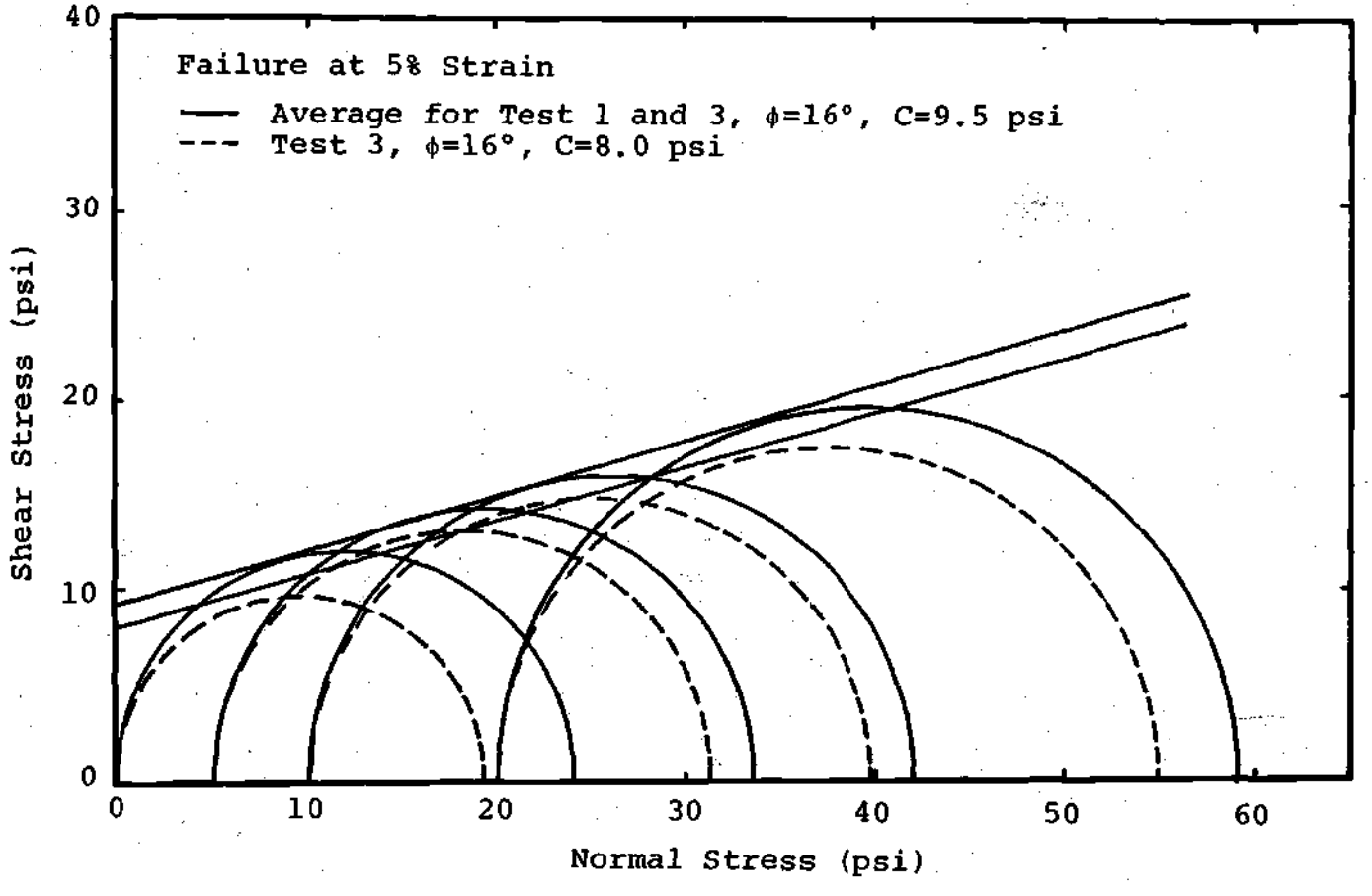

Figure 26. Mohr Envelopes for Compacted Sandy Clay.

samples from all three test sections show comparable peak strength at the same confining pressures except for the samples from Test 3 which exhibit slightly lower strength than those from Test 1 and Test 2 (Figure 25). This drop of peak strength could be attributed to the nonuniform density of the soil samples. The Mohr envelope which also uses the strength at 5 percent strain is shown in Figure 26, indicating considerable cohesion for sandy clay.

The stress-strain curves for medium sand using both remolded laboratory samples and undisturbed samples recovered from the test pit are shown in Figure 27. The Mohr envelopes for both laboratory and test pit samples are shown in Figure 28. The shear strength parameter ϕ of sand was comparable to that given by Vesic [129] for the same relative density.

Triaxial shear tests on crushed stone were conducted on laboratory compacted specimens. Two different dry densities were used to represent the conditions in which the stone was lightly and highly compacted. The stress-strain curves and Mohr envelopes for both conditions are presented in Figures 29 and 30. Both sand and crushed stone Mohr envelopes exhibit no cohesion but significant friction.

Modulus of Elasticity. The stress distribution within a uniform, homogeneous soil mass, according to Boussinesq theory, is not dependent upon the modulus of elasticity of the soil. Analysis of the stress distribution within the

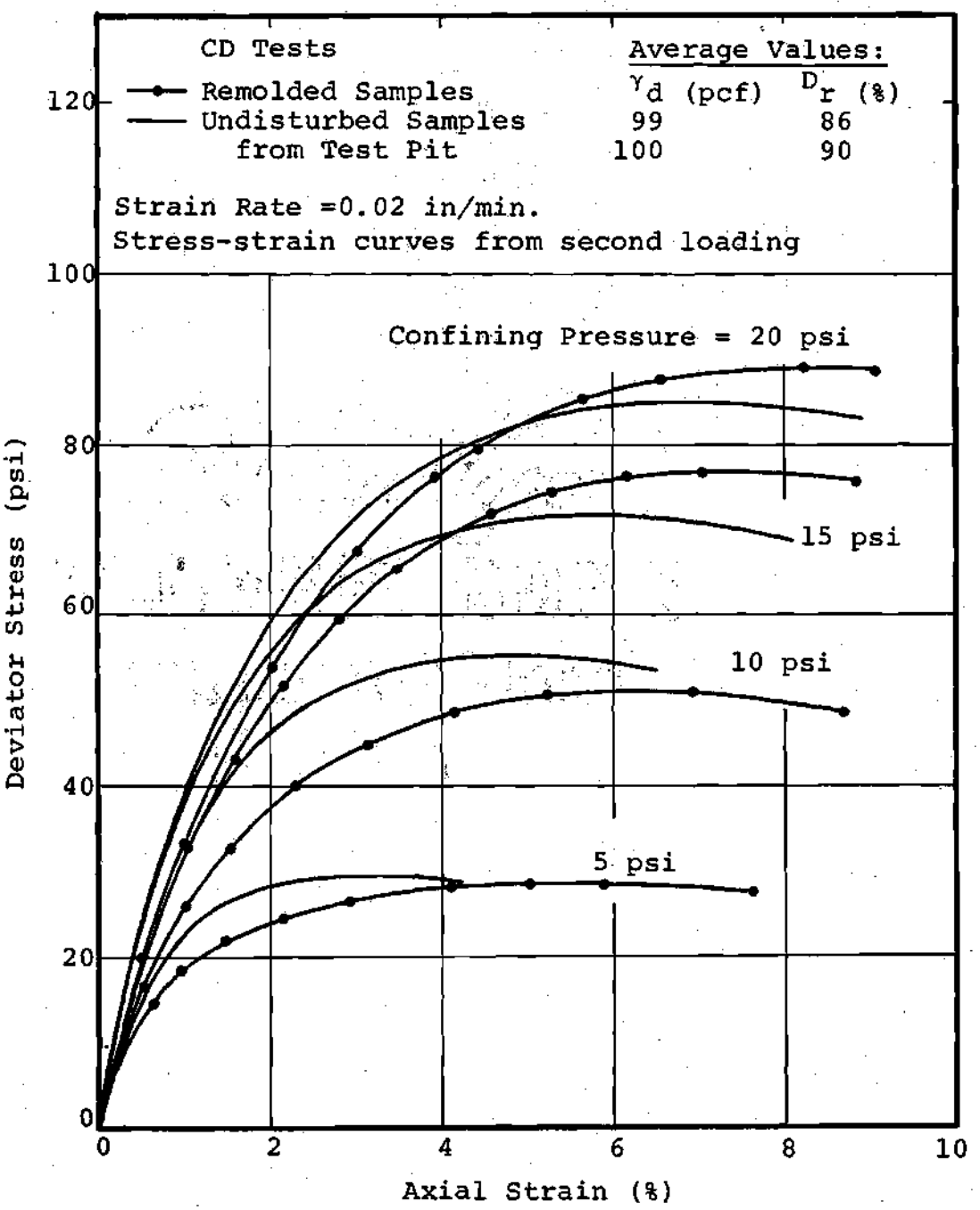

Figure 27. Triaxial Test Results of Compacted Sand From Test Series III.

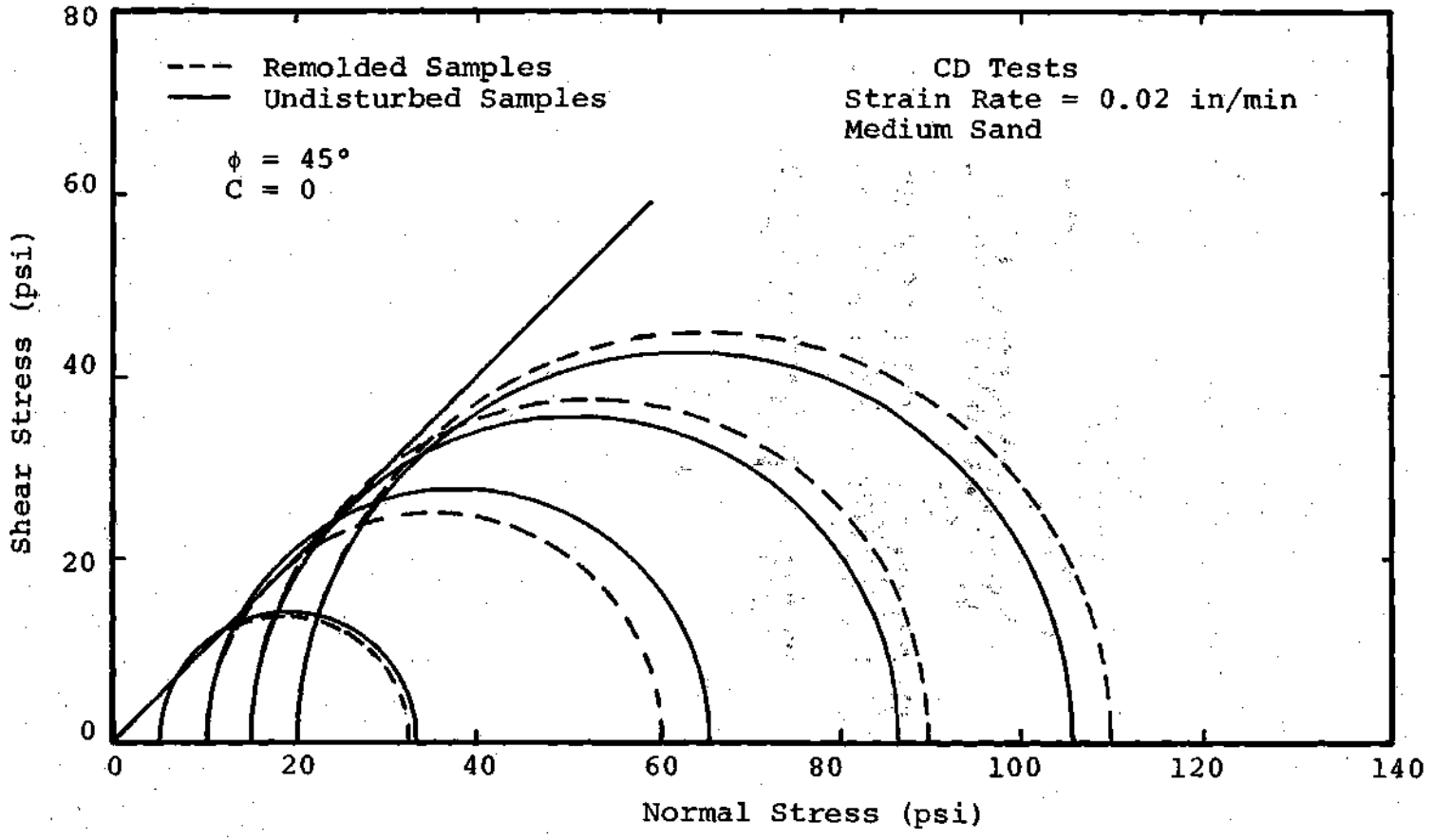

Figure 28. Mohr Envelopes for Compacted Sand, Test Series III.

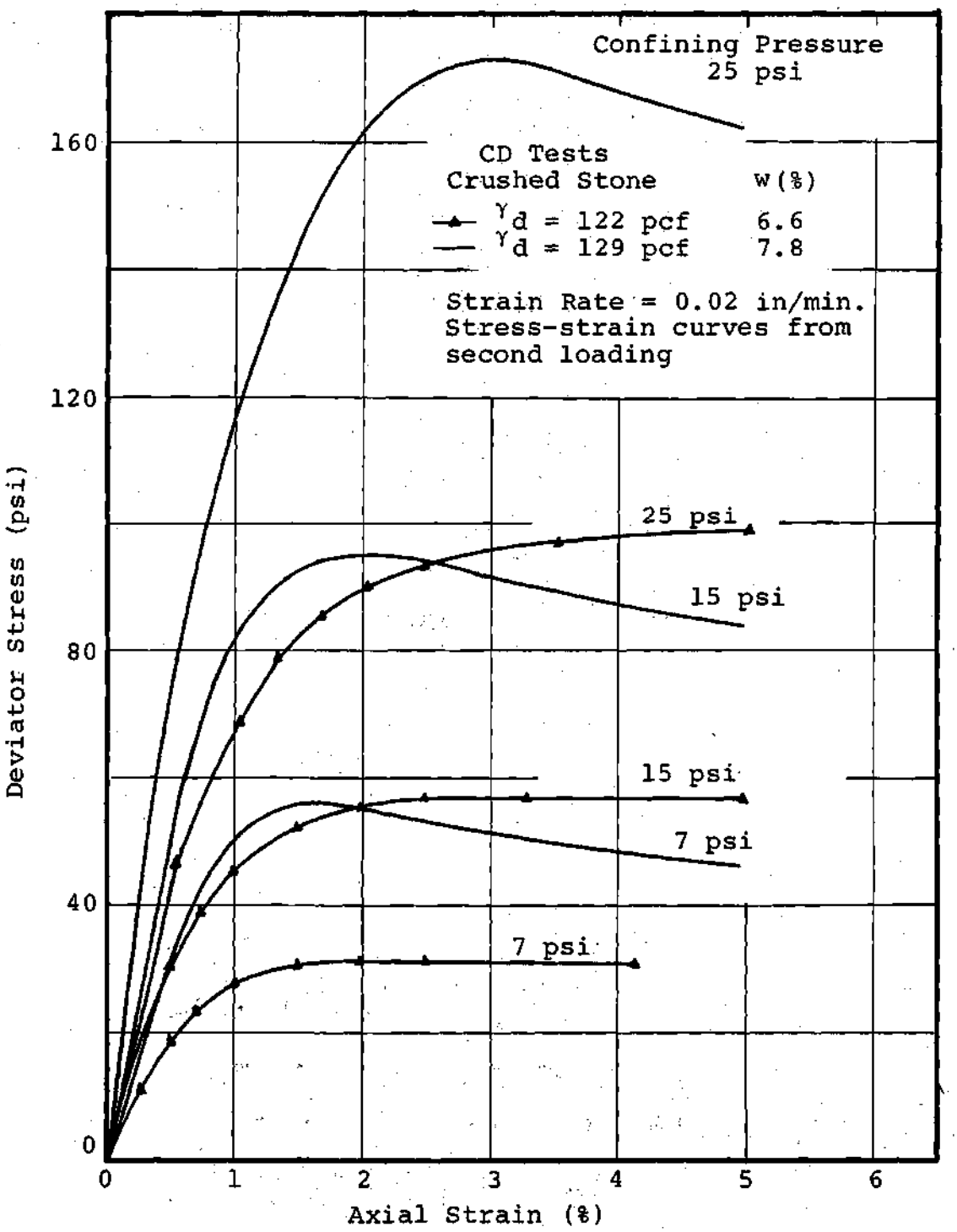

Figure 29. Triaxial Test Results of Compacted Crushed Stone at Two Dry Densities.

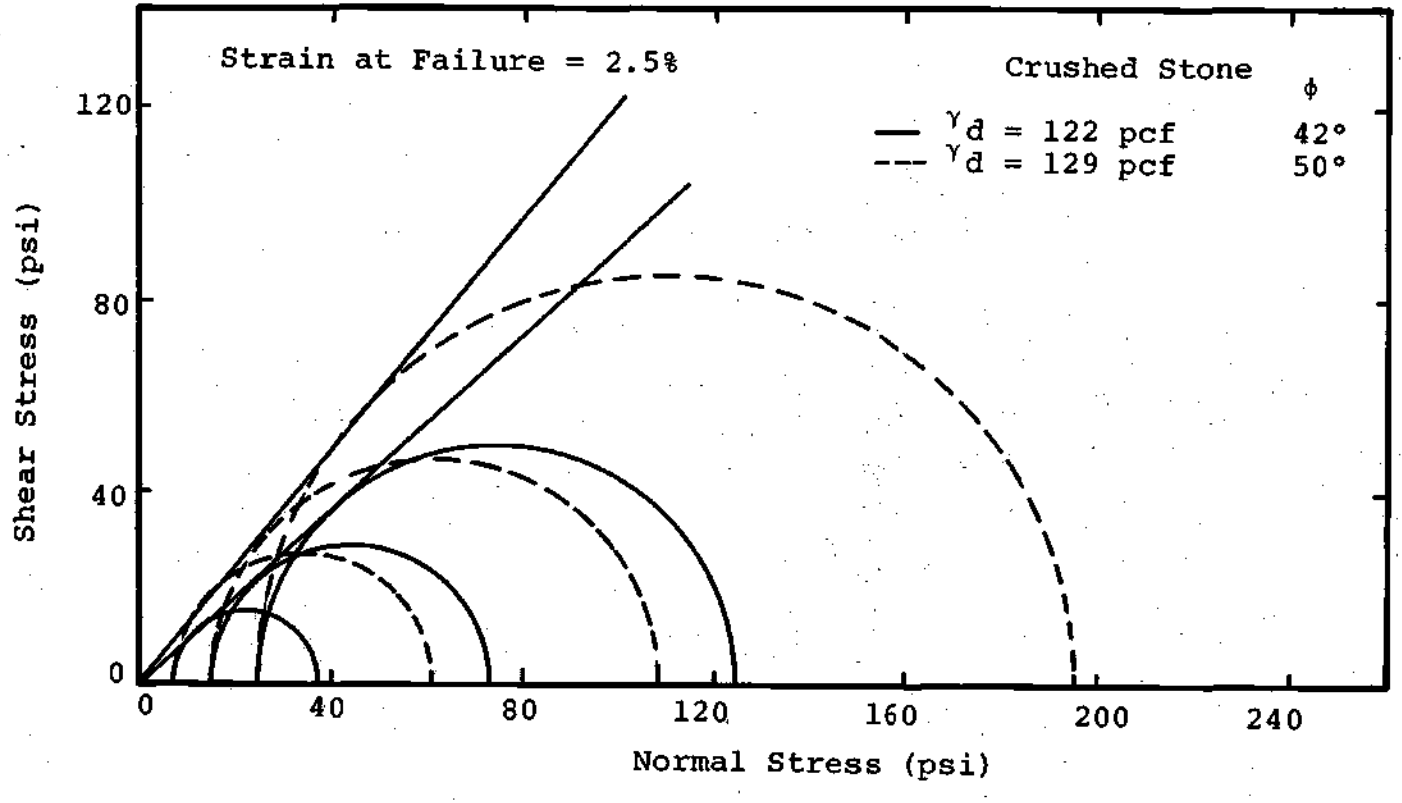

Figure 30. Mohr Envelopes for Crushed Stone.

fill-subsoil system according to the two-layer theory, however, requires a knowledge of the moduli of the fill and subsoil, which are usually assumed to be constant for each layer. The plots of the stress-strain characteristics of the materials used indicate that the material properties are far from being linear and strongly dependent on confining pressure.

Plots of the initial tangent moduli versus confining pressures are given in Figure 31. All the curves show an increase in the modulus with increasing confining pressure.

The curves indicated for sand and crushed stone show essentially continuing linear increase with confining pressure. This linear relationship can be represented by an equation:

$$E = K \sigma_3^n$$

where E = modulus of elasticity

σ_3 = confining pressure

K, n = constants to be evaluated.

For compacted sandy clay the modulus E increases slightly for the range of confining pressures tested. This is expected because the modulus of sandy clay which has been well compacted is not strongly influenced by confining pressure. The curve marked for micaceous clayey silt exhibits a moderate increase in E with confining pressure in a linear fashion. Since the micaceous clayey silt was lightly compacted in the test pit, the application of confining pressure during consoli-

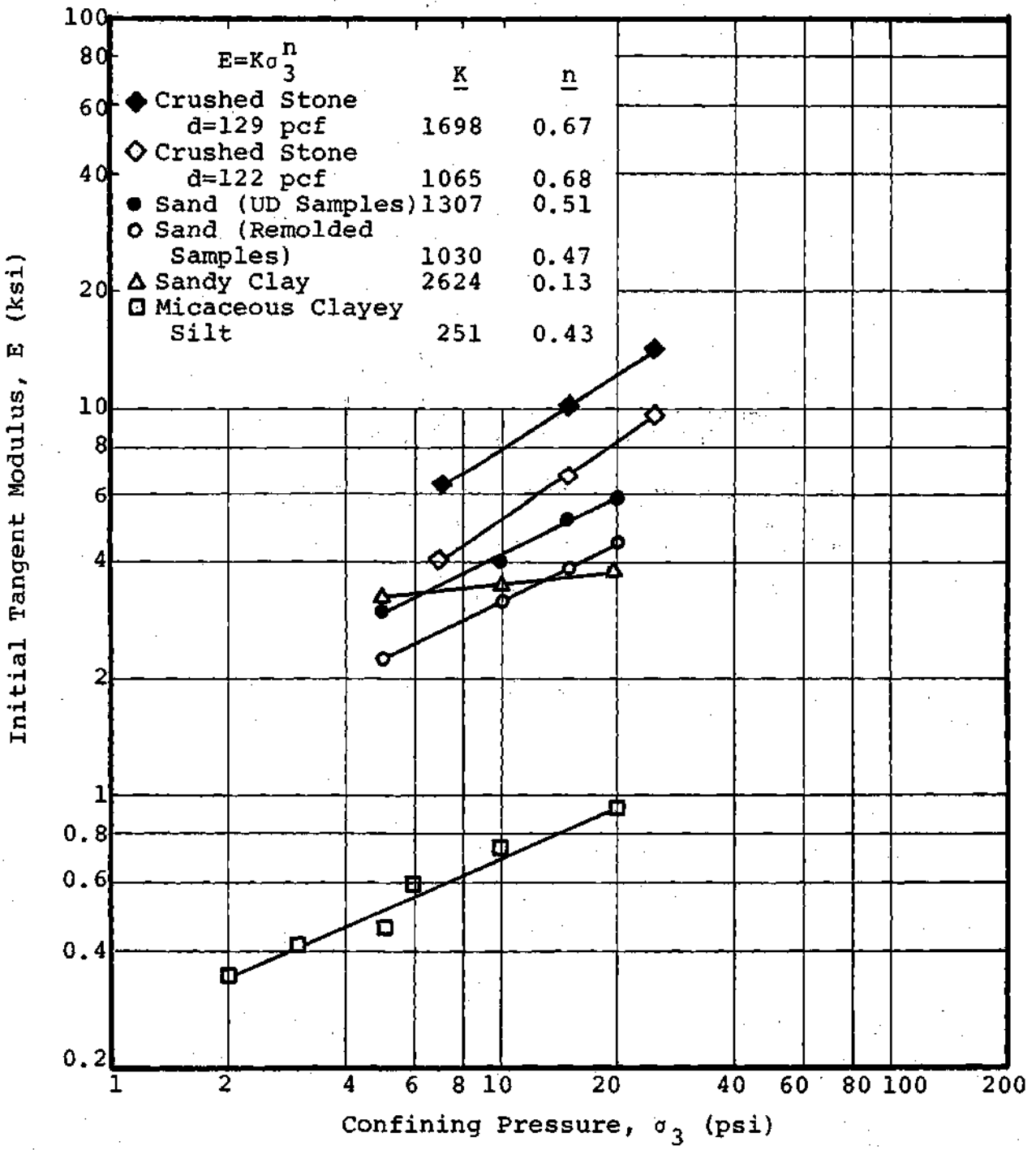

Figure 31. Initial Tangent Modulus as a Function of Confining Pressure.

dation process increases the strength of the soil resulting in an increase in E.

Figure 32 shows the ratio of the initial tangent modulus of elasticity of the subsoil to those of the fill materials. For sand, the modular ratio varies from 6 to 7 while for sandy clay, the ratio decreases from 8 to about 4 as the confining pressure increases. The modular ratio of crushed stone increases rapidly with increasing confining pressure up to a value of 14.5.

Consolidation Tests

Standard consolidation tests were performed on undisturbed samples of micaceous clayey silt obtained from the soft layers of Test Series I, II, and III and on sandy clay from the stiff layers of Test Series II. The test were performed in general as outlined in Lambe [61]. The device was a fixed ring type fabricated at the shop of the School of Civil Engineering. It was similar to commercial lever-type consolidometers. A 2.375 inch diameter by 1.1 inch high stainless steel test ring was used in the tests. Since a maximum total stress of 16 ksf was employed, the deflection of the system under load was checked by loading in increments without a soil specimen. The deflection of the system under loads was used to correct the consolidation test data. A standard load increment ratio of 1 was used. Loading was done as soon as primary consolidation for the previous increment was 100 percent completed, based on Taylor's square root

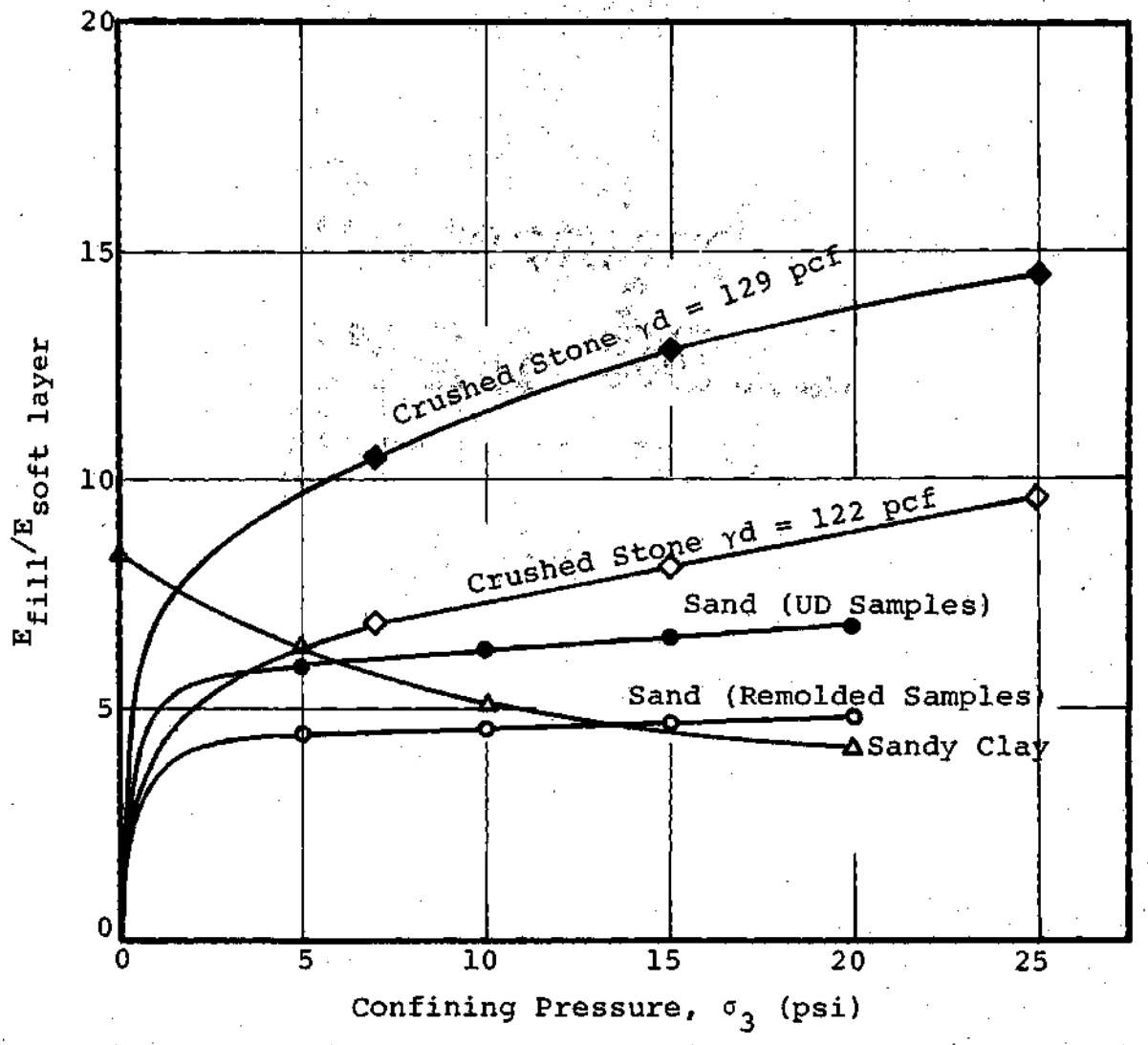

Figure 32. Modular Ratio of Stiff to Soft Layers as a Function of Confining Pressure.

of time method of determining time for completion of 90 percent consolidation.

The test results are presented in Figures 33 and 34. The consolidation test results for micaceous clay silt are shown in Figure 33. Each curve was constructed using the average data obtained from three or more consolidation tests conducted on separate undisturbed samples from the same test series. Strain-log p rather than e-log p curves were plotted as recommended by Brumund, et. al. [27] so that the compressibility characteristics of the soft subsoil from each test series could be compared even though the initial void ratio might be different. The ε_v-log p curves of compacted sandy clay from Test Series III are shown in Figure 34. Each curve represents an average data from at least two consolidation tests.

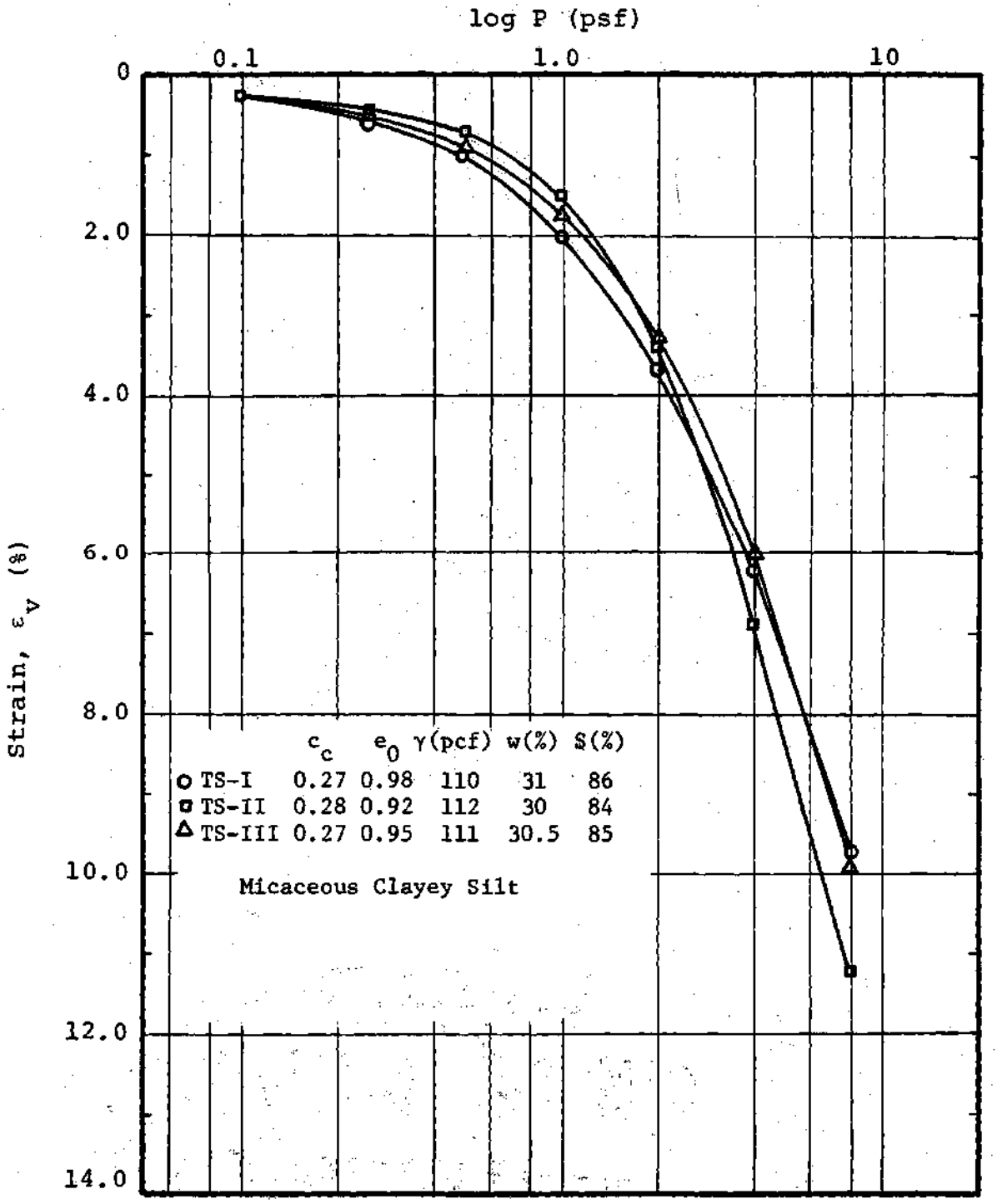

Figure 33. Consolidation Test Results of Micaceous Clayey Silt from Soft Soil Layers of Test Series I, II, and III.

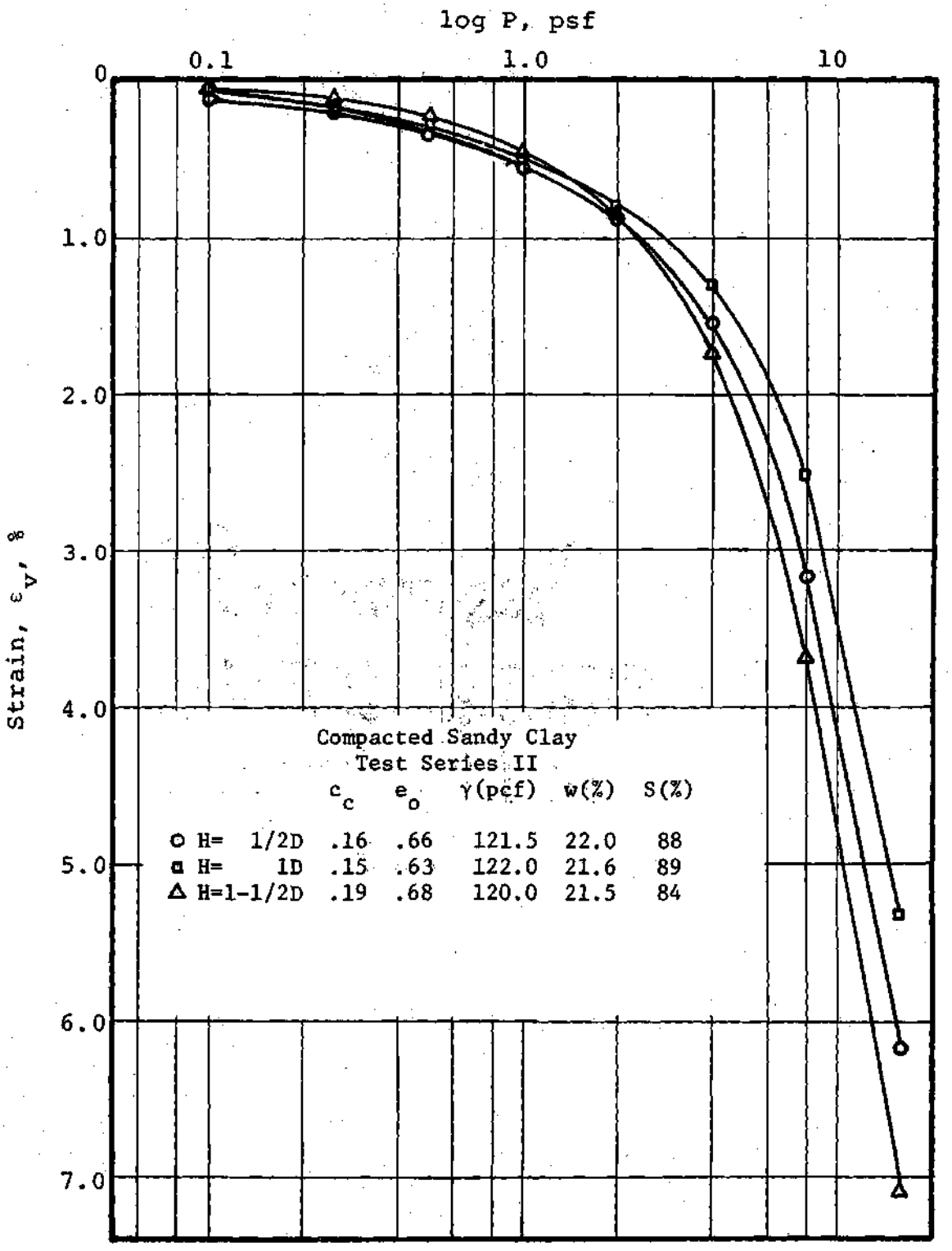

Figure 34. Consolidation Test Results of Stiff Layers: Compacted Sandy Clay, Test Series II.

CHAPTER VI

TEST RESULTS

Settlement Measurements

Surface Settlements

The long-term surface settlement of footings on the uniform soft soil and on the structural fill were measured for each test. The measured settlement was taken as an average of readings from four dial gages. For each load increment, a time settlement relationship was plotted using the square root method to determine the time for completion of the primary settlement. Since a period of two to three days was involved in measuring the long term settlements, the square root method was preferrable to Cassagrande log-time method in that it did not allow secondary consolidation to accumulate. Also the time for completion of the primary settlement could be predicted using this method. Each load increment was maintained until the change in the dial gage readings was less than 0.001 inch per hour. Because the soft subsoil was partially saturated (saturation = 83%), most of the settlement occurred quickly and the immediate settlement accounted for up to 80 to 85 percent of the total settlement.

The results of surface settlement measurements are presented in a graphical form in Figure 35 through 40. The

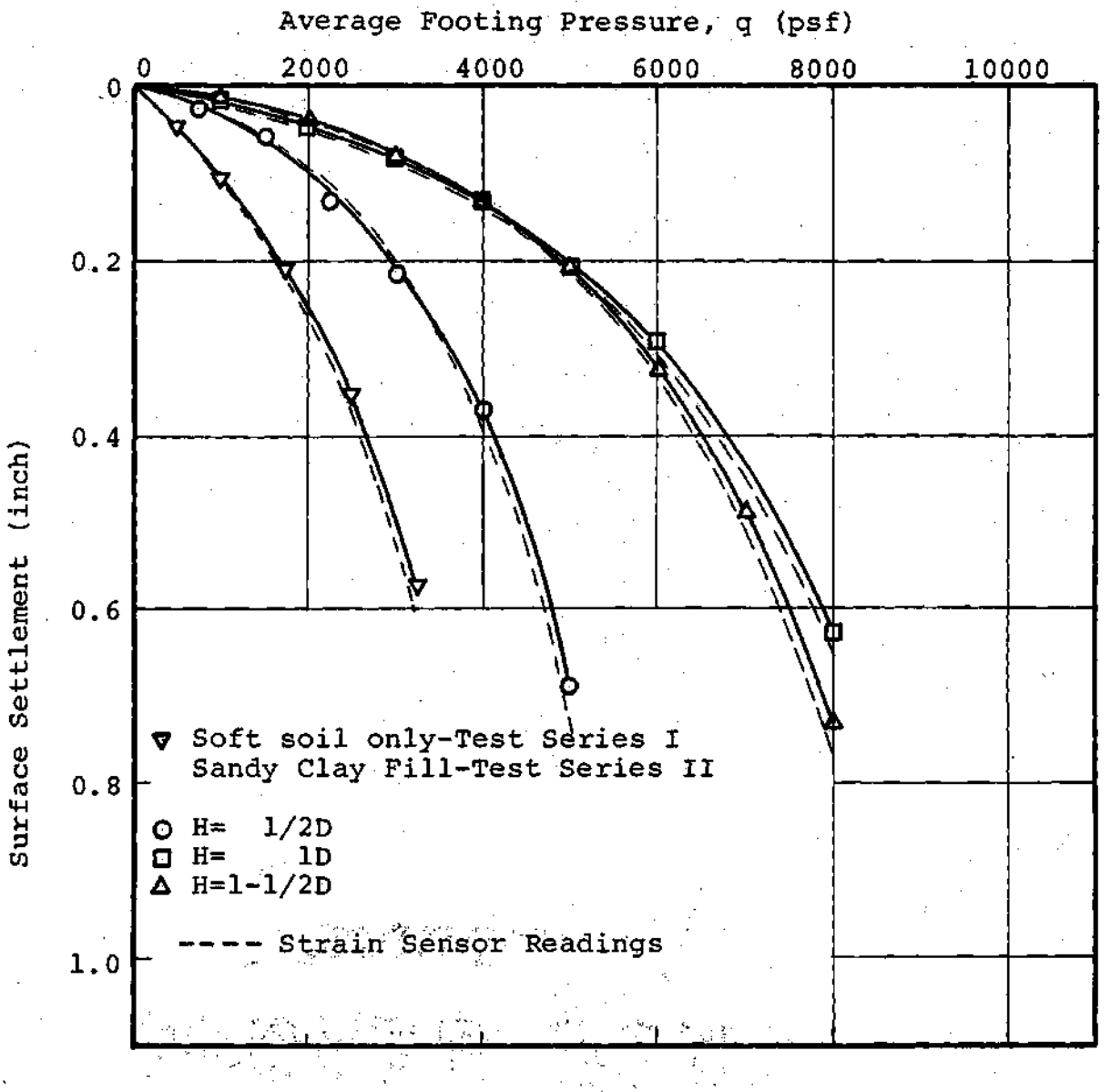

Figure 35. Comparison of Rigid Footing Settlement of Sandy Clay Fills Over Soft Micaceous Clayey Silt Layer with Footing Settlement on Homogeneous Layer.

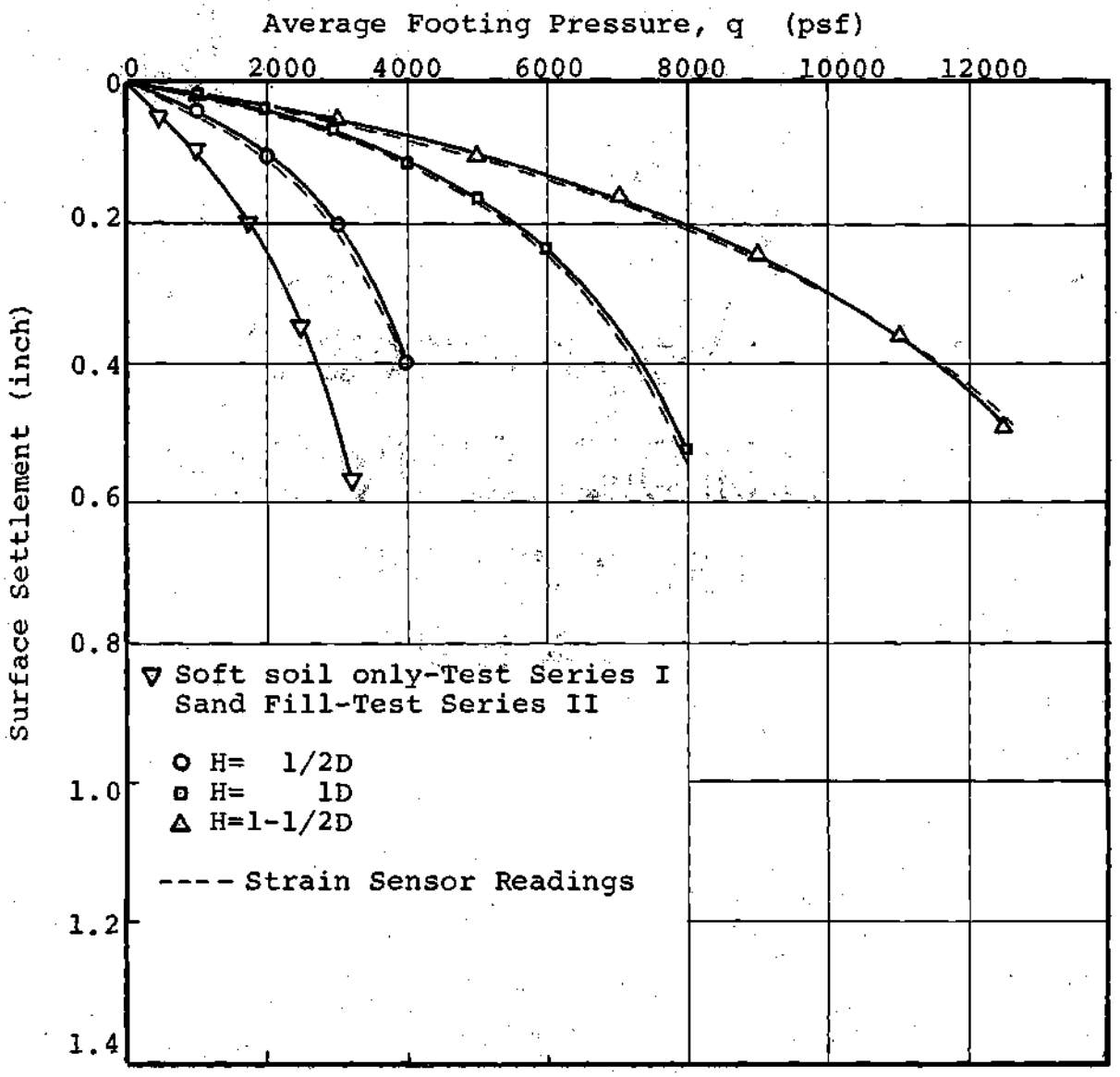

Figure 36. Comparison of Rigid Footing Settlement of Sand Fills Over Soft Micaceous Clayey Silt Layer with Footing Settlement on Homogeneous Layer.

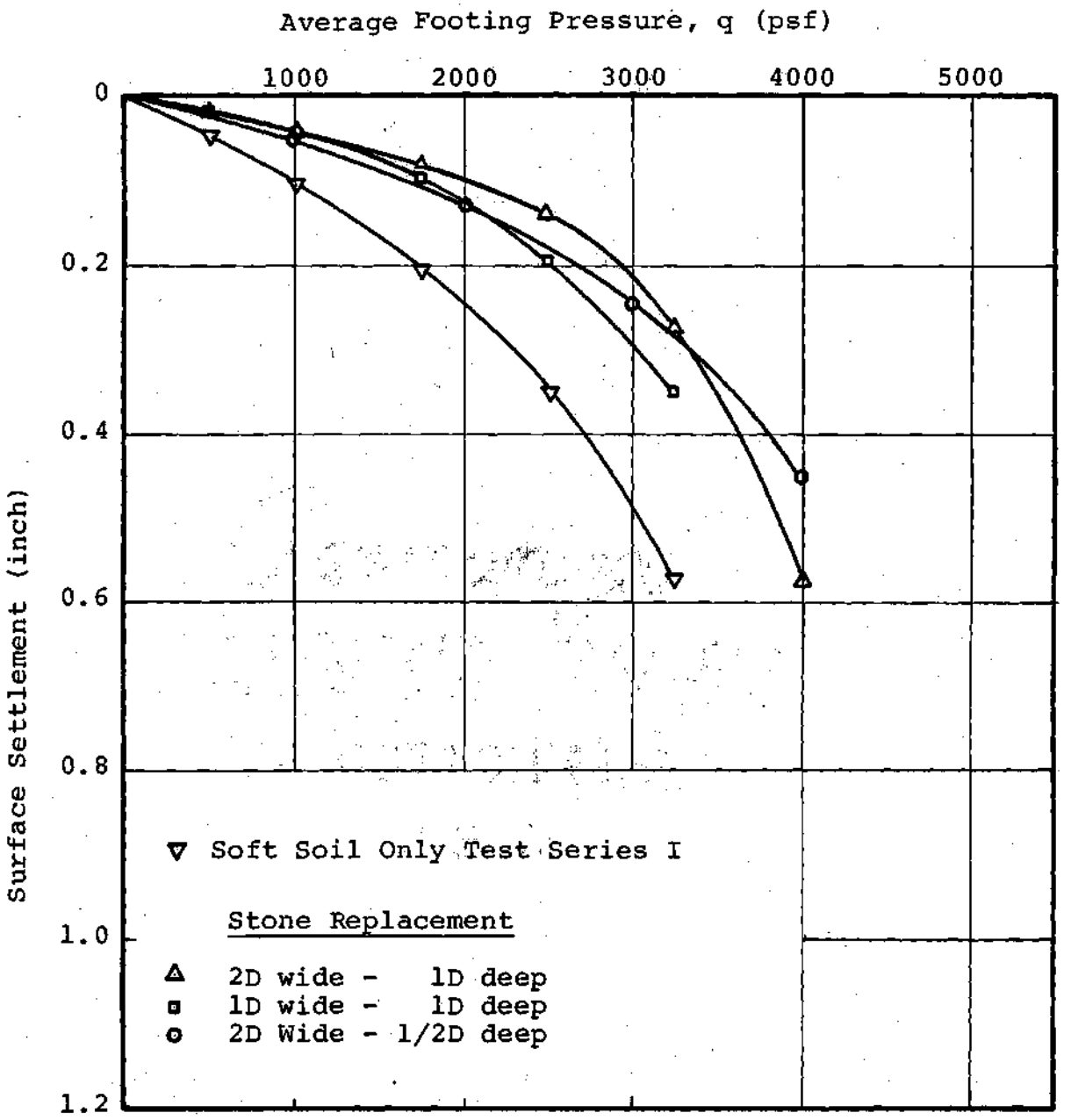

Figure 37. Comparison of Rigid Footing Settlement of Stone Replacement Over Soft Micaceous Clayey Silt Layer with Footing Settlement on Homogeneous Layer.

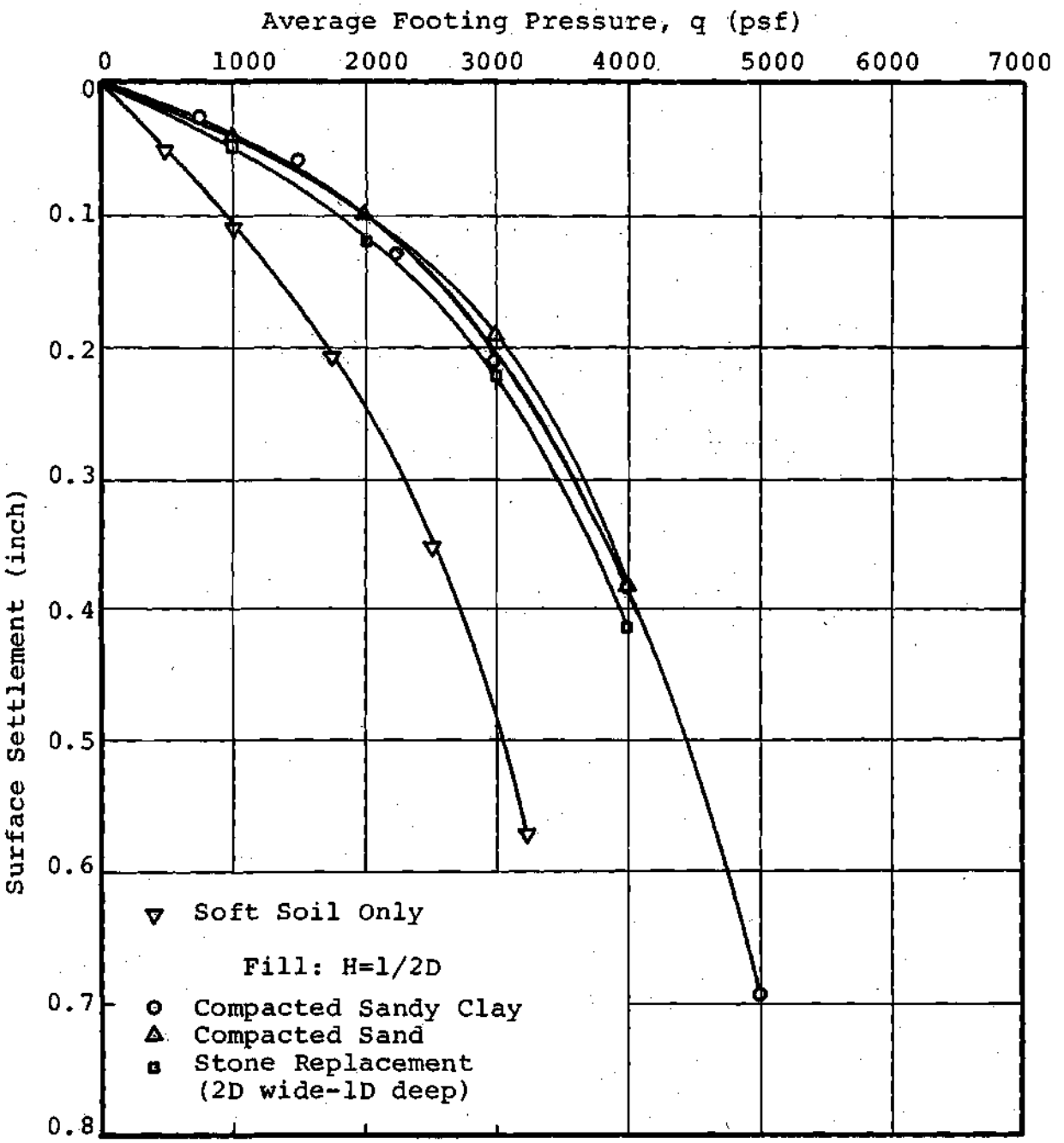

Figure 38. Comparison of Rigid Footing Settlement of Compacted Fill Over Soft Micaceous Clayey Silt Layer: H=1/2D.

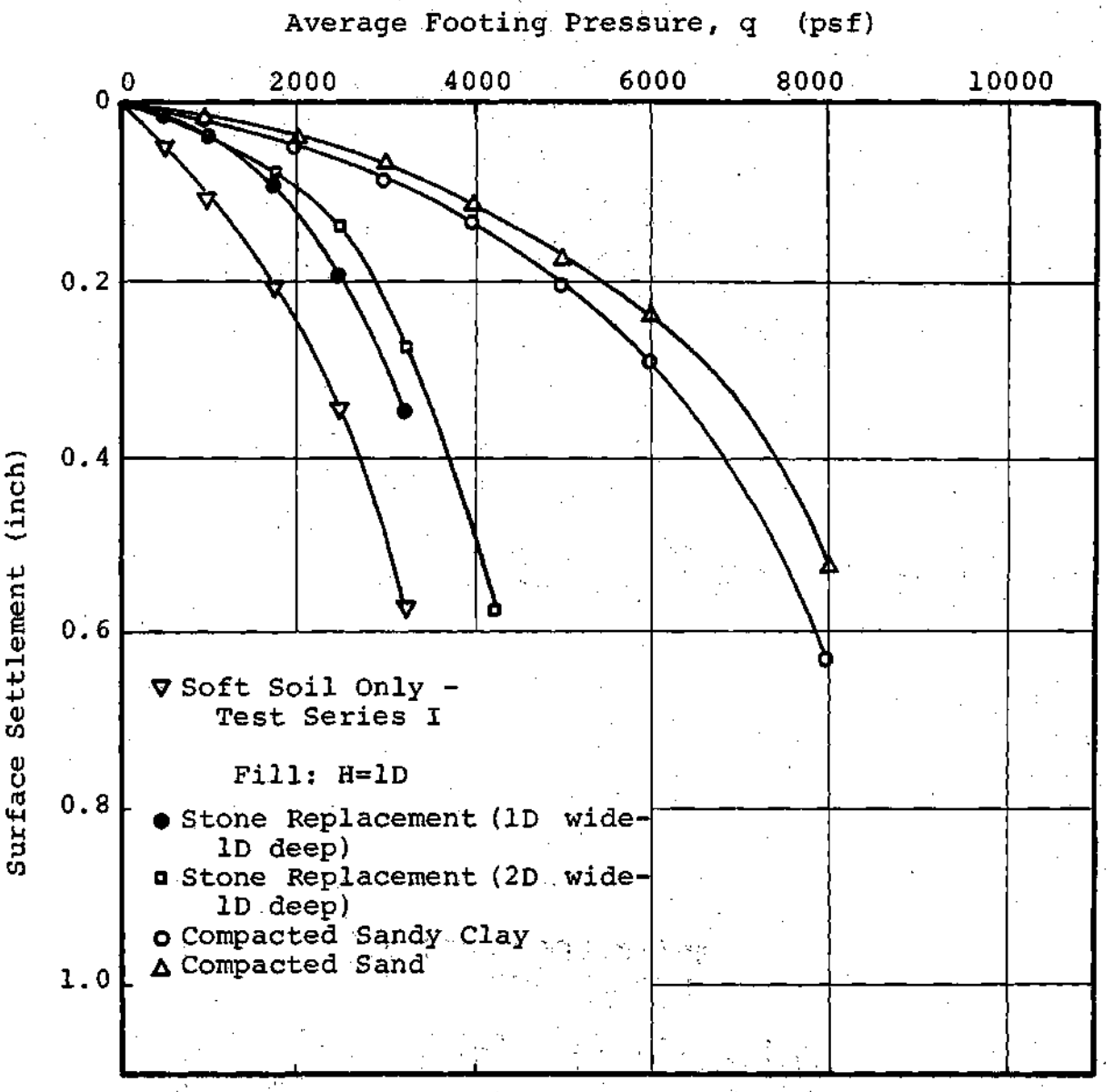

Figure 39. Comparison of Rigid Footing Settlement of Compacted Fill Over Soft Micaceous Clayey Silt: H=1D.

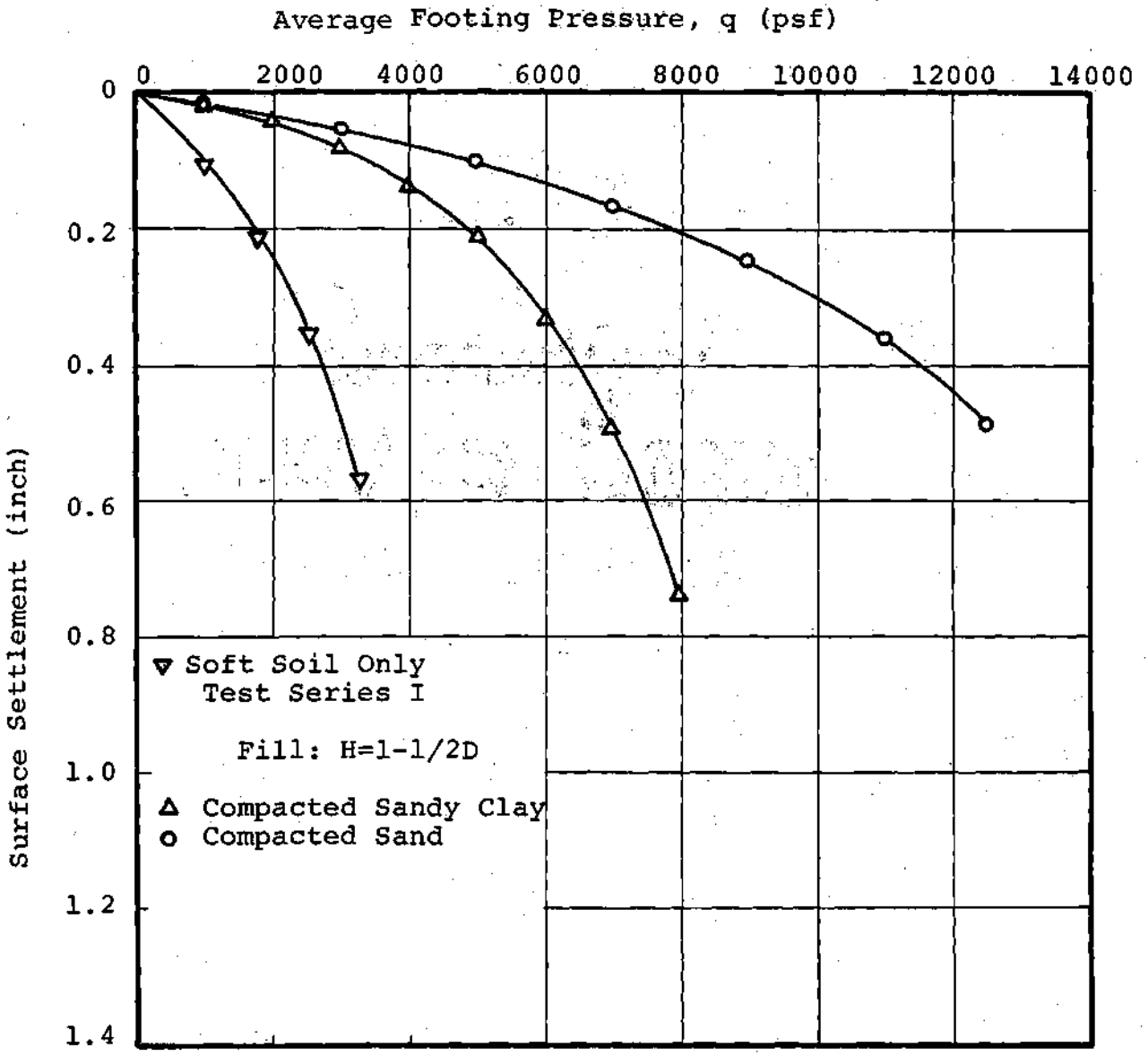

Figure 40. Comparison of Rigid Footing Settlement of Compacted Fill Over Soft Micaceous Clayey Silt: H=1-1/2D.

settlements shows are total settlements which include both immediate and consolidation settlement. Figures 35, 36, and 37 show a comparison of footing settlements on structural fills having three different thicknesses with the footing settlement on the homogeneous soft layer. The footing settlements on the stone replacement are shown in Figure 37. The settlement of footing on the structural fill which had the same thickness are compared in Figures 38, 39, and 40.

Settlement of Soft Layers

The results of settlement measurement of soft layers under the structural fill as compared with the settlement of the homogeneous soft layer below the depth which was equal to the fill thickness are presented in Figures 41, 42, and 43. These results were used in the analysis of the beneficial effects of structural fill in reducing settlement in the soft layer using the method proposed in Chapter III.

Stress Measurement

The measured stress values in the following plots were obtained from cumulative readings of stress cells for each footing pressure. These stress readings were not averaged but plotted as they were representing a single stress reading under the footing pressure for which the stress was measured. Therefore, some scatter in the results is present. Erratic readings, which could be due to several possible causes, i.e., malfunctioning of the cells or effects of temperature variations, were included unless it was absolutely apparent that

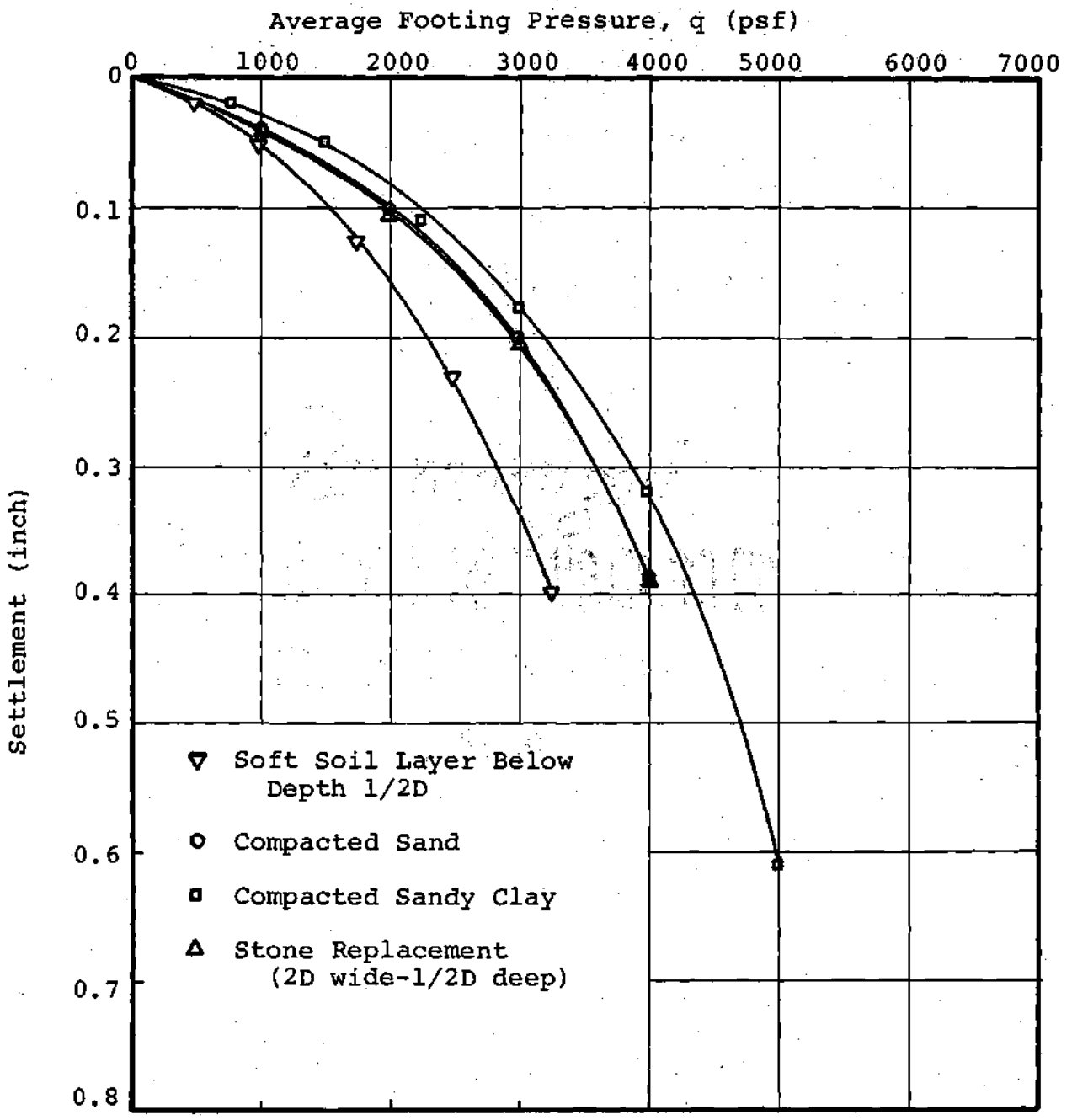

Figure 41. Settlement of Soft Subsoil Beneath 1/2D Compacted Fill.

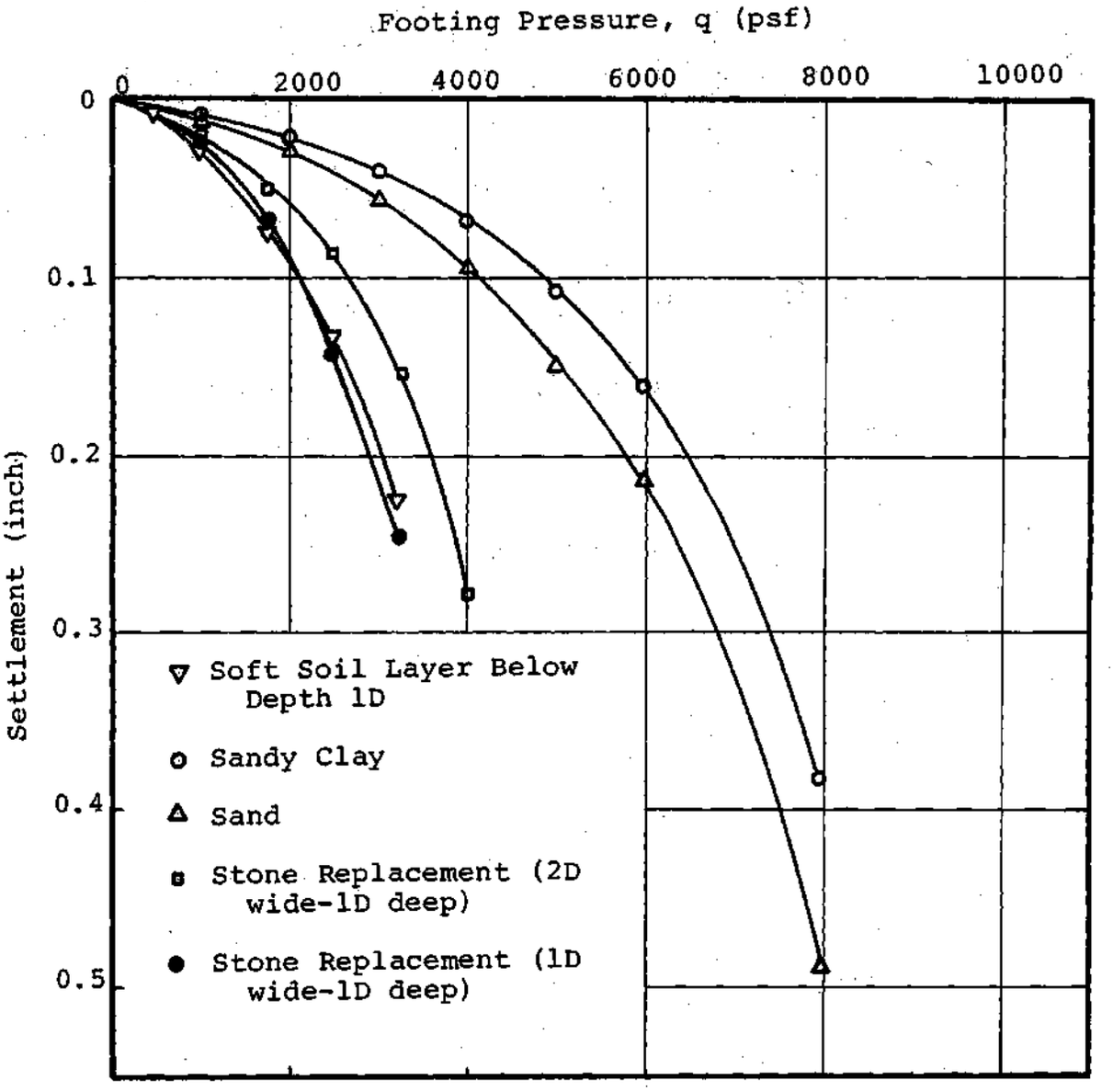

Figure 42. Settlement of Soft Subsoil Beneath 1D Compacted Fill.

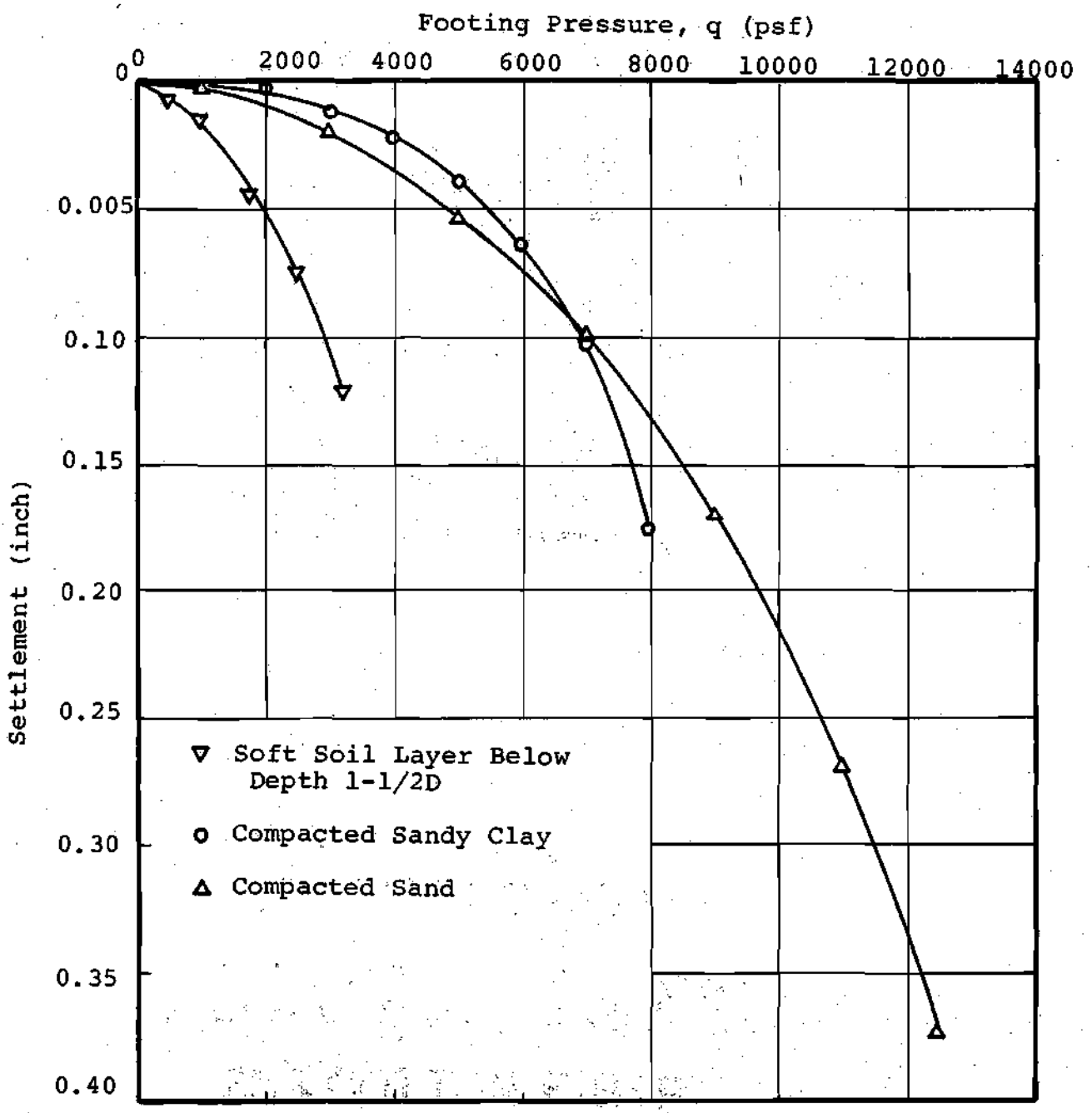

Figure 43. Settlement of Soft Subsoil Beneath 1-1/2D Compacted Fill.

the cell readings were faulty. The measured stresses were plotted in a normalized form by dividing the measured values by the footing pressure, q. The depth at which the stresses were measured was expressed as depth to footing diameter ratios, Z/D.

Homogeneous Clayey Silt Layer - Test Series I

The results of stress measurements are presented in graphical form as shown in Figures 44 and 45 for a variation of vertical stresses with depth and with radii at a given depth. Theoretical plots of Boussinesq solutions for both rigid and flexible loading are included for comparison.

Sandy Clay Fill Over Soft Soil - Test Series II

Figures 46 through 51 show the results of stress measurement in the sandy clay fill as well as in the soft layers using three fill thicknesses which were equal to 1/2D, 1D, and 1-1/2D. Theoretical results from a finite element method and closed form solutions are also presented for comparison.

Sand Fill Over Soft Soil - Test Series III

The results of vertical stress measurement using compacted sand as structural fill are presented in Figures 52 through 57. Fill thicknesses equal to 1/2D, 1D, and 1-1/2D were used as was performed in Test Series II.

Stone Replacement

The measured vertical stresses varying with depth and

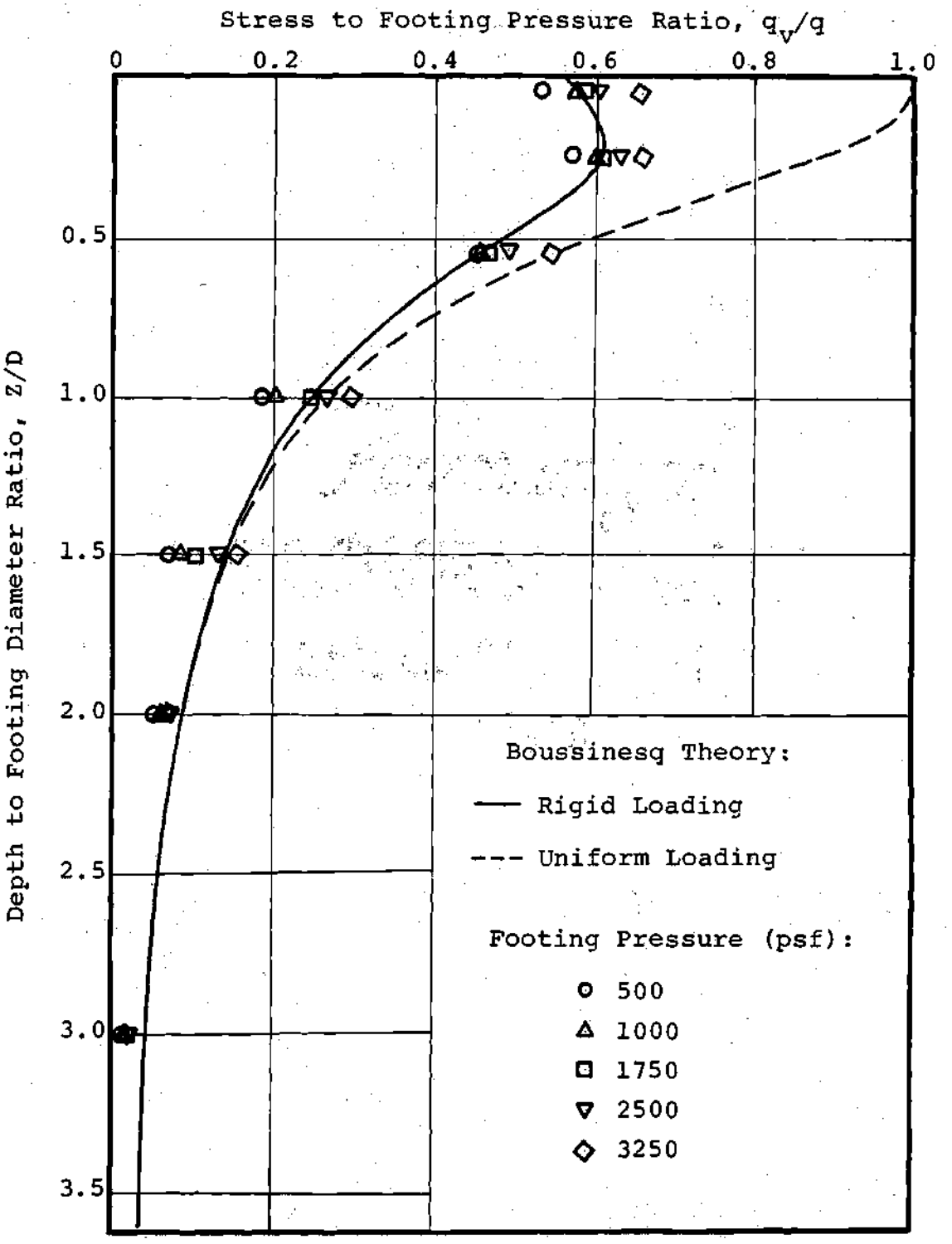

Figure 44. Vertical Stresses at 4 Inch Offset From Load Axis: Homogeneous Layer, Test 1 - Test Series I.

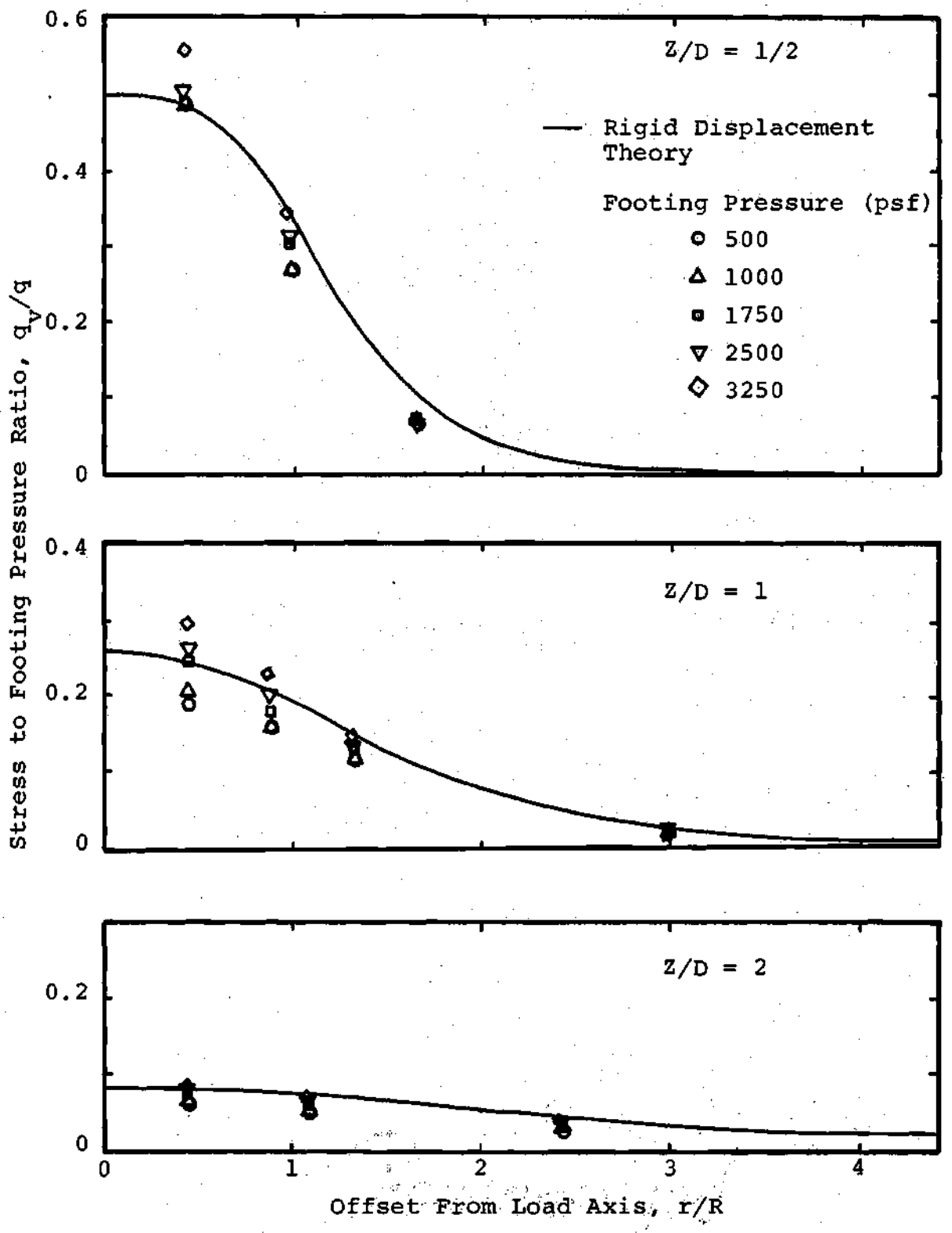

Figure 45. Measured Vertical Stresses with Radii: Homogeneous Layer, Test 1 - Test Series I.

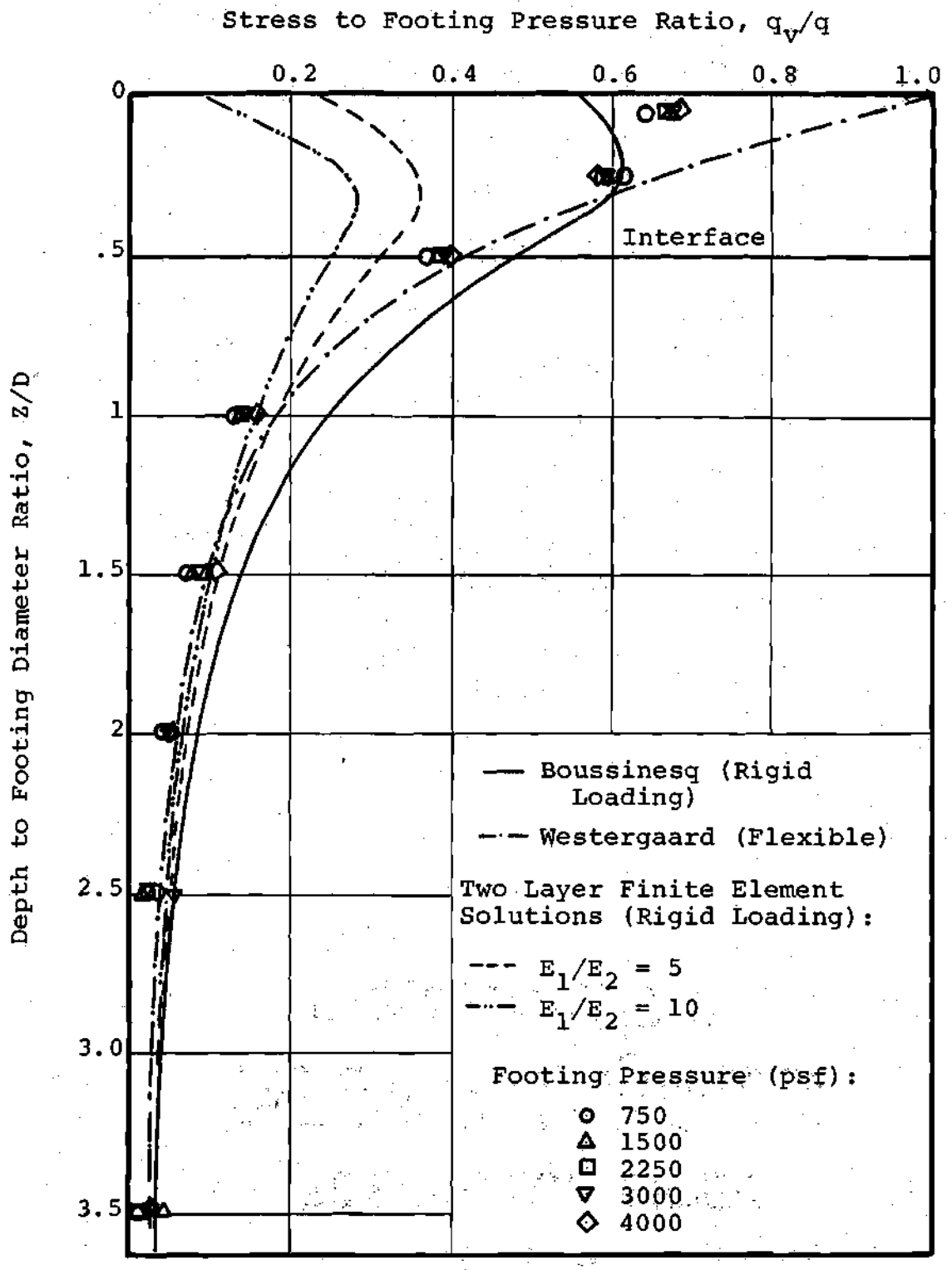

Figure 46. Vertical Stresses at 4 Inch Offset From Load Axis: Compacted Sandy Clay Over Soft Layer, Test 1 - Test Series II (H=1/2D).

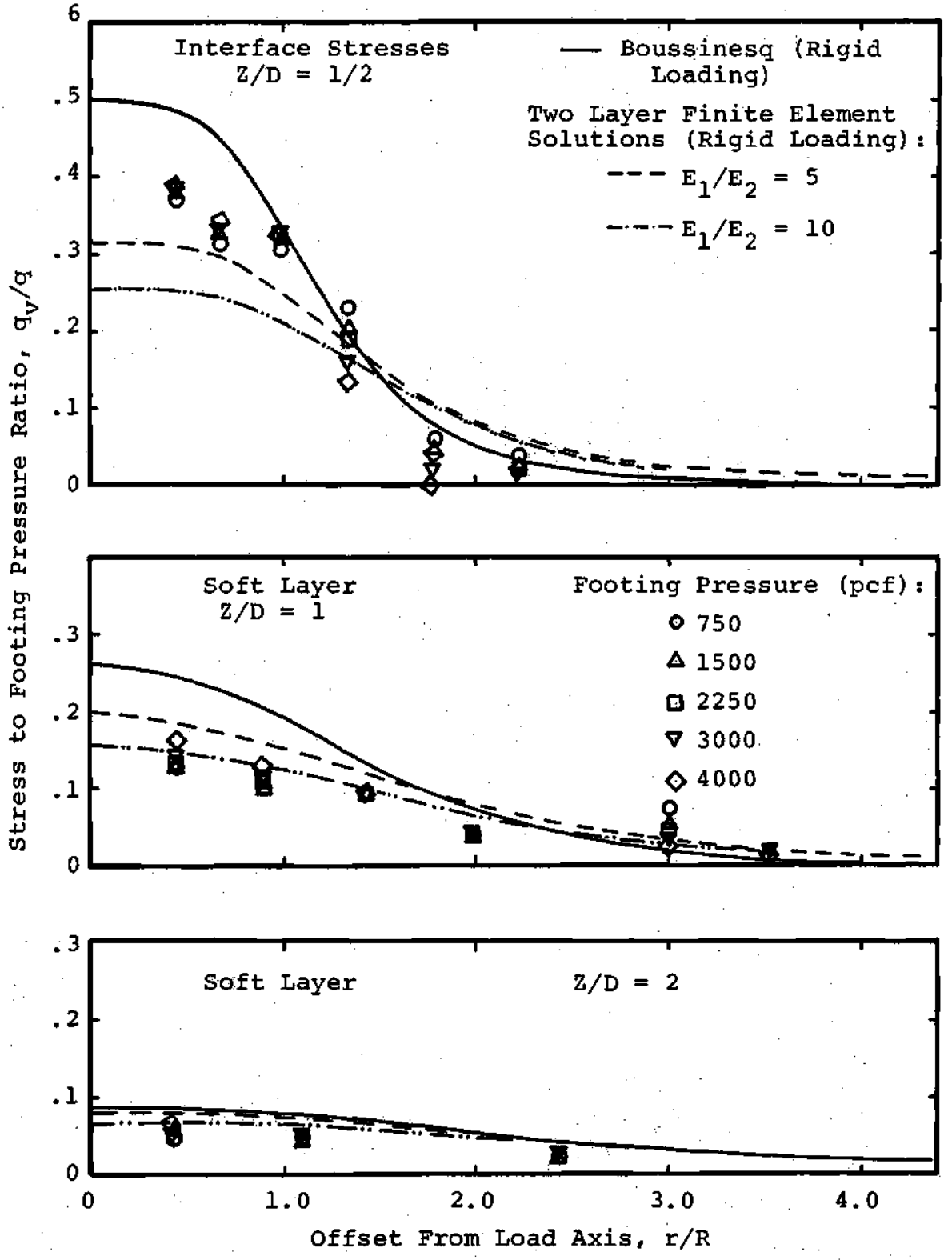

Figure 47. Vertical Stress with Radii: Compacted Sandy Clay Over Soft Layer, Test 1 - Test Series II (H=1/2D).

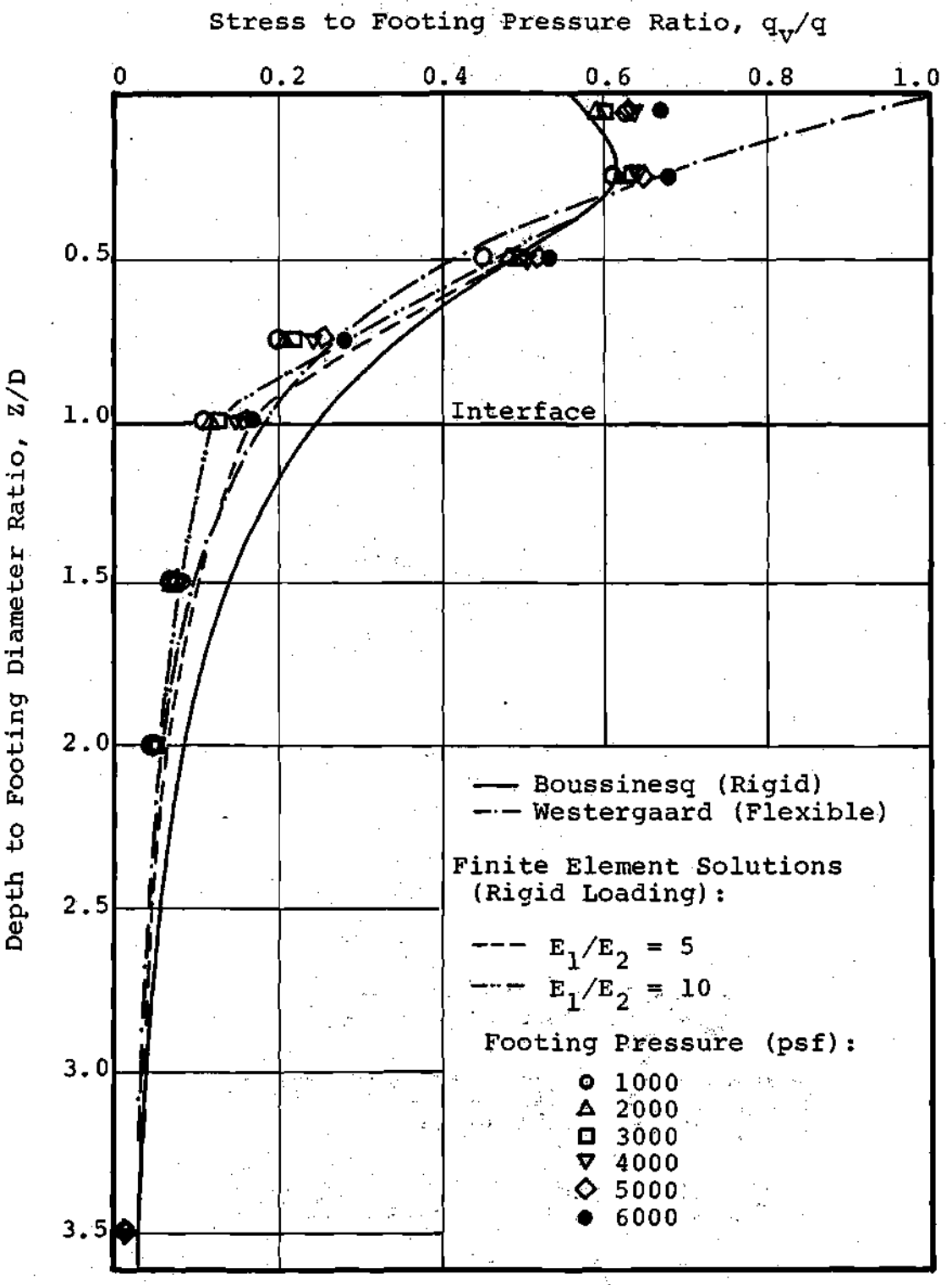

Figure 48. Vertical Stresses at 4 Inch Offset From Load Axis: Compacted Sandy Clay Over Soft Layer, Test 2 - Test Series II (H=1D)

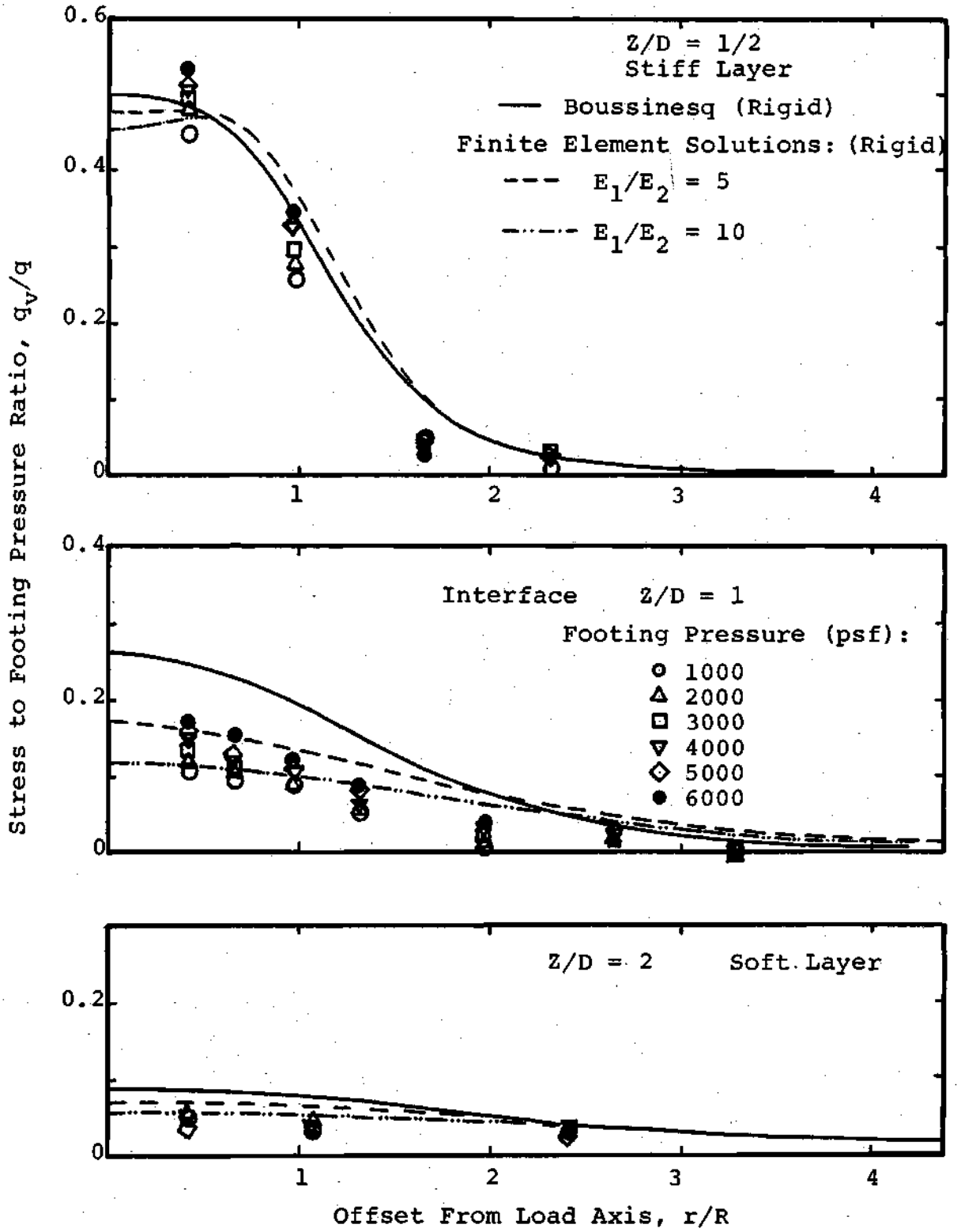

Figure 49. Vertical Stresses With Radii: Compacted Sandy Clay Over Soft Layer, Test 2 - Test Series II (H=1D)

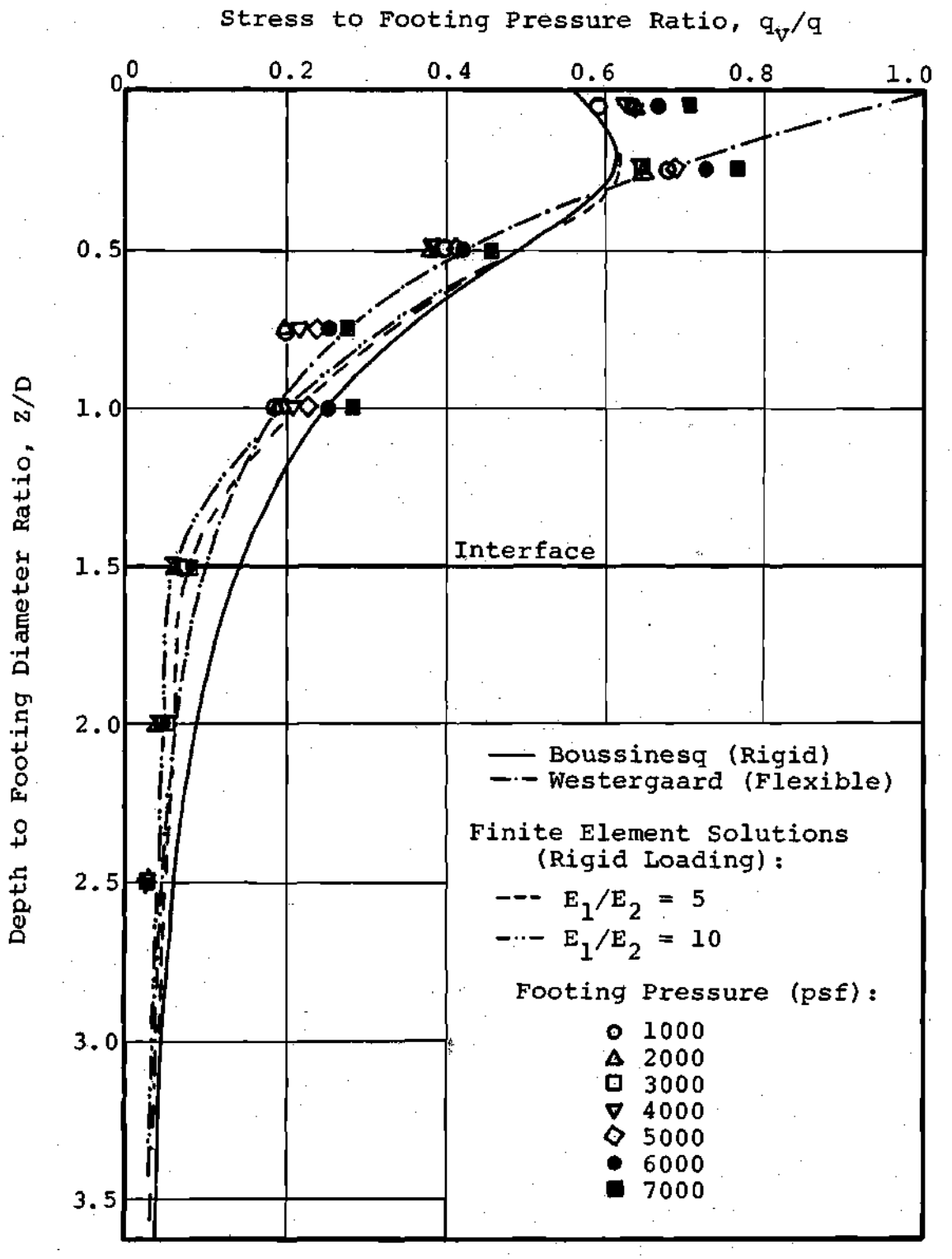

Figure 50. Vertical Stresses at 4 Inch Offset From Load Axis: Compacted Sandy Clay Over Soft Layer, Test 3 Test Series II (H=1-1/2D)

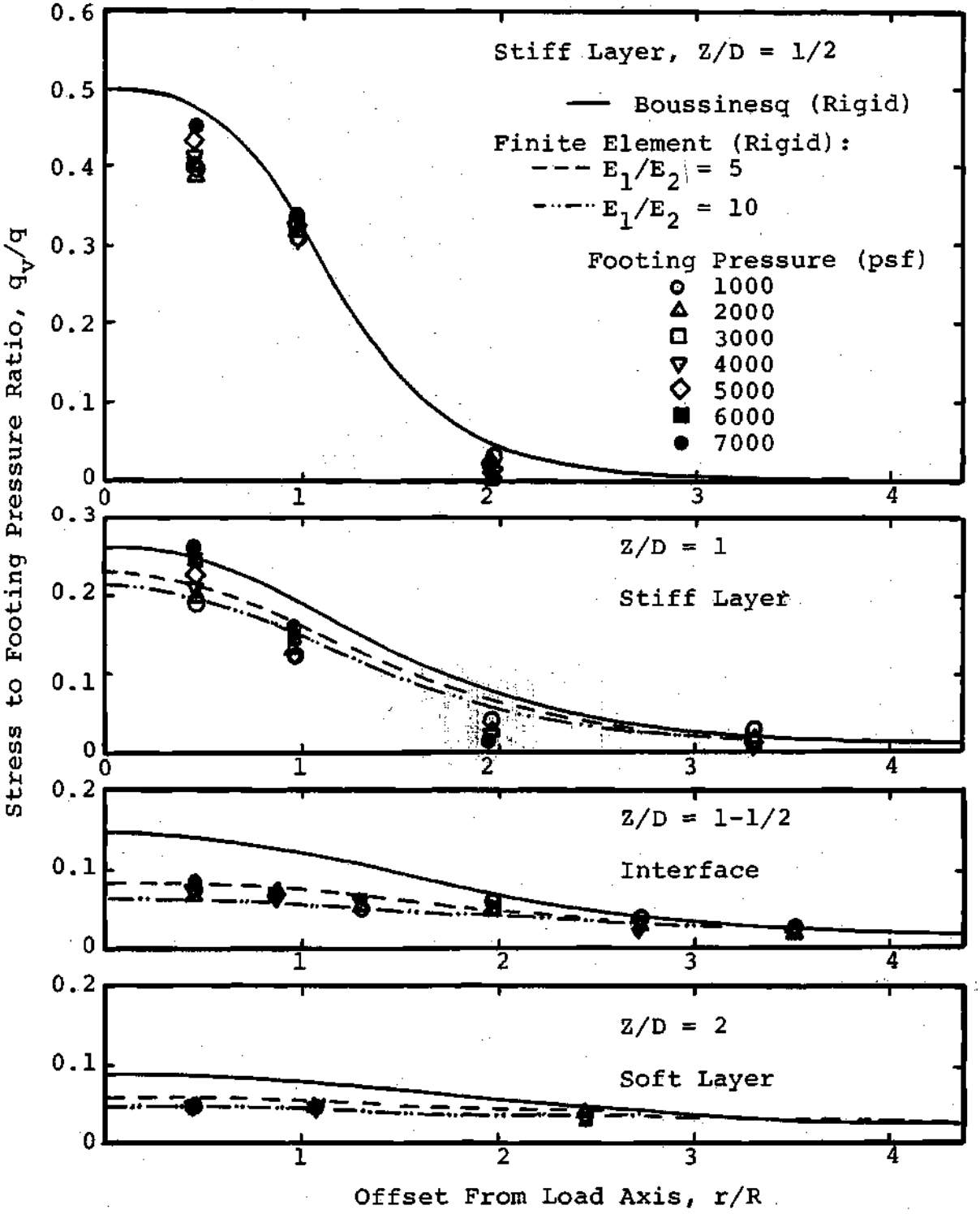

Figure 51. Vertical Stresses with Radii: Compacted Sandy Clay, Test 3 - Test Series II.

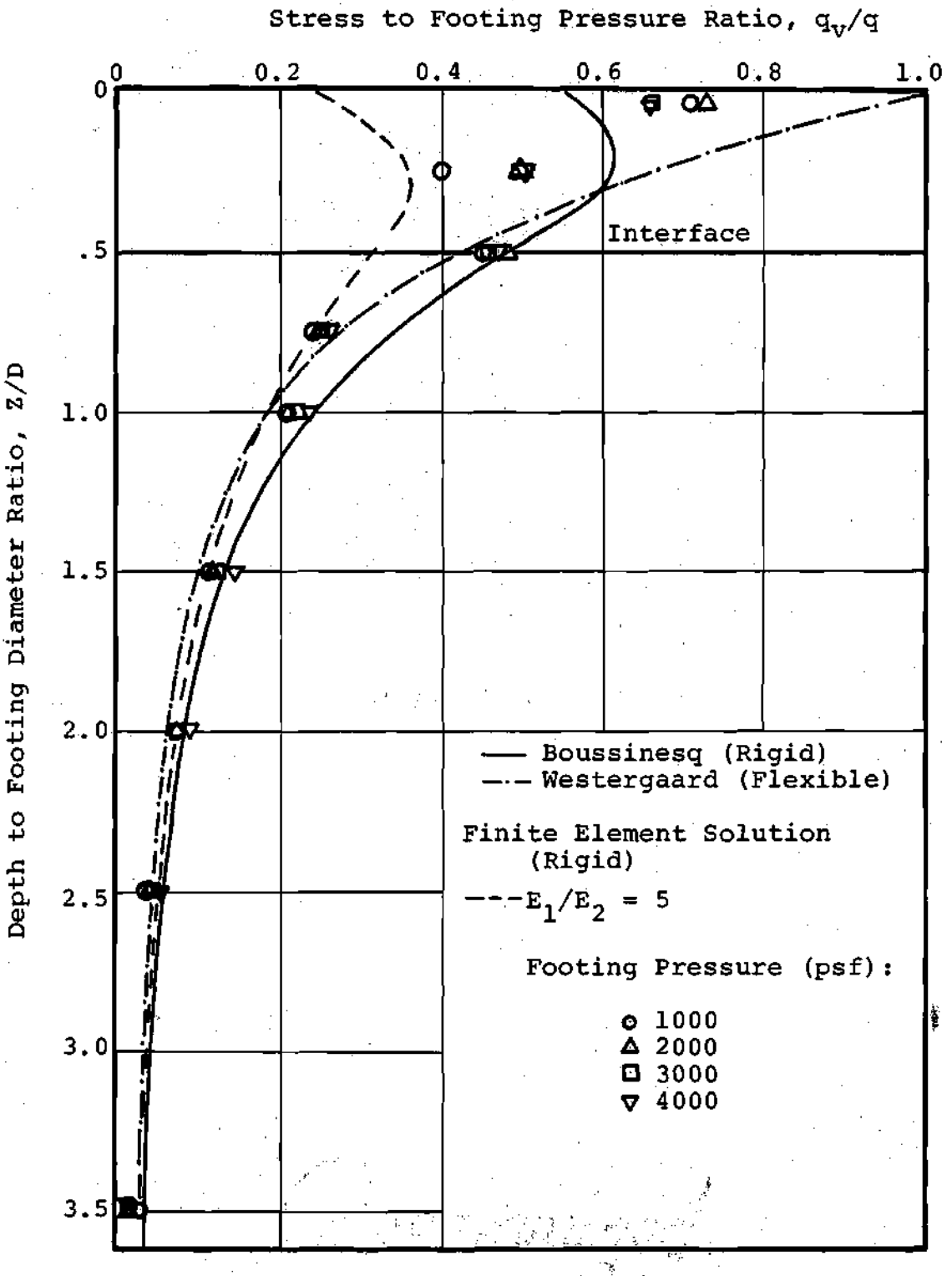

Figure 52. Vertical Stresses at 4 Inch Offset from Load Axis, Compacted Sand Over Soft Layer, Test 1 - Test Series III (H=1/2D)

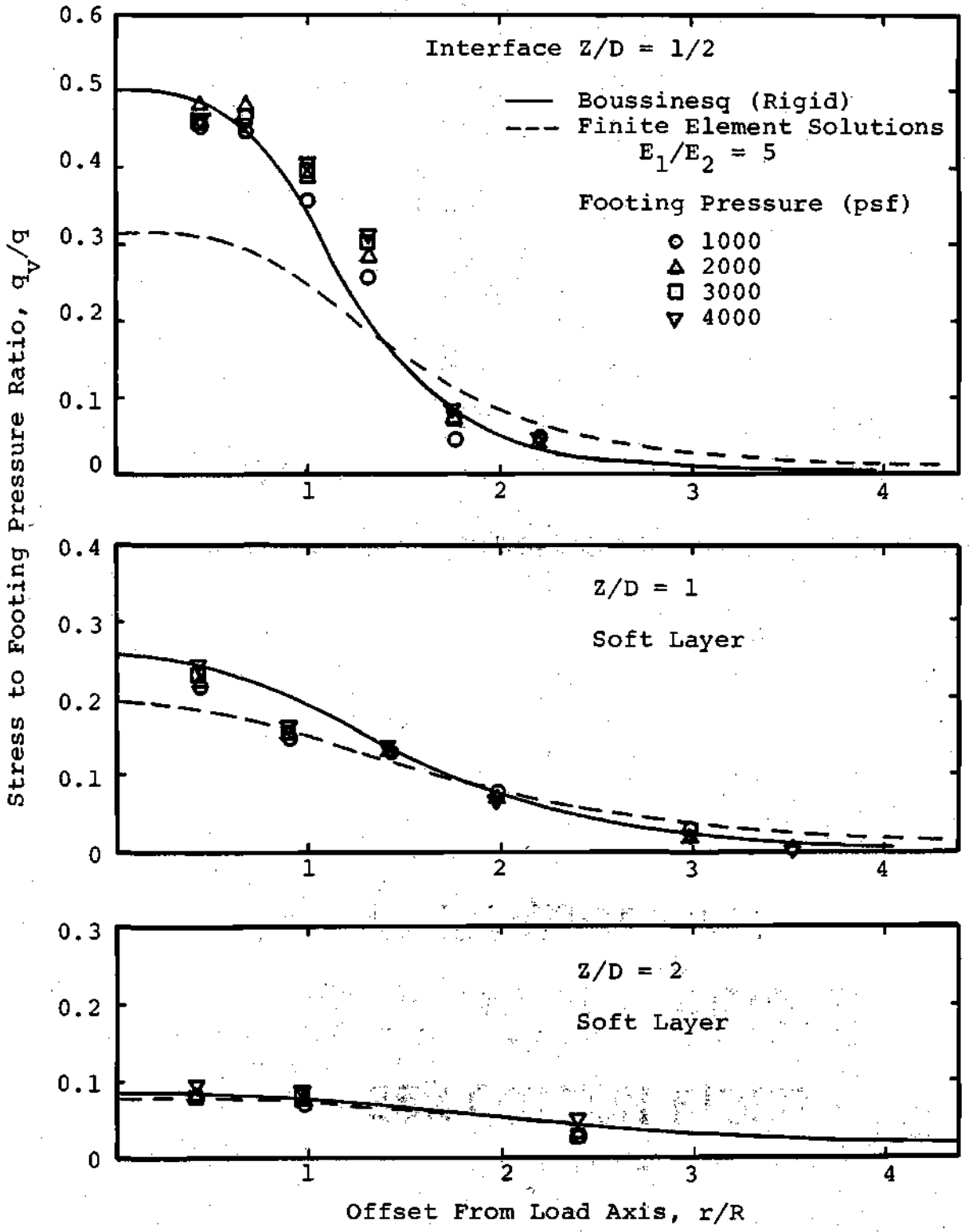

Figure 53. Vertical Stresses with Radii for Compacted Sand Over Soft Layer, Test 1 - Test Series III (H=1/2D).

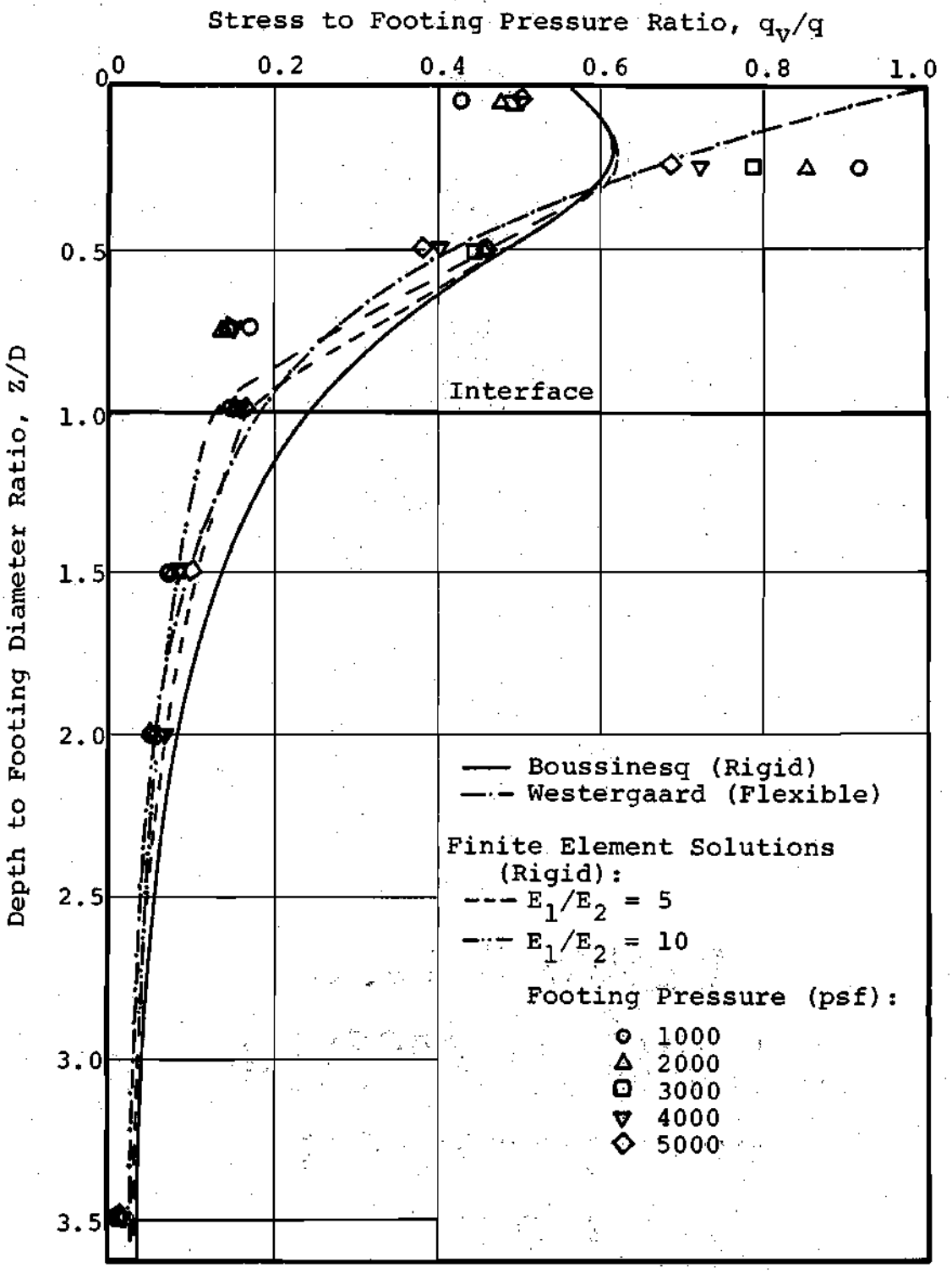

Figure 54. Vertical Stresses at 4 Inch Offset From Load Axis of Compacted Sand Over Soft Layer, Test 2 - Test Series III (H=1D).

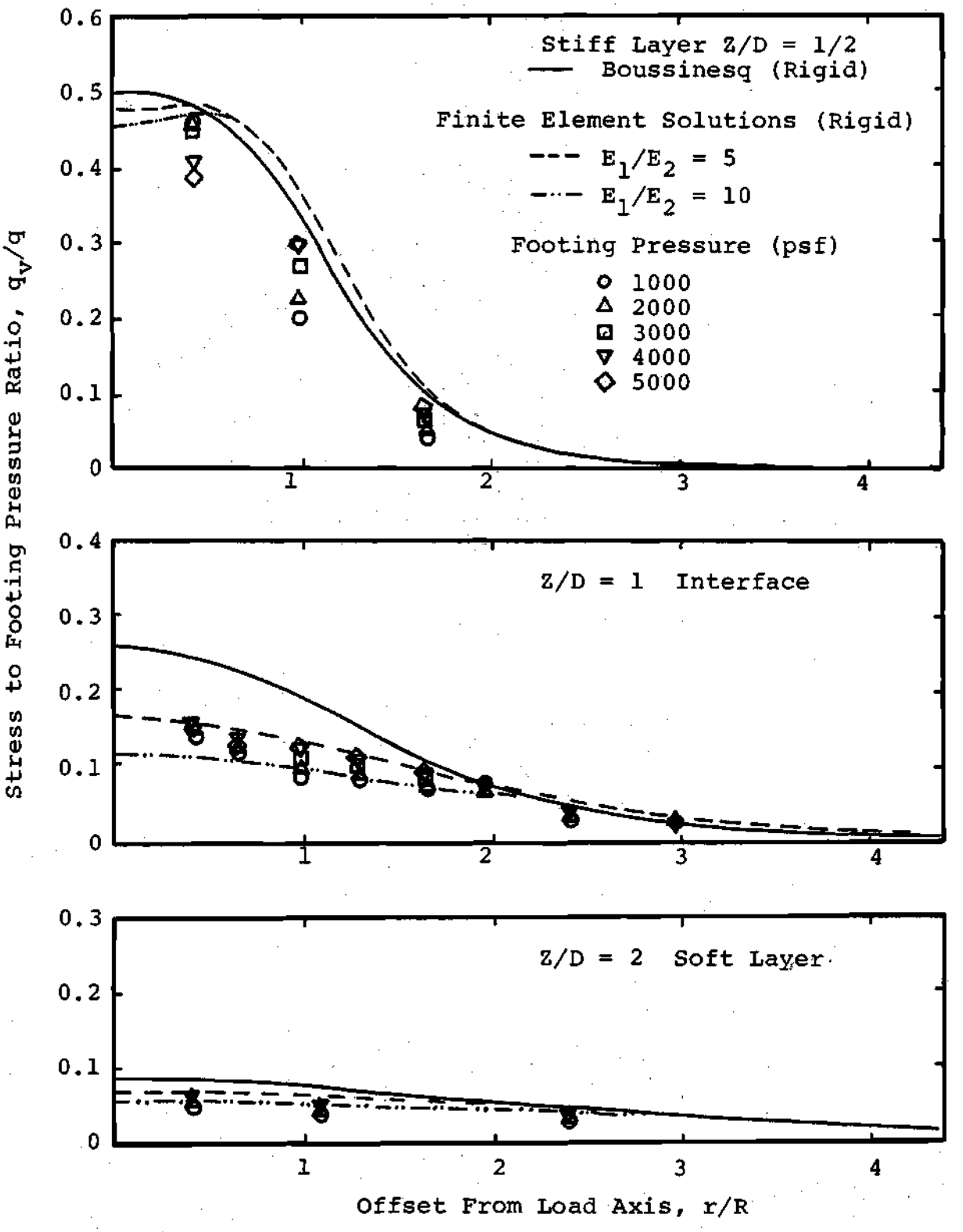

Figure 55. Vertical Stresses with Radii: Compacted Sand Over Soft Layer, Test 2 - Test Series III (H=1D).

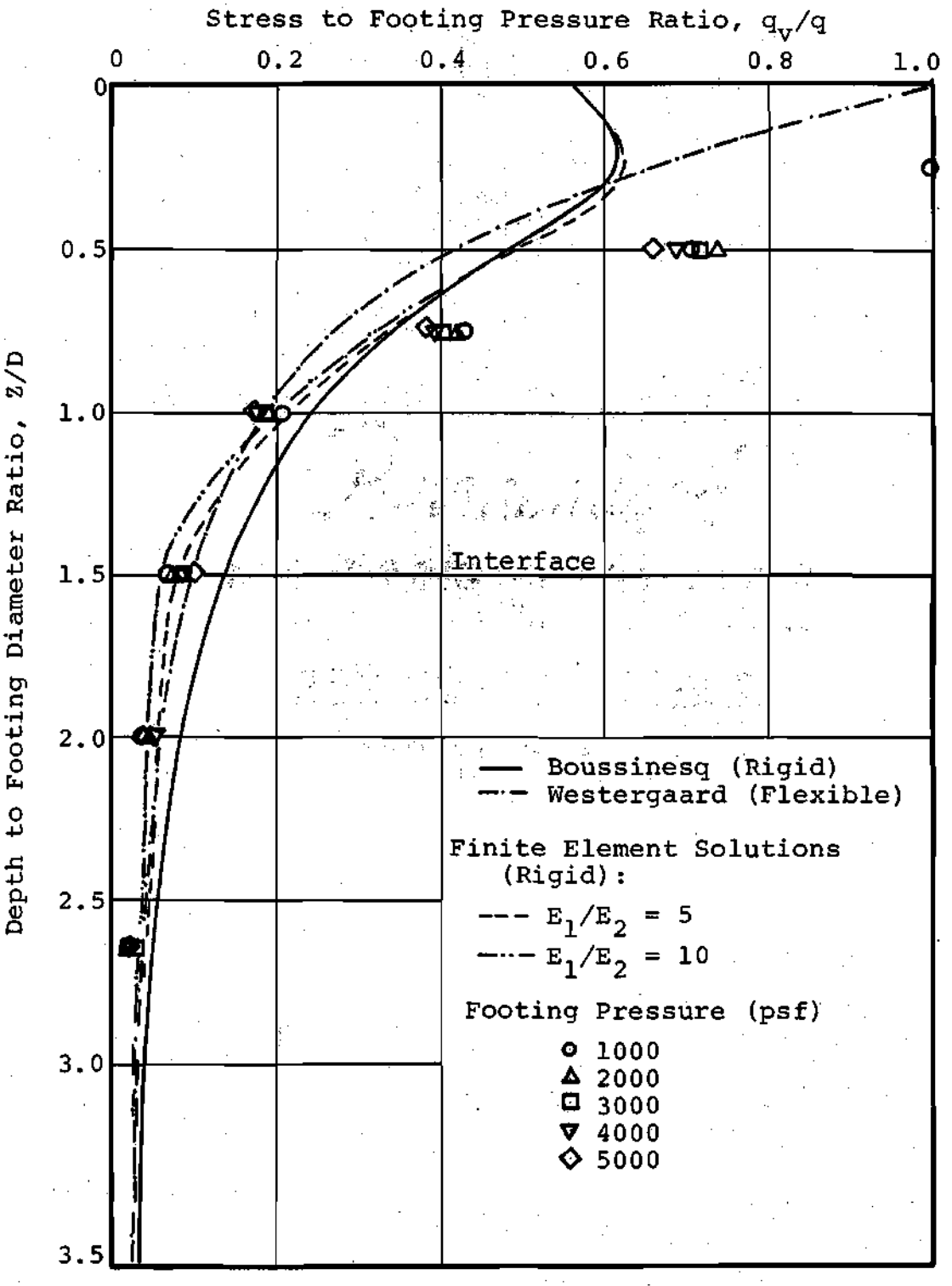

Figure 56. Vertical Stresses at 4 Inch Offset From Load Axis for Compacted Sand Over Soft Layer: Test 3 - Test Series III (H=1-1/2D).

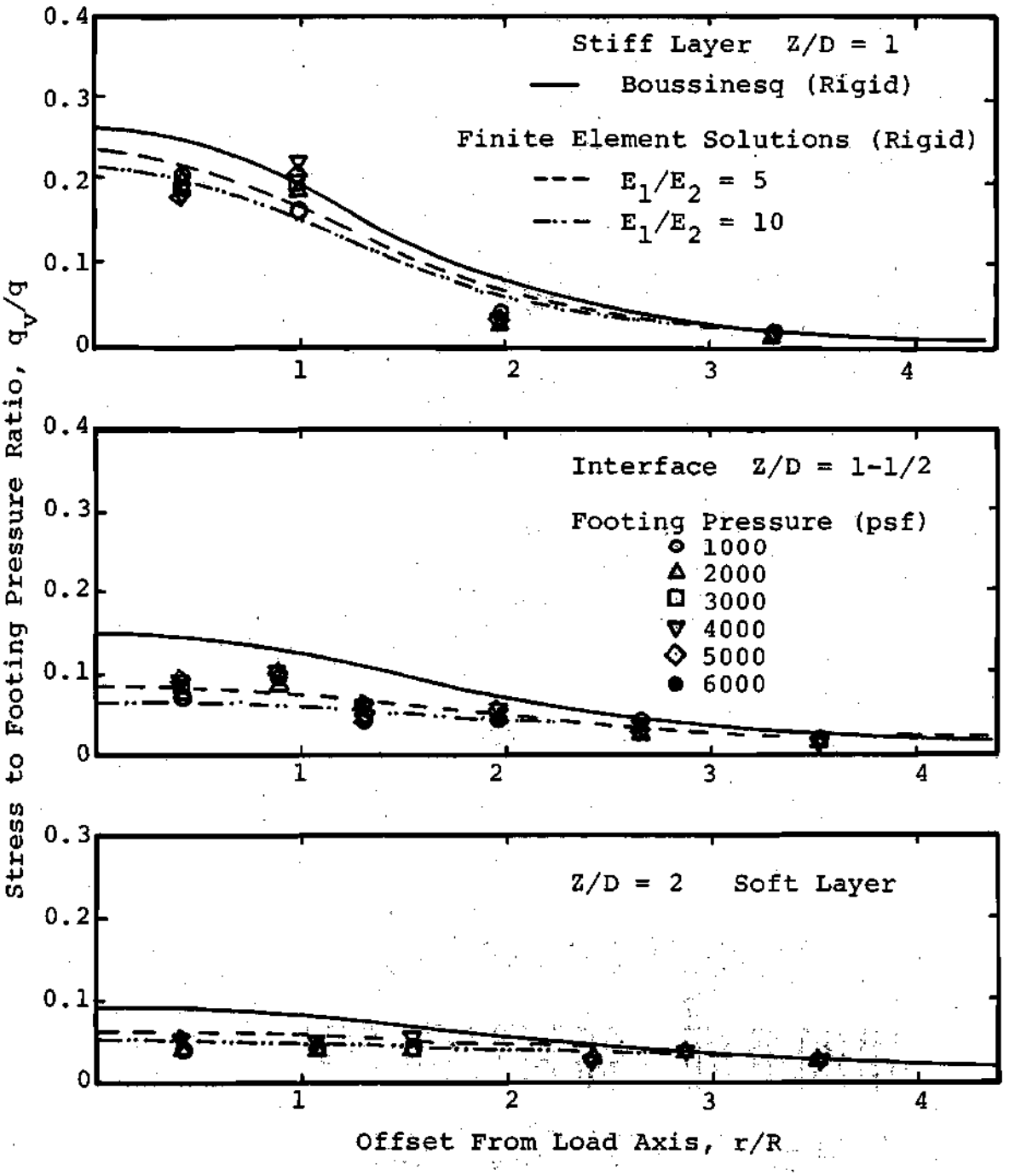

Figure 57. Vertical Stresses with Radii for Compacted Sand Over Soft Layer: Test 3 - Test Series III (H=1-1/2D).

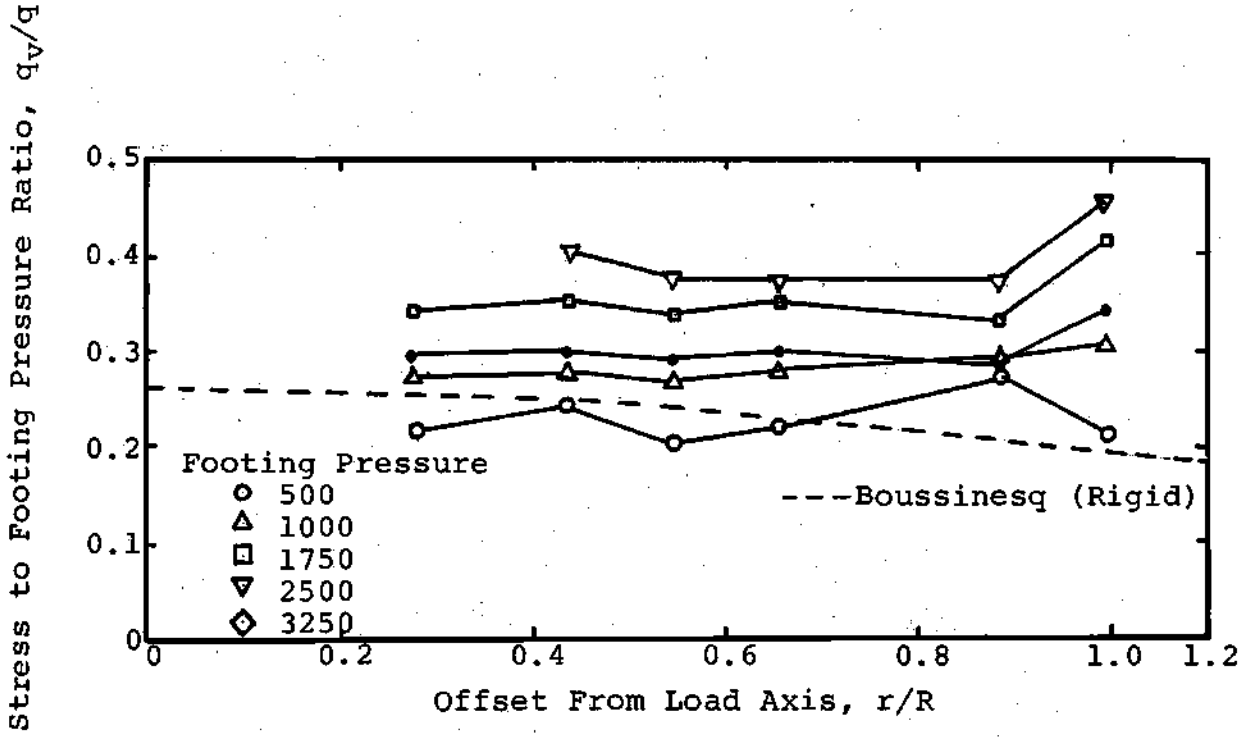

Figure 58. Vertical Stresses Beneath Stone Replacement Footing (1D wide-1D deep), Test 2 - Test Series I.

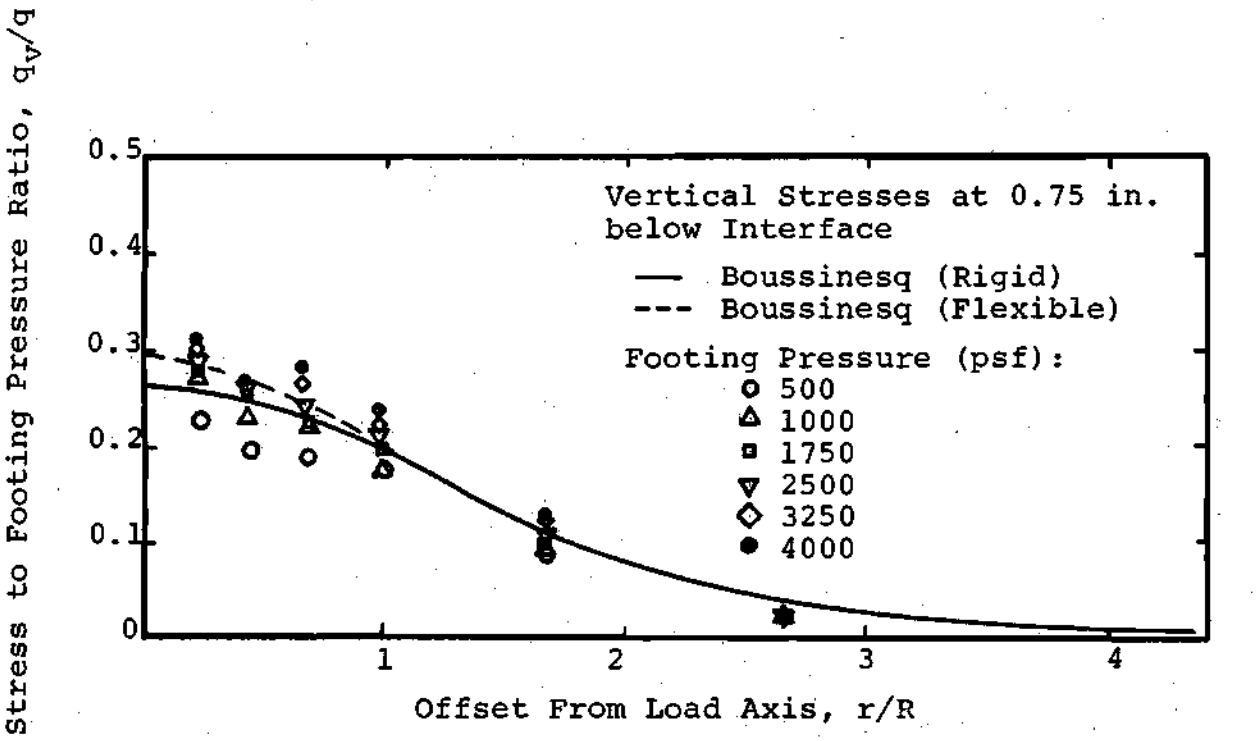

Figure 59. Vertical Stress Variation with Radii for Stone Replacement Footing (2D wide-1D deep), Test 3 - Test Series I.

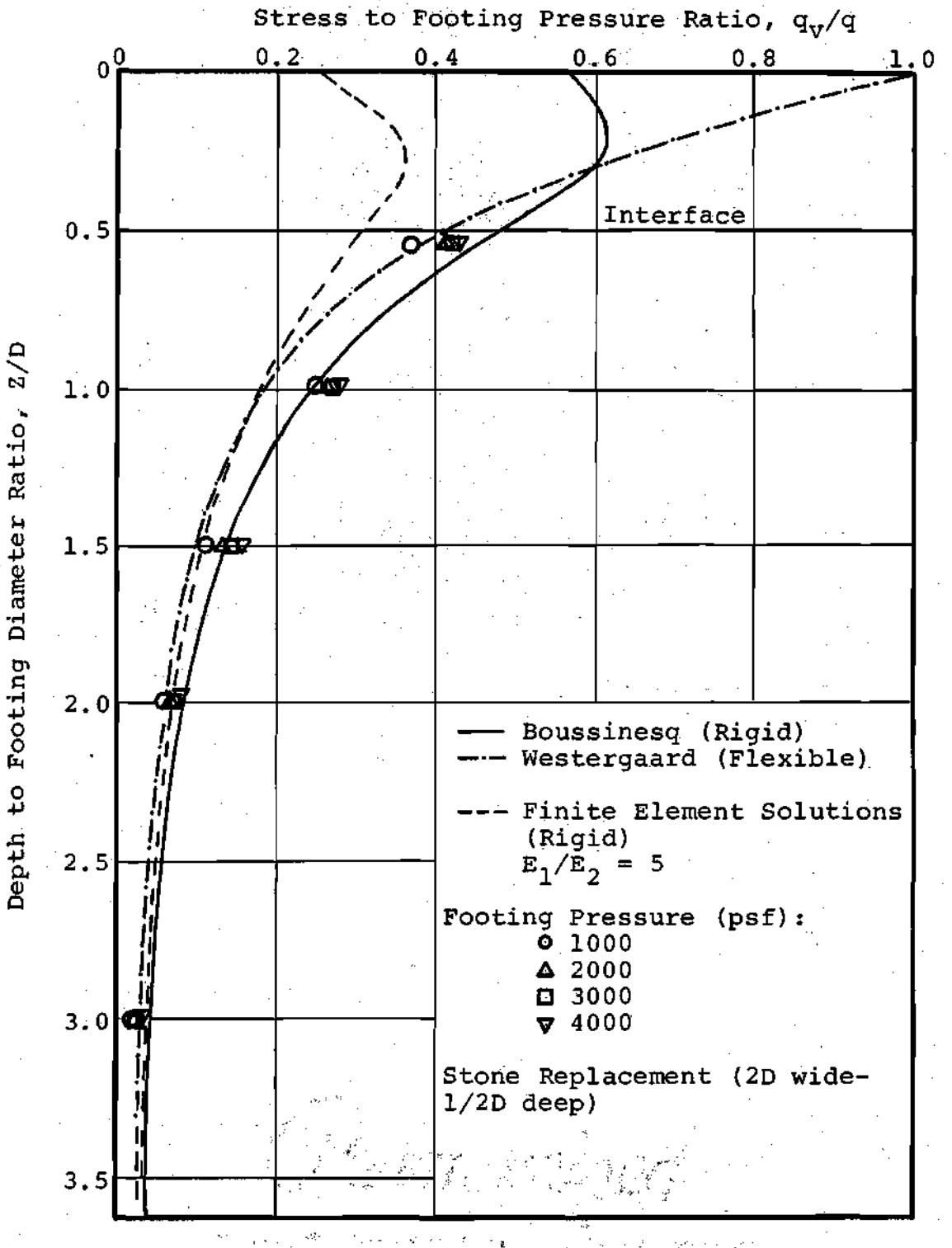

Figure 60. Vertical Stresses at 4 Inch Offset From Load Axis, Stone Replacement, Test 4 - Test Series III.

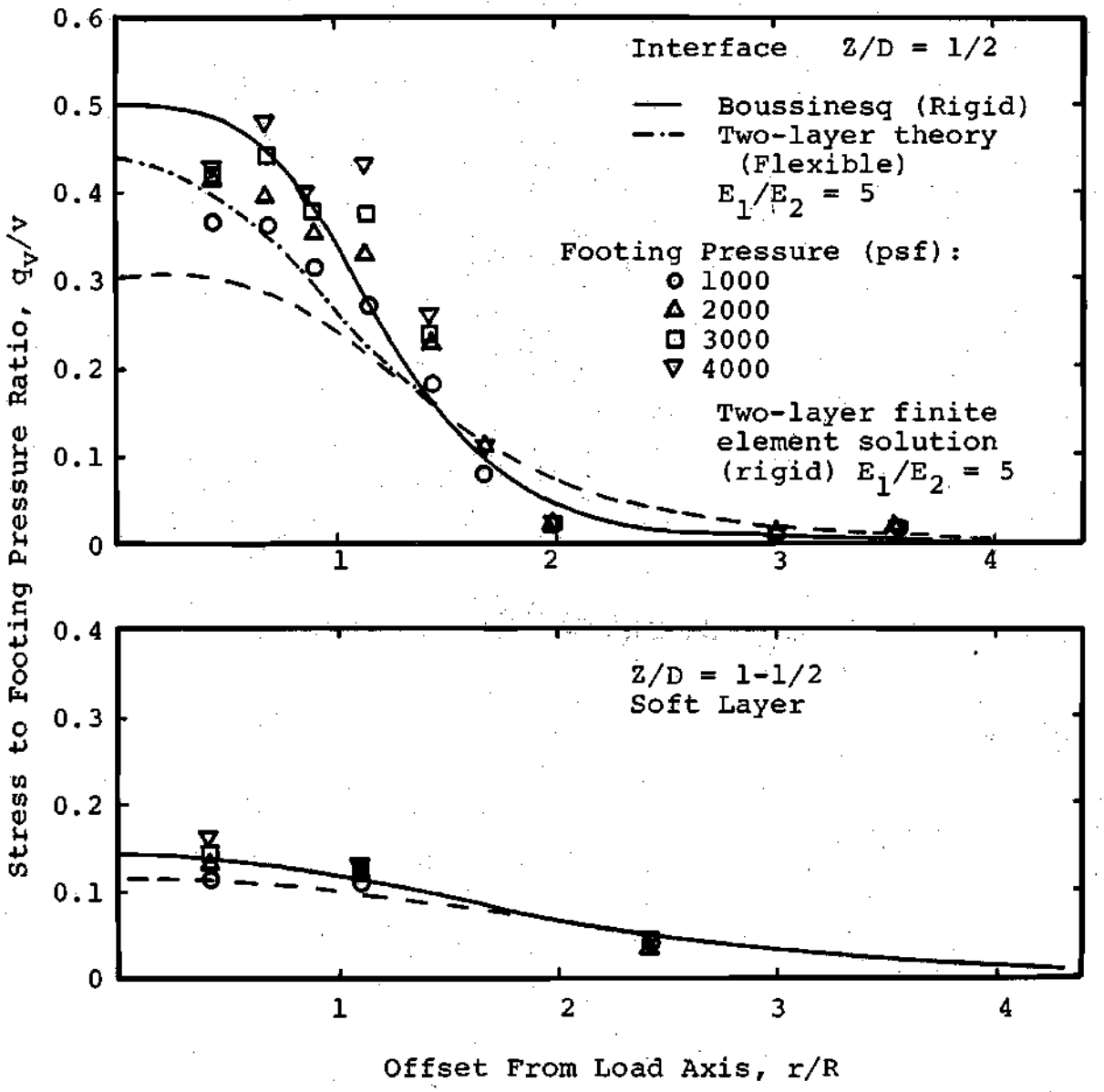

Figure 61. Vertical Stresses with Radii: Stone Replacement (2D wide-1/2D deep), Test 4 - Test Series III.

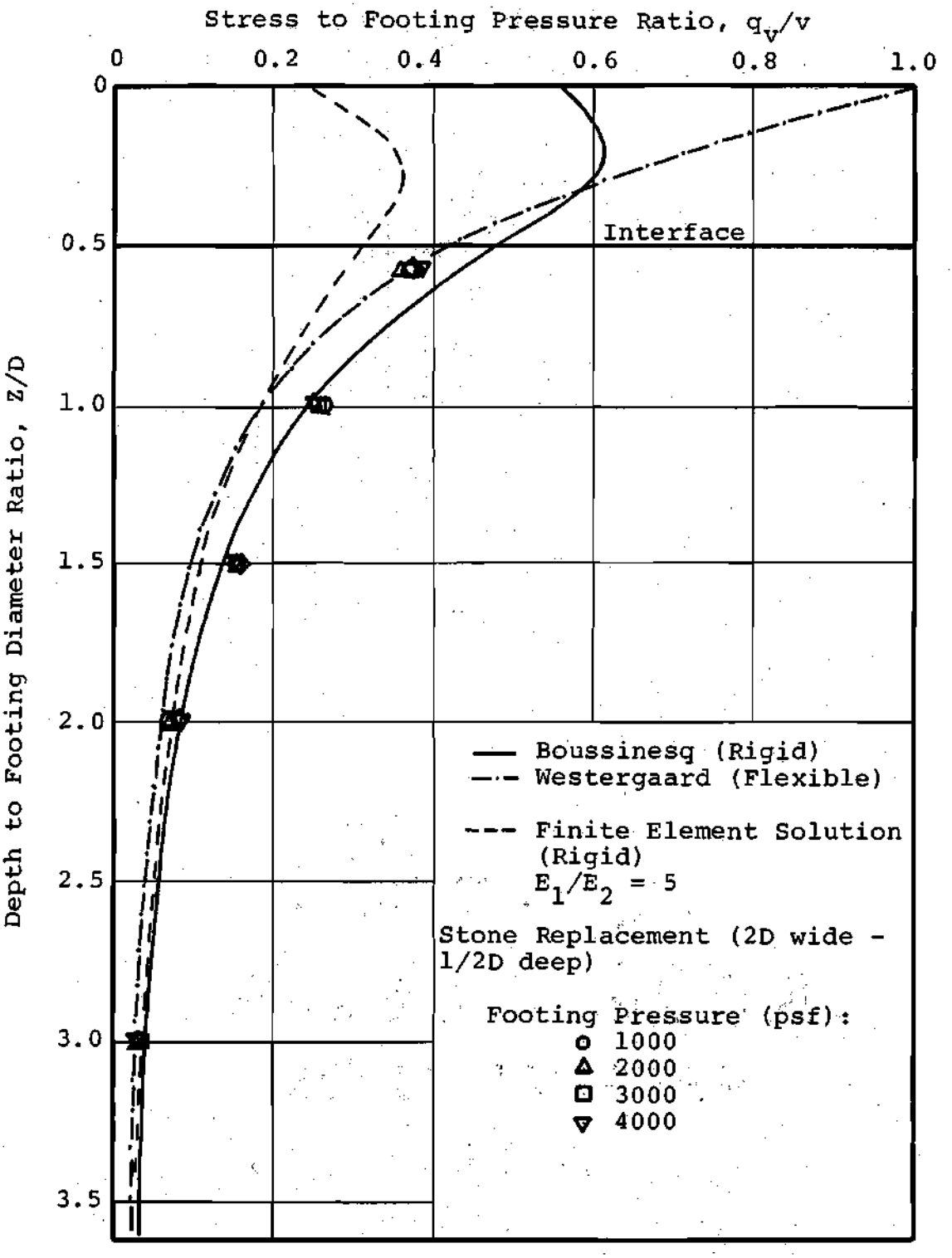

Figure 62. Vertical Stresses at 4 Inch Offset From Load Axis: Stone Replacement (2D wide-1/2D deep), Test 5 - Test Series III.

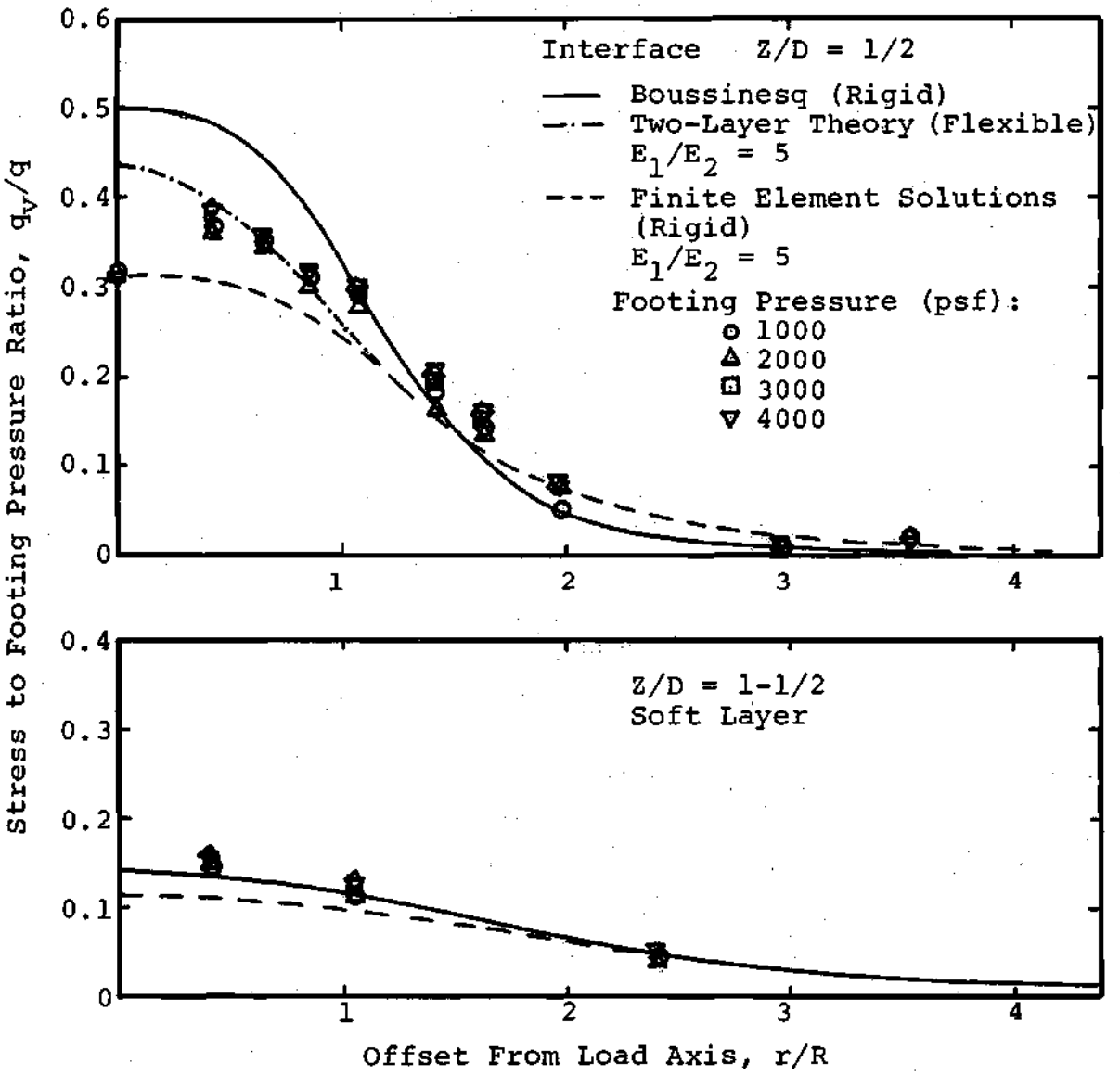

Figure 63. Vertical Stresses with Radii, Stone Replacement (2D wide-1/2D deep), Test 5 - Test Series III.

with radii were measured in the soft layers beneath the stone replacement pads. These test results are shown in Figures 59 through 63.

Strain Measurements

The results of strain measurements were expressed in a normalized form by dividing the measured strains by the footing pressure so that comparison may be made with theoretical solutions.

Homogeneous Clayey Silt Layer - Test Series I

The variation of vertical strain with depth and with radius is shown in Figures 64 and 65. In Figure 64, theoretical solutions using Boussinesq theory for a rigid loading was superimposed for comparison. Schmertmann's approximation of strain distribution [98] was also included.

Sandy Clay Fill Over Soft Soil - Test Series II

The measured strain values from three test conditions using fill thickness equal to 1/2D, 1D and 1-1/2D, are presented in Figures 66, 67, and 68 for vertical strains in both fill and soft layers. The variation of vertical strain with radius within the stiff layer of compacted sandy clay is shown in Figures 69 and 70.

Sand Fill Over Soft Soil - Test Series III

Figures 71, 72, and 73 show the results of strain measurement in sand fill-subsoil systems. Variations of vertical strain with depth along the load axis and at an offset of r/R = 0.5 are plotted. Figures 74 and 75 show the

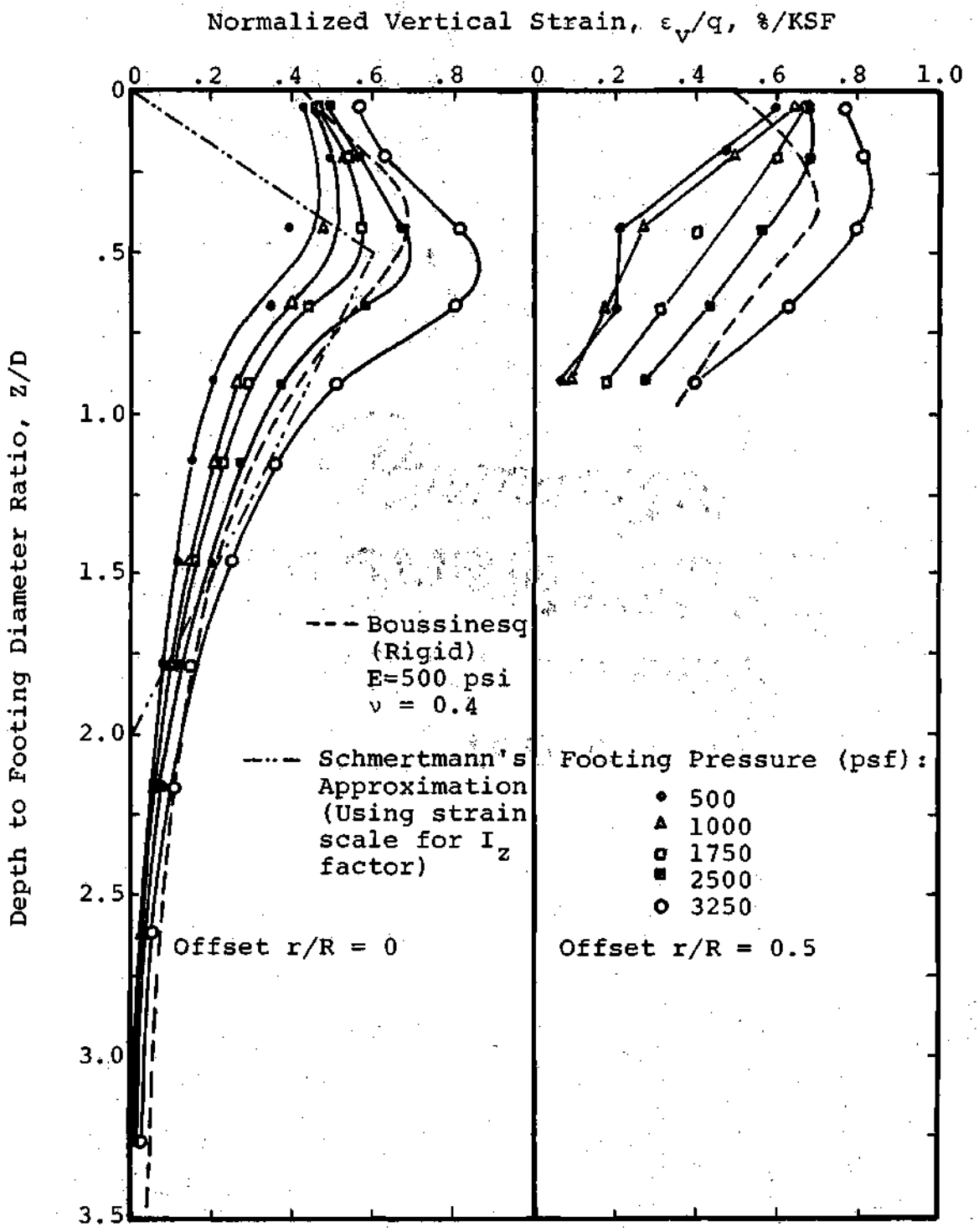

Figure 64. Variation of Vertical Strain with Depth for Homogeneous Soft Layer.

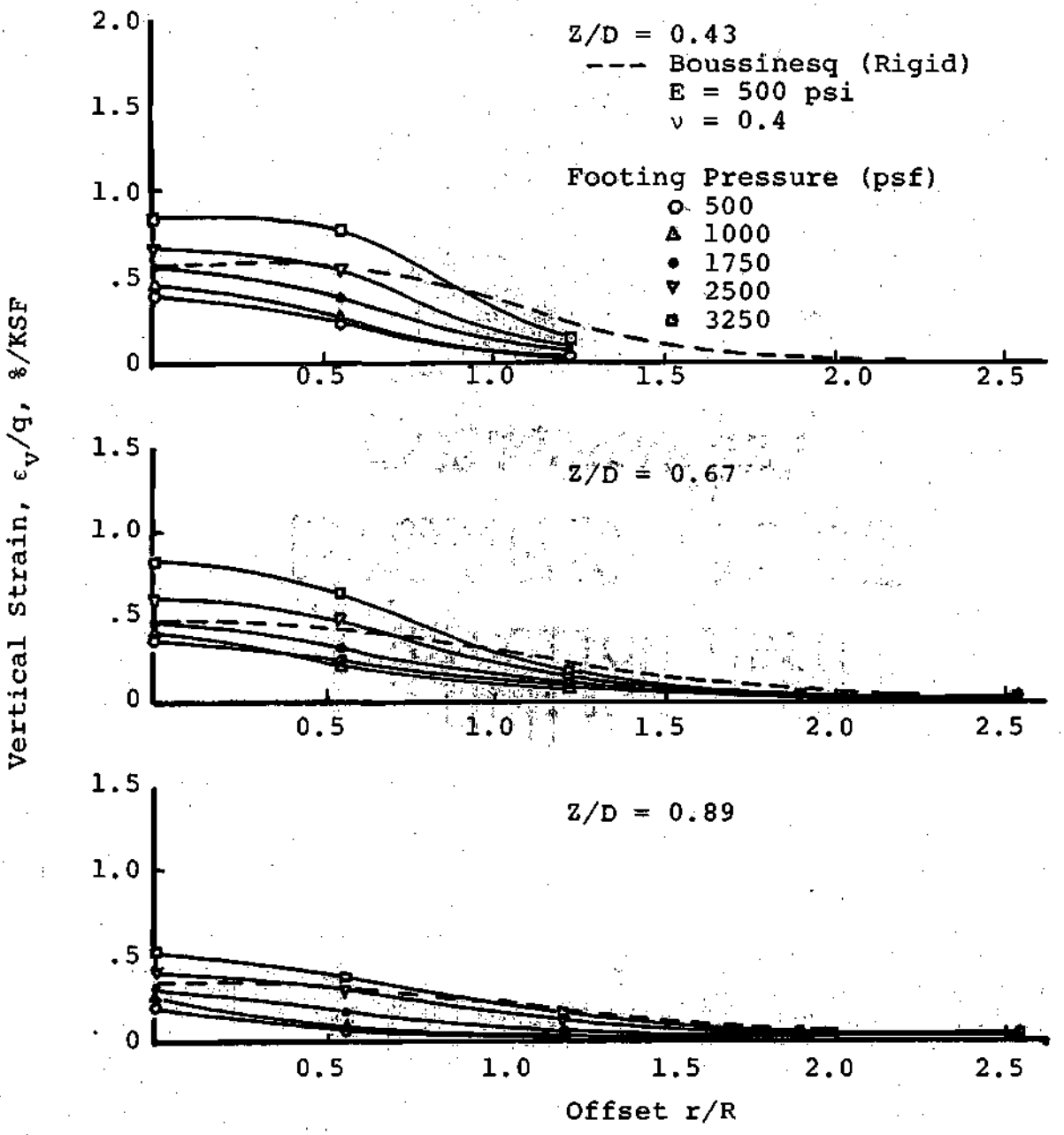

Figure 65. Variation of Vertical Strains with Radii for Homogeneous Soft Layer

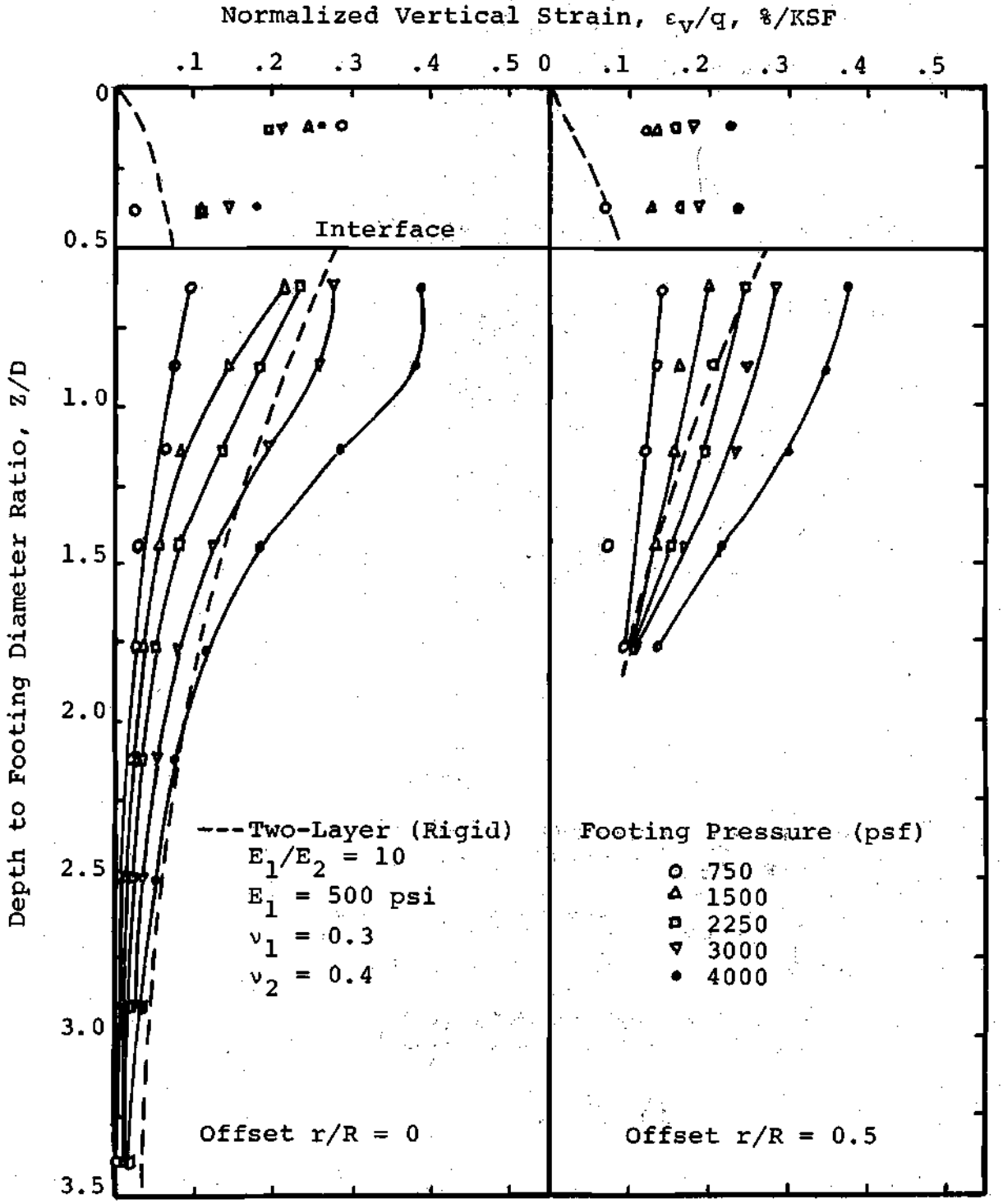

Figure 66. Variation of Vertical Strain with Depth for Sandy Clay Over Soft Layer: H = 1/2D.

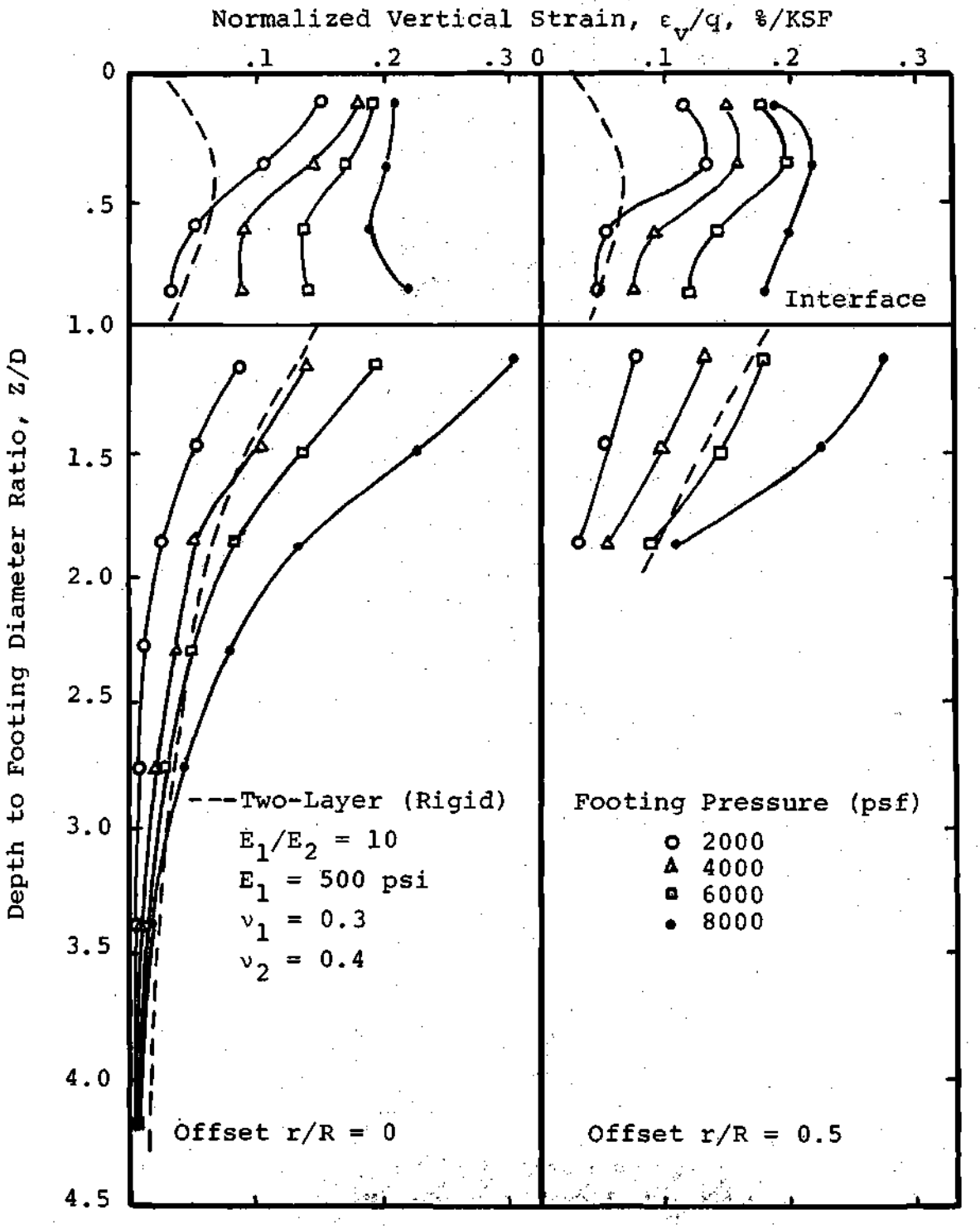

Figure 67. Variation of Vertical Strain vs. Depth for Sandy Clay Over Soft Soil: H = 1D.

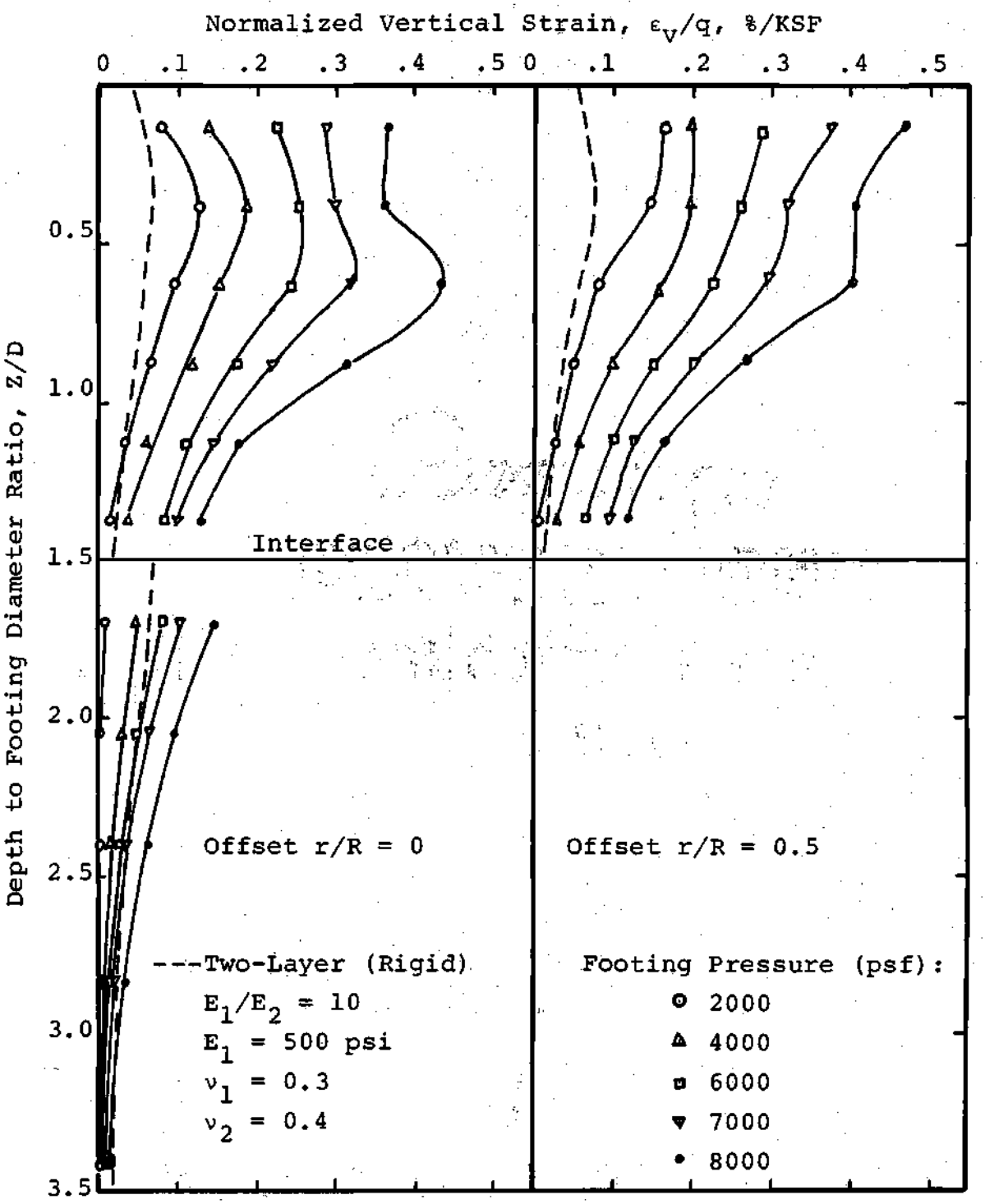

Figure 68. Variation of Vertical Strain vs. Depth for Sandy Clay Over Soft Soil: H = 1-1/2D.

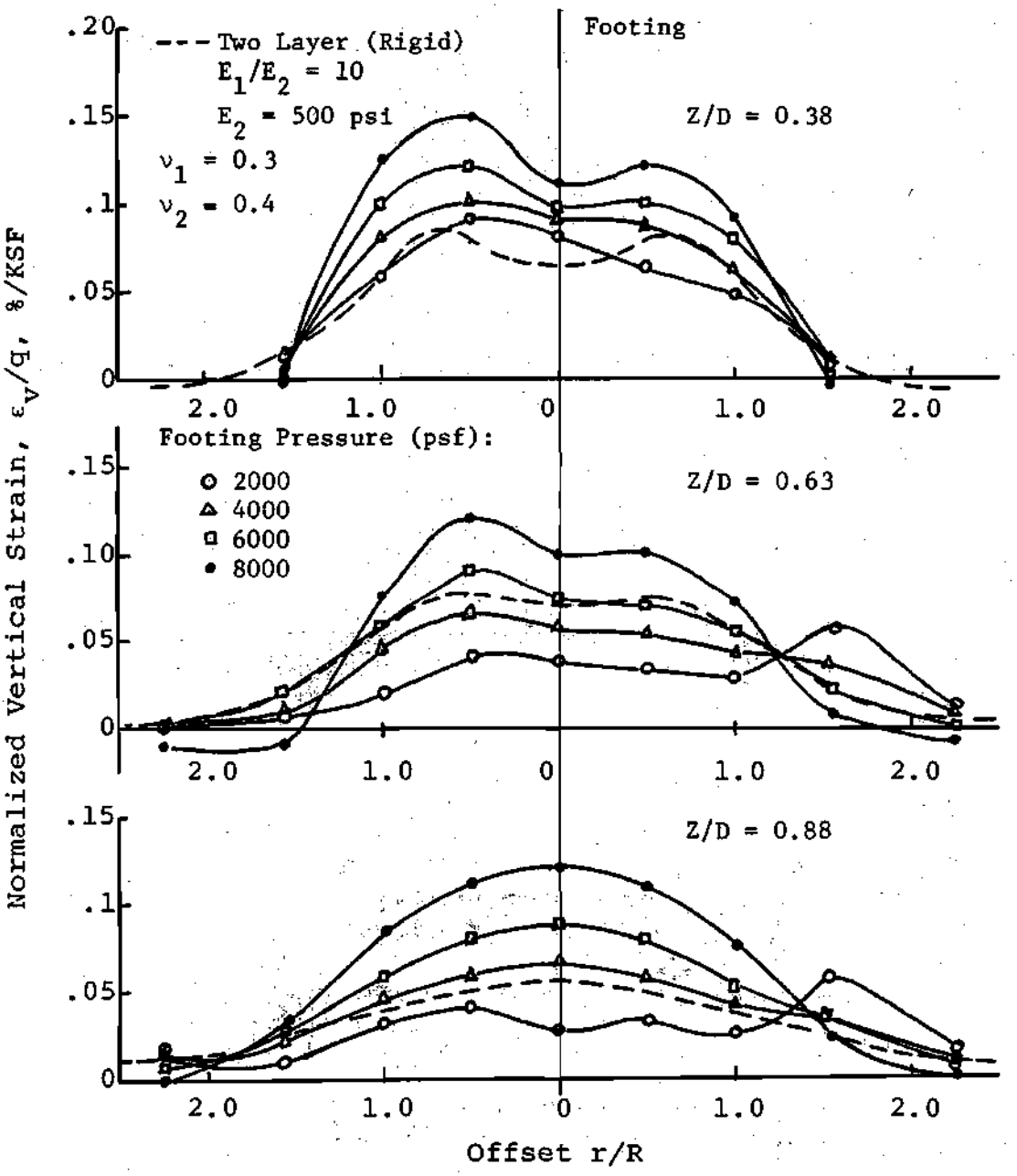

Figure 69. Variation of Vertical Strains with Radii for Compacted Sandy Clay: H = 1D.

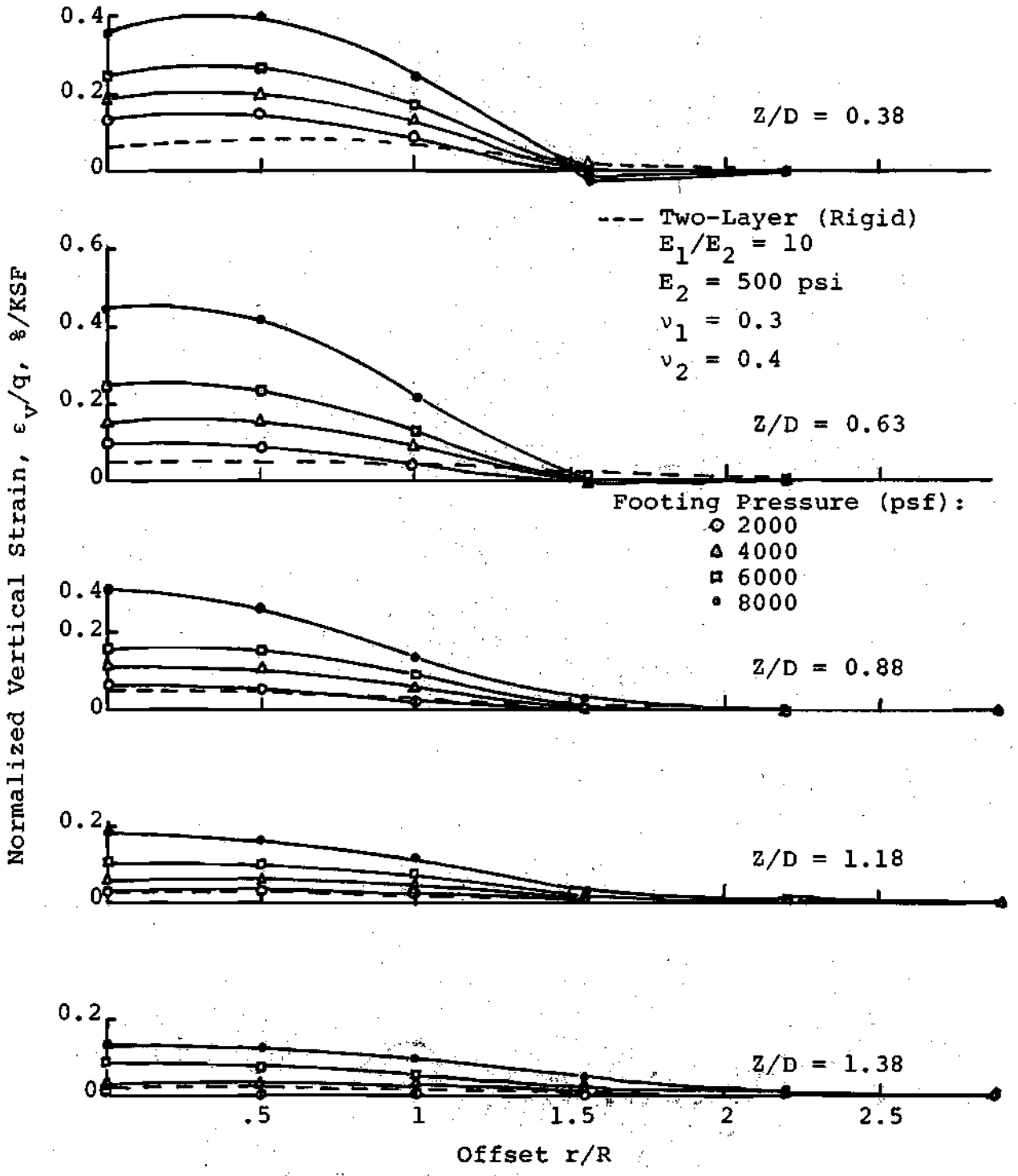

Figure 70. Variation of Vertical Strains with Radii for Compacted Sandy Clay: H = 1-1/2D.

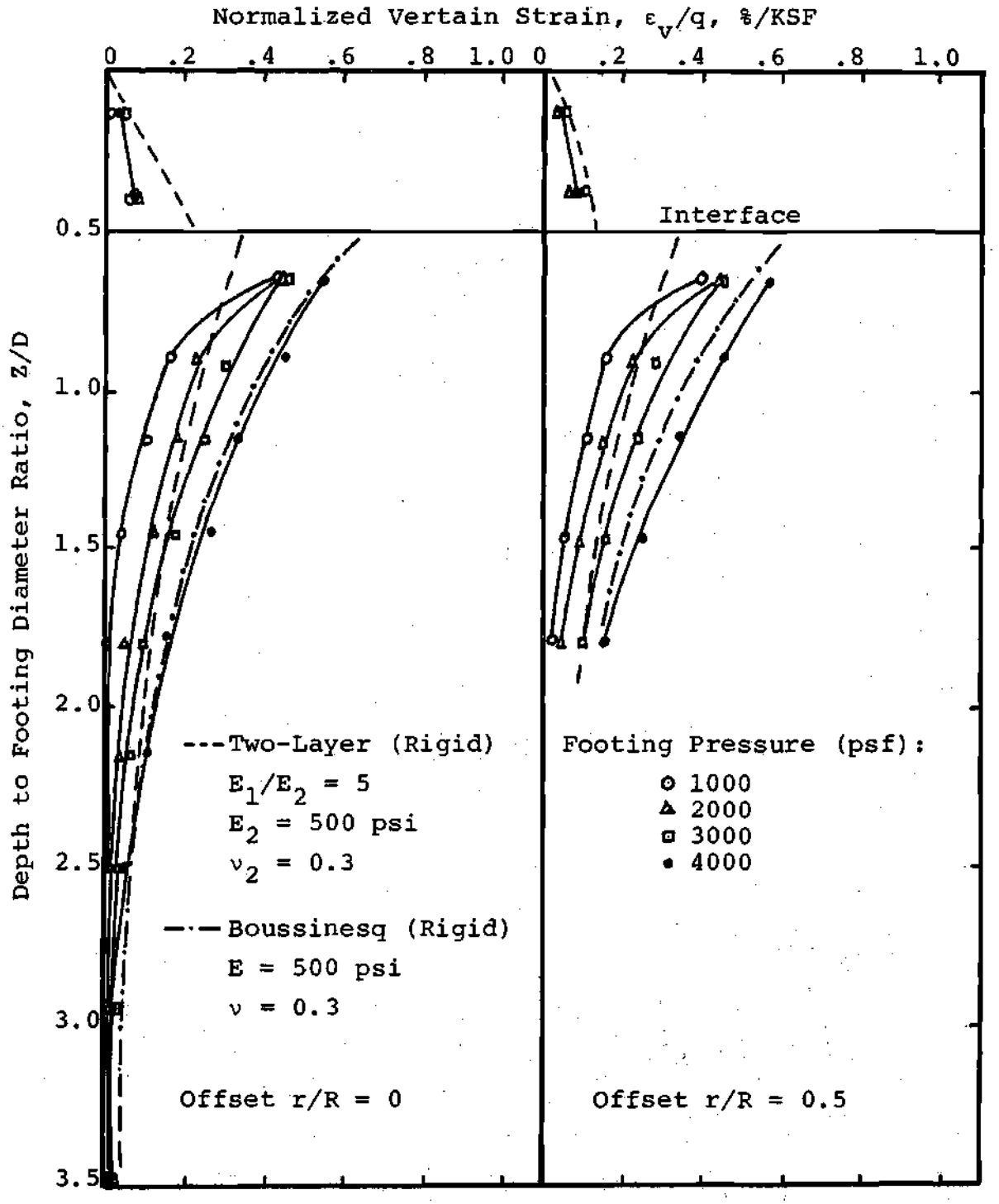

Figure 71. Variation of Vertical Strains with Depth for Sand Over Soft Layer: H = 1/2D.

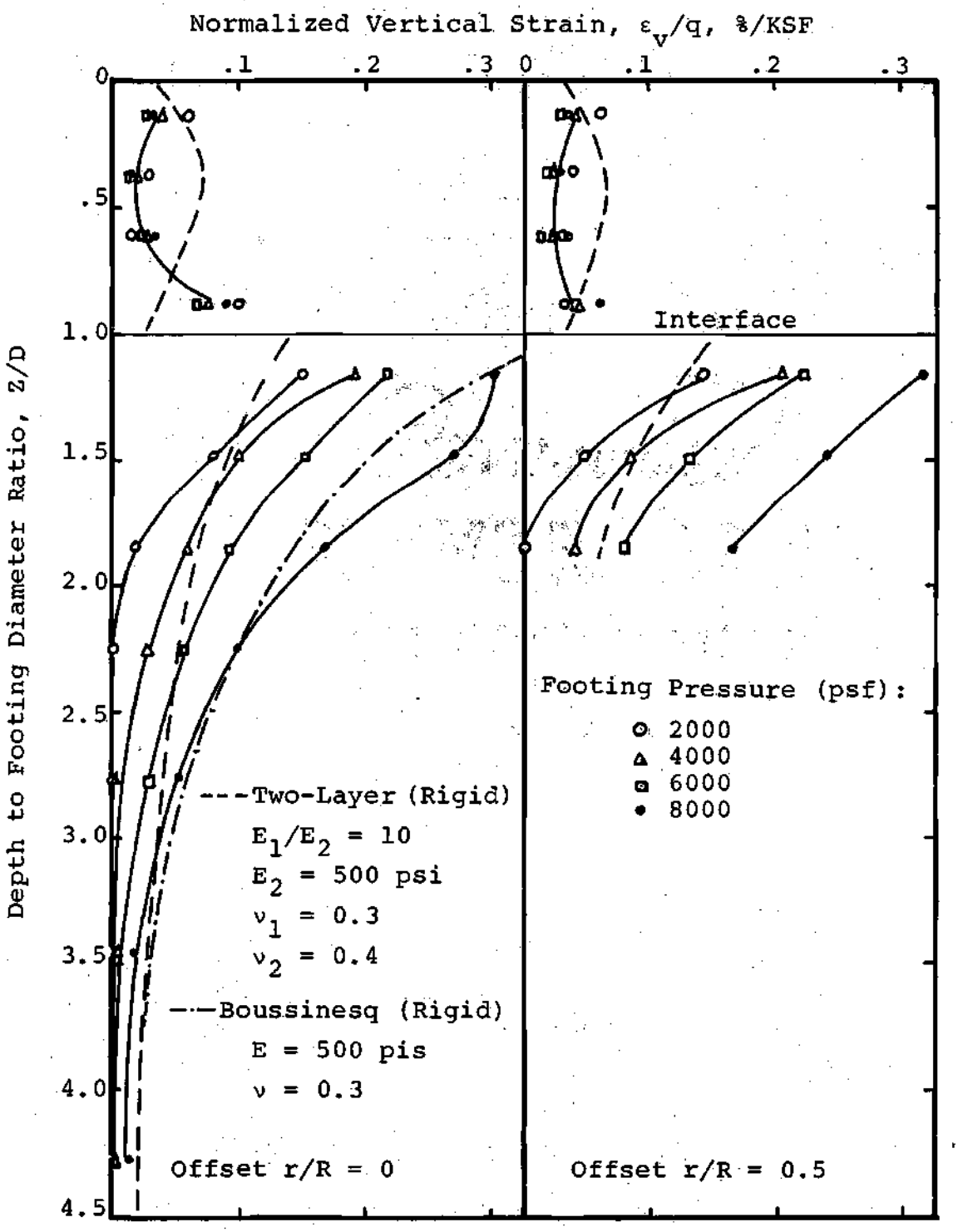

Figure 72. Variation of Vertical Strain with Depth for Sand Over Soft Layer: H = 1D.

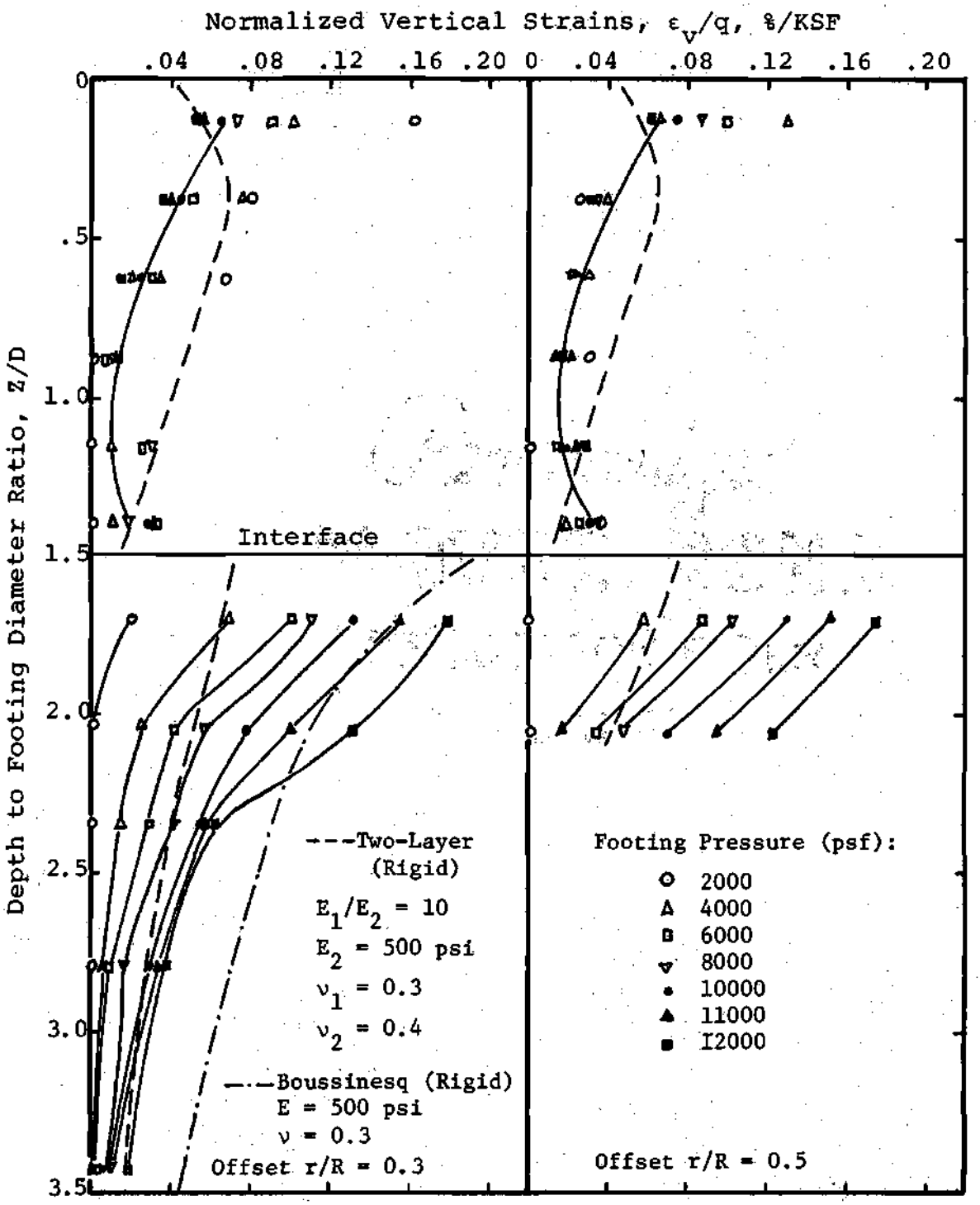

Figure 73. Variation of Vertical Strain vs. Depth for Sand Over Soft Subsoil: H = 1-1/2D.

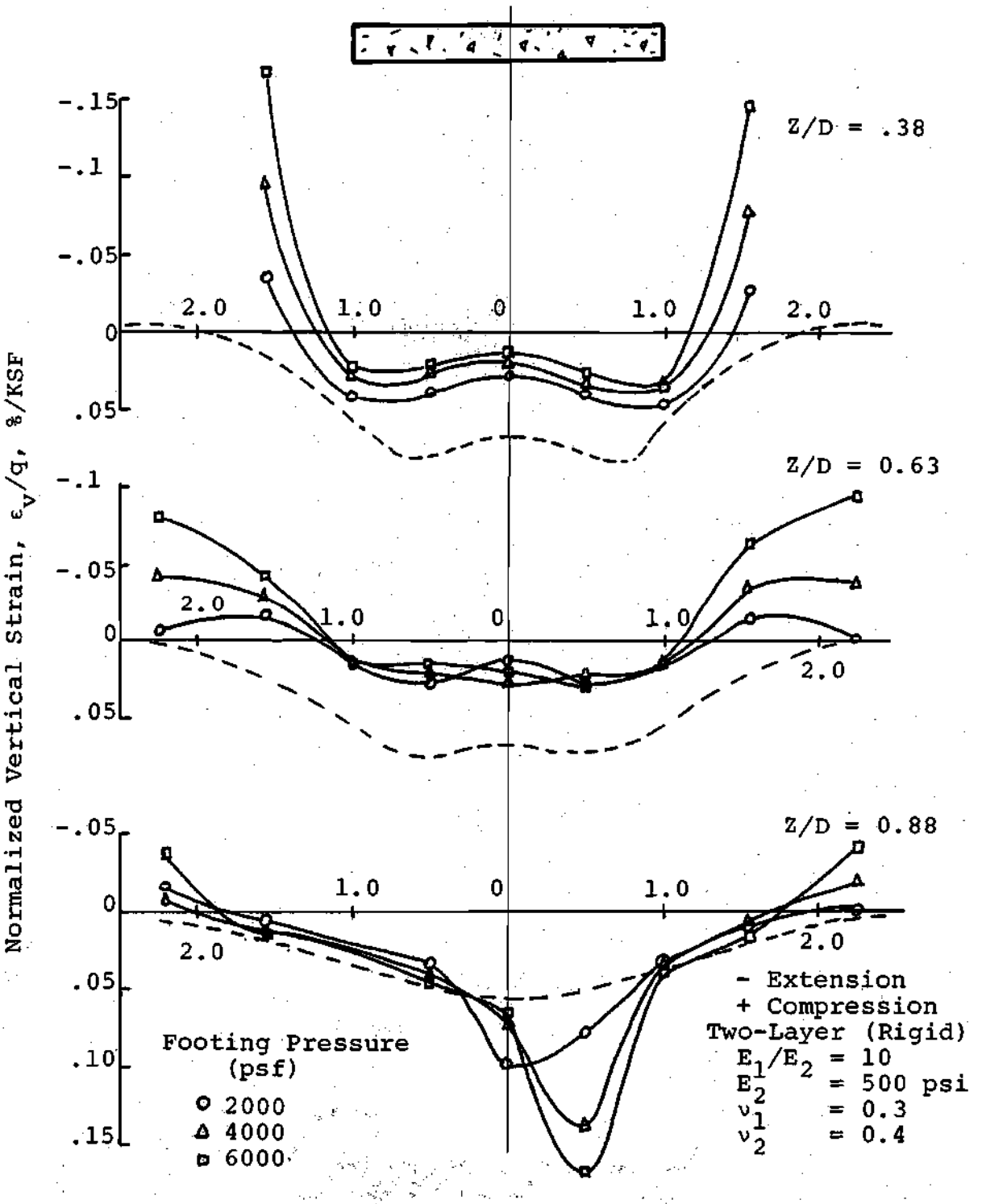

Figure 74. Variation of Vertical Strains with Radii for Sand Over Soft Layer: H = 1D.

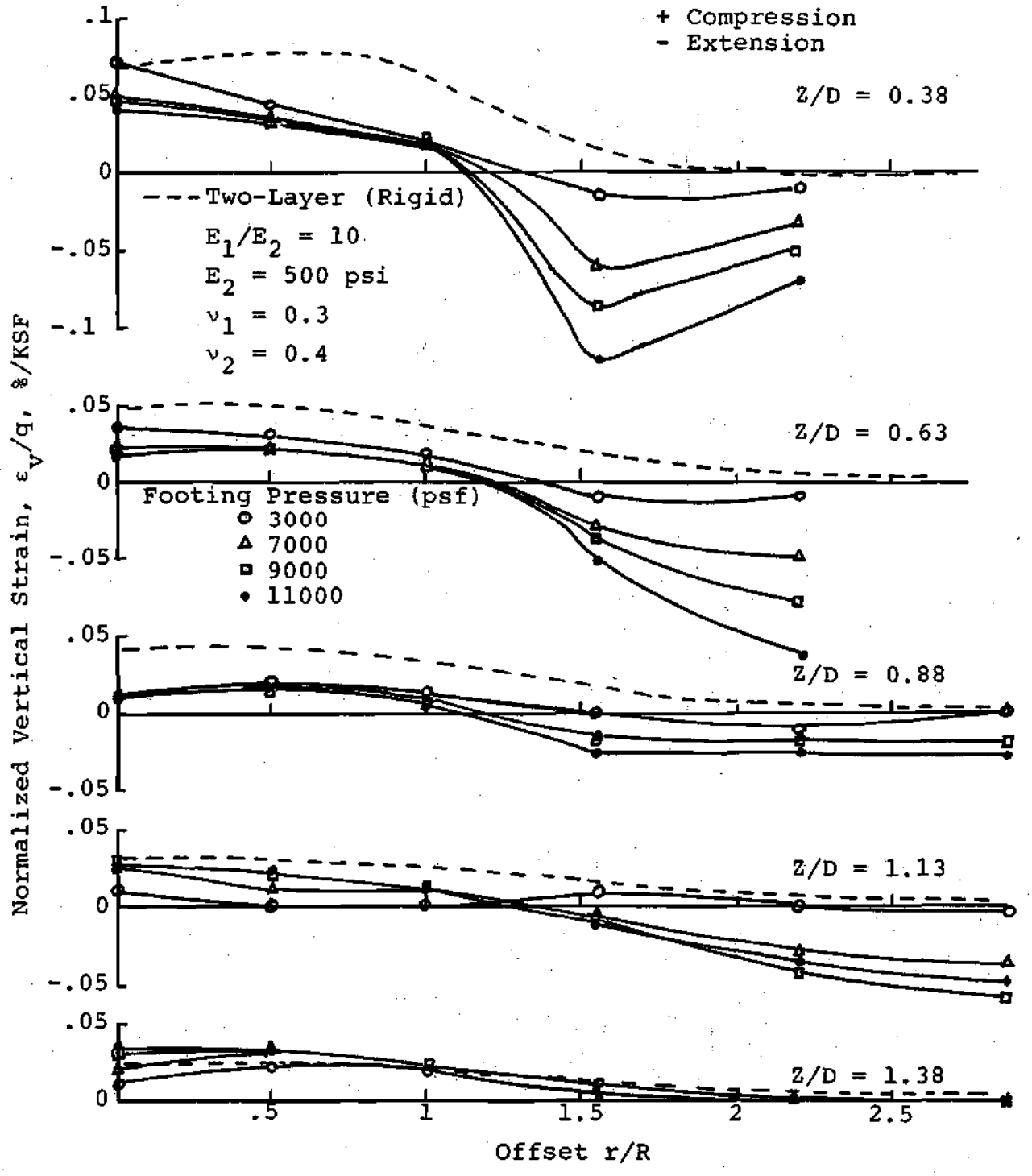

Figure 75. Variation of Vertical Strain with Radius for Compacted Sand: H = 1-1/2D.

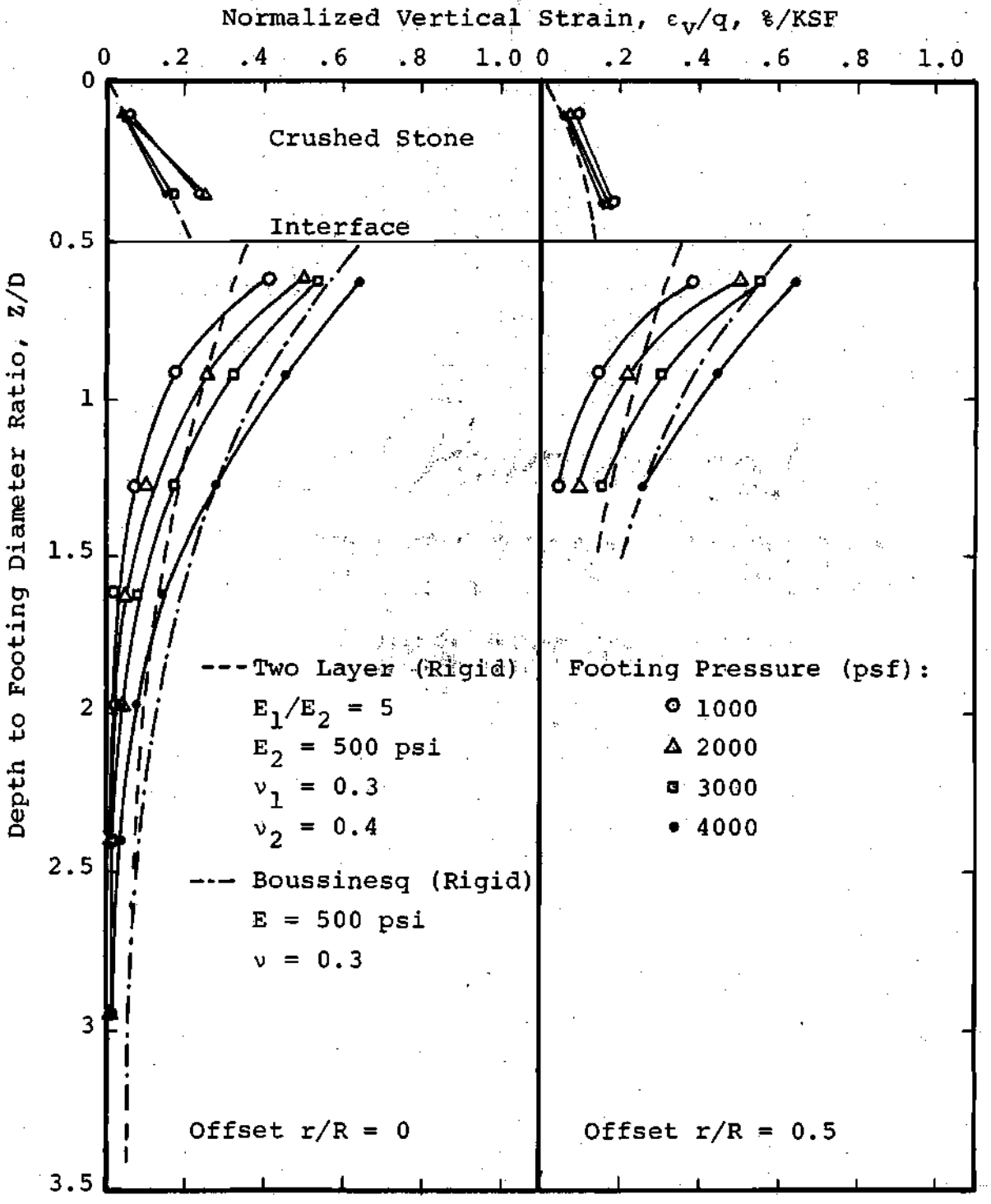

Figure 76. Variation of Vertical Strain with Depth for 1/2D by 2D Stone Replacement Footing.

variation of vertical strain with radius in the sand layers for a fill thickness equal to 1D and 1-1/2D.

The results of strain measurement in the stone replacement pad and in the soft layer are shown in Figure 76.

CHAPTER VII

DISCUSSIONS OF RESULTS

Settlement Measurements

Surface Settlement

Figure 35 shows the load settlement relationships for the rigid footing placed on sandy clay fills having different thicknesses compared with the settlements occurring on a uniform soft soil. The load settlement curves for all tests are nonlinear. As would be expected, replacing portions of the soft soil with compacted structural fill resulted in reduction of settlement considerably. It is seen that the greater the thickness of fill relative to the footing diameter, the smaller the total surface settlements. One exception is for a sandy clay fill having a thickness equal to 1-1/2D. The footing settlements on this fill should have been less than that for a fill thickness of 1D but was not. These results suggest that the fill material was not as well compacted as that for the fill with a thickness of H=1D. The triaxial test results also showed that this fill had a lower strength as compared with the samples from fill with H = 1/2D and 1D.

For each load test, footing settlement under each load increment was also obtained by summing up the change in gage length between each pair of coils which were vertically

stacked along the axis of footing to a depth of at least 4D or to the bottom of the test pit. Beyond the depth 4D, the soil deformations under loads were small and considered to be negligible. These results are presented as dashed lines and can be compared with the measured surface settlements for each load test as shown in Figure 35. All of the settlements from strain sensor readings were found to be greater than the measured settlements, with the difference being not greater than 15 percent.

The results of settlement measurements for sand fill over soft subsoils (Test Series III) are shown in Figure 36. These results are also compared with the load settlement curve for the uniform subsoil condition. The reduction in surface settlements for all cases is evident, indicating that compacted sand fill can be used effectively to reduce the settlement of a foundation on a weak subsoil. The amount of settlement reduction, however, depends upon how much soft soil was replaced. As would be expected, increasing the thickness of sand fill decreased the surface settlement similar to the results obtained for the compacted sandy clay fill. The settlements obtained using strain sensor readings are also superimposed on the load settlement curves for each test. Good agreement was obtained between the measured surface settlement and settlements obtained using strain coil readings.

The surface settlement for different thicknesses and

widths of foundations using stone replacements are presented in Figure 37. It is evident that replacing only a small portion of the soft subsoil beneath the footing with crushed stone is effective in reducing the settlement. The stone replacement with a width of 2D is more effective in reducing surface settlement than using a width of only 1D and the same depth. This is expected because increasing the diameter of the stone replacement decreases shear stresses at the circumferential stone-soft soil interface. When the thickness of the stone area is reduced to 1/2D, the settlement is not much different from that for thicknesses 1D. This could be due to the stone with 1/2D depth having a higher density. The 1/2D stone replacement foundation was conducted at the test location used for the 1/2D sand fill test after the soft subsoil was further excavated to a depth of 1/2D. The soft subsoil was partially loaded once. Therefore, the settlement of this stone replacement was not as much as it would have been had it not been previously loaded.

The load settlement curves for strucutral fill and stone replacements of thickness H = 1/2D, 1D, and 1-1/2D are presented separately in Figures 38, 39, and 40 for comparison. The load settlement curves for the fills and stone replacements with H = 1/2D fall in a narrow band as shown in Figure 38. The settlement reduction is evident in all cases. The load settlement relations for fills and stone replacements with a thickness 1D are shown in Figure 39. It is seen that

compacted sand and clay fills are more effective in reducing surface settlement than stone replacement having the same thicknesses. The compacted sand fill, however, produced less surface settlement than the sandy clay fill. It will be later shown that most of the settlement of the sand fill came from the soft subsoil whereas for the sandy clay fills a significant amount of settlement occurred in the fill itself. Figure 40 compares the surface settlement of the sandy clay fill with that of sand fill. This figure indicates that the settlement in the fill contributed a significant portion to the total settlement.

If a total settlement of 1/4 inch is used as a design criterion, the effect of increasing the thickness of fill on the magnitude of the allowable bearing pressure can be evaluated as shown in Table 7. It is seen that as the fill thickness increases, the allowable bearing pressure that would cause a 1/4 inch settlement also increases. For a fill thickness of 1/2D, using either compacted sandy clay or sand as fill increases the footing pressure to about 1.7 times that for footings placed on the uniform soft soil. Increasing the fill thickness to 1D increases the footing pressure ratio to 2.75 for sandy clay fill and 3.0 for sand fill. When the fill thickness is further increased to 1-1/2D, sand fill increases the footing pressure to about 4.6 times that for the footing on the uniform soft soil. The results for sandy clay fill with H = 1-1/2D were not as good as those

Table 7. Comparison of Footing Pressures for Different Fill Thicknesses Based on a Settlement of 1/4 Inch.

Type	Pressure, psf	Pressure on Fill / Pressure on Uniform Soil
Uniform Soft Soil Only	2000	
Sandy Clay Fill:		
H = 1/2D	3300	1.7
H = 1D	5500	2.75
H = 1-1/2D	5400	2.7
Sand Fill:		
H = 1/2D	3350	1.7
H = 1D	6000	3.0
H = 1-1/2D	9100	4.6
Stone Replacement:		
2D wide-1/2D deep	3000	1.5
2D wide- 1D deep	3300	1.7
1D wide- 1D deep	2800	1.4

for sand fill. Partially replacing soft soil with crushed stone in all cases increases the footing pressure to about 1.4 to 1.7 times that for a footing on a homogeneous soft layer.

If the footing is proportioned for a normal allowable bearing pressure of 2000 psf, the reduction of footing settlement with increasing fill thickness can also be determined as shown in Table 8. Using a fill thickness of 1/2D can reduce the surface settlement by about 60 percent for sandy clay or sand fills. Increasing the fill thickness to 1D, the percent reduction is increased to about 80 to 84. Further increase in fill thickness to 1-1/2D does not reduce the settlement significantly because most of the settlement occurs in the fill material, which set the limit of settlement reduction.

Figure 77 summarizes the results of the surface settlement of a footing placed on structural fill overlying a soft soil based on the two design criteria as previously used. In Figure 77a using 1/4 inch settlement as the design limit, it is seen that the footing pressure increases rapidly as the fill thickness increases. If the allowable bearing pressure of 2000 psf is shown in Figure 77b, the percentage of the settlement reduction sharply increases when thin fill layers are used. As the fill thickness further increases, the percentage reduction in footing settlement approaches asymptotically a constant value of approximately 90 percent, where the settlement of the fill layer rather than of the soft subsoil governs the design.

Table 8. Comparison of Footing Settlements for Different Fills Thicknesses Using a Design Pressure of 2000 psf.

Type	Settlement, inch	% Settlement Reduction*
Uniforn Soft Soil Only	.25	0
Sandy Clay Fill:		
H = 1/2D	.10	60
H = 1D	.05	80
H = 1-1/2D	.03	88
Sand Fill:		
H = 1/2D	.10	60
H = 1D	.04	84
H = 1-1/2D	.03	88
Stone Replacement:		
2D wide-1/2D deep	.13	48
1D wide- 1D deep	.12	52
2D wide- 1D deep	.10	60

*Based on the footing settlement on the homogeneous condition.

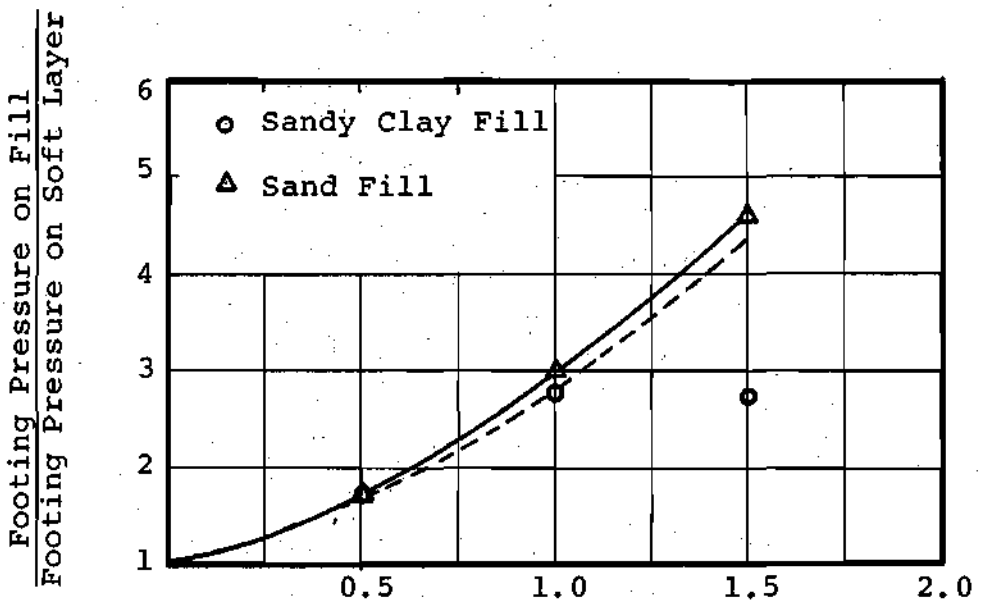

a) Based on a 1/4 inch settlement.

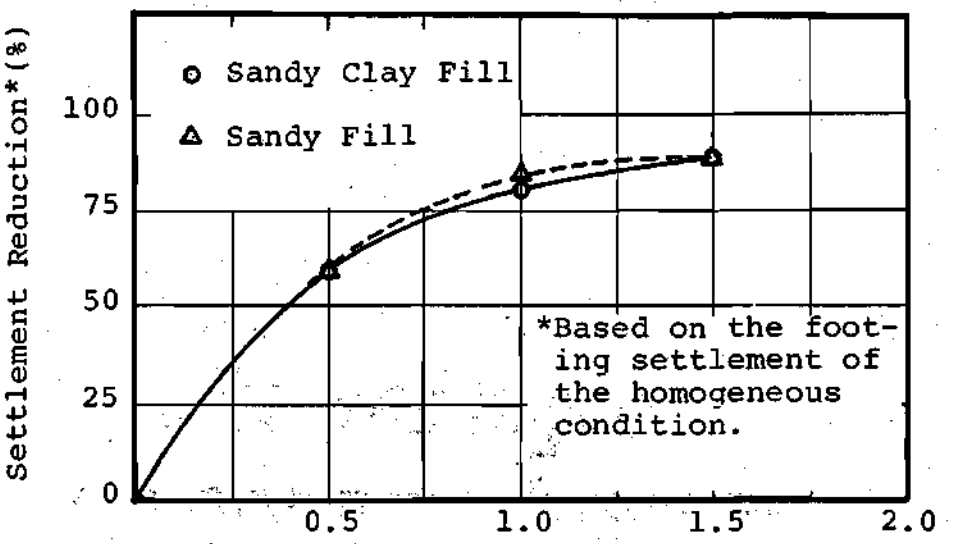

b) Based on an allowable bearing pressure of 2000 psf.

Figure 77. Effects of Compacted Fills in Reducing Pressures and Settlement.

For an allowable footing pressure of 2000 psf, using stone replacements is effective in reducing the surface settlement which can be reduced by as much as 60 percent. Since the stone was lightly compacted to simulate the field conditions where the stone is simply dumped in the prepared area, a significant amount of settlement occurred in the stone. These results seem to indicate that for lightly loaded structures where the footing pressure can be kept in the range of 2000 psf, uncompacted stone replacement can be used effectively to reduce the settlement.

Settlement of Soft Layer

The reduction of surface settlement as the fill thickness increases partially reflects that greater portions of the highly compressible material have been replaced with less compressible soils resulting in a settlement reduction. It does not necessarily indicate whether the fill layer is beneifical in reducing the settlement beneath and, thus reducing the stress, to less than that indicated for a homogeneous soil condition. The settlement of the soft subsoil under the fill was determined by subtracting the settlement occurring in the fill from total settlements. The settlements in the fills were obtained using the strain sensor readings. Because the total settlement obtained from strain coil readings were 10 to 15 percent greater than the measured settlements as discussed previously, the settlement in the fill layers using the strain

sensor readings were adjusted in direct proportion. The load settlement relationship is nonlinear for all cases.

Figure 41 shows a comparison between the settlement of the soft layer beneath the compacted fill and beneath stone replacements having a thickness of 1/2D with that occurring in the uniform soft soil below the same depth. The settlement reduction in the soft layer due to placement of structural fill to less than that indicated by the homogeneous soft soil condition is evident, indicating the protection afforded by the fills. The settlement of soft subsoil beneath the sandy clay fill is less than that for the sand fill and stone replacement foundation. This is expected because the compacted clay fill is more capable of spreading the load than compacted sand with comparable thicknesses. The settlements of the soft subsoils for sand fill and stone replacements with a width of 2D and 1/2D thickness are practically the same indicating that replacing only a portion of soft subsoil with crushed stone is as effective in protecting the soft subsoil as placing a layer of sand fill.

As the fill thickness increased to 1D, the settlements of the underlying soft subsoil decrease considerably using sandy clay or sand as compacted fills as shown in Figure 42. The beneficial effect of the structural fill in reducing the settlement in the soft subsoil is clearly evident when compared with the settlement of the soft soil at the same depth for the homogeneous condition. As would be expected, the

sandy clay fill is more effective in reducing the settlement of the soft layer than a sand fill. The compacted clay fill is capable of carrying tension whereas the sand cannot carry significant amounts of tension. The very lightly compacted stone replacements having 2D width and 1D depth are not as effective in reducing the settlement of subsoil as compacted sandy clay and sand fills. The settlement of the soft soil beneath the 1D deep by 1D wide stone column is very nearly the same as the settlement of the soft soil at the same depth from the homogeneous condition, indicating stresses similar to those for a homogeneous condition.

Figure 43 compares the settlement of the soft soil underlying the compacted fill with a thickness of 1-1/2D to that of the soft soil for the uniform, homogeneous condition at the same depth. A considerable amount of reduction of the soft subsoil settlement was obtained showing the beneficial effect of the fill in reducing the settlement of the soft subsoil. It is seen that the sandy clay fill is more effective in reducing settlement at low footing pressures. At high footing pressures, the sand fill is more effective because the ultimate bearing capacity of the sand layer is greater than that of the sandy clay.

For an allowable footing pressure of 2000 psf, the settlement reduction as a function of the fill thickness can be evaluated (Table 9). For a pressure of 2000 psf, placing a footing on the sandy clay structural fill with

Table 9. Comparison of Settlements of Soft Subsoil Beneath Different Fill Thicknesses at a Design Footing Pressure of 2000 psf.

Type		Settlement, inch	% Settlement Reduction*
Uniform Soft Soil:	1/2D	0.16	-
	1D	0.095	-
	1-1/2D	0.05	-
Sandy Clay Fill:	1/2D	0.08	50
	1D	0.03	68
	1-1/2D	0.01	80
Sand Fill:	1/2D	0.095	41
	1D	0.035	63
	1-1/2D	0.0125	75
Stone Replacement:			
2D wide-1/2D deep		0.11	31
1D wide- 1D deep		0.095	No Reduction
2D wide- 1D deep		0.06	37

*Based on the settlement of the homogeneous condition at the same depth.

H = 1/2D could reduce the settlement in the soft layer by as much as 50 percent. If a compacted sand fill is used, the reduction is about 41 percent. Increasing the fill thickness to 1D increases the percentage reduction to 68 for sandy clay fill and 63 for sand fill. Further increase in fill thickness to 1-1/2D does not reduce the settlement of the soft layer appreciably. When stone replacement is used, the settlement of soft soubsoil is reduced 37 percent or less for the low level of compaction of the stone used in these tests.

These results are plotted in Figure 78 to develop a relationship between the fill thickness and percentage reduction of the soft subsoil settlement. As the fill thickness increases, the curves asymptotically approach a value of 100 percent.

Stress Measurements

Theoretical Stress Distribution

One of the main objectives of this study is to check the validity of elastic theory as applied to a homogeneous soft soil and structural fill-subsoil systems. On each plot of measured stresses, there are superimposed theoretical solutions for comparison with the experimental points.

Even though the stress-strain characteristics of the soils used are non-linear, a linear elastic theory was used to predict the stress distribution. Theoretical investigations [52, 53, 67] have shown that non-linearity and non-homogeneity of soils have little effect on the distribution of vertical

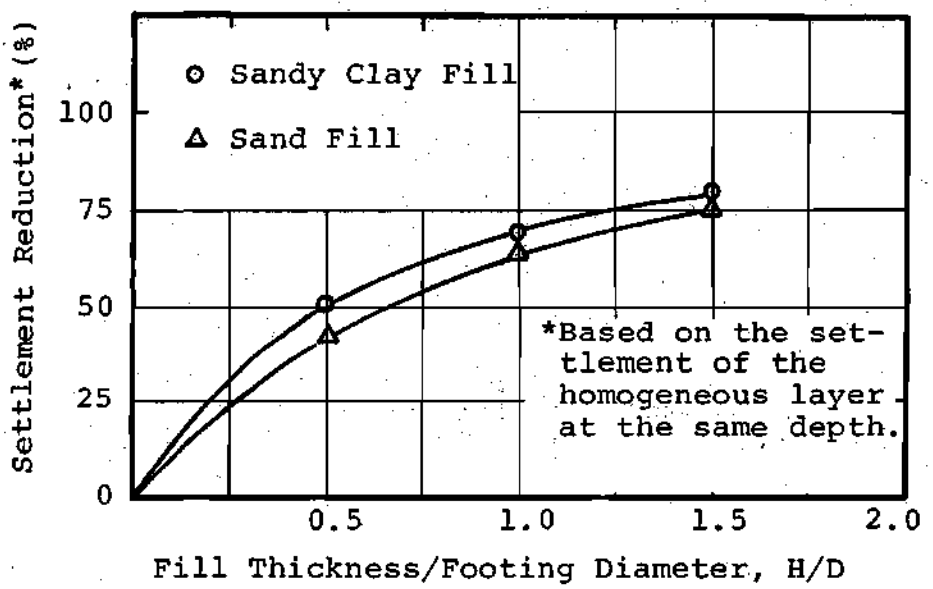

Figure 78. Reduction of Settlements in Soft Layer Based on an Allowable Footing Pressure of 2000 psf.

stress and a linear elastic theory may be used to predict the stress distribution in non-linear, non-homogeneous soil media. It will later be shown that the results of this study support these findings.

Rigid Displacement Theory. The footing load tests were conducted using a rigid concrete footing to simulate the nearly rigid condition of the actual foundation of structures. The closed form solutions developed by Gerrard and Harrison [46] were used to calculate vertical stresses at an offset of 4 inches from the load axis with depths and with radii at different depths. The results were superimposed on the plots of measured stresses from Test Series I - uniform soft soil and Test Series II and III - fill-subsoil systems.

Finite Element Approximation. Since theoretical solutions for a rigid footing loaded on the surface of a two-layer system of a stiff over a softer stratum are not presently available, a finite element method was used to approximate the stress distribution for the fill-subsoil systems. A linear finite element program rather than a non-linear one was used because it had been found [53] to give a good approximation of vertical stress distribution in a non-linear and stress-dependent soils. The program was for an axisymmetric solid by Barksdale [11].

Finite element grids were evaluated in an effort to optimize the results within the constraints imposed by the storage capacity of the computer. The array that was ulti-

mately selected is shown in Figure 79 and consists of 247 rectangular elements connected at 280 nodes. The elements were constructed to be small and numerous in the region of high stress gradients beneath the rigid footing and increase in size and decrease in number away from the footing in the radial r and vertical z direction. The elements in the z-direction were arranged in such a way that a two-layer system of a stiff over softer layer having H/D = 1/2, 1 and 1-1/2 could be modeled. Since the calculated stresses are given as an average value at the center of each element, the interface stresses between the fill and soft layers were determined by using a layer of thin elements close to the fill layer.

A series of computer runs was performed to insure accuracy of the finite element analysis in predicting the stress distribution in elastic media. Several runs were made for a single layer and two-layer system using both rigid and flexible loading conditions. The computer solutions of vertical stresses at an offset of r/R = 0.028 are compared with closed form solutions [44, 46] in Figure 80. The solutions of vertical stresses with radii were presented in Figure 81.

For uniform loading conditions, equal pressures were simply applied over the elements beneath the footing. For a rigid displacement condition, a uniform displacement at the nodal points beneath the footing was initially specified.

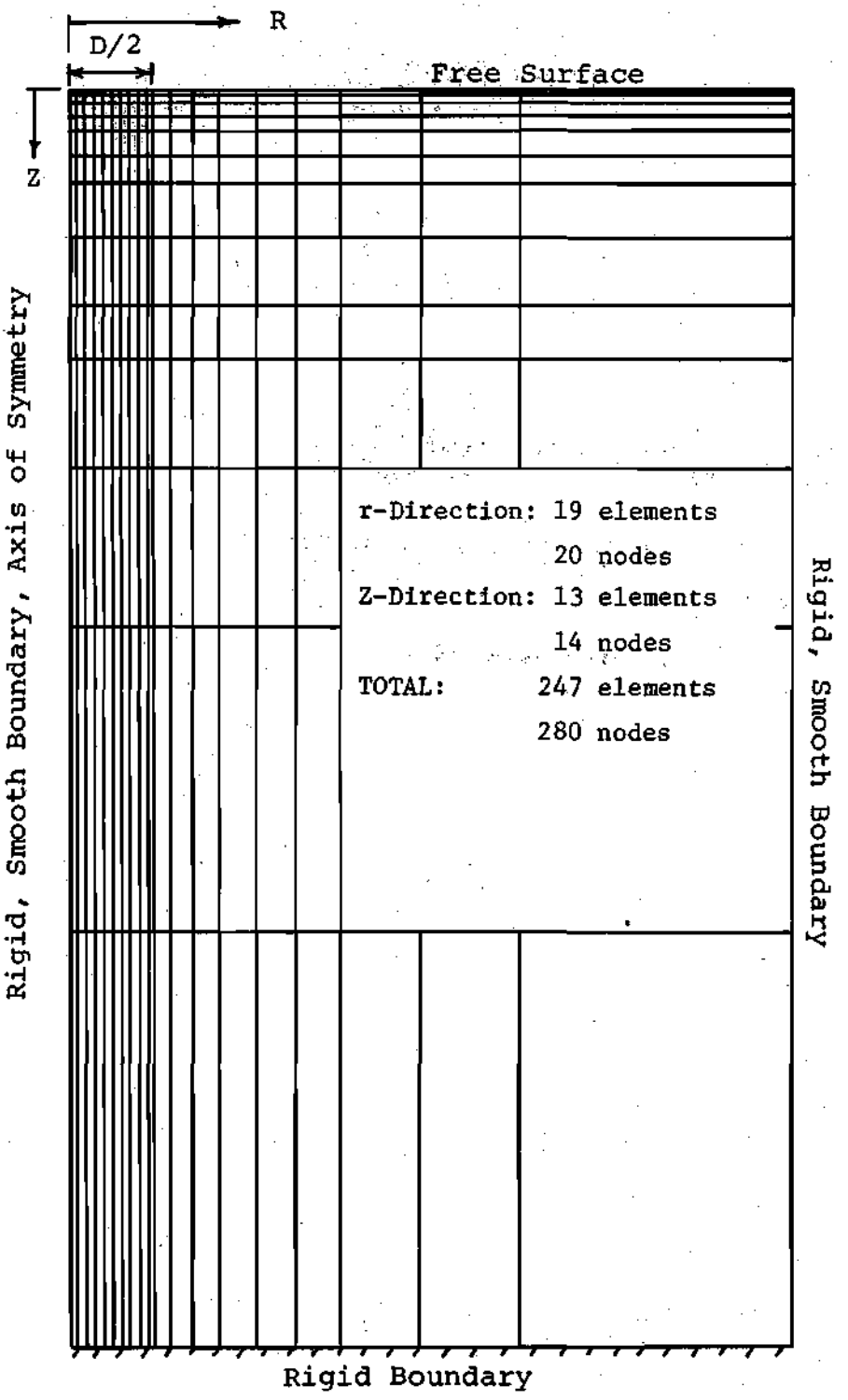

Figure 79. Finite Element Grid Used to Analyze Structural Fill Loaded with a Rigid Footing.

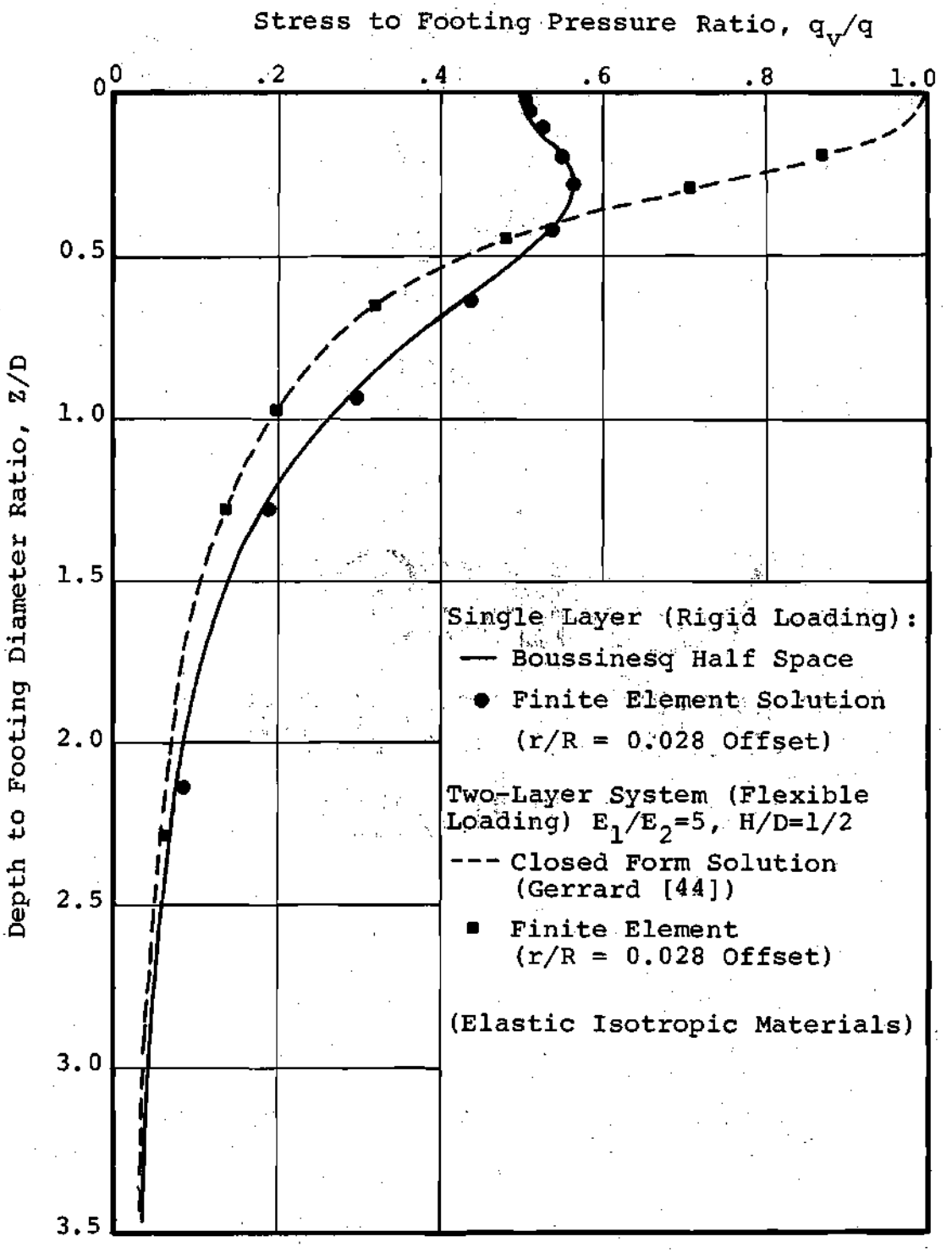

Figure 80. Distribution of Theoretical Vertical Stresses With Depth on Load Axis.

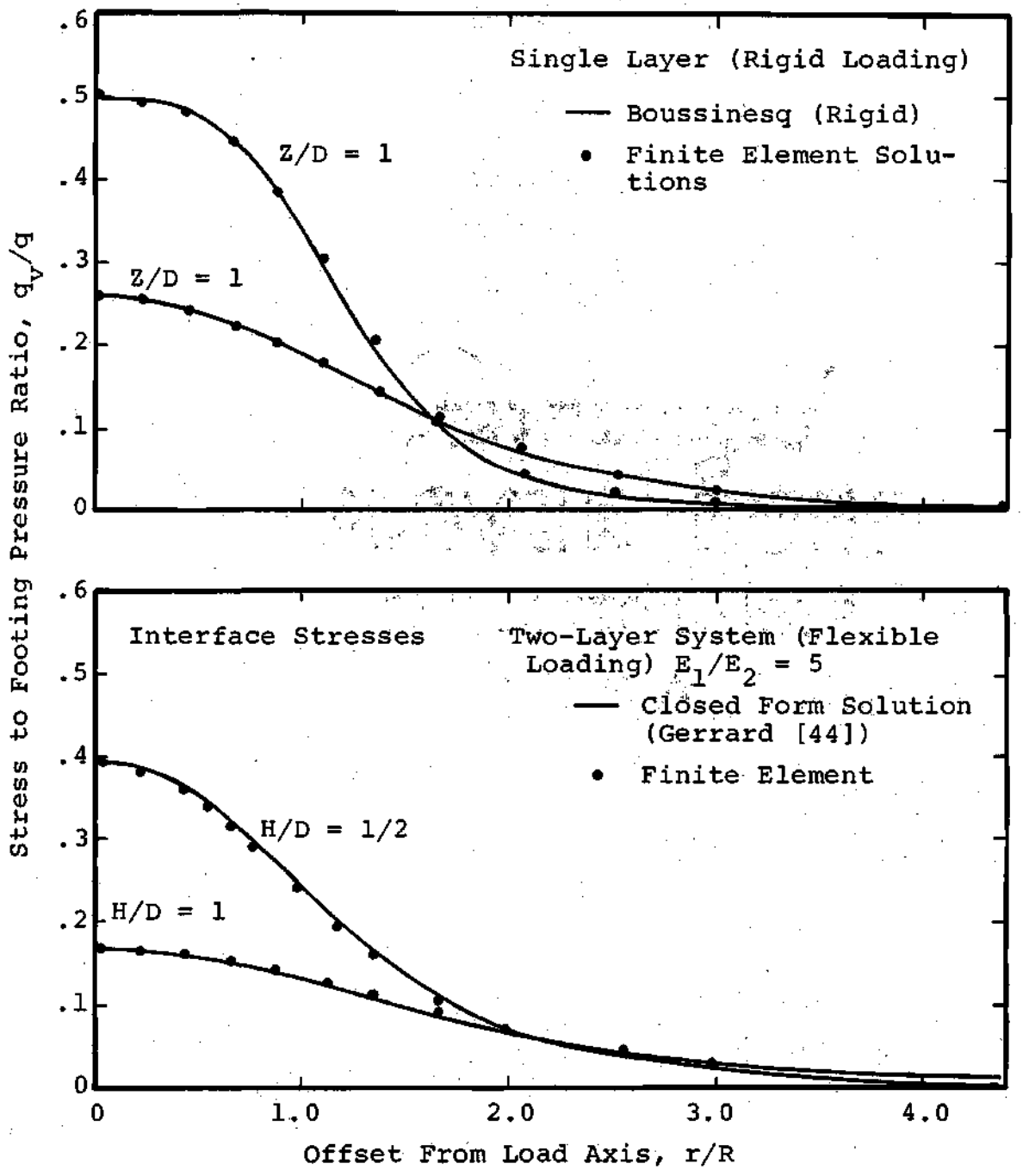

Figure 81. Theoretical Vertical Stresses with Radii: Single and Two-Layered Systems.

The footing was assumed to be smooth since the nodes were allowed to move in the r-direction. Only one half of the footing was loaded along the axis of symmetry.

To determine the average footing pressure for a rigid condition, the computed stresses from the elements immediately beneath the footing were plotted as a function of radial distance from center line axis. The footing contact pressure was then integrated using an approximate method to obtain a total applied force which was divided by the footing area to obtain an average footing pressure. All of the finite element results were plotted in a normalized form as shown in Figures 80 and 81. The stresses calculated by finite elements for a rigid displacement case and a two-layer system using a flexible foundation agree well with the theoretical solutions.

The finite element solutions for a two-layer system using a rigid loading area are compared with theoretical solutions of a two-layer elastic theory [44] which assumes a flexible foundation as shown in Figures 82, 83, and 84. The comparison is made for a modular ratio of E_1/E_2 = 5 and 10. When the fill thickness is equal to 1/2D, the vertical stresses at the interface produced by a rigid foundation are much less than those obtained using a two-layer elastic theory and flexible loading (Figure 82). As the fill thickness increases to 1D and 1-1/2D (Figures 83 and 84), the vertical stresses at the interface and at greater depths are

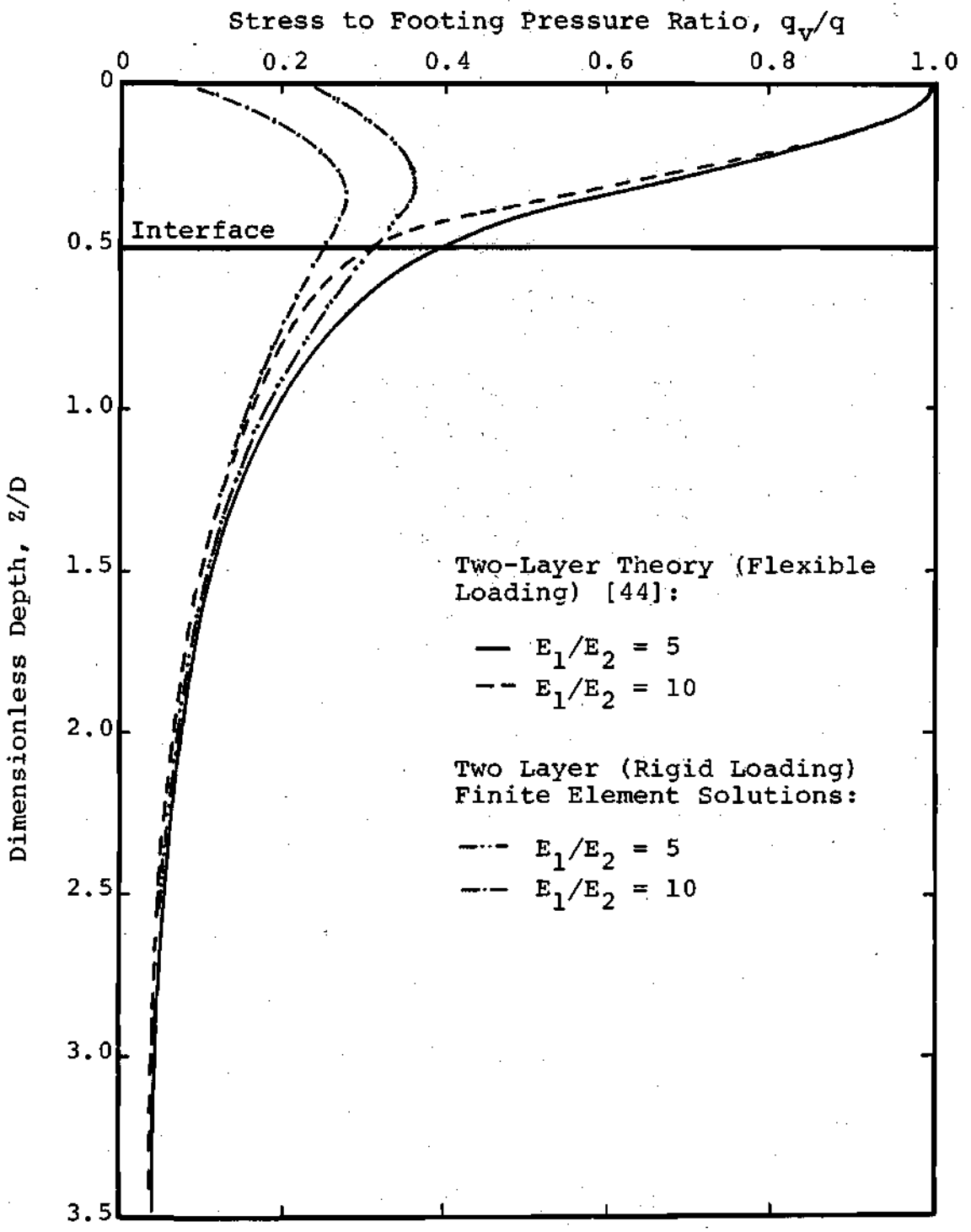

Figure 82. Comparison of Vertical Stress Distribution in a Two-Layer System Using Flexible and Rigid Loading, H = 1/2D.

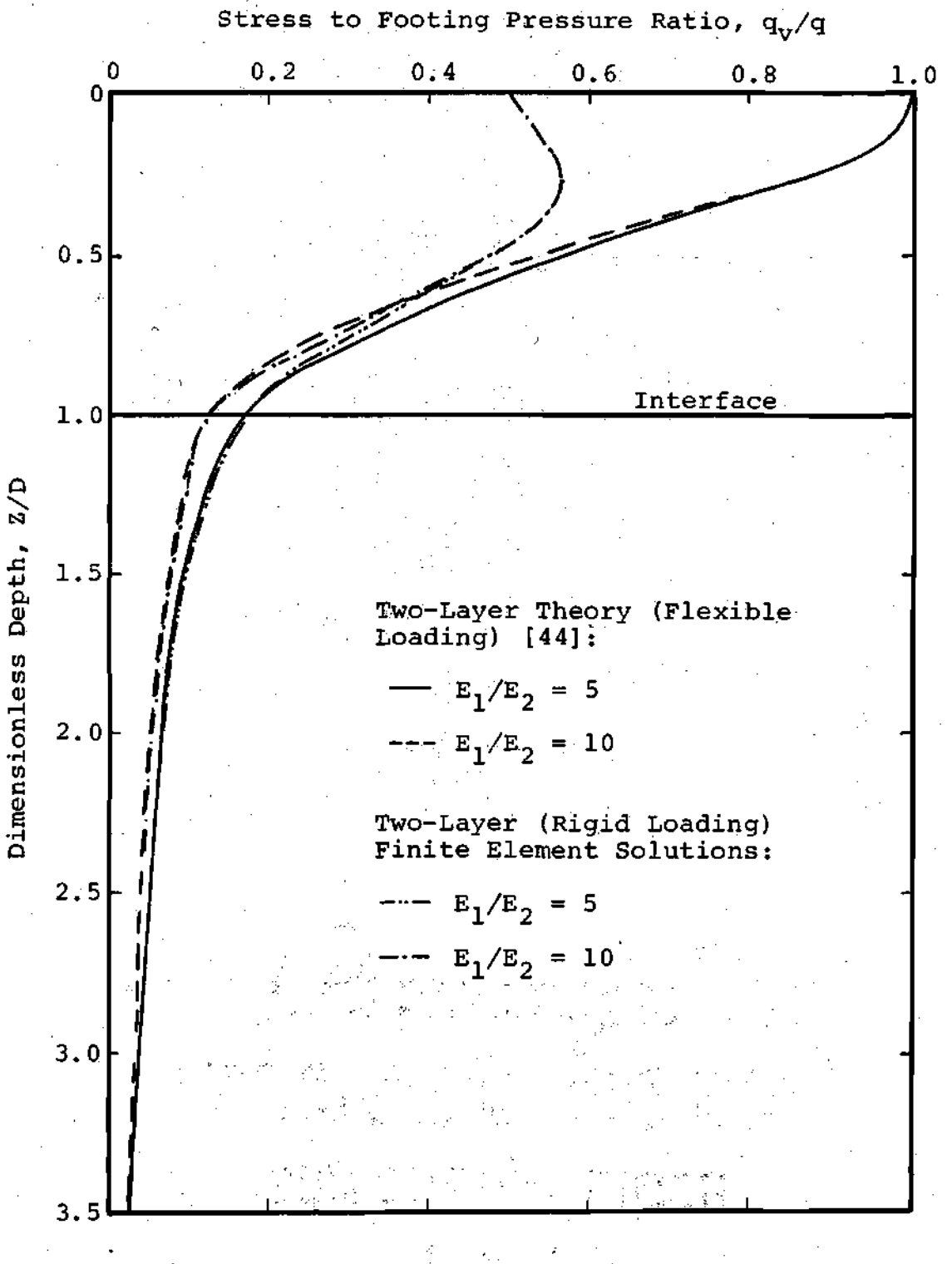

Figure 83. Comparison of Vertical Stress Distribution in Two-Layer System Using Flexible and Rigid Loading, H = 1D.

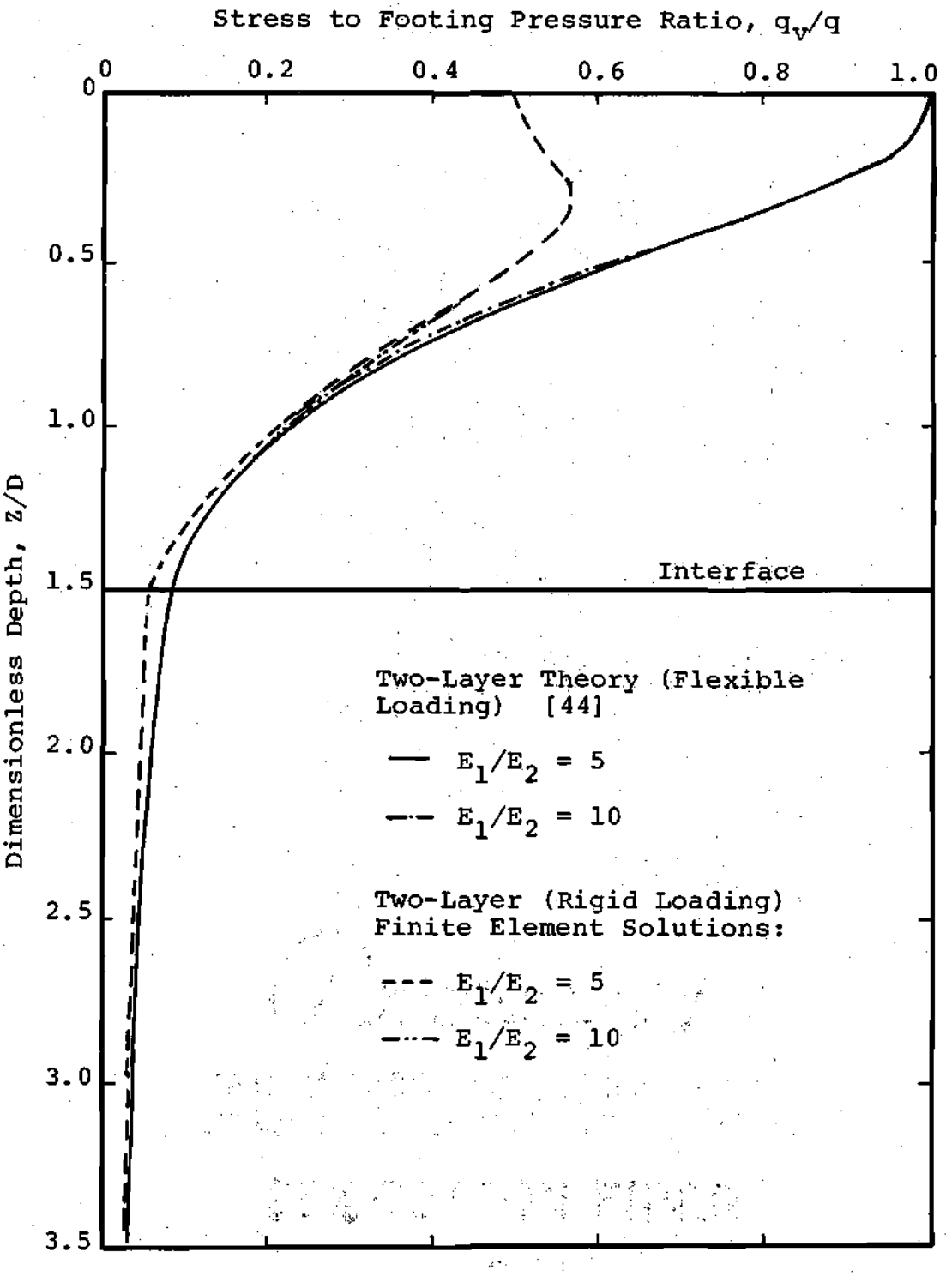

Figure 84. Comparison of Vertical Stress Distribution in a Two-Layer System Using Flexible and Rigid Loading, H = 1-1/2D.

comparable. These results of the finite element study indicate that when the thickness of the stiff layer is approximately 1D or greater, the stresses at the interface and in the soft layer produced by a rigid load area may be approximated using the solutions of a two-layer elastic theory for a uniform loading condition. For the case of fill thickness equal to 1/2D, it will be later shown that using either a cohesive or granular fill, the measured stresses at the interface and in the soft layer closely follow the theoretical solutions using a flexible rather than a rigid foundation even though a rigid footing was used in the test.

The computer solutions for a rigid foundation on a two-layer system consisting of a stiff over softer layer were obtained for two modular ratios E_1/E_2 equal to 5 and 10. The results are superimposed on the plots of measures stresses. The vertical stress distribution by Westergaard [132] was also included in the plots for comparison.

Uniform Clayey Silt Layer - Test Series I

The plots of measured vertical stresses in a normalized form are shown in Figures 44 and 45.

The results of measured vertical stress in Test Series I - uniform soil layer reveal that the peak stress under a rigid foundation does not occur immediately beneath the foundation. The results show some scatter but generally follow the pattern of the theoretical line for a rigid displacement condition. At greater depth, however, the measured

stress values are less than those indicated by theoretical results. A theoretical line for stresses using Boussinesq theory and a flexible foundation was also superimposed on the plot of Figure 44 for comparison. The calculated stresses for these two conditions are not much different at a depth 1D below the footing.

The measured stresses tend to increase with increasing footing pressure. This is due to the effect of non-linearity of the soils. Terzaghi and Peck [121] have indicated that the contact pressure at the center of the base of a rigid footing supported by a subgrade soil whose properties have both cohesion and friction, increases and approaches a uniform distribution as the load increases. From the plots of vertical stress variation with depth (Figure 44) it appears that the measured values attenuate with depth faster than indicated by Boussinesq theory.

The plots of measured vertical stresses on a horizontal plane at different depths as shown in Figure 45 also show generally good agreement with the theoretical results for a rigid loading. These test results support the theoretical findings [53] that vertical stress distribution beneath a vertically loaded foundation is relatively insensitive to the stress-strain relationship of the material. The stress distribution in the uniform layer of micaceous clayey silt confirms the finginds of other workers [22, 124], although in some cases flexible foundations and dynamic loading were

used.

Sandy Clay Fill Over Soft Subsoil - Test Series II

The results of streee measurements for different fill thicknesses are presented in Figures 46 through 51. For the fill having a thickness of 1/2D, the finite element solutions and the measured values do not agree well for the stresses in the fill layer and at the interface. At a greater depth below the interface a good agreement was obtained. The superimposed line of Westergaard theory which assumes a flexible loading shows a reasonably good agreement with measured stresses at all levels except immediately beneath the footing. The measured vertical stresses distributed in radial directions at the interface and in the subsoil are shown in Figure 47. At the interface, the stresses are less than those indicated by Boussinesq rigid displacement theory but closer to the two-layer theory line with $E_1/E_2 = 5$. The measured stresses in the soft subsoil are closer to the theoretical lines with $E_1/E_2 = 10$ than 5 even though the modular ratio E_1/E_2 from laboratory triaxial tests results ranges from 8.5 to 7 for a lateral confining pressure from zero to 2.5 psi.

Figures 48 and 49 show the results of stress measurements for the case where the fill thickness is increased to 1D. A comparison of the measured stresses with the theoretical distributions indicates that the majority of the measured values fall between $E_1/E_2 = 5$ and 10 solutions for vertical stresses with depths and with radii, and are generally less than those indicated by Westergaard theory. The measured

stresses at the interface and in the fill (Figure 49) show a systematic variation, which is caused by the non-linear behavior of the fill material and subsoil as the footing pressure increases.

Further increase of the fill thickness to 1-1/2D also results in a stress reduction in the lower layer to less than that predicted by Boussinesq rigid displacement theory as shown in Figures 50 and 51. The measured vertical stresses generally follow the theoretical lines of finite element solutions for E_1/E_2 = 5 and 10. Good agreement between measured and theoretical stresses is confirmed from the plots of vertical stresses with radii (Figure 51), especially at the interface. Appreciable scatter of vertical stresses with depth in the fill layer is observed. Good approximation of the measured vertical stresses can be made using the Westergaard theory for the sandy clay fill tested.

It can be concluded that the results of stress measurements in Test Series II using sandy clay as compacted fill for all three thicknesses indicate that the beneficial effect of the structural fill in reducing stresses to less than that indicated by Boussinesq theory is evident. These results are consistent with the measured settlement reduction of the soft layers observed beneath the compacted sandy clay fills. A reduction is expected because compacted sandy clay fills are capable of resisting tensile stresses induced in the fill thus providing ability to spread the load. The results of

beam bending tests (Appendix C) indicate that the modulus in tension and in compression of compacted sandy clay determined from the stress-strain curves using measured strains are comparable. Thus, the assumption of equal moduli in tension and in compression for the two-layer theory and in the finite element approximation may not be too critical for low strain levels.

The stress distribution in the soft layer beneath the fill due to a rigid surface load can be predicted reasonably well using the finite element method and $E_1/E_2 = 10$. This modular ratio is slightly higher than the measured values from the triaxial shear tests. A good approximation of vertical stresses with depth can be made in all three cases using the Westergaard theory especially for stresses below the interface of the two layered system.

Sand Fill Over Soft Soil - Test Series III

The stress distribution data obtained for three test conditions using three different fill thicknesses are presented in Figures 52 and 57. The measured vertical stress at various depths for the fill thickness of 1/2D is plotted in Figure 52. The measured points in the sand layer are somewhat scattered but those below the interface increase slightly with increasing footing pressure. It is seen that a small reduction in stress to less than that predicted by the Boussinesq rigid displacement theory occurs at a low level of footing pressure (1000 psf) and the measured points lie

closer to the theoretical values obtained using a rigid footing and $E_1/E_2 = 5$. As the footing pressure increases, the load-spreading ability of the sand layer decreases, and the measured stresses closely follow the theoretical stresses computed by the Boussinesq theory for a rigid loaded area. These test results are confirmed from the plots of measured vertical stress variation with radii at the interface, and at depths Z/D = 1 and 2 in the soft layer as shown in Figure 53. The measured interface stresses closely follow the theoretical line for Boussinesq rigid displacement theory. Good agreement between the measured stresses and the Boussinesq theoretical stresses is further evident at two depths below the interface.

It is difficult to determine the modular ratio between the compacted sand and the soft subsoil from the laboratory triaxial test results because the modulus of sand is greatly dependent upon the confining pressure. The modulus of sand prior to conducting the load tests may be estimated from the relationship between the confining pressures and moduli as shown in Figure 32 if an average lateral confining pressure in the sand layer is known. The lateral confining pressure, σ_h, in the sand layer can be calculated using the following relationship [114].

$$\sigma_h = K_0 \gamma z \qquad (3)$$

where K_0 = coefficient of earth pressure at rest

γ = unit weight of sand

z = depth below the sand fill surface.

The coefficient of earth pressure at rest, K_0, for sand compacted by tamping in layers is approximately equal to 0.8 [121]. For sand fills compacted using vibratory rollers, the studies of D'Appolonia, Whitman, and D'Appolonia [33] have shown that K_0 is likely to be greater than 1.0. Since the J-Tamper vibratory compactor was used to compact the sand in this study, it is most likely that K_0 is greater than 1. A value of K_0 = 1.0 was used in the analysis. Using an average unit weight of 110 pcf for compacted sand and the thickness of fill and surcharge equal to 1.25 feet, the overburden pressure at the bottom of the sand layer is approximately 1 psi. The lateral confining pressure due to the weight of the fill and surcharge is equal to 1.0 psi. From Figure 32, using the curve for undisturbed samples, the modular ratio between that of sand and micaceous clayey silt is found to be about 4.5. Heukelomp and Klomp [50] have found from field vibratory tests that the ratio of the moduli of untreated granular materials to that of the subgrade is not much higher than about 2.5. Using gravel as the base course material over a clay subgrade, Seed, et. al. [101] report a modular ratio varying from 0.4 to 1.8 depending upon the stress conditions. Because of a thin sand layer used in Text No. 1 of Test Series III, a very small lateral confining stress due to the weight of the fill is expected. Hence, the modular ratio

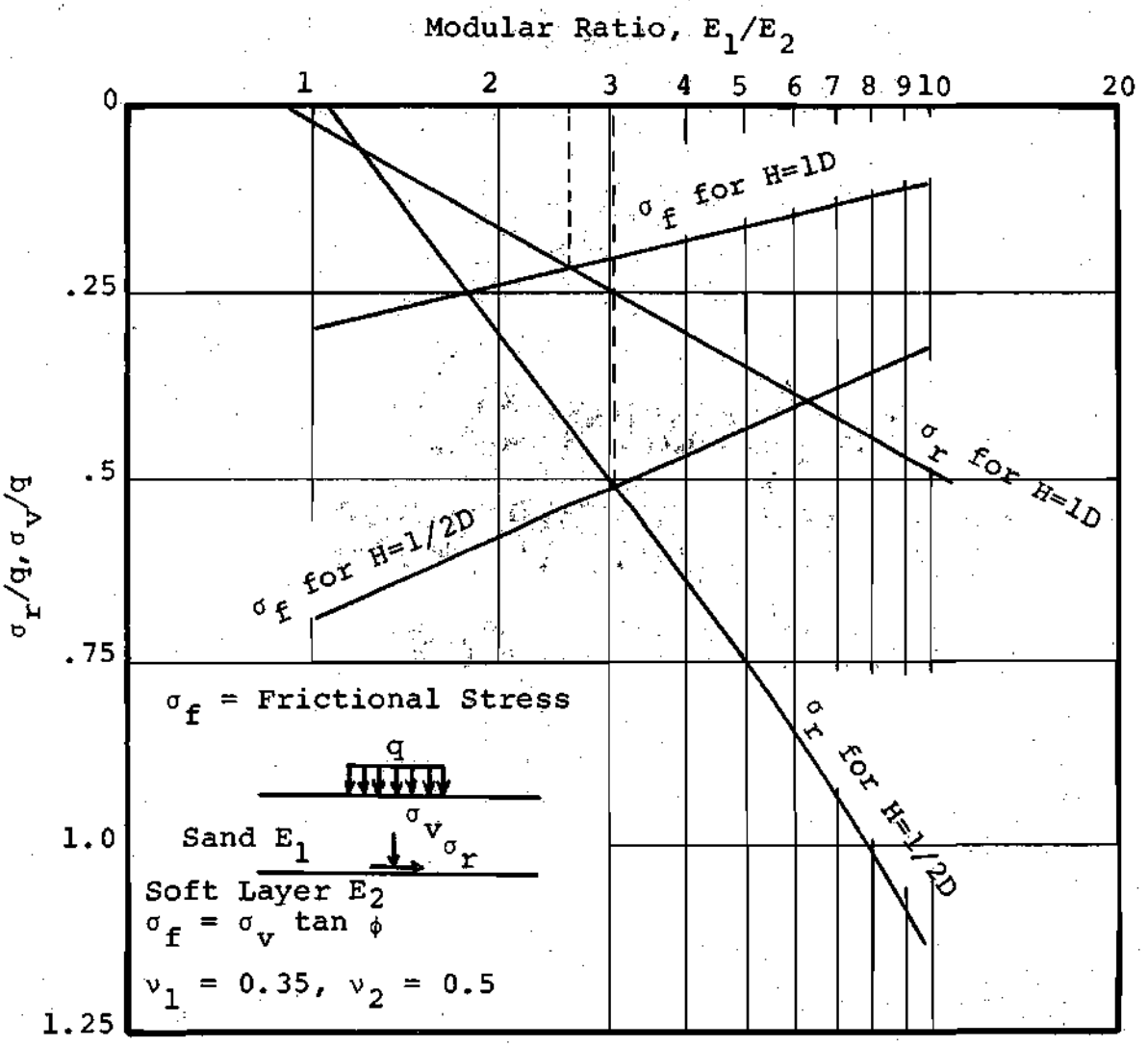

Figure 85. Effect of Frictional Stress of Sand in Resisting Tensile Stresses.

between the sand and underlying soft soil is probably not greater than 3 to 5.

An analysis similar to Heukelomp and Klomp's [50] is used for a two-layer system to determine the modular ratio between the sand fill and the soft layer. Plots of the ratio of the tensile stress, σ_r, at the bottom of the sand layer to the applied footing pressure, q, for H/D = 1/2 and 1 are shown in Figure 85 using the solutions of a two-layer elastic theory for a uniform footing pressure on a circular area as given by Gerrard [44]. It is seen that the radial stress, σ_r, is slightly compressive when the ratio E_1/E_2 is close to unity, and tensile when this ratio is greater than one. If sand cannot resist tension, E_1 decreases due to radial tensile stress which tends to produce expansion, until the ratio E_1/E_2 at the base of the sand layer is close to one which will cause the sand to stablize. However, the frictional stress due to interlocking of sand grains as a function of the vertical stress component allows the sand to sustain certain radial stresses without expanding. The frictional stress is related to the frictional resistance of sand and may be expressed as:

$$\sigma_f = \sigma_v \tan \phi \qquad (4)$$

where σ_f = frictional stress

σ_v = vertical stress component due to footing pressure, q

ϕ = frictional angle

The value of ϕ for compacted sand from the results of triaxial shear tests is approximately 45°. Thus, the frictional stress is equal to the vertical stress component or $\sigma_f = \sigma_v$.

The plots of σ_f in terms of the applied surface load, q, are shown in Figure 85. The figure shows that the frictional stress, σ_f, is greater than the tensile radial stress, σ_r, if E_1/E_2 is less than about 3.0 for H/D = 1/2. If E_1/E_2 is greater than 3.0, the radial stresses are higher than the frictional stresses and thus higher than the assumed tensile strength of sand. However, when the weight of the sand layer is taken into account, it contributes to the confining effect, allowing modular ratios in the range of 3 to 5. Therefore, only a small stress reduction using low applied pressure is expected when a thin layer of sand is used as compacted fills.

Figures 54 and 55 show the plots of measured stresses varying with detph and with radii for the sand fill-subsoil system having an H/D of 1. The measured vertical stresses in sand show some scatter, particularly at a depth 0.25D. This anomaly cannot be explained. However, the stress cell at this depth was checked after the test and was found to function properly. Some erratic results have been knwon to occur for measurement of stress in sand [127]. The stresses at the interface and at various depths below are less than those indicated by Boussinesq theory for a rigid load area. Most of the measured points fall between the lines of rigid load, elastic layered solutions for E_1/E_2 = 5 and 10. A similar

analysis to that for H = 1/2D was used to determine the modular ratio between the sand and subsoil for H/D = 1, which indicates a limiting ratio of about 5. From Figure 85, the highest theoretical modular ratio at the base of the sand layer which could be obtained without exceeding the frictional stress is 2.6. In the analysis, however, weight of the sand layer was not included. As the fill thickness was increased from 1/2 to 1D, the tensile stresses induced by applied loads decreased. Also, the confining effect due to the fill increased, resulting in modular ratios in the range of 3 to 5. A good agreement between the measured and layered system theoretical stresses for E_1/E_2 = 5 (Figure 55) is obtained at the interface and at a depth Z/D = 2.

The beneficial effect of the compacted sand fill in reducing stresses in the subsoil to less than those computed by Boussinesq theory for a rigid foundation is expected because as the fill thickness increases the effective modular ratio increases, thereby increasing the load-spreading capability of the sand fill.

The variation of measured stress with depth and with radii as the fill thickness increased to 1-1/2D is shown in Figures 56 and 57. Using the same procedure based on laboratory tests previously described, the modular ratio of the sand-subsoil system was found to be about 5 to 6. Measured stresses at the interface and in the lower layer closely followed the theoretical relation for E_1/E_2 = 5 and 10. Since

the spread between these two lines is small, it is difficult to distinguish which modular ratio gives a better correlation. However, definite stress reduction to less than that obtained by Boussinesq theory is observed. The plots of vertical stresses varying with radii (Figure 57) also show similar stress reduction at the interface and at a depth 2D. The measured stresses compared well with the elastic layer system solutions for $E_1/E_2 = 5$, particularly at the interface.

The stress reduction in the soft layer below the sand fills are consistent with the settlement reduction of the soft layers shown in Figures 41, 42, and 43 for a fill thickness equal to 1/2D, 1D, and 1-1/2D. These results support the finding of Mitchell and Gardner [78] who analyzed the problem using a non-linear finite element method, that compacted sand fills are effective in reducing the stresses in the soft soil. In their analysis, the sand fill elements were not permitted to carry tension by reducing the modulus of sand to a very low value (100 psf) when the shear strength of sand was exceeded during loading. The results of stress measurement for a sand fill thickness of 1/2D (Figure 52) indicated that once the footing pressure approaches a bearing capacity failure, a stress reduction to less than that calculated by Boussinesq theory was not obtained and the measured stresses in the soft layer closely followed the solutions by Boussinesq theory. The measured stress distribution for sand fill thickness equal to 1D and 1-1/2D follows this similar

trend in which the stress reduction is less as the footing pressure increases.

The stress distribution by Westergaard theory was found to give a good approximation for measured stresses at and below the interface for fill thickness of 1D and 1-1/2D.

The stress cell readings in the sand layer close to the footing (Figure 56) were erratic and consequently were not included in the plots. The stress cells used in the sand layer at these depths, however, still functioned properly after the tests. The cause for this aberration might be due to arching resulting from the high stress imposed on the cells during compaction.

Stone Replacement

Measured vertical stresses beneath the footings having stone replacement over a width 1D and a depth 1D are shown in Figure 58. The stone was lightly compacted to replace only the weak soil beneath the footing. The distribution of measured stresses with radii increases with increasing footing pressure and the magnitude of the stress is greater than that indicated by Boussinesq theory. The stress distribution pattern, however, is approximately uniform suggesting that the stone acts as a short column and transfers surface applied loads to the base more than that indicated by Boussinesq theory. Part of the stress was transferred to the surrounding soil through shear. Since the stone was lightly compacted, the modular ratio between the stone and the soft subsoil was

probably equal to one or less, and since the stone replacement behaves more as a rigid inclusion in the soil medium, a two-layer theory is not applicable in this case.

The width of the stone replacement was increased to 2D and the results of stress measurement at the bottom of the stone are presented in Figure 59. It is seen that by increasing the width to 2D, the stress distribution beneath the base of the stone is similar to the theoretical solutions obtained by using Boussinesq theory for a flexible or rigid foundation. A stress reduction was obtained, however, at a very low footing pressure (500 psf). As the pressure increases, the measured points approach the theoretical values for Boussinesq theory which assumes a semi-inifinite solid. These results agree with the findings of other workers [72, 101] that the stress distribution beneath a compacted crushed stone layer can be predicted using Boussinesq theory for a homogeneous, elastic medium. It appears that replacing only a portion of the weak foundation soil with stone using a limited width of 2D is as effective as placing a continuous layer of crushed stone in that the stress distribution in the soft layer for both cases is similar. Using the procedure previously described and laboratory test data, the modular ratio between the stone and the subsoil was found to be about 2.0. The ratio was probably closer to one as a result of radial tensile stress induced by applied loads.

Figure 60 shows the variation of vertical stresses

with depths in the soft soil below a stone replacement of a width 2D and a depth of only 1/2D. The stone was lightly compacted to a dry density of 122 pcf as for the previous two tests. As can be seen, the measured stress compare well with those computed using Boussinesq theory for a rigid loaded area. The stress variations with radii immediately below the interface and at a depth of 1-1/2D are shown in Figure 61. The measured stresses for the first increment of footing loads (1000 psf) are less than the theoretical stresses for a homogeneous soil, indicating that some stress reduction was obtained. Increasing the footing pressure also increases the tension in the stone layer, which gradually eliminates the load-spreading ability of the stone. The modular ratio between the stone and the soft subsoil was probably close to one since the stone was lightly compacted and a thin layer was used.

The test results at the soil-stone interface show appreciable scatter, particularly for points at r/R = 1. This scatter could be due to a stress concentration as a result of placing the stress cells too close to the bottom of the stone layer. Each cell, however, had a soil cover of at least one-half inch and the bottom of the excavation was covered with a thin layer of sand before placing the stone. It should be pointed out that measured vertical stresses at a depth of 1-1/2D show good agreement with the stresses computed by Boussinesq theory for a rigid loading.

To determine if significant stress concentration occurred over the stress cells, a second test was conducted at the same location. The stress cells, however, were embedded at least one inch below the bottom of the pit and a thin sand layer was also spread on the bottom prior to placing the stone. The stone was heavily compacted to obtain a dry density of approximately 129 pcf which was much higher than the 122 pcf used in the previous tests. The results of vertical stress measurements with depth and with radii are shown in Figures 62 and 63. The measured variation in vertical stress with depth (Figure 62) compared favorably with those indicated by Boussinesq rigid displacement theory except in the zone directly below the soil-stone interface where there was a definite reduction of stress. This reduction is more evident as shown on the plots of stress variation with radii in Figure 63, but became negligible at greater depths. McMahon and Yoder [72] report a similar stress reduction beneath the crushed stone base. Using Figure 32, the modular ratio between the stone and the soft subsoil was found to be about 2.5. The theoretical limit of the modular ratio for this two-layer system is probably not greater than 3 as shown in Figure 85.

The measured points immediately beneath the interface did not show as much scatter as those in Test 4 (Figure 61), indicating that some stress concentration did occur in the previous test.

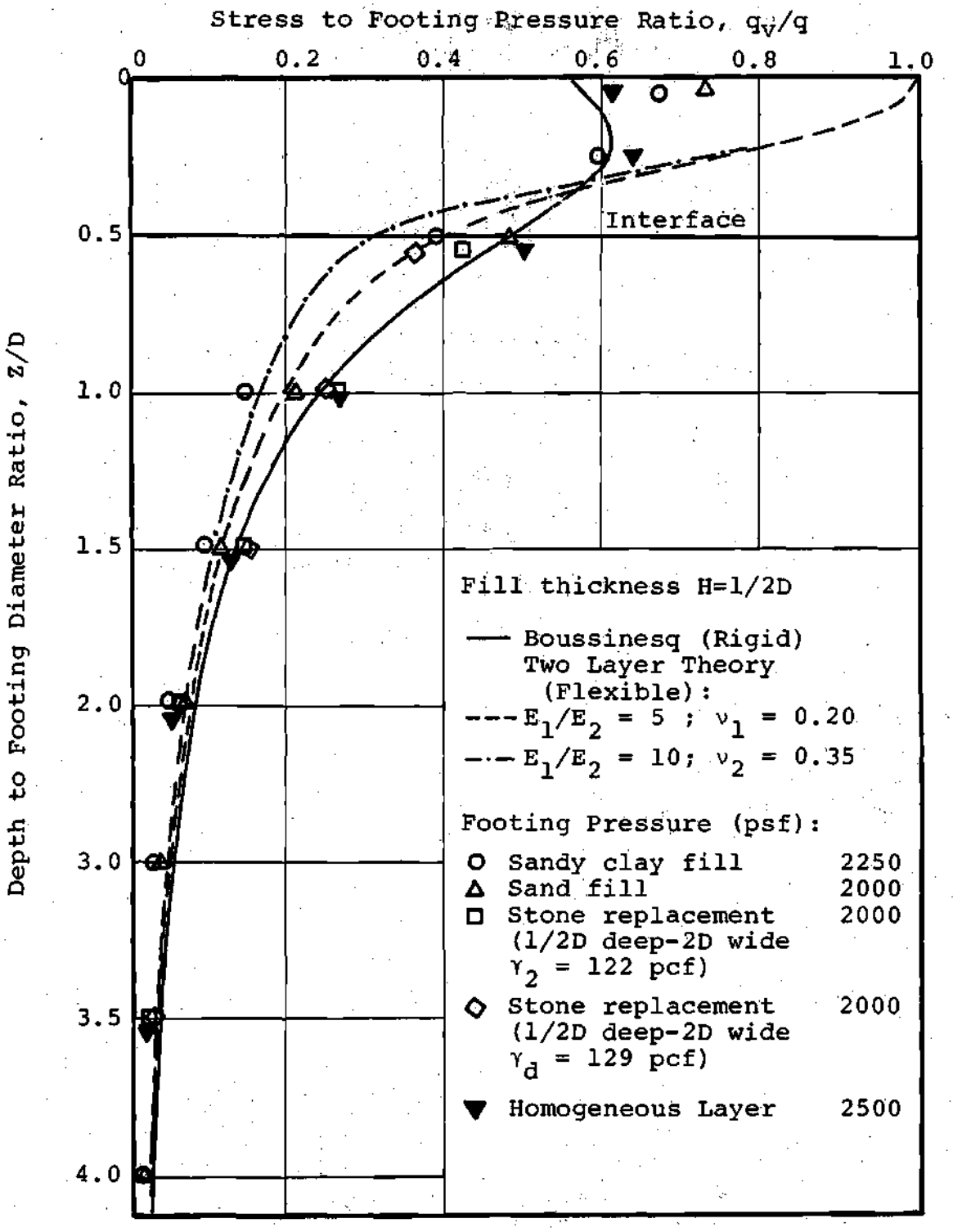

Figure 86. Comparison of Vertical Stresses at Selected Footing Pressure for Different Fill Materials, H = 1/2D.

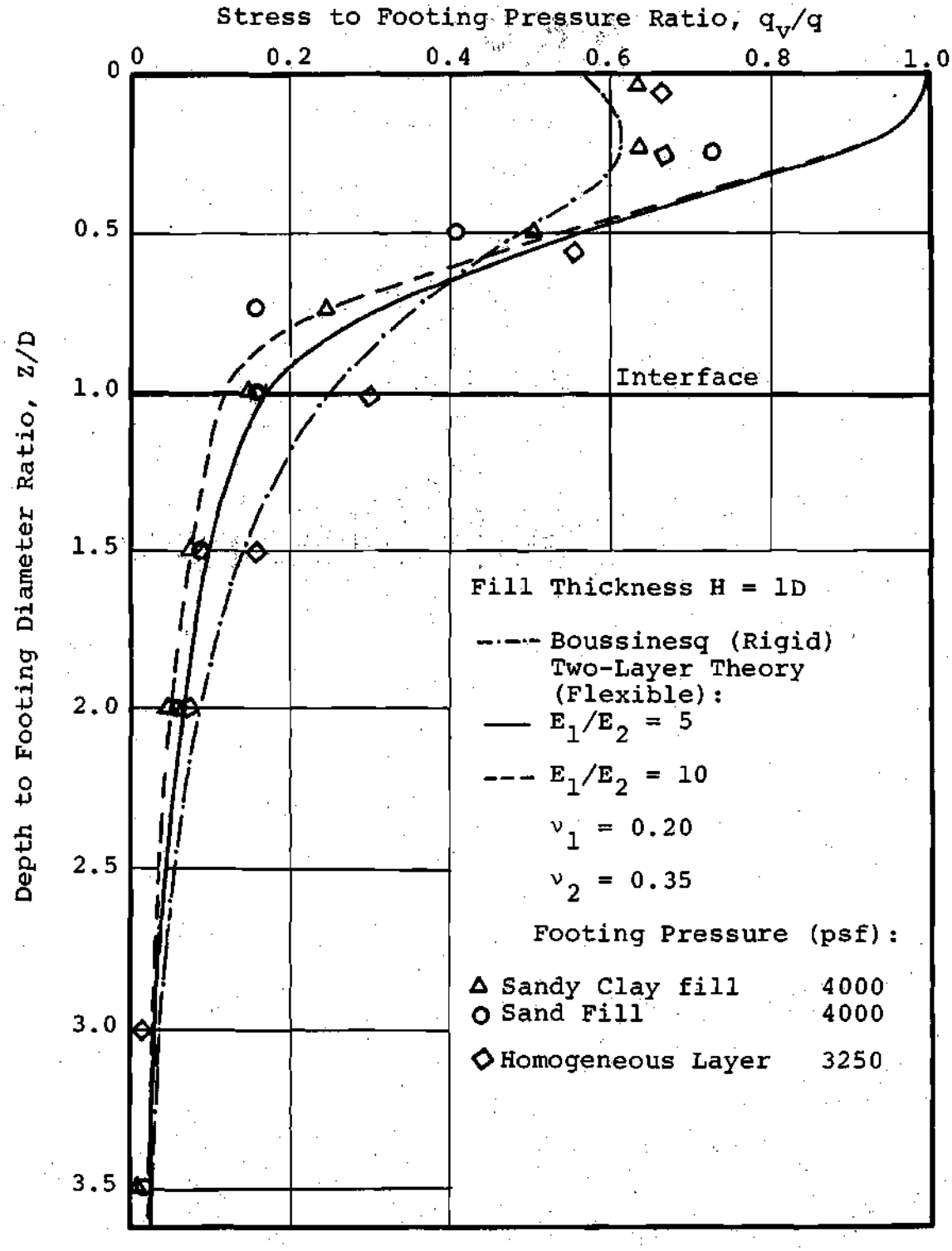

Figure 87. Comparison of Vertical Stresses at Selected Footing Pressures for Different Fill Materials, H = 1D.

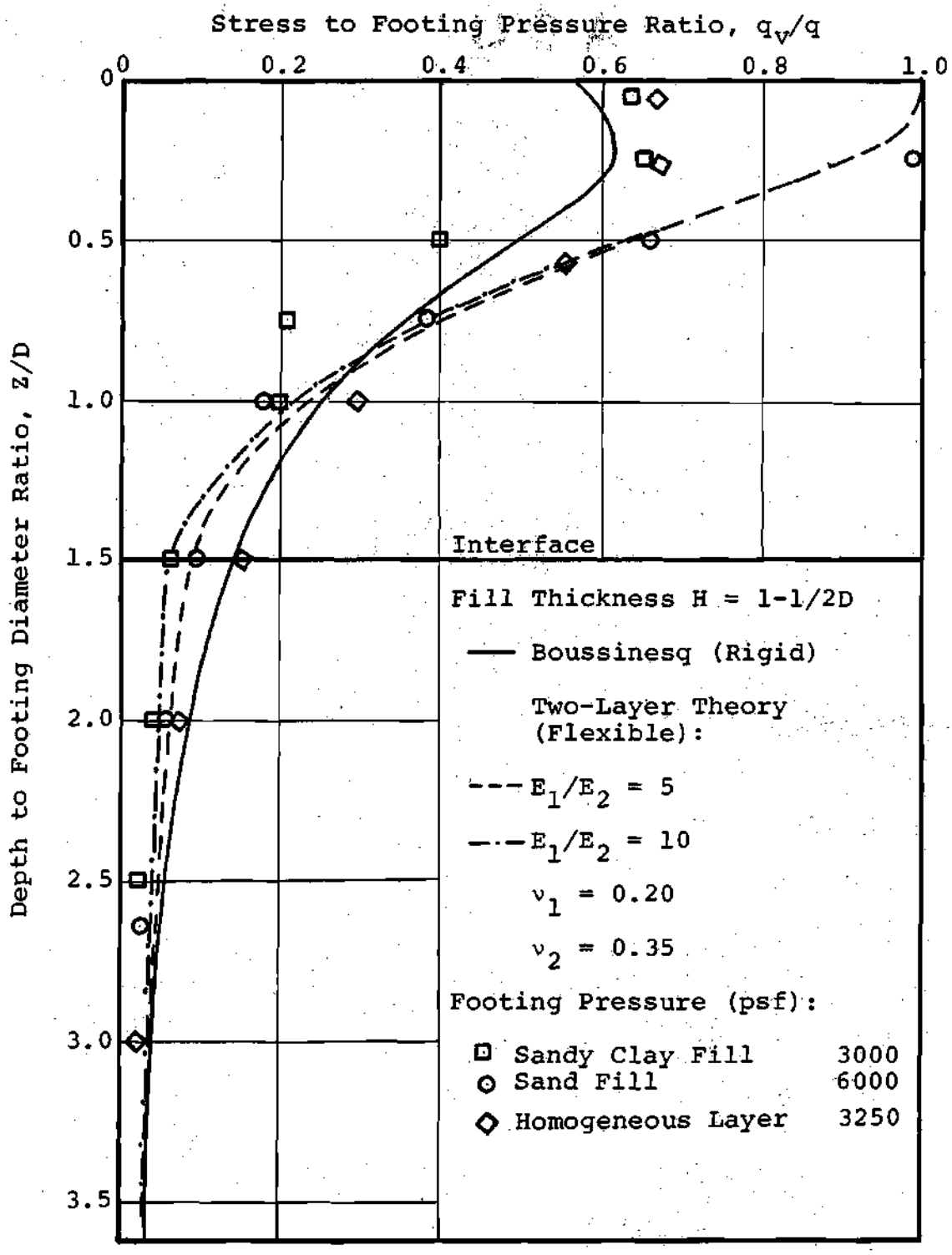

Figure 88. Comparison of Vertical Stresses at Selected Footing Pressure for Different Fill Materials, H = 1-1/2D.

The variations of measured vertical stress with depth for a fill thickness of 1/2D, 1D, and 1-1/2D were plotted for selected footing pressures and compared with theoretical solutions in Figures 86, 87, and 88. The allowable footing pressure for each fill-subsoil system was obtained by dividing the ultimate bearing capacity values obtained from the load-settlement curves as given in Table 11 by a safety factor of 2. Figure 86 shows the plots of measured vertical stresses at working footing pressures shown for the fill thickness H = 1/2D. It is seen that a significant stress reduction to less than that computed by Boussinesq theory for a rigid loading foundation is obtained when sandy clay and sand were used as fill materials. Using crushed stone as a footing replacement pad, produced only a small stress reduction close to the soil-stone interface. Theoretical solutions using a two-layer linear elastic theory [44] for a flexible foundation and modular ratios E_1/E_2 of 5 and 10 were used to predict the stress distribution in the soft layer. It seems that the two-layer theory using a flexible foundation can be used to calculate stresses in the soft layer. The measured stresses, however, seem to attenuate faster with depth than that indicated by theoretical solutions.

The variations of measured vertical stress with depth at allowable bearing pressures for a fill thickness H = 1D and 1-1/2D using sandy clay and sand fills are shown in Figures 87 and 88. It is seen that for both cases, the theo-

retical solutions of two-layer theory for a flexible loading condition using modular ratios of 5 and 10 may be used to predict the measured stresses in the soft layer even though a rigid footing was used to apply the loads. The plots of measured vertical stresses with depth from the homogeneous layer (Test Series I) were also shown in Figures 86, 87, and 88. A comparison between the measured stresses in the soft layers of the compacted fills and those in the homogeneous layer indicates that a considerable stress reduction in the soft layers was obtained. Thus, the beneficial effects of the compacted fills in reducing stresses were evident.

Strain Measurements

Uniform Soft Soil - Test Series I

The variation of vertical strains measured in the test pit are shown in Figure 64 for strains varying with radii. All measured vertical strains were expressed in a normalized form by dividing the measured strains by the footing pressure.

Since the settlement and strain are dependent on modulus values, measurements of in situ strain are going to be influenced by any variations in elastic modulus of the material. This is reflected in all strain distribution plots, since experimental points show much more scatter than those for stress where the influence of modulus variation is less.

The strain distribution plots as shown in Figures 64

and 65 (and those for two-layer systems which will later be presented), clearly indicate that the vertical strain is greatly affected by the non-linear properties of the soils. The modulus of elasticity E, to which the strains are directly related, is stress-dependent and decreases with increasing stress level. The stress level at a point is dependent on both the overburden and applied footing pressure. Thus, when the footing pressure varies, the modulus also varies and results in different values of strain as shown in Figure 64. As previously shown, stress measurements are affected to a lesser extent by the non-linear nature of the soils.

To draw a theoretical curve for comparison, it is necessary to use an average value of E and Poisson's ratio, ν. In these plots, an average modulus value of 500 psi from triaxial test results and Poisson's ratio of 0.40 were used for the soft micaceous clayey silt in the calculations of vertical strains using the closed-form solutions for strains under a rigid loaded area given by Gerrard and Harrison [46].

Plots of measured vertical strain as a function of depth are shown in Figure 64. Despite the dependence of vertical strain on the footing pressure, there is generally reasonable agreement between the experimental and the theoretical values. The peak vertical strain occurring beneath a rigid footing loaded with light surcharge load placed on a uniform micaceous clayey silt does not occur immediately beneath the footing but reaches the maximum value at a depth

Z/D ranging from 0.4 to 0.55, depending on the magnitude of the footing pressure. The maximum strain from the theoretical plot, however, occurs at a depth Z/D = 0.38. The results of small footing load tests on a uniform sand using a rigid, circular footing conducted by Eggestad [42], indicate that the depth to maximum vertical strain was about (Z/D) = 0.75 for both loose and dense sand. A non-linear finite element study of strain distribution beneath a rigid circular footing on homogeneous sand by Schmertmann [98] also shows that the peak strain value occurs at a depth Z/D increasing from 0.36 to 0.6 as the footing pressure increases. The Schmertmann's simplified strain distribution which shows a peak strain value at Z/D = 0.5 is plotted in Figure 64 The measured vertical strains at a design pressure of 1750 psf (using safety factor = 2) also show a peak value at about Z/D = 0.5 which agrees with Schmertmann's approximation. However, the measured strains did not indicate zero values at the footing level as shown in Schmertmann's plot.

It can, therefore, be stated that the results of this large scale footing load test confirm the theoretical prediction and findings of other investigators that the maximum strain under a rigid footing resting on a homogeneous soil mass does not occur immediately beneath the footing, and that the depth to the maximum strain in non-linear soils varies and is stress-dependent.

From the plot of vertical strain (Figure 64), it is

seen that the majority of strain and thus settlement occurs within a depth of 2D, and that measured strain dissipates with depth faster than those theoretically predicted.

The variations of measured vertical strains with radii are shown in Figure 65. Theoretical Boussinesq solutions for elastic half space were also superimposed for comparison. The dependence of strain on footing pressure and modulus of elasticity is further emphasized in these plots. It is obvious that the measured strains cannot be predicted using a single value of the modulus E, indicating that a linear elastic theory cannot be used to calculate strains in non-linear, stress-dependent soils. These results support the findings of Huang [53] who reached similar conclusions.

A comparison between the theoretical and measured strains generally indicates the same general distribution pattern despite the stress-dependent nature of the vertical strains.

Sandy Clay Fill Over Soft Layer - Test Series II

The plots of measured vertical and horizontal strains with depth for compacted fill over a soft layer with H = 1/2D, 1D, and 1-1/2D are presented in Figures 66 through 70. On each plot of vertical strain theoretical distributions obtained from the finite element solutions for a rigid displacement condition on an isotropic, elastic two-layer system having E_1/E_2 = 10 were superimposed. In the analysis, an average value of E = 500 psi and ν = 0.4 were used for the soft sub-

soil. It is seen that the non-linear nature of the soil has a great effect on the variation of strain with load level and that a linear elastic theory using a single modulus value cannot be used to predict the strain distribution adequately. Because the moduli of the compacted sandy clay fill and the soft subsoil are stress-dependent and decrease with increasing level of vertical stress, the measured strains increase as the modulus decreases. A finite element method which incorporates the nonlinear properties of the soils such as that given by Duncan and Chang [41] is probably more suitable to be used for prediction of strain distribution. A linear program has been used in this study to make a general comparison between measured and computed strains.

Figure 66 shows vertical strain distribution for each load increment as compared with the theoretical values. In the soft layer, the pattern of strain distribution is similar to the theoretical line. The majority of measured strains particularly at low footing pressures are less than the theoretical values indicating that the equivalent in situ modular ratio E_1/E_2 is probably equal to or greater than 10. The results of stress measurements for this test (Figure 46) also indicate that the stress distribution in the soft subsoil was close to that computed using a modular ratio of 10. Therefore, the results of stress and strain measurements are reasonably compatible and tend to reinforce each other.

The comparison of measured vertical strain for the

fills with H = 1D and 1-1/2D with theoretical distribution as shown in Figures 67 and 68 also show similar results, confirming that the stress distribution below the compacted sandy clay fill could be predicted adequately using a two-layer theory and E_1/E_2 = 10 for low footing pressures.

The plots of measured strains in the fill layers show considerable scatter and do not compare well with the theoretical predictions. This random variation in strain can be considered as a difference from theoretical solutions or variations of the local strain in the compacted clay fills due to a non-homogeneous condition or probably both.

The distribution of vertical strain with radii within the fill layer for the structural fill-soft soil system having H = 1D and 1-1/2D shown in Figures 69 and 70. The trend of strain distribution follows those of the theoretical lines for E_1/E_2 = 10.

Figures 89 and 90 show the plots of vertical and radial strains in the fill layers at the failure loads. Measured strains indicate that tension occurred at the bottom of the fill layers and the maximum tensile strain was on the order of 0.35 to 0.71 percent. These results compare reasonably well with the maximum tensile strains at failure obtained from beam bending tests, which were in the range of 0.35 to 0.45 percent. Thus, the results of beam bending tests on compacted clay can be used to predict the failure strains of compacted clay fills overlying a soft subsoil.

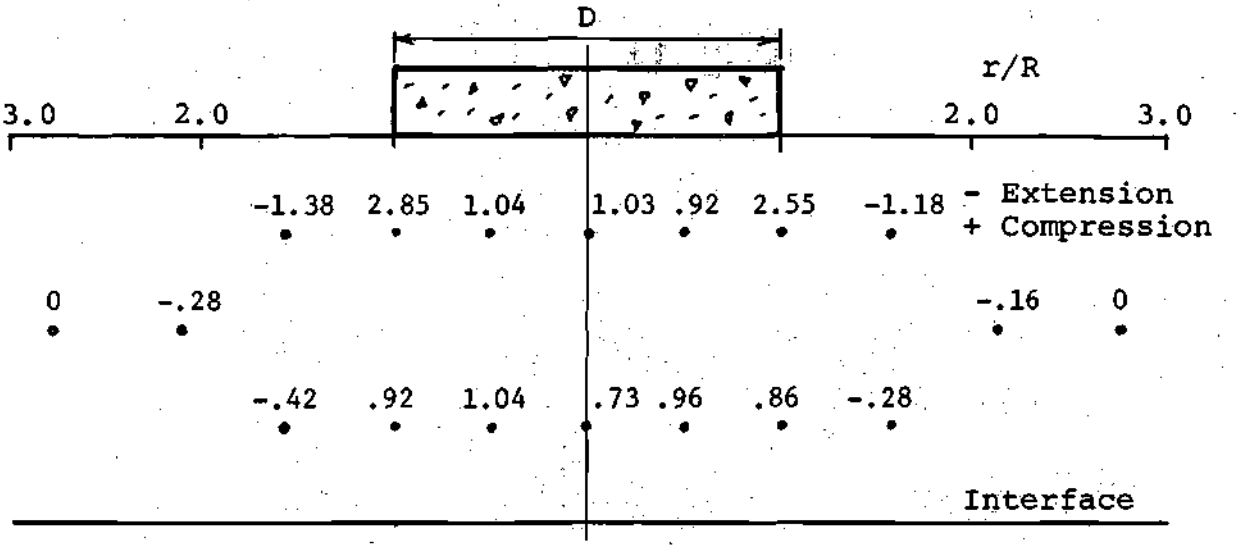

a) Vertical Strain at q = 4000 psf (%)

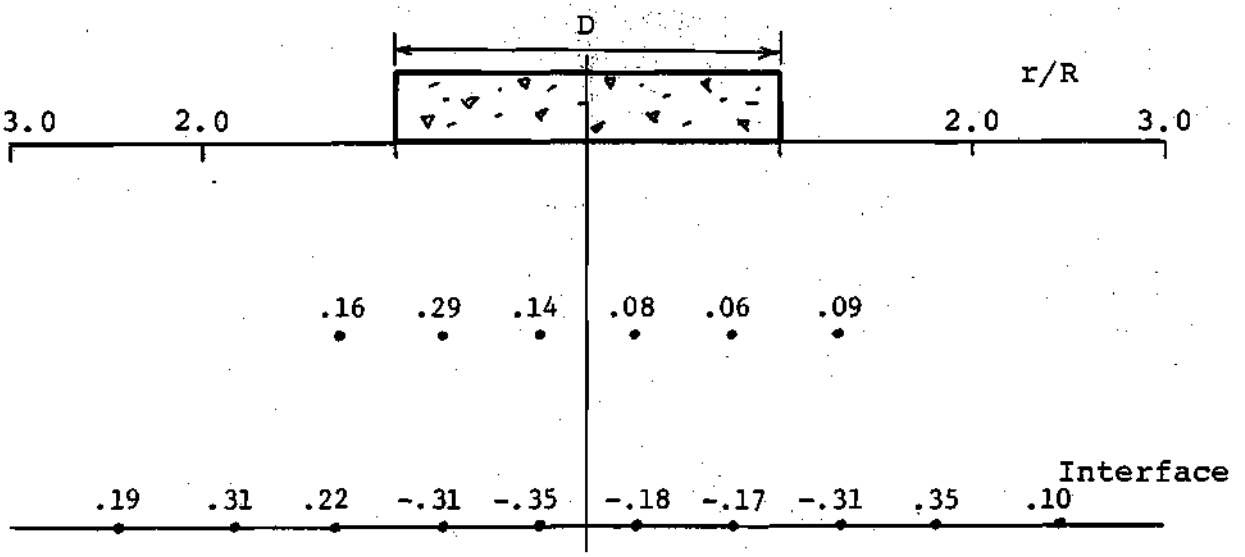

b) Radial Strains at q = 4000 psf (%)

Figure 89. Measured Strains in Compacted Sandy Clay at Ultimate q = 4000 psf, H = 1/2D.

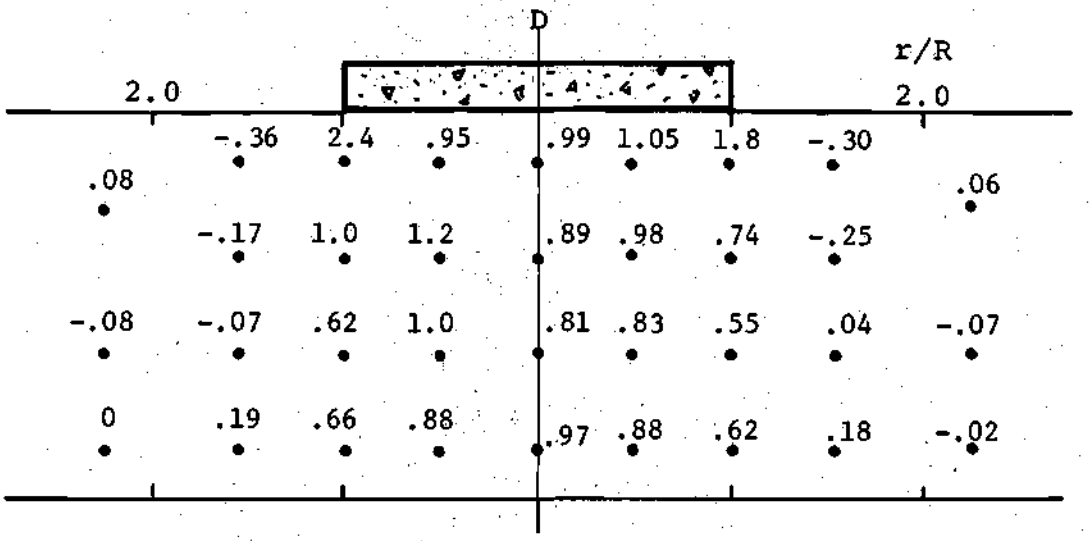

a) Vertical Strains at q = 8000 psf (%)

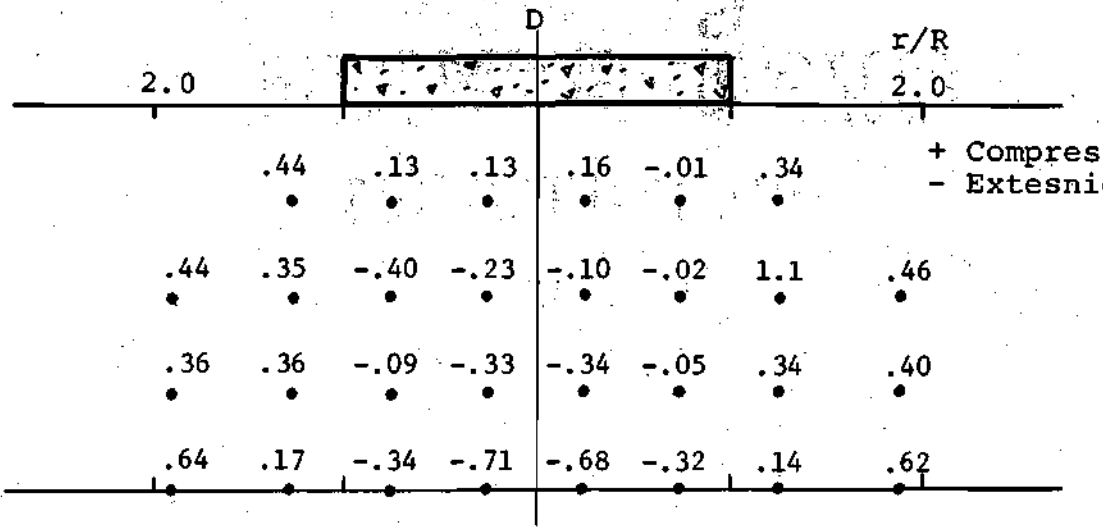

b) Radial Strains at q = 8000 psf (%)

Figure 90. Measured Strains in Compacted Sandy Clay, at Ultimate q = 8000 psf, H = 1D.

The initial tangent modulus of compacted sandy clay obtained from bending tests on test pit samples indicates a value of about 6500 to 7500 psi as compared with a value of 2750 psi obtained from unconfined compression tests (Appendix C). If E from the beam bending tests for the compacted fill is used in the evaluation of the modular ratio E_1/E_2, the ratio varies from 13 to 15 using E_2 = 500 psi for the soft subsoil. Therefore, this ratio is considerably greater than the value of 5 to 8 obtained from the results of the triaxial compression tests. Using a modular ratio of 10 in the theoretical analysis was found to give a good correlation between the measured and predicted values for both stress and strain at an allowable bearing pressure of 4000 psf (use S.F. = 2). This result suggests that the in situ modulus of compacted clay is higher than that obtained from compression tests and that a better estimate of E can be obtained from bending test. Since a compacted fill under load behaves in a general way similarly to a beam subjected to bending, using E from beam bending test appears to be appropriate.

Sand Fill Over a Soft Layer - Test Series II

Figure 71 shows the plot of vertical strain as compared with theoretically predicted values using a modular ratio E_1/E_2 = 5. A good agreement was in general obtained, particularly for the shape of the strain distribution with depth both in the fill and the soft subsoil. A theoretical line for Boussinesq theory for a rigid displacement condition is

also superimposed on the plot. These results are in agreement with the plot of measured stresses (Figure 52) in that a reduction in vertical strains was obtained at low footing pressures. As the footing pressure increases and approaches failure, the load-spreading ability of the sand layer has been destroyed and the strain distribution is similar to that obtained from Boussinesq rigid theory.

The variation of vertical strains with depth for H = 1D and 1-1/2D is shown in Figures 72 and 73, which are compared with the theoretical lines using E_1/E_2 = 10 and that of Boussinesq theory for a rigid loading. The effects of nonlinearity and stress-dependent moduli of the soft layer on measured strains are evident as the strain increases at an increasing rate as the footing pressure increases. At a low footing pressure, i.e., 2000 to 4000 psf, considerable strain reduction to less than that computed by the two-layer method using E_1/E_2 = 10 is observed. These results indicate that the beneficial effect of sand fill in reducing strain and stress in the underlying soft subsoil to less than that indicated by Boussinesq theory, decreases as the footing pressure increases. The strains computed by Boussinesq theory for a homogeneous solid half-space using E = 500 psi are considerably greater than the measured values.

The distribution of vertical strains with radii in the sand layers for a fill thickness H = 1D and 1-1/2D is shown in Figures 74 and 75. The theoretical solutions from the

finite element method for a two-layer system using a rigid footing and a modular ratio of 10 are superimposed on the plots for comparison. The variation of measured strains with radii for H = 1D as shown in Figure 74 generally follows the shape of the theoretical curves within 1R from the center of the footing. At a distance greater than 1R, the strains were in extension rather than compression shown by the theoretical curves. These results indicate that punching rather than a bending action occurred. This is different from the strain plots for the compacted clay fill using H = 1D (Figure 69) which shows a bending action in general. These strain plots in the sand layer demonstrate the inability of sand to resist large tension stresses.

The plot of measured vertical strains in the sand fill varying with radii at different depths are shown in Figure 75. The measured curves do not follow the general shape of the theoretical plots using a linear elastic two-layer system solution. This is also evident in the plot of vertical strains with depth in the sand layer (Figure 73) that the measured values are different from the theoretical predications. This could be attributed to the non-homogeneous property of the sand fill, the modulus of which is dependent on confining pressure and the state of stress.

Surface Deflection

The surface deflection profile for the homogeneous

test section of Test Series I was plotted using the measured values at footing pressures of 1000 and 1750 psf (Figure 91). The theoretical deflection profile was predicted using the solutions given by Gerrard and Harrison [46] for a Boussinesq solid loaded with a rigid foundation using E = 500 psi and $\nu = 0.4$. It is seen that the settlement of the ground surface is localized around the loaded area, much more than the Boussinesq theory for a rigid load condition predicts. These results could be due to the influence of non-homogeneity of the soil. Burland, Sills, and Gibson [24] have shown that the theoretical deflected shapes of the ground surface for an oil tank founded on chalk were much greater than the observed displacements. They postulated that it was due to the influence of non-homogeneity of the chalk.

The surface settlement profiles of sandy clay and sand fills over soft layers are shown in Figures 92 and 93. Since theoretical solutions for a two-layer system of a stiff over soft layer loaded on the surface with a rigid foundation is not available to predict the surface settlement profile at the present time, no attempt was made to compare the measured settlements with theory. All the plots in Figures 92 and 93 show that punching of the footing into the soft layers rather than a general bearing capacity failure occurred. Most of the settlements were concentrated around the footing. The settlement profiles of sandy clay fill show practically no movement at a distance r/R of about 3 from the footing

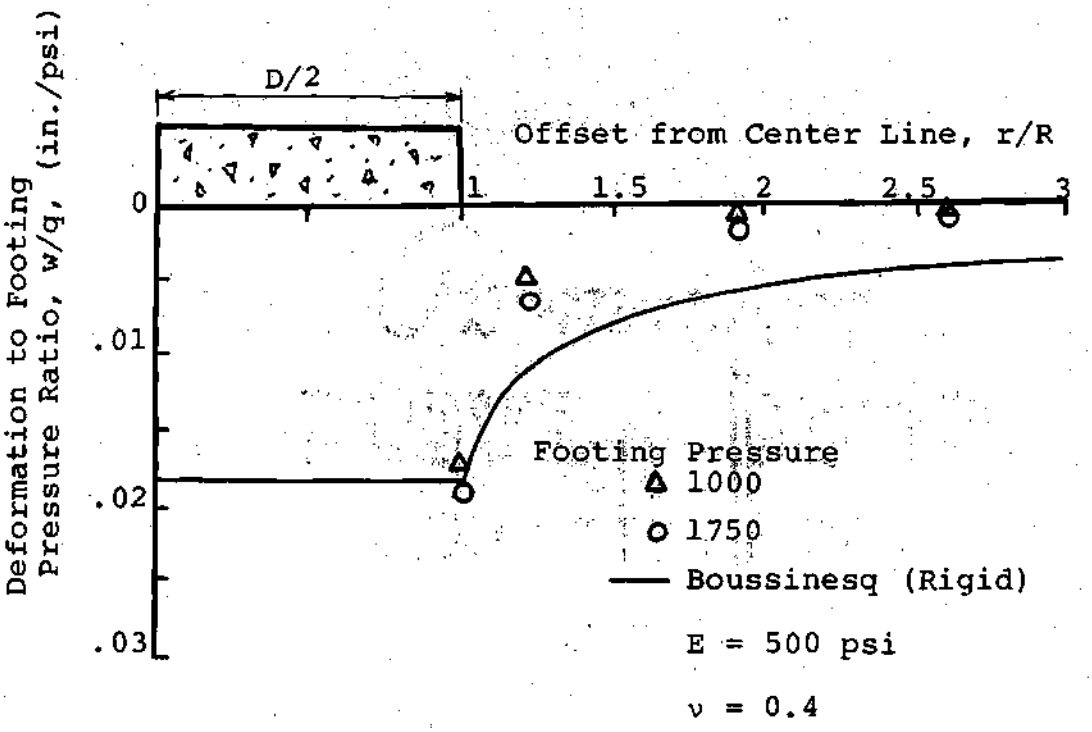

Figure 91. Comparison of Surface Deflection Profile with Theoretical Predictions for Homogeneous Layer - Test Series I.

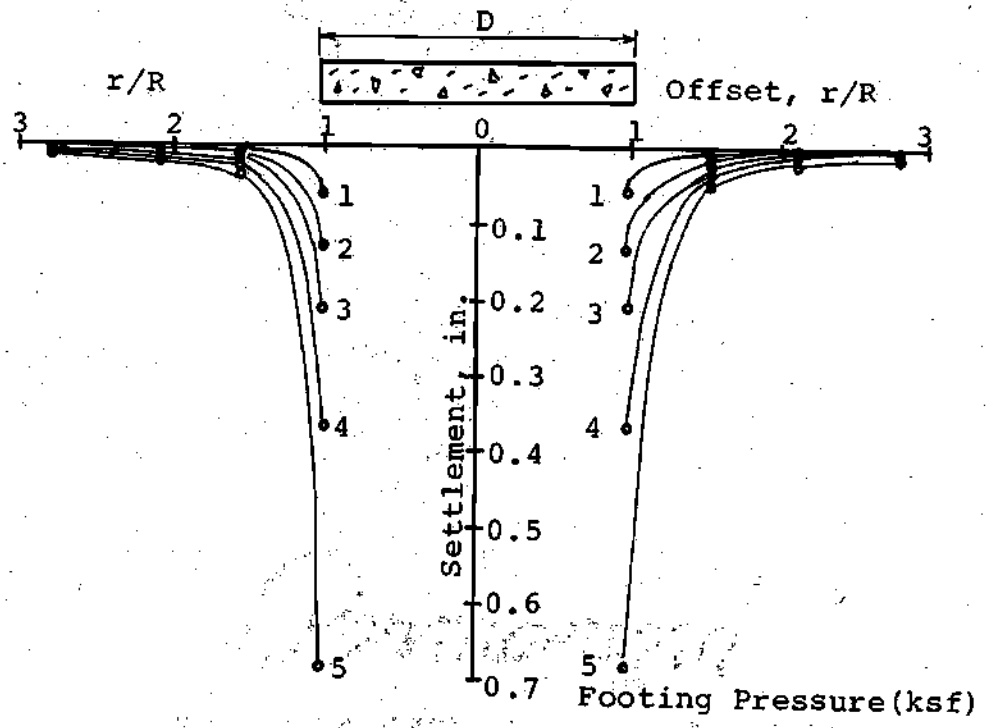

a) Fill Thickness H = 1/2D

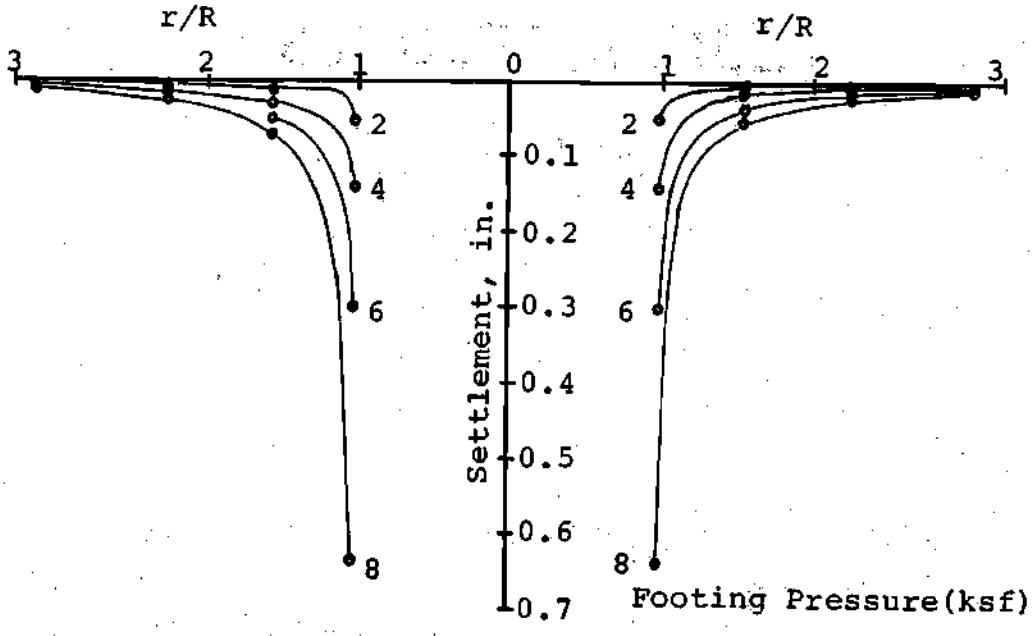

b) Fill Thickness H = 1D

Figure 92. Surface Deflection Profiles of Sandy Clayey Fills over Soft Layers - Test Series II

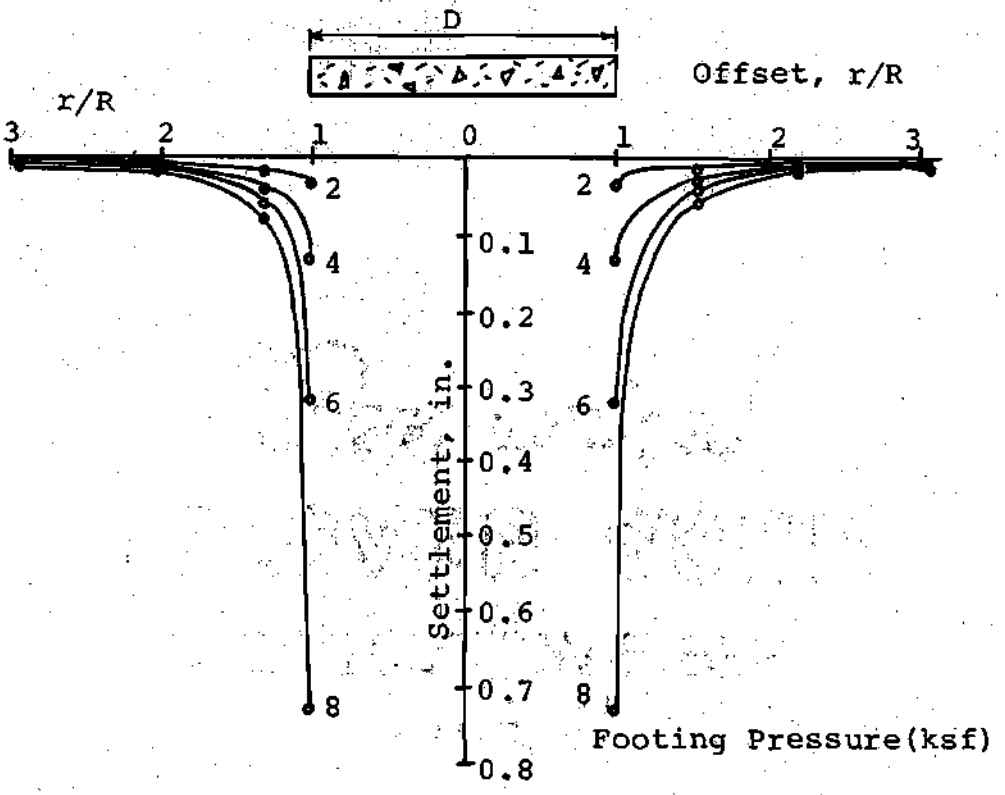

c) Fill Thickness H = 1-1/2D

Figure 92. (continued) Surface Deflection Profiles of Sandy Clay Fills over Soft Layers - Test Series II

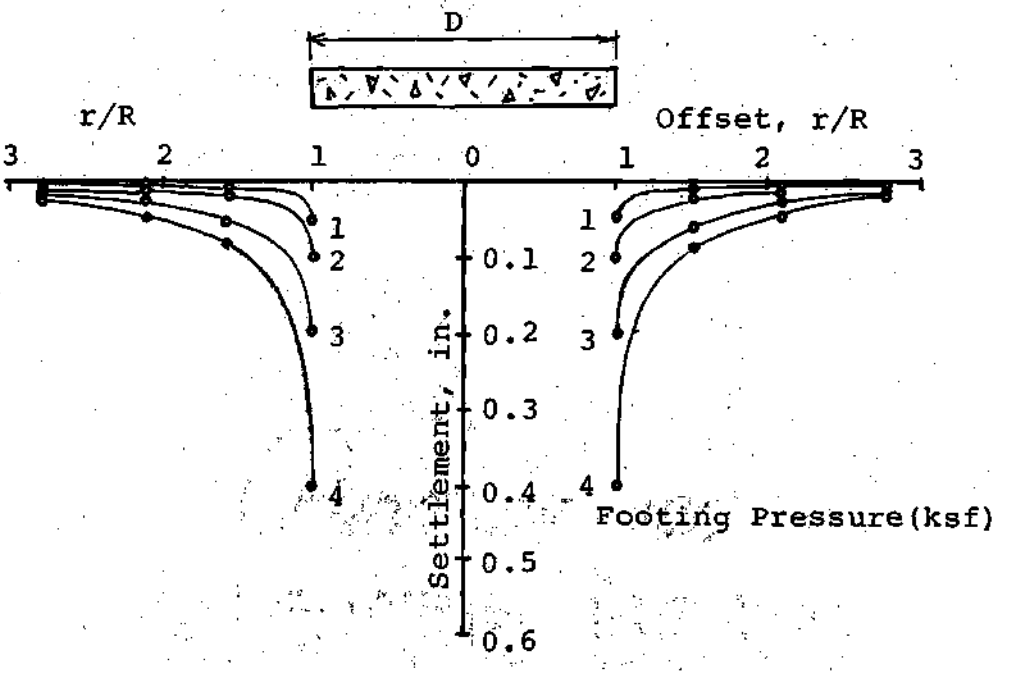

a) Fill Thickness H = 1/2D

Figure 93. Surface Deflection Profiles of Sand Fills over Soft Layers - Test Series III

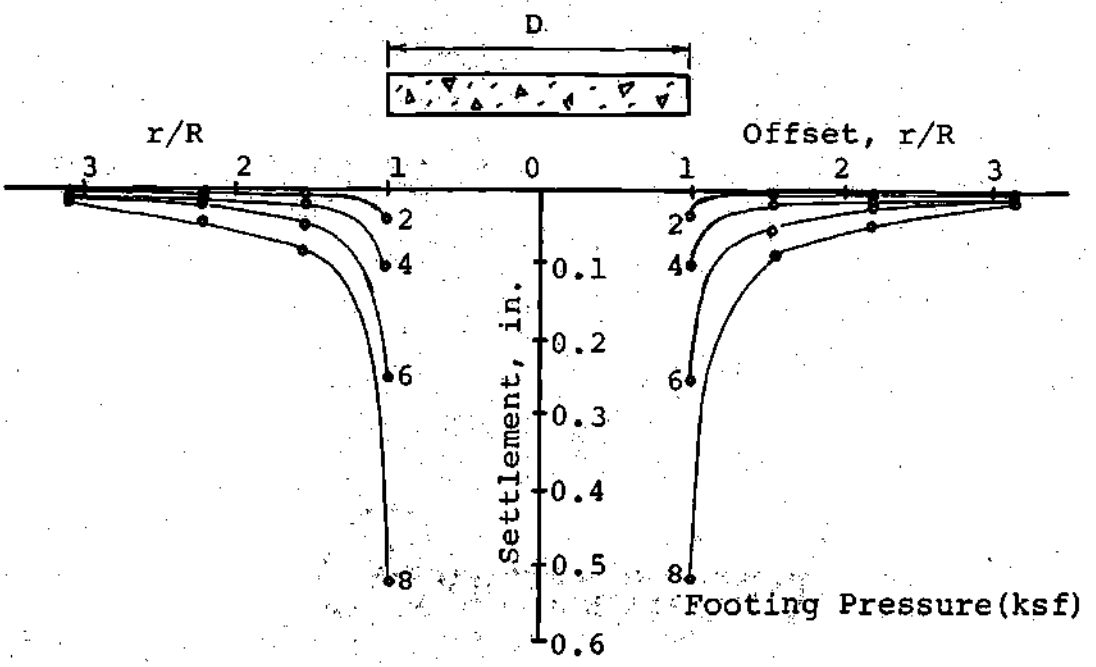

b) Fill Thickness H = 1D

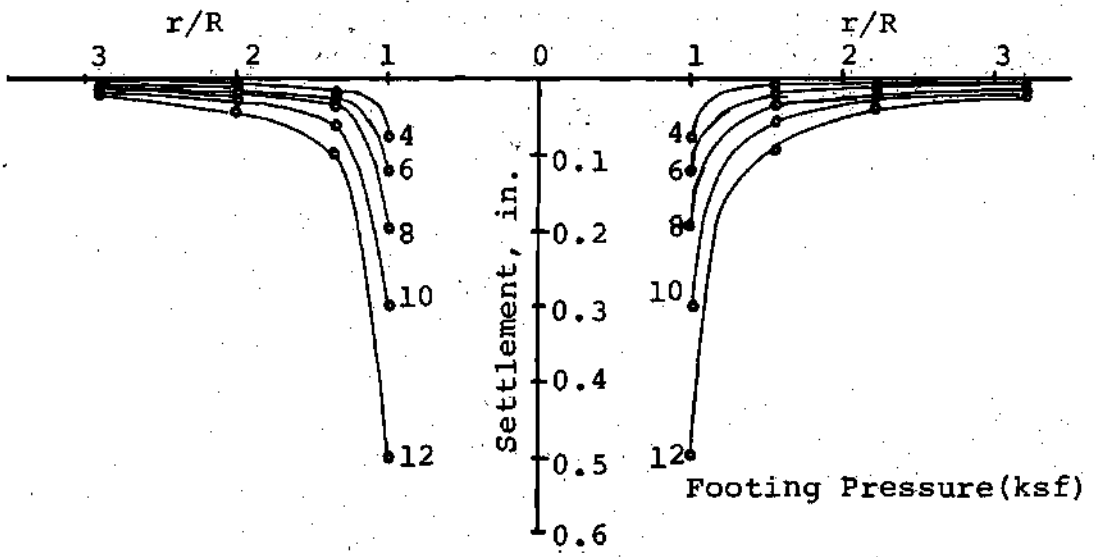

c) Fill Thickness H = 1-1/2D

Figure 93. (continued) Surface Deflection Profiles of Sand Fills over Soft Layers - Test Series III

center. For sand fills, the surface displacements occurred beyond the distance r/R = 3 for all three fill thicknesses used. No surface rise was measured as the footing pressure approached a bearing capacity failure. Visual inspection after the tests confirmed that punching failure occurred.

Ultimate Bearing Capacity Analysis

The ultimate bearing capacities of the structural fill-subsoil systems and of the homogeneous soil layer were determined from the load-settlement curves for each test series. These results are presented in Table 10. Figure 94 shows the plots of the ratio of ultimate bearing capacity of compacted fill to that of the homogeneous soil layer for sandy clay and sand fills. As would be expected, the bearing capacity ratio increases as the fill thickness increases.

The ultimate bearing capacity of the uniform soft soil layer was calculated using the relationship given by Terzaghi and Peck [121] for a circular loaded area (Appendix D) and triaxial test data which are summarized in Table 11. The calculated bearing capacity was compared with the results of footing load tests as shown in Table 10. The effects of soil compressibility on bearing capacity was considered in the analysis following the Terzaghi and Peck's recommendation. It is seen that good agreement between calculated and measured maximum bearing capacity was obtained.

The ultimate bearing capacity of the fill-subsoil systems may be analyzed using several available procedures. Two

Table 10. Comparison of Measured and Calculated Maximum Bearing Capacity.

Type	Calculated, psf		Measured, psf
	Terzaghi and Peck [121]		
Uniform Soil	2808 psf		3000
Sandy Clay Fills	Vesic [130]	Meyerhof [76]	
H = 1/2D	5,620	-	4500
H = 1D	8,414	-	8000
H = 1-1/2D	16,433	-	8000
Sandy Fills			
H = 1/2D	5,031	4737	4000
H = 1D	9,833	8589	8000
H = 1-1/2D	19,316	14217	12500
Stone Replacements			
2D wide- 1D deep	9,833	3945	3000
2D wide-1/2D deep	5,031	3331	3400
1D wide- 1D deep	-	-	2550

Table 11. Summary of Triaxial Test Results.

Soil Type	γ_d (pcf)	W (%)	Effective Strength Parameter C′ (psi)	Effective Strength Parameter ϕ'
Micaceous Clayey Silt[1] (Average Value)	85	30.5	3	10°
Sandy Clay[2]				
Test 1 and Test 2	99.5	22.5	9.5	16°
Test 3	99.5	22.0	8.0	16°
Sand				
Crushed Stone:	122	6.0	0	42°
	129	6.5	0	52°

[1] and [2] Five percent strains were used as failure criteria.

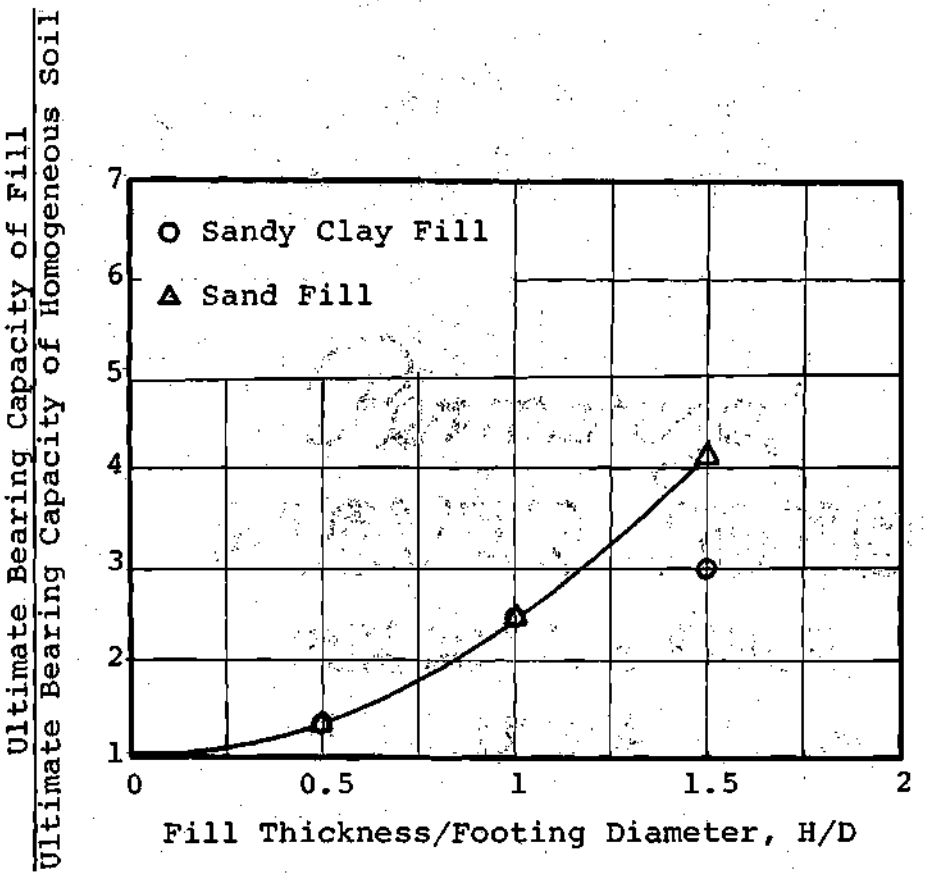

Figure 94. Effects of Fill Thickness on Ultimate Bearing Capacity.

methods which are applicable to this study are those of Vesic [130] and Meyerhof [76]. Details of these equations are given in Appendix D. Vesic's method is applicable to soils which possess both cohesion and friction in fill layers and the underlying soft layer. His method was based on experimental studies which indicated that the mode of failure was punching along vertical slip lines following the foundation perimeter. The method by Meyerhof [76] which is applicable only to a foundation resting on a sand layer overlying clay also assumes that punching occurs through the sand layer into the clay. The footing load tests conducted in this experiment were not carried out to obtain a complete bearing capacity failure or ultimate punching into the soft subsoil. Each load test was terminated as soon as the plot of load versus surface settlement indicated a marked deviation from the approximately linear portion of the curve and when the rate of settlement increased at an increasing rate. This was done to prevent excessive disturbance of the soft subsoil adjacent to the test area. The results of surface deflection measurements shown in Figures 93 and 94 indicated that a punching rather than a general bearing capacity failure occurred in all tests, which supports the findings of Vesic and Meyerhof.

The calculated ultimate bearing capacities using both methods are compared with the measured values as shown in Table 10. For both sandy clay fill and sand fill, Vesic's method gave excessive estimates of bearing capacity for the

case where the fill layer was relatively thick (H = 1-1/2D). The measured bearing capacity of sandy clay fill with H = 1-1/2D was considerably lower than anticipated maybe because of some variation in the density of the fill layer. The dynamic penetration test results show a weaker material than that for sandy clay fill of 1D thickness (Figure 105). This effect, however, was taken into account in the analysis by using the shear strength parameters from samples obtained from this fill.

The Meyerhof method was found to predict the ultimate bearing capacity of the sand fill-subsoil system accurately for all three cases. The Vesic method gave considerably higher estimates than the measured values as the fill thickness increased. This could be attributed to the fact that the solution given by Vesic for a sand layer over clay is applicable for a range of ϕ between 25° and 50°. However, the measured shear strength parameter ϕ of the sand layer is not used in the analysis. The Meyerhof method on the other hand takes into account the actual ϕ of the sand layer in the solution.

Attempts were also made to apply both methods to calculate the ultimate bearing of stone replacements with the width of 2D. Since the stone was lightly compacted, the compressibility effect was taken into account by reducing the shear strength from triaxial tests as recommended by Terzaghi and Peck [121]. It is seen that the Meyerhof method may be used to reliably estimate the ultimate bearing capacity of

the stone replacement with a width of 2D. The method by Vesic gave considerably higher estimates than the measured values.

Settlement Analysis

The footing settlements and settlements of soft subsoils were estimated using the consolidation test results and the Terzaghi one-dimensional consolidation theory [121]. In this method, the total settlement is assumed to be equal to the consolidation settlement. The results of consolidation tests on samples of soft subsoils from all three test series are presented in Figure 33. The settlement was calculated by direct proportion to vertical strain using the ε_v-log p plots of consolidation test data as recommended by Brumund, et. al., [27]. The allowable bearing pressure for each load test, which was used in the settlement analysis, was obtained by reducing the measured maximum bearing capacity in Table 10 by a safety factor of 2. For the homogeneous soft soil layer an elastic approach referred to as the layer-strain method proposed by Barksdale, et. al., [13] to calculate foundation settlement in a residual soil was also used to compute the total settlement. This method requires a plot of effective reload modulus versus confining pressure and a value of K_0 of the soil to be analyzed. In this method the soil profile beneath the foundation is divided into small layers and the stress increase at the center of each layer determined using

the stress distribution theory as shown in Table 12. The total horizontal stress due to the overburden pressure and stress increase at the center of each layer is determined assuming a K_0 condition. A typical value of K_0 equal to 0.5 for micaceous clayey silt was used. The effective modulus of each layer was then determined from the relationship of modulus versus confining pressure as shown in Figure 32. An average vertical strain at the center of each layer below the centroid of the load was determined by dividing the stress increase by effective modulus. The total settlement is then obtained by multiplying the average vertical strain by the layer thickness and summing up the resulting settlements. The layer-strain approach admittedly neglects the effects on the vertical strain due to the change in horizontal stress. The calculated settlements using the consolidation and layer-strain methods are compared with the measured value in Table 12. It is seen that using the stress distribution theory by Boussinesq for a flexible foundation over-estimates the measured settlement considerably. The settlement prediction was markedly improved when Boussinesq theory for a rigid displacement case (which is compatible with the test condition) was employed in both methods.

The rigid footing settlements of the fill subsoil systems (Test Series II and III) were calculated using the consolidation method and the stress distribution theories which were similar to the results of stress measurements as

Table 12. Comparison of Measured and Calculated Settlements for Homogeneous Layer (Test Series I) at an Allowable Footing Pressure of 1500 psf.

Method	Stress Distribution Theory	Settlement, in.		Ratio*
		Calculated	Measured	
Consolidation Method	Boussinesq (Centerline) (Flexible)	0.40		2.0
	Westergaard (Centerline) (Flexible)	0.29		1.4
	Boussinesq (Centerline) (Rigid)	0.27	0.20	1.35
Layer-Strain Method (Barksdale, et. al., [13])	Boussinesq (Centerline) (Flexible)	0.34		1.7
	Boussinesq (Centerline) (Rigid)	0.25		1.25
	Westergaard (Centerline) (Flexible)	0.24		1.2
Schmertmann [98]		0.42		2.1

*Calculated/measured.

shown in Figures 86, 87, and 88. The settlements in the sand layers were calculated using the elastic layer-strain method and E from triaxial test data. The settlements within the stone replacements were calculated in the same manner.

As shown in Table 13, the measured settlements were over-estimated using the theoretical methods in all cases. The differences in the calculated and measured settlements can be attributed to the following conditions:

1. Long term settlements under footing loads were not completed.
2. Consolidation test results were not representative.
3. Stress distribution theory used was not correct.
4. Errors in the settlement measurements.
5. Use of centerline stress instead of average over an area.

During the footing load tests, each load increment was maintained until the primary consolidation was reached. Additional settlements which might have occurred due to adding the next load increment too soon, would have been small. Consolidation tests were conducted on samples from various depths in the soil layer and the average results plotted. Disturbance during sampling and the test preparation could be the cause of these errors. The stress distribution theories used in the settlement calculation were similar to the measured stresses. Errors in the settlement measurement should be relatively small.

The settlement of the test footing on the fill-subsoil

Table 13. Comparison of Measured and Calculated Settlements for Structural Fills Over Soft Layers - Test Series II and III Using Consolidation Method.

Type	Stress Distribution Theory	Calculated, in.		Measured, in.		Ratio[a]	
		Surface Total	Soft Layer	Surface Total	Soft Layer	Surface Total	Soft Layer
Sandy Clay Fill:							
H = 1/2D	$E_1/E_2 = 10$[b]	.14	.11	.11	.09	1.3	1.2
	Westergaard[c]	.18	.12			1.6	1.3
H = 1D	$E_1/E_2 = 10$	.20	.09	.14	.08	1.4	1.2
	Westergaard	.24	.13			1.7	1.6
H = 1-1/2D	$E_1/E_2 = 10$	.16	.04	.08	.02	2.0	2.0
	Westergaard	.18	.06			2.2	3.0
Sand Fill:							
H = 1/2D	$E_1/E_2 = 5$	.17	.16	.11	.10	1.5	1.6
	Westergaard	.18	.15			1.6	1.5
H = 1D	$E_1/E_2 = 5$	.17	.13	.10	.09	1.7	1.4
	Westergaard	.18	.14			1.8	1.5
H = 1-1/2D	$E_1/E_2 = 5$	.18	.13	.14	.08	1.3	1.6
	Westergaard	.20	.14			1.4	1.7
Stone Replacement:							
2D wide-1/2D deep	Boussinesq (Rigid)	.17	.15	.10	.09	1.7	1.6
	Westergaard	.12	.10			1.2	1.1
2D wide- 1D deep	Boussinesq (Rigid)	.13	.10	.07	.04	1.8	2.5
	Westergaard	.10	.06			1.4	1.5
1D wide- 1D deep	Boussinesq (Rigid)	.10	.08	.05	.04	2.0	2.0
	Westergaard	.07	.05			1.4	1.3

[a] Calculated/observed settlement.
[b] Two-layer rigid displacement for linear elastic isotropic materials.
[c] Westergaard solution used a flexible surface loading.

systems used in this study could be conservatively predicted using the Terzaghi theory and consolidation test results provided the appropriate stress distribution theory is used. The calculated settlements were on the order of 13 to 63 percent overestimate of the measured settlements.

The layer-strain method was also used to calculate the total settlement and the settlement in the soft layers of the fill-subsoil systems and the stone replacements. For sand fills compacted in layers, K_0 equal to 1.0 was used to calculate the horizontal confining pressures under loads in the sand layers. For the compacted sandy clay fills and lightly compacted stone replacements, K_0 equal to 0.5 was used. The stress distribution theories used produced results similar to the stress measurements, which were for a two-layer rigid footing elastic analysis. Table 14 shows a comparison between the observed and calculated settlements using this method. Good agreement between the calculated and observed settlements was obtained using this method. Since the settlement was primarily elastic, the layer-strain method, therefore, gave good estimates of the settlements to within $\pm$25 percent of the measured values.

Boundary Effects on Stress Distribution

In the theoretical analysis of stress distribution, the soil mass is assumed to be semi-infinite in both horizontal and vertical directions. The dimensions of the test pit did not meet this assumption; therefore, some deviation

Table 14. Comparison of Measured and Calculated Settlements for Compacted Fills Over Soft Layers - Test Series I and II Using Layer-Strain Method [13].

Type	Stress Distribution Theory	Calculated (in.)		Measured (in.)		Ratio[1]	
		Surface Total	Soft Layer	Surface Total	Soft Layer	Surface Total	Soft Layer
Sandy Clay Fill:							
H = 1/2D	$E_1/E_2 = 10$[2]	0.13	0.12	0.11	0.09	1.2	1.3
H = 1D	$E_1/E_2 = 10$	0.17	0.11	0.14	0.09	1.2	1.3
H = 1-1/2D	$E_1/E_2 = 10$	0.09	0.03	0.08	0.02	1.2	1.5
Sand Fill:							
H = 1/2D	$E_1/E_2 = 5$	0.14	0.13	0.11	0.10	1.3	1.3
H = 1D	$E_1/E_2 = 5$	0.14	0.11	0.10	0.09	1.4	1.2
H = 1-1/2D	$E_1/E_2 = 5$	0.19	0.08	0.14	0.08	1.4	1.0
Stone Replacement:							
2D wide-1/2D deep	Boussinesq (Rigid)	0.17	0.14	0.10	0.09	1.7	1.5
2D wide- 1D deep	Boussinesq (Rigid)	0.10	0.06	0.07	0.04	1.4	1.5
1D wide- 1D deep	Boussinesq (Rigid)	0.09	0.06	0.05	0.04	1.8	1.5

(1) Calculated/observed settlement.
(2) Two-layer rigid displacement for linear elastic isotropic materials.

from the theoretical results would occur. The effect of the concrete walls on the stress distribution pattern was investigated using a finite element method. One analysis was made assuming a finite element grid close to a semi-infinite extent (10R and 27R in horizontal and vertical directions, respectively) and the other was performed using the dimensions of the test pit. It was found that by having the footing load test located a distance of two diameters of the footing from the center line to the concrete wall, the maximum stress value at the wall was increased from 0.019q to 0.029q where q is the applied footing pressure, an increase of approximately 50 percent. The results of the finite element analysis, however, indicated the concrete side walls had no observable effect on the vertical stress distribution under the loaded area. The concrete bottom of the test pit which was located at a depth of 4.5D below the footing level was also found to have no significant effect on the vertical stress distribution.

Design and Development of Stress Cells

Stress cells were designed and developed as a portion of this study. The available literature was studied to ascertain the extent of the knowledge of the design of a stress cell and its limitations in use. The cells were designed according to the latest design criteria which have already been enumerated in Chapter IV and discussed in Appendix A.

The stress cells were tested to establish their

behavior characteristics in water, micaceous clayey silt, sandy clay, and sand. The calibration tests indicate that the degree of accuracy of the stress cell was in all cases within an accuracy of ±5 percent, and usually much less.

Field Applications

The results of this study for the materials tested and loading conditions showed that sandy clay fill tested when compacted to 95 percent of the dry density obtained by Standard Proctor, could be used effectively to reduce the settlement of the soft subsoil beneath the fills. The measured stresses in the weak subsoil were less than that indicated by Boussinesq theory for a homogeneous soil condition and could be predicted using a two-layer theory for a flexible foundation and a modular ratio $E_1/E_2 = 10$. The sand fill tested when compacted to a relative density of 90 percent also reduced the settlement of the soft layers. At allowable bearing pressures equal to one-half the ultimate bearing capacity, the measured stress in the soft subsoil were found to be less than that computed by Boussinesq theory and corresponded to that indicated by a two-layer theory using a modular ratio $E_1/E_2 = 5$. The compacted sand fill tested, as expected, was not as effective in reducing the stresses in the soft layers as the sandy clay fills.

Lightly compacted stone replacement footing could be used effectively to reduce the surface settlement. Using a width of two times the footing diameter and one diameter

deep was effective in reducing the settlement in the soft layer beneath the stone.

For good engineering practice and until more data are available, the thickness of the fill should be at least equal to the width of the footing in order to insure adequate protection against bearing capacity failure of the fill-subsoil system.

The results of this study have not been verified in the field by a large scale footing load test comparable to a building foundation (6 to 8 feet in diameter). Since the experiment was conducted using a 1.5 foot diameter footing in a controlled condition, the scale effect should be considered in applying the test results to a field problem. For compacted sand, the scale effect may not be unfavorable because increasing the fill thickness would be beneficial in that the modulus of elasticity of sand increases with depth of overburden. The scale effect also should not be very significant for sandy clay fill because the modulus of sandy clay is not very sensitive to the increase of overburden pressures. When the footing size increases, the fill thickness must also increase in order to maintain the same fill thickness to footing diameter ratio. For this condition, the increase in footing size has no influence on the vertical as well as radial and tangential stresses in the fill-subsoil system when the same footing pressure is applied. However, from elastic theory the settlement of footing increases for a

given footing pressure as the footing size increases.

The time-effect on the strength of compacted sandy clay fills could be significant, particularly if utilized in the area with high ground water table. The strength of sandy clay fill will be adversely affected by a rise of ground water level or a capillary rise, which will cause a reduction of strength and tensile modulus on wetting. Wetting from the surface down of sandy clay fill due to seasonal rainfall could also cause a strength reduction which in turn reduces the load-spreading ability of the sandy clay fill. Therefore, utlizing a compacted sandy clay fill in the field should be made after verification with full-size footings.

CHAPTER VIII

CONCLUSIONS

The beneficial effects of two compacted fills in reducing the settlement and stress in an underlying soft micaceous clayey silt were investigated experimentally utilizing 1.5 feet diameter footing load tests. Based on the test results, the following general conclusions can be made:

1. Compacted sandy clay and sand fills were effective in reducing the settlements of the soft layers to less than that of the soft soil measured at the same depth in a homogeneous condition, thus indicating the beneficial effects of the compacted fills in reducing the consolidation settlement of the soft layers.
2. The beneficial effect of the sandy clay and sand fills in reducing the settlement increased as the fill thickness increased. Based on a design footing pressure of 2000 psf., sandy clay and sand fills caused a settlement reduction in the soft layers from 50 to 80 percent and 41 to 75 percent, respectively, as the fill thickness increased from one-half to one and one-half times the footing diameter.
3. The stone replacement beneath the footing lightly compacted with no density control was found to reduce the

surface settlement. The beneficial effect of the stone replacements in reducing the settlement in the soft layers depends on the replacement width.

4. The measured vertical stresses beneath a rigid footing in homogeneous micaceous clayey silt compared favorably with that computed by Boussinesq theory for a rigid loaded area. The measured stresses and strains, however, attenuated faster with depth than indicated by Boussinesq theory.
5. At footing pressures equal to one-half the ultimate bearing capacity, the measured vertical stresses beneath the compacted sandy clay and sand fills tested having a thickness of 1/2D, 1D and 1-1/2D were less than the measured vertical stresses in the homogeneous condition, thus indicating the beneficial effects of the compacted fills in reducing the stress in the soft layers. This stress reduction was in agreement with the reduction of measured settlement of the soft layers.
6. At footing pressures equal to one-half the ultimate bearing capacity, the measured vertical stresses with depth in the soft layers beneath the compacted fills could be predicted adequately using a two-layer linear elastic theory for a flexible foundation and a modular ratio E_1/E_2 = 10 and 5 for compacted sandy clay and sand fills, respectively. The theory by Westergaard could be used to approximate stress distribution.

7. The stress distribution beneath the stone replacements tested having a width twice the diameter of the footing could be predicted using Boussinesq theory for a rigid displacement condition. Using a width of one diameter, the measured stresses at the soil-stone interface were 25 to 30 percent greater than those computed by Boussinesq theory.
8. The maximum bearing capacity of the sandy clay fills tested which overlay the soft subsoil was predicted aequately using the method of Vesic [130]. For sand fills the method by Meyerhof [76] gave good estimates of the maximum bearing values.
9. Using the elastic layer-strain method [13] and the stress distribution theories for a rigid foundation on a homogeneous layer and two-layer systems gave good estimates of the settlements of the footing on the homogeneous micaceous clayey silt and on compacted fills over soft layers. The calculated settlements were from 1.0 to 1.5 times the measured values. Using the consolidation test results and stress distribution theories for a rigid foundation, the estimated settlements range from 1.4 to 2.2 times the measured settlements.

CHAPTER IX

RECOMMENDATIONS FOR FURTHER STUDY

The experimental investigation on the beneficial effects of compacted fills performed in this study has indicated several other areas which need to be investigated. Some of these are:

1. A full scale footing load test using a 6 to 8 foot square footing should be conducted on compacted fill overlying a weak subsoil in the field to verify the findings in this study. To be of most value, the test should be instrumented with stress cells and strain sensors to measure stress and settlement of the soft subsoil.
2. A 1.5 foot diameter footing load test and even full scale should be performed on a real structural fill-subsoil system using materials which are normally available at marginal sites to verify the results of this study.
3. The stress-reduction ability and the ultimate bearing capacity of sand fills placed over soft subsoils possibly can be increased by placing reinforcing metal strips or fiber fabrics in the tension zone of the fill layer. This problem needs investigation. A 1.5 foot diameter footing load test similar to this study is recommended. Measurement of stress and deformation in the soft layer could be made using the same stress cells developed in

this study and Bison strain sensors.

4. The data gathered in this study indicate that the stress and strain attenuate with depth faster than that indicated by elastic theories. Further investigations are needed to better define the stress and strain distribution at greater depths.
5. The load-deformation behavior as well as the stress and strain distribution of sandy clay and sand fills overlying soft subsoil tested in this study should be predicted using a finite element method which incorporates non-linear and stress-dependent properties of the soils and uses different moduli in tension and in compression.

APPENDIX A

STRESS CELLS

Stress cells which have frequently been used in the measurement of stresses in soil are of the diaphragm type having one active sensing area [20]. Various sensing elements have been used to measure the deflection of the diaphragm including bonded strain gages of various type, vibrating wire gages and others. Bonded strain gages are most commonly used as the sensing element because of simplicity and low production cost. Important design considerations for stress cells have been reviewed by Selig [102], Triandafilidis [122], and recently by Brown [21].

Limitations

If a stress cell, being a rigid body, is introduced into a soil mass, it disturbs the stress distribution pattern in the vicinity of the cell causing a stress concentration around it, which is higher than the free field stress. The stress cell therefore has a natural tendency to indicate measured stresses higher than the true stresses. If the stress cell is to indicate true soil stresses, it must have the same elastic properties as those of the surrounding soil. The possibility of developing such a cell is remote. Therefore, the only recourse is to design a stress cell

which will disturb the stress patterns as little as possible and will measure stresses close to the actual values. A theoretical analysis [122] indicates that a stress cell stiffer than the soil medium will give stresses closer to the free-field values and is more preferable than a softer one.

For laboratory soil stress measurements, Hadala [54] reports variations in the over registration ratio as large as 40 percent. These variations were attributed primarily to variations in the placement technique. Ideally the bedding material around the cell should be compacted to the same density and stiffness as the soil mass. Unfortunately this condition is difficult to satisfy.

The determination of in situ stress remains a difficult problem because it cannot be measured directly and must rely on a measurement of strain or deformation within the instrument using an appropriate sensor. Becuase of the many difficulties involved, accuracies much better than about 20 percent cannot be expected [21, 54].

Design Criteria

The design of the stress cells used in this study follows closely the procedure given by Brown [21]. Two variables which will affect the cell registration are the cell geometry and the stiffness of its diaphragm relative to that of the soil. The cell registration factor is defined as

$$C = \frac{\text{measured stress}}{\text{true stress}} .$$

The geometry is expressed in terms of

$$\text{Aspect Ratio} = \frac{\text{cell thickness } B}{\text{cell diameter } D} .$$

and the relative stiffness of the diaphragm is expressed as

$$\text{Flexibility Factor} = \frac{\text{soil stiffness}}{\text{diaphragm stiffness}}$$

or

$$F = \frac{E_s d^3}{E_c t^3} \qquad \text{(A-1)}$$

where E_s, E_c = modulus of elasticity of soil and cell material

t, d = cell diaphragm thickness and diameter, respectively.

Brown [21] presents a series of curves relating these three variables. The flexibility factor should be less than 2 [7] for a stress cell to measure stresses to within a few percent of the true values.

Steps in Design

1. Select the type of material to be used, i.e., aluminum, stainless steel, titanium, etc. Aluminum was selected for this study.
2. Determine the diameter of the diaphragm by following the suggestion by Kallstenius and Bergau [58] that the

diaphragm diameter should be at least 50 times that of the largest soil particle to prevent arching effects of the diaphragm. Later theoretical studies based on probability [133] indicate that this criterion is valid.

3. The diameter of the cell can now be determined by keeping the area of the diaphragm to less than 45 percent of the total area of the cell face [84]. This criterion is intended to keep the sensing area away from the edge where stress concentration occurs. Audibert and Tavenas [7] suggest that the aspect ratio should be less than 0.1. The only limitation is to have adequate thickness for cable entry.
4. The thickness of the diaphragm can be determined by estimating the magnitude of stress to be measured in the field. To prevent the effect of arching the central deflection of the diaphragm under the anticipated field stress should not exceed 1/2000 of its diameter [125]. The deflection of the diaphragm can be calculated using the following relationship [94] for a clamped plate:

$$y_c = \frac{3\ Pd^4(1-\nu^2)}{256\ Et^3} \qquad \text{(A-2)}$$

where d = diameter of diaphragm

P = applied pressure

t = diaphragm thickness

ν = Poisson's ratio of the plate, and

E = modulus of elasticity of the plate.

By keeping the diaphragm deflection to within the limit, the diaphragm thickness can be adjusted to have a flexibility factor less than 2. Equation (A-1) is rearranged for F = 2 as

$$[\frac{d}{t}]^3 = 2[\frac{E_c}{E_s}]$$

E_s has to be estimated for the type of soil used.

Cell Construction

The stress cells used in this study were designed according to the procedure previously described. To determine the diaphragm diameter, the maximum grain size of micaceous clayey silt which was used to construct the soft layers was first determined. The grain size distribution curve (Figure 4) for this soil shows more than 97 percent passing No. 30 sieve which has an opening of 6 millimeters. Using this as the diameter of the largest soil particles, the required diaphragm diameter was 1.18 inches.

The stress cells were machined from grade 2024 T-3 aluminum which had a yield strength of 42 ksi and a modulus of elasticity of 10×10^6 psi. The stress cell had a diameter of 2 inches and a final diaphragm diameter of 1.25 inches. The ratio of the diaphragm area to the total area for this cell was 39 percent which was within the limit of the third design criteria. To provide adequate area for

cable entry, the thickness of the cell was limited to 0.25 inch. The cover plate thickness was 0.05 inch giving a total thickness of 0.3 inch. The aspect ratio of this stress cell was 0.15 which is slightly greater than the desired value of 0.1. The minimum diaphragm thickness which could be used in micaceous clayey silt without exceeding the flexibility factor of 2 was 0.03 inch, based on the modulus value of 500 psi which was determined from triaxial shear test results. The thickness of the diaphragm was varied depending on the anticipated field stresses. The diaphragm thickness of 0.03 inch was designed for a maximum pressure of 15 psi and 0.075 inch for 200 psi to keep the central diaphragm deflection within the limit of the fourth criterion. The stress cells which were made for Test Series II and III had two different diaphragm thicknesses because adequate sensitivity using one thickness could not be obtained for the range of stresses to be measured. Four of the cells had a diaphragm thickness of 0.075 inch and the remaining twenty were 0.05 inch.

Figure 4 shows a detail of the stress cell. One Micro-Measurement "JB" type diaphragm strain gage was used for each cell. This strain gage is designed to give a maximum output by summing the absolute value of both tangential and radial strains developed in the diaphragm when subjected to pressure. These gages were connected to form a four arm bridge capable of self temperature compensating.

To install the diaphragm strain gages, the cell body was first sprayed with a degreasing agent. The area to receive the strain gage was then scrubbed using a cotton tip while being sprayed with a mild acid solution (Conditioner A). The acid was neutralized using Neutralizer 5. Both products were manufactured by Micro-Measurements, Inc. Isopropyl alcohol was applied to the surface as the final step. The strain gage was then epoxied to the diaphragm by applying Micro-Measurements M-Bond AE 10/15 adhesive to the surface. A pressure of 10 psi was applied using dead weights to the strain gage and the cell was placed in the oven at 120°C to speed up the curing time to about one hour. To prevent contamination and corrosion, after removing from the oven, the strain gage was immediately covered with Micro-Measurements M-Coat C, a rubber based waterproofing agent. The connections between the strain gages and the lead wires were soldered and all bare wires were insulated with electrical tape. The lead wires were insulated and shielded to reduce signal interference. Before closing the lid, M-Coat C was applied on the edge to waterproof the cell. The lid was then lightly screwed down. After the silicon sealant was cured, the cover plate was then screwed tightly.

As mentioned in Chapter III, two sets of stress cells were made. The cells made in the first set were not anodized. In the second set, a commercial clear anodizing protective finish was applied and the cells were also sprayed with

corrosion resistant paint.

Cell Calibration

Each of the stress cells was calibrated individually using the calibration tank shown in Figure 95. The tank had a diameter nine times that of a stress cell which meets the criterion given by Triandafilidis [122].

Hydrostatic Calibration. To determine the true registration of the stress cells the hydrostatic calibration tests were conducted for each stress cell. The cell was sandwiched between two rubber membranes in the center of the tank which was filled with water. A rubber membrane was used to seal the tank and to apply pressure to the water. The top of the tank was bolted down securely prior to applying the air pressure. An Ashcroft pressure gage having a knife edge needle and a reflecting mirror was carefully calibrated using a dead weight tester and used to monitor the air pressure. A pressure three to four times greater than the anticipated field stresses was first applied and cycled to relieve the metal of residual stresses caused during manufacture and to minimize hysteresis effects.

Soil Calibration. It is desirable to calibrate stress cells under controlled laboratory conditions which correspond as closely as possible to the field situation. The stress cells were therefore placed in the same soil in which they were used and compacted to the same density. Prior to compacting the soil in the tank, the wall of the tank was covered

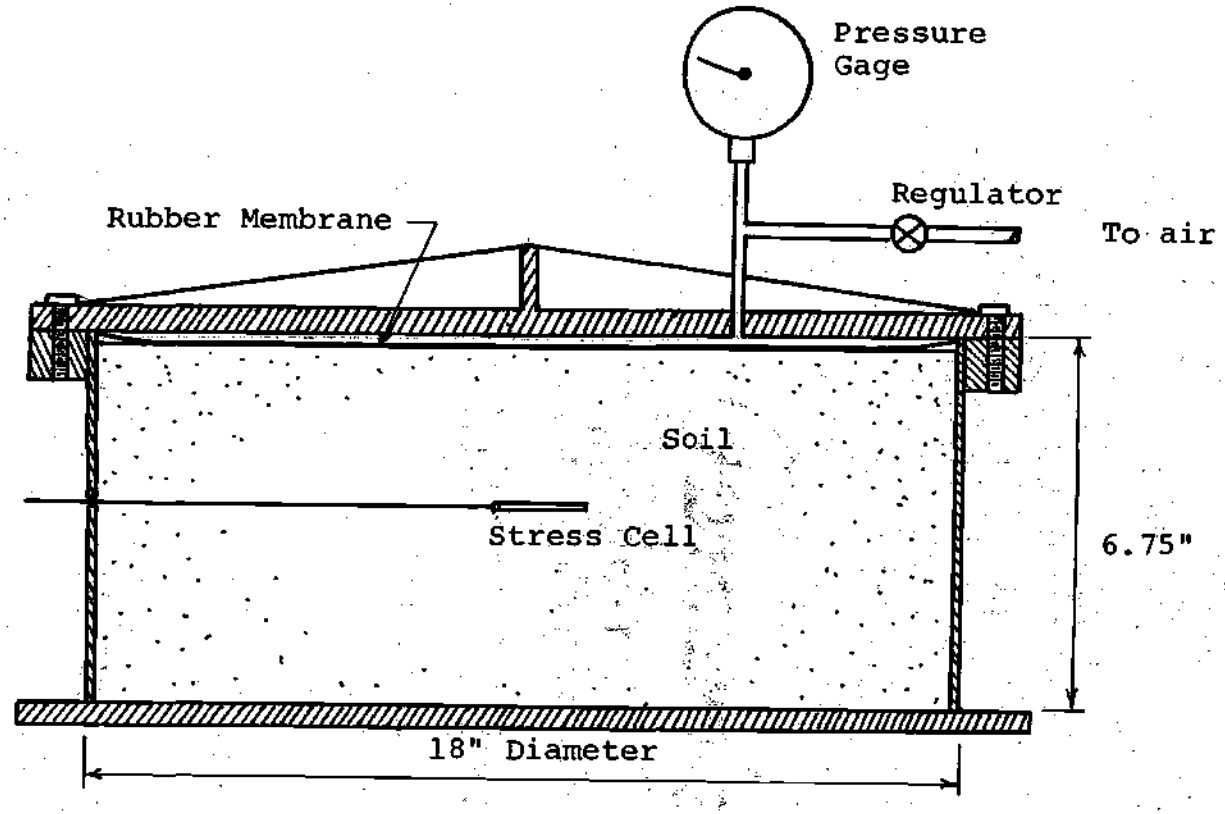

Figure 95. Calibration Chamber.

with rubber membranes attached to it with silicone grease. The stress cells were positioned at the center of the tank using the same technique of installation to be used in the test pit.

The pressure was increased in increments to the design pressure and then cycled 2 to 3 times to check the reproducibility of the output. Subsequent cell readings were found not to be much different from those of the first cycle. The strain output was recorded and the strain differences were computed to develop calibration curves for each cell. Typical curves for both hydrostatic and soil calibrations are shown in Figure 96. The calibration relationship was found to be linear within the design stress range. Table 14 contains a comparison between experimental cell registration and the theoretical ones as given by Brown [21]. The over or under registration of the gage was determined by comparing the strain output which is greater or less than the hydrostatic by the reference (hydrostatic) output at the same applied pressure. All of the stress cells were found to give over registration, and the experimental cell registration values were slightly less in most cases than those indicated by the theoretical approach of Brown [21].

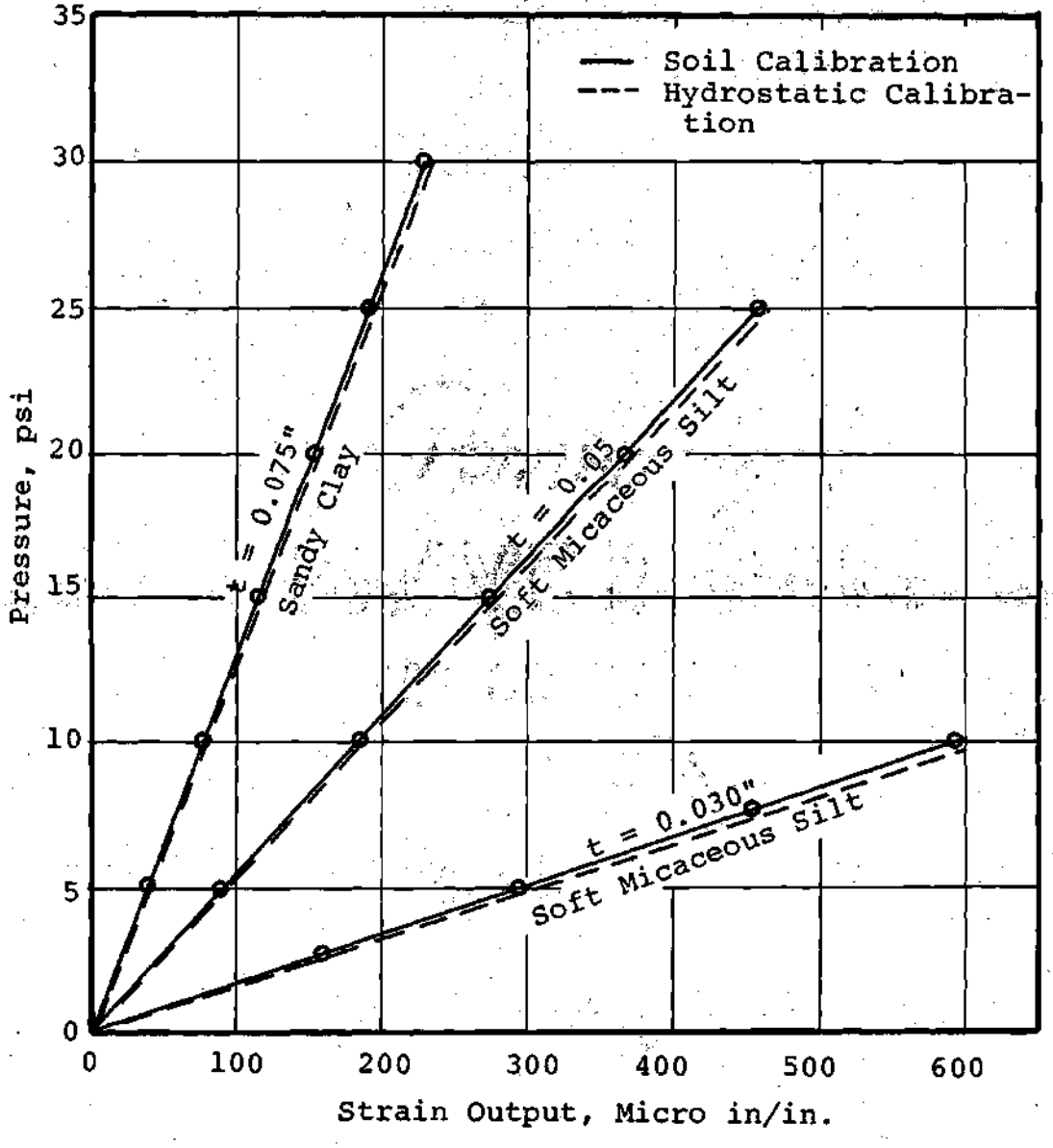

Figure 96. Stress Cell Calibration Curves.

Table 15. Comparison of Experimental and Theoretical Cell Registration of Typical Cells.

Cell Designation	Diaphragm Thickness, t, inch	Cell Registration	
		Experimental	Theoretical
A	0.05	1.01	1.05
B	0.075	1.06	1.05
C	0.030	1.054	1.05

APPENDIX B

SOIL STRAIN SENSORS

Strain measurements in soil mass have received very little attention in the past and a few attempts to measure strain in soil have been reported [22, 103]. There have been also relatively few strain cells described in the literature.

A strain measuring device should move with the soil in which it is placed without reinforcing it in any way. To determine strain in the soil mass, deformation has to be measured over a known gage length. This implies that the instrument must determine the relative movement of two points in the soil. There are several types of soil strain cells that may be used. Basically, two types of instrument are available. The TRRL Version [21] has two end discs which move relative to one another, the movement being determined by a built-in displacement transducer. The main shortcoming of this instrument is the mechanical linkage between the ends of the gage length. This causes problems of installation and friction which inhibits free movement. This type of strain cells can measure only strain at a certain point in soils and is not as versatile as the second type.

The other type of strain measuring instrument consists of a pair of strain sensors of wire wound induction coils [104]. These strain sensors which are commercially available from

Bison Instrument, Inc., were considered to be the most suitable for this study because they are free-floated thus providing minimum interference with the soil movement. The effect of change of moisture, temperature and cable length is in general negligible. The sensors are relatively easy to install, durable and fairly tolerant to errors caused during installation or subsequently which involves movements in directions other than the one in which measurements are being taken [103, 104]. Both laboratory and field measurements of dynamic and static strains have been made successfully [66, 116].

Three different sizes of sensors were used in this study with their size being 1.125 inches in diameter by 0.125 inch thick, 2.125 inches in diameter by 0.25 inches thick, and 4.125 inches in diameter by 0.25 inches thick. The sensors are machined-lined phenolic bases with electrical coils potted in epoxy for environmental stability. The unit Model 4101A is used to excite the electronic sensors with a 20 KHz frequency signal with a peak to peak amplitude of 15 volts. The maximum sensitivity of these sensors is 0.0004 inches of movement per amplitude dial division on the indicator box.

The sensors may be placed in coaxial or coplanar positions with the separations of the coils of from one to four diameters. The sensor separation selector on the read-out unit is used to control the range over which the amplitude

dial was effective. For sensor separations of one to two diameters, two to three diameters, and three to four diameters, the coil separation selector was set at one, two, or three. Some overlap between the three exists. Thus, by changing the sensor separation selector, the sensitivity of the read-out unit remained approximately constant for any sensor separation.

The bridge balance in the read-out unit is accomplished by means of phase and amplitude controls using a meter to indicate null. After a null condition of both phase and amplitude was obtained for a given sensor separation, the amplitude dial reading (0 to 1000 divisions) of the read-out unit corresponds to the sensor spacing. Changes in spacing are determined by renulling and noting the changes in the amplitude dial reading.

To establish the relationship between sensor separation and null amplitude and phase dial reading for each separation range, each pair of sensors was calibrated. The coil sensors were placed on a device which could measure the distance between the gages to 0.001 inch. For each coil separation range, sensor separations corresponding to null amplitude and phase dial readings at each 100 division from zero to 1000 were recorded. The relationship between sensor separation and amplitude dial reading for a coil separation range of three is indicated in Figure 97 for a one and two inch set of gages, two inch set of gages, and a two and four

inch set of gages. Similar relationships for coil separation ranges of one and two and two and four can be obtained.

To facilitate the interpretation of the large amount of strain coil readings taken during the load test series, the relationship between the sensor separation and amplitude reading for each coil separation range and sensor pair was approximated by a polynomial curve fit method using a fourth order curve. A typical relationship between the coil spacing and amplitude reading is given for 2 inch diameter coils in Equation (B-1). A typical fit is shown in Figure 97.

$$y = 3.57759 + 9.09473 \times 10^{-4} x + 2.03667 \times 10^{-6} x^2 - 3.2885 \times 10^{-9} x^3 + 3.18292 \times 10^{-12} x^4 \ldots \quad \text{(B-1)}$$

A computer program was written to convert the readings into gage lengths (spacing) and interpret the change in gage length for each load increment. The strains in percent are then calculated as:

$$\varepsilon_n = \frac{L_n - L_o}{L_o} \times 100 \quad \text{(B-2)}$$

where ε_n = strain at the nth load increment

L_o = initial spacing with no load

L_n = spacing at the nth load increment

The calculated strain is assumed to be the average value of strain at the center of the initial gage length.

Movement of the sensors within the soil mass can be

monitored both in coaxial and coplanar directions. This versatility gives the advantage of being able to measure relative movement of one sensor to another vertically and horizontally. If the sensors are installed in columns along the vertical axis of the footing, the change of spacing between each pair of sensors due to the imposed footing loads, can be measured by a leap frogging method. Simple switching units using terminal strips attached to wood blocks were used to facilitate the sensor readings.

The sensitivity of the sensor movement can be best obtained if the sensor spacing is set so that the initial null amplitude reading is in the range of 0-400 for each coil separation because of the nonlinearities of the sensor calibration curve. The sensitivity actually obtained for sensors one and two inches in diameter ranges from 0.0015 to 0.0025 inch per unit change in amplitude.

Two major problems were found using these sensors. First, the lead wires of the sensor had to be shielded in order to obtain consistent results and maximum sensor spacing for each coil separation according to those given in the literature provided by the manufacturer. Secondly, any metal within four diameters of any sensor affected the output of the sensors. The effect is to move up or down the calibration curves shown in Figure 97 but not to change the shape of the curve. The stress cells which were made of aluminum were placed at not less than two sensor diameters from the

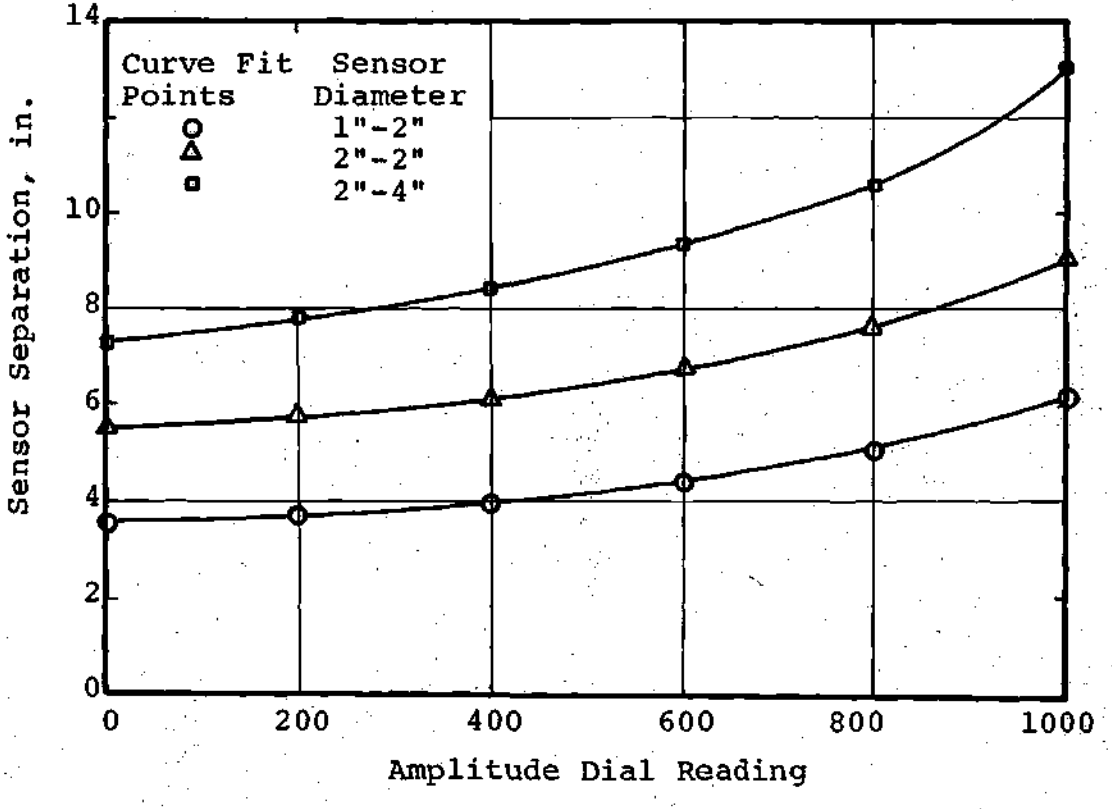

Figure 97. Amplitude Dial Reading vs. Sensor Separation.

sensors as recommended by the manufacturer to minimize the influence on the sensor output by the stress cells. The effects were eliminated by placing a stress cell two diameters from the sensors during calibration.

APPENDIX C

BEAM BENDING TESTS

Introduction

When a compacted structural fill is placed over a weak subsoil and subjected to a surface load, three-dimensional bending action produces tension at the base of the fill layer. According to the two-layer theory, the analysis of stress distribution usually assumes equal moduli of elasticity in tension and in compression. The modulus of elasticity of compacted clay in compression is normally determined from compression tests. Recent studies [3, 4] indicate that values of modulus of compacted clay from bending tests may be two to four times greater than those obtained from unconfined compression tests.

The purpose of performing beam bending tests was to determine the tensile-stress strain characteristics of compacted sandy clay used as the structural fill in Test Series II. Bending tests were conducted on a laboratory compacted sample and beams trimmed from block samples recovered from the test pit. From the test results the maximum tensile strains at failure were determined. The modulus of elasticity of the compacted clay from bending tests were also compared with the modulus of elasticity obtained from unconfined compression tests.

Table 15 gives a summary of test results from previous investigations in bending tests.

Test Procedure

Specimen Preparation

Laboratory Specimens. A beam specimen was prepared by compacting sandy clay mixed with betonite at 4 percent by weight in a rectangular steel mold with a compaction hammer having a 1.5 inch by 2.0 inch shoe. The steel mold 20 inches long and three inches by three inches internal dimensions had removable sides and end plates. The clay was compacted in the mold in six layers. The moisture content and the density of the clay beam was selected to be the same as those of the compacted sandy clay fills in the test pits.

Before placing the next layer, the smooth surface of the compacted soil in the mold was scarified in order to prevent weak planes. After the final layer was compacted, the surface of the beam was screeded to a smooth finish. The mold was then weighed and the wet density of the beam determined. The beam was transferred to the wooden block (see Figure 99) without lifting the beam to prevent unnecessary pre-stressing. The beam was coated with paraffin (mixed with 60 percent petrolatum oil) by first gently brushing the molten wax on the beam surface and manually working with a knife to produce an even layer. A template with two rows of predrilled holes 0.03 inch in diameter at 0.85 inch apart was placed on the beam surface and a small pin 0.025 inch diameter was

Table 16. Summary of Existing Bending Test Results on Compacted Soils Tested at Standard Proctor Density and Optimum Moisture Content.

Source	LL	PI	< No. 200 Sieve	Standard Proctor γ_d pcf	Standard Proctor W_{opt} %	Tensile Strain at Failure %	Initial Tangent Modulus psi	Secant* Modulus psi
Leonard and Narain [70]								
Limestone	72	45	82	96.0	25.9	0.3	-	5250
Portland Dam	29	8	25	112.0	16.3	0.18	-	3000
Rector Creek Dam	36	16	11	103.0	19.8	0.15	-	4025
Woodorest Dam	Non-Plastic	-	21	127.0	10.2	0.24	-	4500
Willard Dam	31	11	28	110.0	16.4	.07	-	4300
Shell Oil Dam	Non-Plastic	-	22	120.0	11.2	.22	-	2100
Ajaz and Parry [3]								
Gault Clay	73	39	90	95.6	24.6	0.80	14500	2200
Balderhead Clay	34	14	65	129.0	13.0	0.65	16600	2681

*Secant modulus was determined at failure strain.

inserted in each hole to a depth of 3/4 inch. These pre-drilled holes on the beam were made to later receive miniature coils for measuring strains in the beam.

Beam Specimens from Test Pit Samples. Two beams hand trimmed from block samples from Test Series II were also tested in flexure. The size of the beam specimens was the same as those compacted in the laboratory. After trimming, the paraffin coat was immediately applied to the beam to prevent moisture loss.

Beam Bending Device

The test arrangement is shown in Figure 98. A two-point loading system was used since this system would produce a uniform pure bending moment in the region between the inner loading points. To monitor the deflection of the beam, three dial gages having an accuracy of 0.0001 inch were mounted on the beam as shown in Figure 99. The internal strains of the beam were measured by using miniature inductance coils 0.3 inch in diameter and 0.15 inch thick. Since metal pins could not be used because of the interference with the coil readings, bamboo skewers were cut to a length of 1.75 inch and a diameter of 0.03 inch and epoxied to the strain coils. After the beam was placed in the test area, the pins with coils attached were then inserted in the predrilled holes in the positions as shown in Figure 98. The movements of the miniature coils during testing were monitored using Bison readout unit Model 4101A. These coils which were especially designed

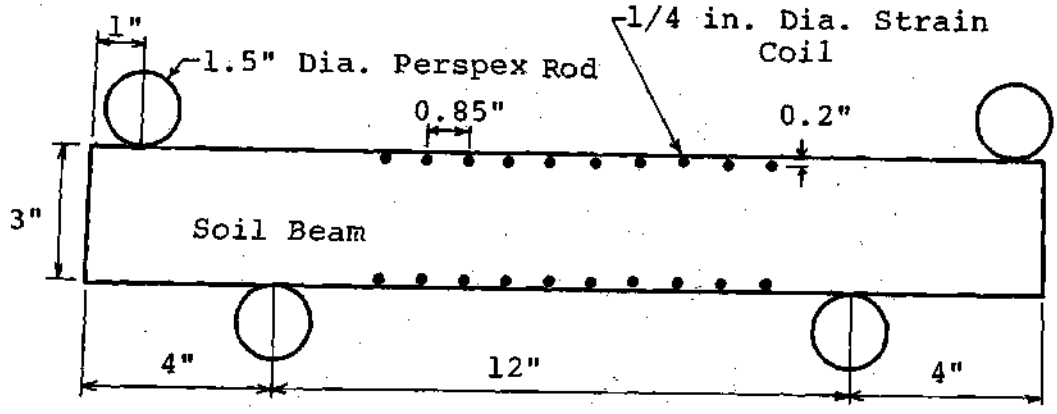

Figure 98. Strain Coil Pattern Layout.

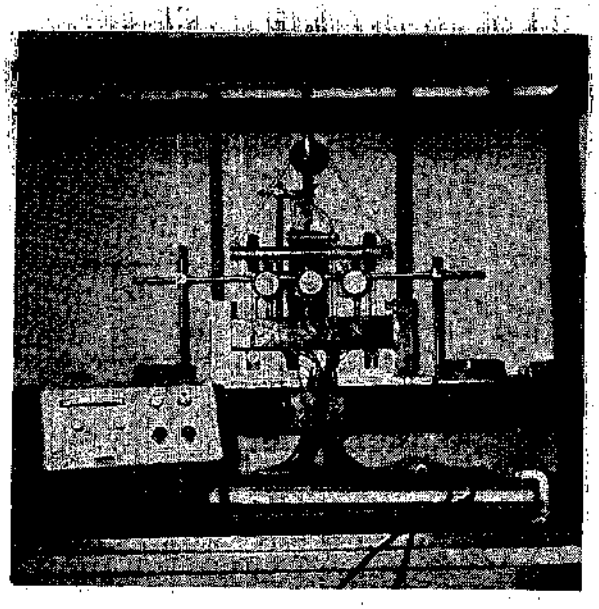

Figure 99. Beam Bending Test in Progress.

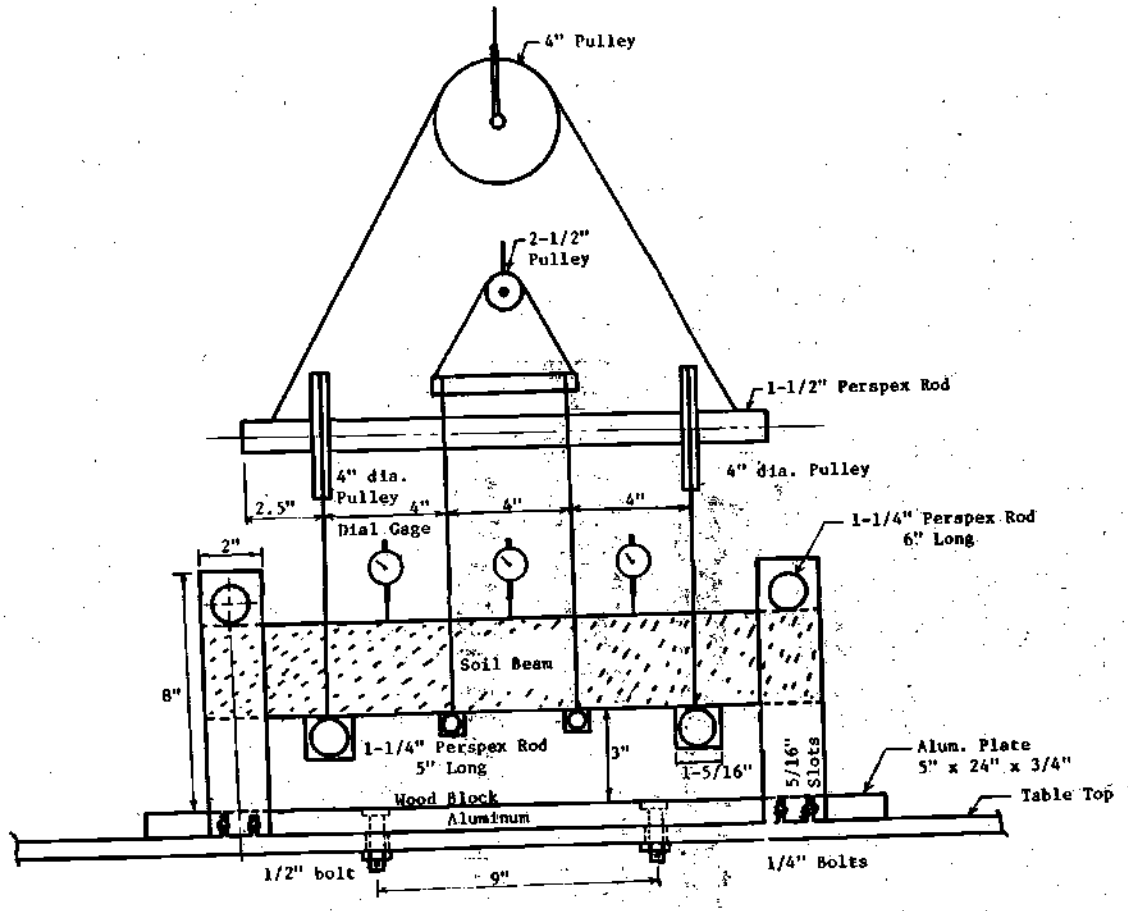

Figure 99. (Continued). Schematic Drawing of Beam Bending Device.

and fabricated for the bending test were capable of measuring deformation to 0.0002 inch per change in amplitude reading. The coil pattern layout is shown in Figure 98.

Load was applied by dead weights (Figure 99). The use of two sets of ball-bearing pulleys (free to move in mutually perpendicular directions) eliminated the possibility of eccentric loading or twisting of the beam. In order to compensate approximately for dead-load stresses, an independent pulley system with dead weights was applied at the two central one-fifth points of the beam as shown in Figure 99. Before commencing the test, counter weights were added so that the beam was lifted 1/4 inch above the wooden block and rested against the reaction rods at each end. To minimize stress concentrations at the points of contact between the beam and the perspex rods, a thin plexi-glass strip one inch wide and 1/8 inch thick was placed on the beam surface at the points of contact.

Loading Procedure

Prior to loading, initial readings were taken for each successive pair of coils and zero readings of the dial gages were taken. Loads were added in increments of 5 pounds, and the dial gage readings versus times were taken. Approximately a six hour interval between load increments was required, and the test was completed in a period of 2 to 2-1/2 days. Strain coil readings were taken at the end of each load increment. After failure, soil trimmings were taken from different depths

of the failed beam specimen section to determine the variation in moisture content throughout the beam. It was found that paraffin coating was effective in preventing moisture loss. The change of moisture content after completion of the test was less than 0.5 percent. Cylindrical specimens 1.4 inch diameter and 2.8 inch were also trimmed from the end portions of the beam specimen.

Unconfined Compression Test

Strain controlled unconfined compression tests were conducted on the trimmed specimens from each compacted beam using a strain rate of 0.02 inch per minute. After failure, moisture content of the specimens was determined.

Analysis of Bending Strains

Compressive and tensile strains were determined by using both the observed deflections of the beam and the miniature coil readings.

Strains Calculated from Deflections

The deflections of the beam under various increments of load in the course of a bending test were used to calculate the corresponding extreme compressive and tensile strains in bending. It was assumed that the beam bent in a circular arc between the two supports with a neutral axis in the mid height of the beam in accordance with elastic beam bending theory. It was further assumed that the bending moment at the center section of the beam was due mainly to the applied load and that the dead weight of the beam after being balanced out had negli-

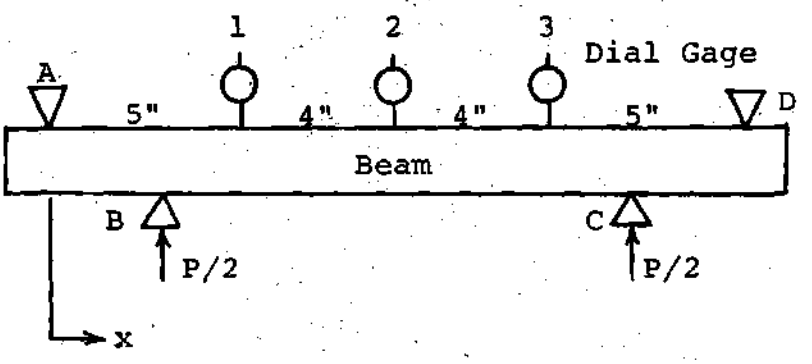

Figure 100. Beam Diagram for Deflection Measurement.

gible effects on the moment distribution in the beam. After the counter weights were applied, the maximum moment at the center of the span due to the beam weight was about 1.2 in-lb.

From Figure 100 bending moment and deflection equations due to the loading applied at B and C are:

$$M = 3/2\ P$$

and

$$y = (\frac{3}{4}\ Px^2 - \frac{27}{2}\ Px)/EI.$$

Using the relationships $\sigma = Mc/I$ and $\sigma = E\varepsilon$, where c = the distance from neutral axis to the extreme fiber, I = moment of inertia and E = modulus of elasticity, the extreme fiber strain at Dial Gage (2) is

$$\varepsilon_2 = 0.02469\ \frac{My}{P}$$

and at Dial Gage (1) and (3) is:

$$\varepsilon_{1,3} = 0.02778 \frac{My}{P}$$

The average strains using the deflection values of all three dial gages were used in the plot of tensile stress-strain curves (Figure 101).

Strains from Coil Readings

Longitudinal strains in the beam specimens were calculated making the assumptions that: (1) displacements of the coils represented the displacement of soil between the coils; (2) the coils lay and remained in a single vertical plane; and (3) the coils and the pins inserted in the beam did not influence the soil behavior.

The average strains for each load increment were calculated by dividing the change in gage length between each pair of coils by the initial spacing. These measured longitudinal tensile and compressive strains (Figures 102 and 103) were used in the calculation of tensile stresses using the following relationship for a bilinear analysis [3].

$$\sigma_c, \sigma_t = \frac{3M}{bd^2} \frac{\varepsilon_c + \varepsilon_t}{\varepsilon_c, \varepsilon_t}$$

where σ_c = compressive stress

σ_t = tensile stress

M = bending moment

b = width of beam

d = breadth of beam

ε_c = compressive strain

ε_t = tensile strain

Test Results

The tensile stress-strain curves using both beam deflections and measured strains are shown in Figures 101, 102, and 103. Figure 104 shows the stress-strain curves from unconfined compression tests. The test results are summarized in Table 16.

A comparison of tensile strains at failure obtained from the bending test results with those from the literature in Table 15 shows a good agreement for the soil types having comparable liquid limits and plasticity indices. The initial tangent moduli in tension and in compression from the measured stress-strain curves appear to be about the same. These results support the finding of Ajaz and Parry [3] who measured the strains in bending using a radiographic technique that the initial tangent moduli in compression and in tension from bending tests were about equal. The initial tangent moduli from bending tests are about 2 to 2.5 times greater than that from unconfined compression tests. Leonards and Narain [70] found the moduli in tension from bending tests and compression from unconfined compression tests to be comparable in magnitude, but were apparently comparing initial tangent modulus in compression with secant moduli at failure in tension.

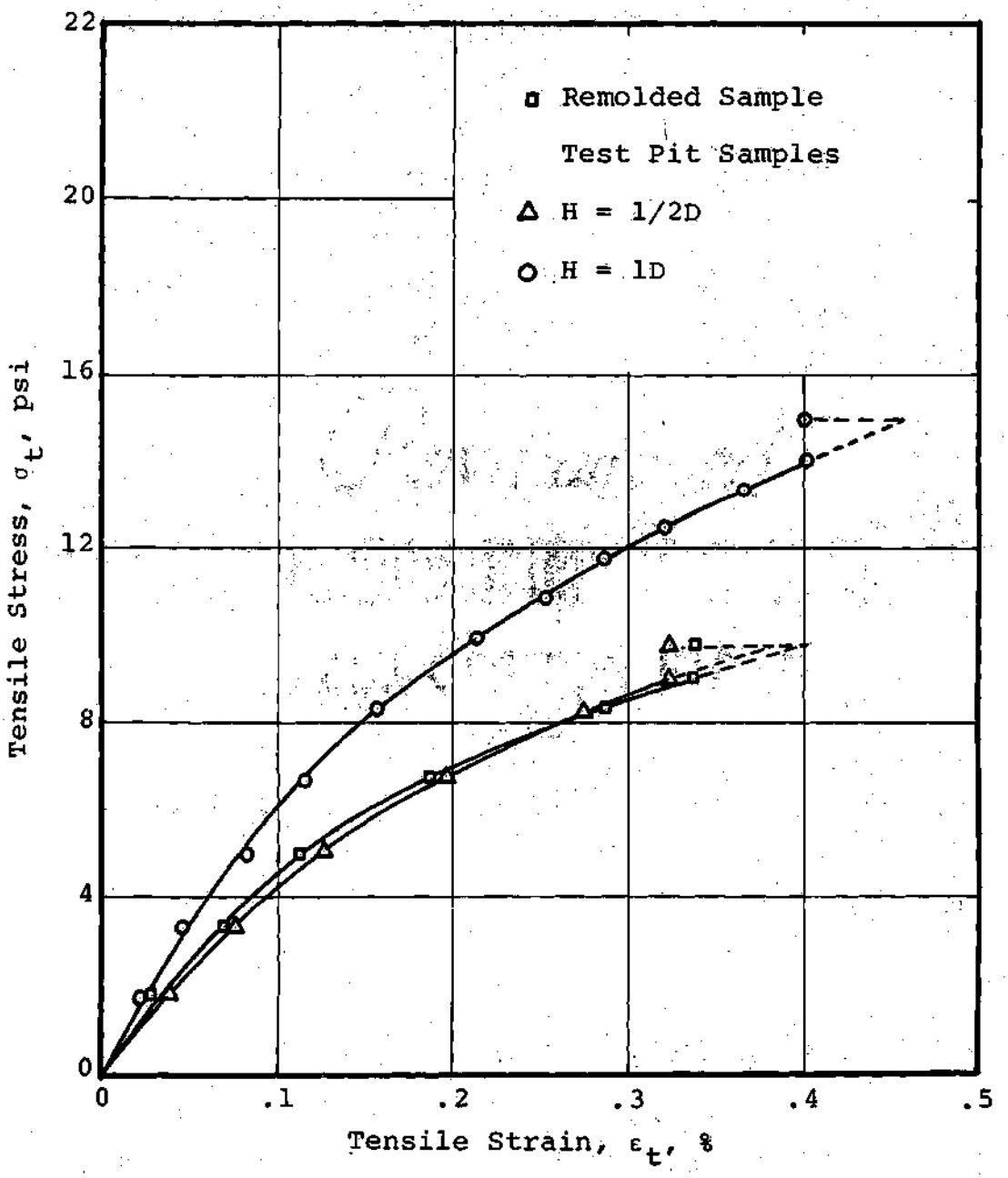

Figure 101. Tensile Stress-Strain Curves Using Beam Deflection.

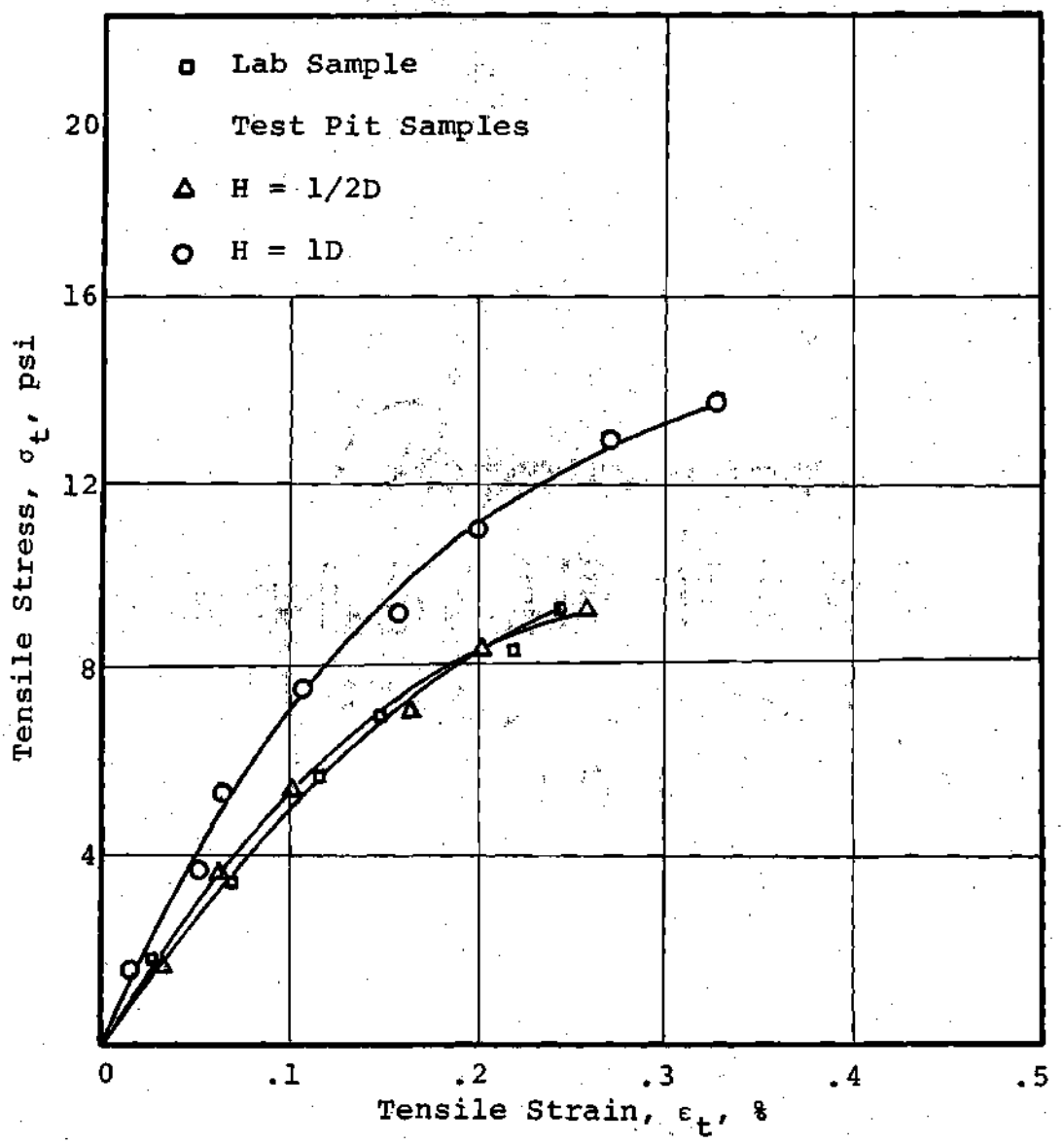

Figure 102. Tensile Stress-Strain Curves Using Measured Strains.

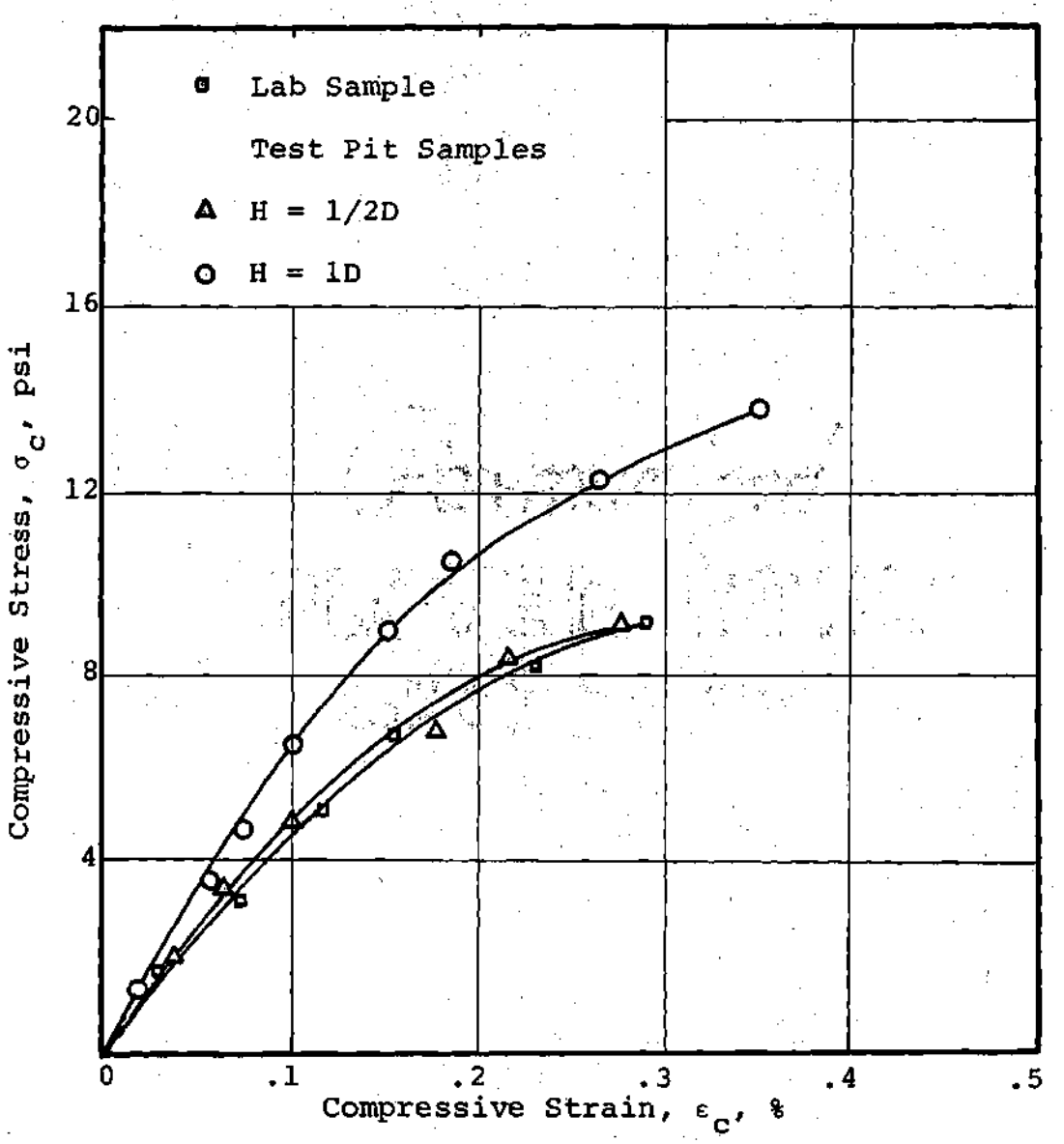

Figure 103. Compressive Stress-Strain Curves Using Measured Strains from Bending Tests.

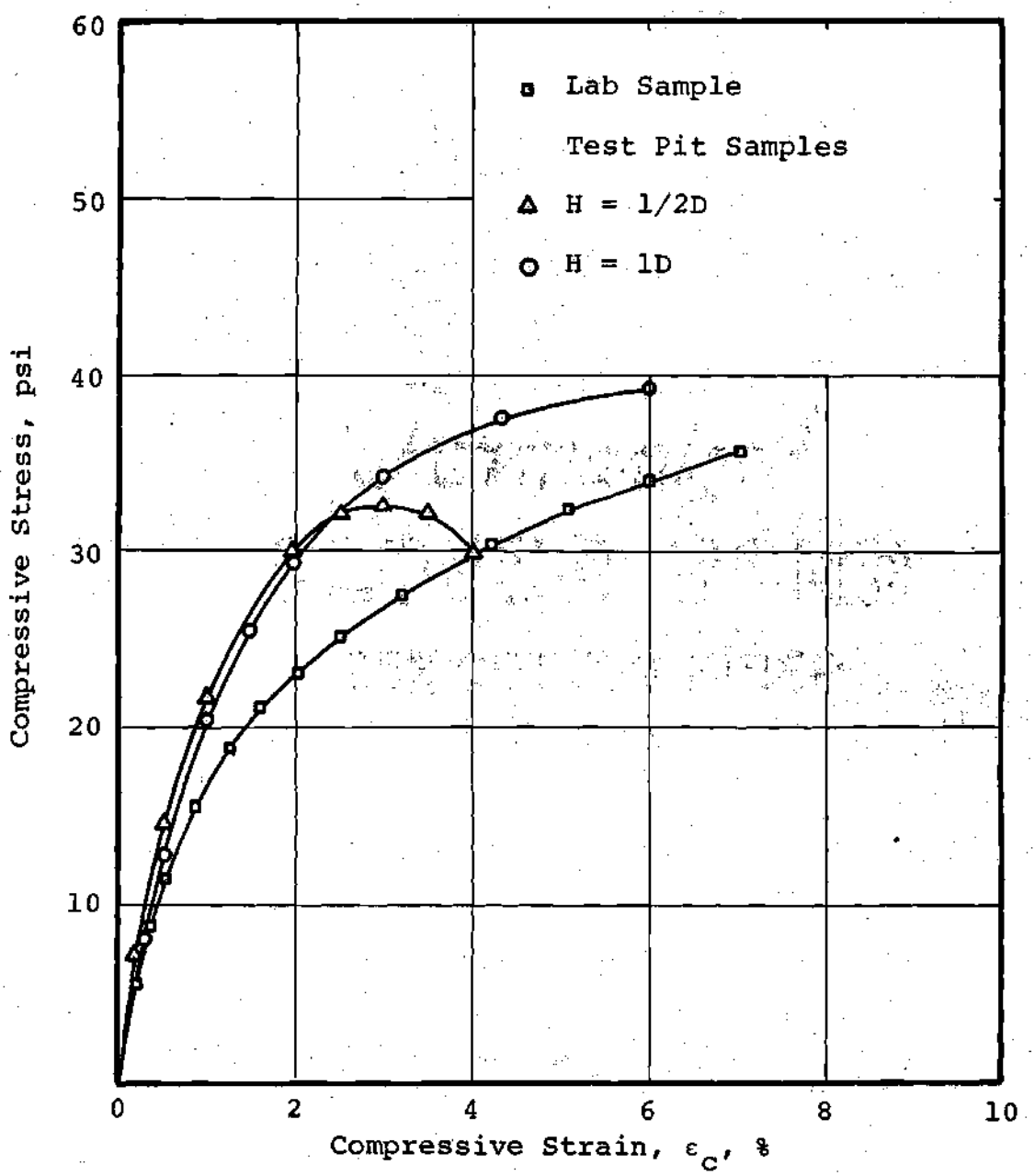

Figure 104. Unconfined Compression Tests.

Table 17. Bending Test Results.

Beam Sample	γ (pcf)	w (%)	Failure Strain ε_t (%) Calculated[2]	Failure Strain ε_t (%) Measured[3]	E_{td}[4] (psf)	Measured[5] E_t (psf)	Measured[5] E_c (psf)	E_{uc}[6] (psf)	$\frac{E_{td}}{E_{uc}}$
Laboratory (Remolded)	121	22.9	0.37	0.25	5500	5600	5200	2750	2.0
Test Series II[1]									
H = 1/2D	120	22.5	0.39	0.26	5500	6150	5750	2800	1.9
H = 1D	123	21.0	0.45	0.33	7220	7900	7500	2910	2.5

[1] Samples cut from block samples.

[2] Using beam deflections.

[3] From strain coil readings.

[4] Initial tangent modulus from tensile stress-strain curves using beam deflections.

[5] Initial tangent modulus from tensile and compressive stress-strain curves using measured strains.

[6] Initial tangent modulus from unconfined compression tests.

APPENDIX D

METHODS FOR BEARING CAPACITY ANALYSIS

Circular Footing on Homogeneous Soil

A well known ultimate bearing capacity equation is that given by Terzaghi and Peck [121] for a circular footing resting on a fairly dense or stiff soil which possesses both cohesion and friction.

$$q_u = 1.2CN_c + \gamma D_f N_q + 0.6\gamma r N_\gamma \qquad \text{(E-1)}$$

where q_u = ultimate bearing capacity

c = cohesion

N_c, N_q, N = bearing capacity factor

γ = unit weight

D_f = surcharge depth

γ = footing radius

When the soil is fairly compressible local shear failure develops. Terzaghi and Peck [121] suggest to modify the bearing capacity factors by reducing the shear strength as follows:

$$c' = 2/3c$$

$$\tan\phi' = 2/3 \tan \phi$$

The ultimate bearing capacity equation for local shear failure

is then:

$$q_u' = 0.8cN_c' + \gamma D_f N_q' + 0.6\gamma r N_\gamma' \qquad \text{(E-2)}$$

in which N_c', N_q', N_γ' = modified bearing capacity factors.

Circular or Square Footing on Compacted Fill

If both the fill layer and subsoil have cohesion and internal friction, Vesic [130] suggests the following expression to calculate the ultimate bearing capacity.

$$q_u = [q_u'' + (1/K)C_1\cot\phi_1]\exp[4K\tan\phi_1(CH/B)] - (1/K)C_1\cot\phi_1 \qquad \text{(E-3)}$$

where $K = (1-\sin^2\phi_1)/(1+\sin^2\phi_2)$

q_u'' = the bearing capacity of a fictitious footing of the same size and shape as the actual footing resting on top of the soft subsoil using c_2 and ϕ_2 in the analysis.

H = fill thickness

B = footing diameter

c_1 = cohesion of fill

ϕ_1 = frictional angle of fill

c_2 = cohesion of subsoil

ϕ_2 = frictional angle of subsoil.

If a granular fill is used, the bearing capacity equation is modified as:

$$q_u = q_u'' \exp[1.34(H/B)]$$

This expression was developed for $25° \leq \phi_1 \leq 50°$.

Meyerhof [76] considers the failure of a footing punching through the granular layer into the subsoil as an inverted uplift problem and suggests the following expression for bearing capacity analysis.

$$q_u = q_u'' + 2\gamma H^2(1+2D_f/H)K_s \tan\phi_1/B + \gamma D_f \qquad \text{(E-4)}$$

where K_s = coefficient of punching shearing resistance given by Meyerhof.

It is seen that for a given H/B, Vesic's method gives a constant value of q_u for $25° \leq \phi_1 \leq 50°$, where as q_u by Meyerhof's equation increases as ϕ_1 increase.

APPENDIX E

RESULTS OF PENETRATION TESTS

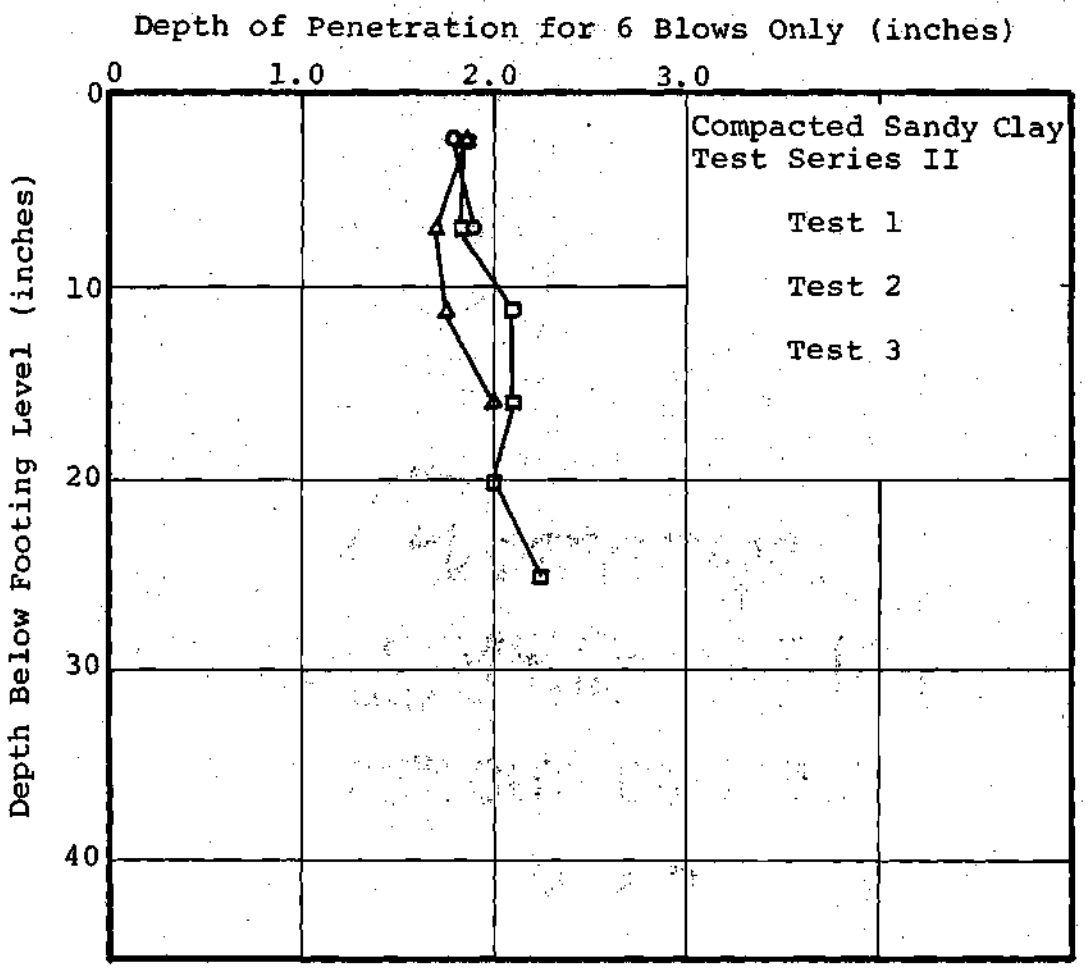

Figure 105. Results of Dynamic Cone Penetration Tests of Compacted Sandy Clay Layers - Test Series II.

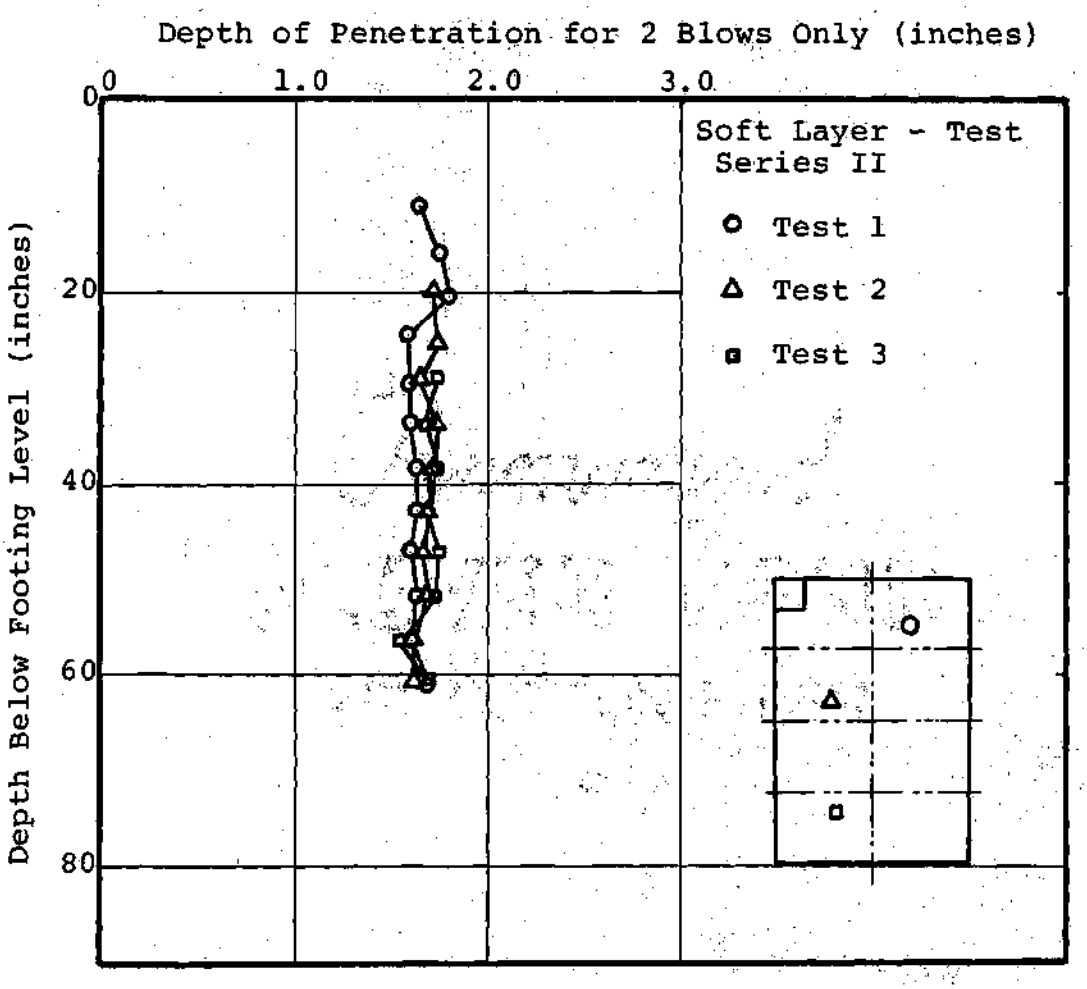

Figure 106. Results of Dynamic Cone Penetration Tests of Soft Layer - Test Series II.

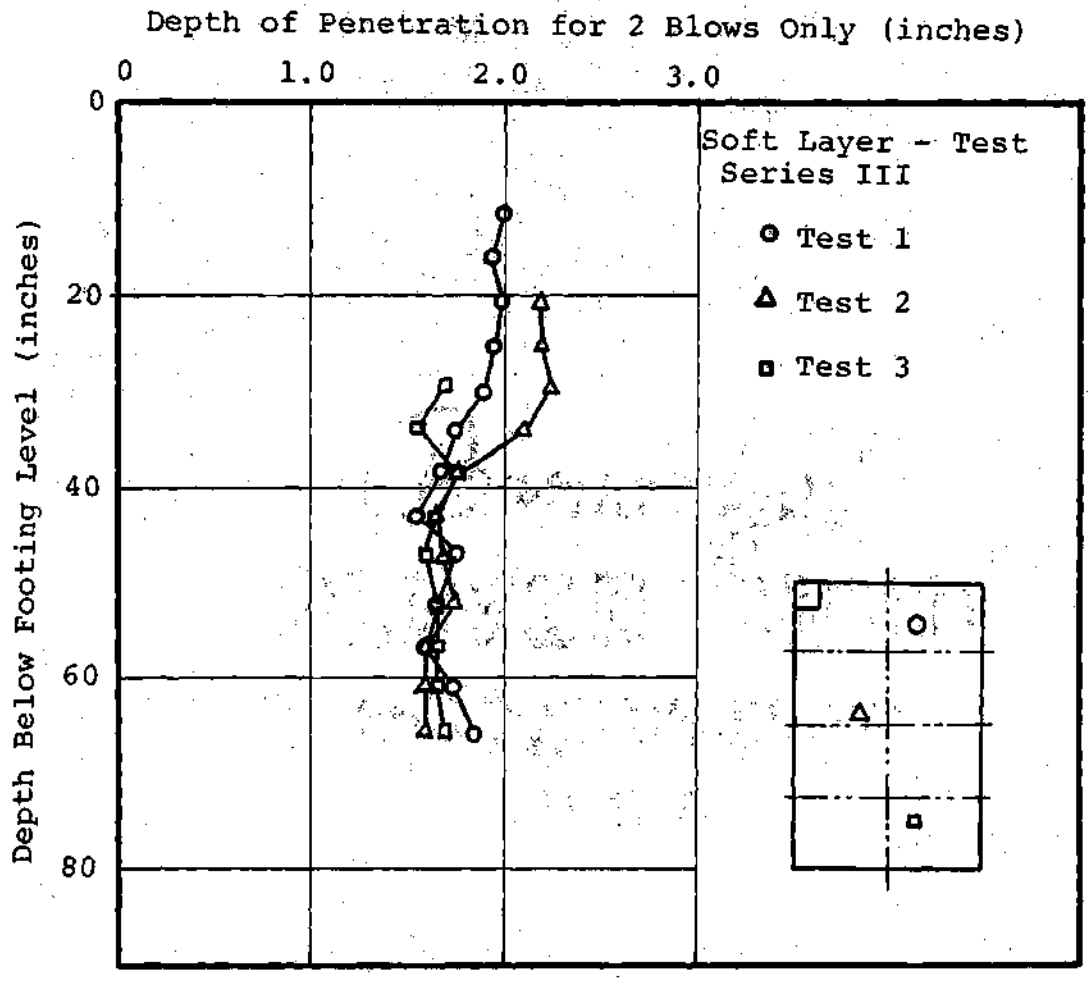

Figure 107. Results of Dynamic Cone Penetration Tests of Soft Subsoil - Test Series III.

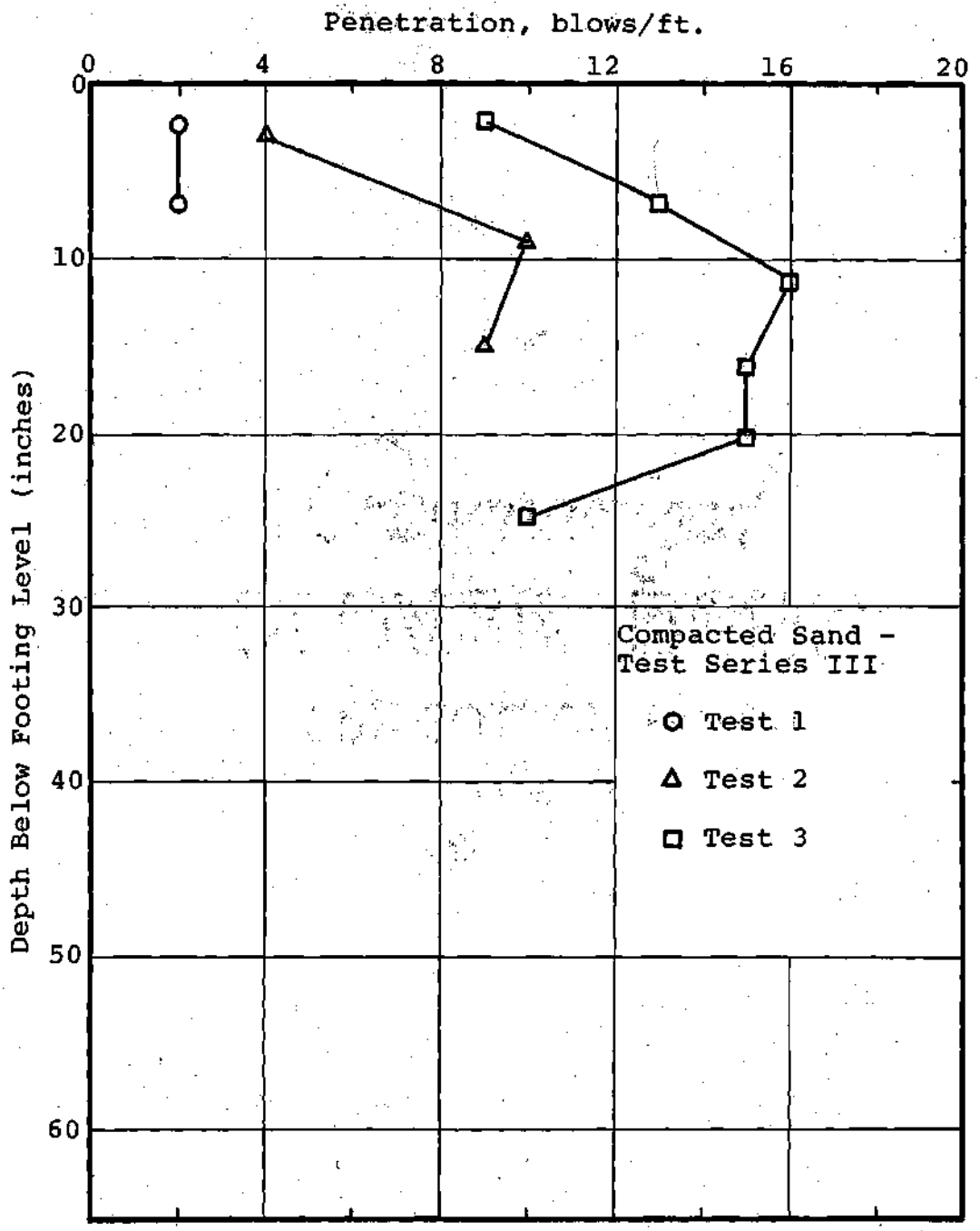

Figure 108. Results of Dynamic Cone Penetration Tests for Compacted Sand Layers - Test Series III.

BIBLIOGRAPHY

1. Acum, W. E. A. and Fox, L., "Computation of Load Stresses in a Three Layer Elastic System," Geotechnique, Vol. 2, 1951, pp. 297-300.

2. Ahlvin, R. C. and Ulery, H. H., "Tabulated Values for Determining the Complete Pattern of Stresses, Strains and Deflections Beneath a Uniform Circular Load on a Homogeneous Half-Space," Highway Research Board Bulletin, No. 342, 1962, pp. 1-3.

3. Ajaz, A. and Parry, R. H. G., "Stress-Strain of Two Compacted Clays in Tension and Compression," Geotechnique 25, No. 3, 1975, pp. 495-4512.

4. Al-Hussaini, M. M. and Townsend, F. C., "Investigation of Tensile Testing of Compacted Soils," M. P., S-74-10, U. S. Army Waterways Experiment Station, Vicksburg, Mississippi, June 1974.

5. Allwood, R. J., "An Experimental Investigation of the Distribution of Pressures in Sand," Ph.D. Thesis, University of Birmingham, 1956.

6. Alpan, I., "Estimating Settlement of Foundation on Sand," Civil Engineering and Public Works Review, Vol. 59, 1964, pp. 1415-1421.

7. Audibert, M. E. and Tavenas, F. A., Discussion: "Evaluation of Stress Cell Performance," Journal of the Geotechnical Engineering Division, ASCE, GT 7, Vol. 101, July 1975, pp. 705-707.

8. Barden, L., "Stresses and Displacements in a Cross-Anisotropic Soil," Geotechnique, Vol. 13, 1963, pp. 198-210.

9. Barden, L., "Consolidation of Clay with Non-Linear Viscosity," Geotechnique, Vol. 15, No. 4, December 1965, pp. 345-362.

10. Barden, L. and Berry, P. L., Closure to "Consolidation of Normally Consolidated Clay," Journal of the Soil Mechanics and Foundations Division, ASCE, Vol. 93, SM 1, January 1967, pp. 121-123.

11. Barksdale, R. D., "Analysis of Layered System," Final Report, Project B-607, School of Civil Engineering, Georgia Institute of Technology, 1969.

12. Barksdale, R. D. and Leonards, G. A., "Predicting Performance of Bituminous Surface Pavements," Proceedings of the Second International Conference on Structural Design of Asphalt Pavements, Ann Arbor, Michigan, 1967, pp. 321-340.

13. Barksdale, R. D., Intraprasart, S., and Crisp, L. P., "Settlement of Footings on a Saprolite Soil," Proceedings, Fifth Panamerican Conference on Soil Mechanics and Foundation Engineering, Vol. 3, November 1975, pp. 545-560.

14. Berre, T., Schjetne, K., and Sollie, S. C., "Sampling Disturbance of Soft Marine Clays," Proceedings of the Seventh International Conference on Soil Mechanics and Foundation Engineering, Special Session 1, 1969, pp. 21-24.

15. Biot, M. A., "General Theory of Three-Dimensional Consolidation," Journal of Applied Physics, Vol. 12, No. 75, February 1941, pp. 155-164.

16. Bond, D., "The Use of Model Tests for the Prediction of Settlement Under Foundations in Dry Sand," Ph.D. Thesis, University of London, 1956.

17. Boussinesq, J., Application des Potentials a L'Etude de L'Equilibre et du Mouvement des Solides Elastiques, Gauthier-Villars, Paris, 1885.

18. Brown, J. D. and Meyerhof, G. G., "Experimental Study of Bearing Capacity in Layered Clays," Proceeding, Seventh International Conference on Soil Mechanics and Foundation Engineering, Vol. 2, 1969, pp. 45-51.

19. Brown, P. T. and Gibson, R. E., "Surface Settlement of a Deep Elastic Stratum Whose Modulus Increases Linearly with Depth," Canadian Geotechnical Journal, Vol. 9, No. 4, 1972.

20. Brown, S. F., "The Measurement of In-Situ Stress and Strain in Soil," Proceeding of the Symposium on Field Instrumentation in Geotechnical Engineering, London, 1973, pp. 38-51.

21. Brown, S. F., "State of the Art on Field Instrumentation for Pavement Experiments," Preprint for Technical Committee A2K01 of the U.S. Transportation Research Board, January 1976.

22. Brown, S. F. and Pell, P. S., "An Experimental Investigation of the Stresses, Strains, and Deflections in a Layered Pavement Structure Subjected to Dynamic Loads," Proceeding, Second International Conference on the Structural Design of Asphalt Pavements, Ann Arbor, Michigan, 1967, pp. 487-504.

23. Brown, S. F. and Pell, P. S., "Subgrade Stress and Deformation Under Dynamic Load," Journal of the Soil Mechanics and Foundations Division, ASCE, Vol. 93, SM 1, January 1967, pp. 17-46.

24. Burland, J. B., Sills, G. C., and Gibson, R. E., "A Field and Theoretical Study of the Influence of Non-homogeneity on Settlement," Proceedings of the Eighth International Conference on Soil Mechanics and Foundation Engineering, Vol. 3., 1973, p. 39-46.

25. Burmister, D. M., "Theory of Stresses and Displacements in Layered Systems and Application to the Design of Airport Runways," Proceedings of Highway Research Board, Vol. 23, 1943, pp. 148-126.

26. Burmister, D. M., "Application of Dimensional Analysis in the Evaluation of Asphalt Pavement Performances," Proceeding of Fifth Asphalt Paving Conference, 1967, pp. 22-28.

27. Brumund, W. F., Jones, E., and Ladd, C. C., "Estimating In Situ Maximum Past (Preconsolidation) Pressure of Saturated Clays From Results of Laboratory Consolidometer Tests," Manual of Practice, Estimation of Consolidation Settlement, Special Report 163, Transportation Research Board, pp. 4-12.

28. Button, S. J., "The Bearing Capacity of Footings on a Two-Layer Cohesive Subsoil," Proceedings, Third International Conference on Soil Mechanics and Foundation Engineering, Vol. 1, pp. 332-335.

29. Carrier, W. D. and Christian, J. T., "Rigid Circular Plate Resting on a Non-Homogeneous Elastic Half-Space," Geotechnique, Vol. 23, No. 1, 1973, pp. 67-84.

30. D'Appolonia, D. J., D'Appolonia, E., and Brisette, R. F., "Settlement of Spread Footings on Sand," Journal of the Soil Mechanics and Foundations Division, ASCE, SM 3, May 1968, pp. 735-760.

31. D'Appolonia, D. J., D'Appolonia, E., and Brisette, R. F., Closure to "Settlement of Spread Footings on Sand," Journal of the Soil Mechanics and Foundations Division, ASCE, SM 2, March 1970, pp. 754-761.

32. D'Appolonia, D. J. and Lambe, T. W., "A Method of Predicting Initial Settlement," Journal of the Soil Mechanics and Foundations Division, ASCE, Vol. 96, SM 2, March 1970, pp. 523-545.

33. D'Appolonia, D. J., Whitman, R. V., and D'Appolonia, E., "Sand Compaction with Vibratory Rollers," Journal of the Soil Mechanics and Foundation Division, ASCE, Vol. 95, No. SM 1, January 1969, pp. 263-284.

34. Das, S. C. and Gangopadhyay, C. R., "Undrained Stresses and Deformations Under Footings on Clay," Journal of the Geotechnical Engineering Division, ASCE, Vol. 104, GT 1, January 1978, pp. 501-525

35. Davis, E. H. and Poulos, H. G., "Triaxial Testing and Three-Dimensional Settlement Analysis," Proceeding, Fourth Australia-New Zealand Conference on Soil Mechanics, 1963, pp. 233-242.

36. Davis, E. H. and Poulos, H. G., "The Use of Elastic Theory for Settlement Prediction Under Three-Dimensional Conditions," Geotechnique, Vol. XVIII, No. 1, March 1968, pp. 67-91.

37. De Beer, E., "Bearing Capacity and Settlement of Shallow Foundation on Sand," Proceeding, Symposium on Bearing Capacity and Settlement of Foundations, Duke University, 1965, pp. 15-33.

38. De Jong, J. and Harris, M. C., "Settlement of Two Multistory Buildings in Edmonton," Canadian Geotechnical Journal, Vol. 8, No. 2, 1971, pp. 217-235.

39. Desai, C. S. and Reese, L. C., "Analysis of Circular Footing on Layered Soils," Journal of the Soil Mechanics and Foundations Division, ASCE, Vol. 96, SM 4, July 1970, pp. 1289-1310.

40. Domaschuk, L. and Villiappan, P., "Nonlinear Settlement Analysis by Finite Element," Journal of the Geotechnical Engineering Division, ASCE, Vol. 101, GT 7, July 1975, pp. 601-614.

41. Duncan, J. M. and Chang, C. Y., "Nonlinear Analysis of Stress and Strain in Soils," Journal of the Soil Mechanics and Foundations Division, ASCE, Vol. 96, SM 5, September 1970, pp. 1629-1653.

42. Eggestad, A., "Deformation Measurements Below a Model Footing on the Surface of Dry Sand," Proceedings of

European Conference on Soil Mechanics and Foundation Engineering, Vol. 1, 1963, pp. 233-238.

43. Egorov, K. E., Kuzmin, P. G., and Popov, B. P., "The Observed Settlements of Buildings as Compared with Preliminary Calculation," Proceeding, Fourth International Conference on Soil Mechanics and Foundation Engineering, Vol. 3, 19, pp. 291-296.

44. Gerrard, C. M., "Tables of Stress, Strains and Displacements in Two-Layer Systems Under Various Traffic Loads," Australian Road Research Board, Special Report, No. 3, 1969.

45. Gerrard, C. M., "Stresses and Displacements in Layered Cross-Anisotropic Elastic Systems," Proceeding, Fifth Australia-New Zealand Conference on Soil Mechanics and Foundation Engineering, 1967, pp. 205-210.

46. Gerrard, C. M. and Harrison, W. J., "Circular Loads Applied to a Cross Anisotropic Half Space," Technical Paper No. 8, Division of Applied Mechanics, Australia.

47. Gibson, R. E., "Some Results Concerning Displacement and Stresses in a Non-Homogeneous Elastic Half Space," Geotechnique, Vol. 17, 1967, pp. 58-67.

48. Gibson, R. E., Brown, P. T., and Andrews, K. R. F., "Some Results Concerning Displacement in a Non-Homogeneous Elastic Layer," Journal of Applied Mathematics and Physics, Vol. 22, 1971, pp. 855-864.

49. Gibson, R. E., England, G. L., and Hussey, M. J. L., "The Theory of One-Dimensional Consolidation of Saturated Clays," Geotechnique, London, Vol. 18, No. 3, September 1967, pp. 261-273.

50. Heukelom, W. and Klomp, A. J. G., "Dynamic Testing as a Means of Controlling Pavements During and After Construction," Proceedings of the International Conference on the Structural Design of Asphalt Pavements, 1963, pp. 667-679.

51. Holl, D. L., "Stress Transmission in Earths," Proceedings Highway Research Board, Vol. 20, 1940, pp. 709-721.

52. Huang, Y. H., "Stresses and Displacements in Non-Linear Soil Media," Journal of the Soil Mechanics and Foundations, ASCE, No. SM 1, January 1968.

53. Huang, H. Y., "Finite Element Analysis of Nonlinear Soil Media," Proceeding of the Conference on the Applications of Finite Element Methods in Civil Engineering, ASCE, November 1969.

54. Hadala, P. F., "The Effect of Placement Method on the Response of Soil-Stress Gages," Proceedings of the Symposium on Wave Propagation and Dynamic Properties of Earth Materials," University of New Mexico, 1967.

55. Janbu, N., "The Resistance Concept Applied to Deformation of Soils," Proceedings, Seventh International Conference on Soil Mechanics and Foundation Engineering, Vol. 1, 1969, pp. 191-196.

56. Jones, A., "Table of Stresses in Three-Layer Elastic Systems," Highway Research Board, Bulletin No. 342, 1962, pp. 176-214.

57. Jorden, E. E., "Settlement in Sand-Methods of Calculating and Factors Affecting," Ground Engineering, January 1977, pp. 30-37.

58. Kallstenius, T. and Bergau, W., "Investigations of Soil Pressure Measuring by Means of Cells," Proceedings 12, Royal Swedish Geotechnical Institute, 1956.

59. Koning, H., "Stress Distribution in a Homogeneous Anisotropic, Elastic Semi-Infinite Solid," Proceeding, Fourth International Conference on Soil Mechanics and Foundation Engineering, Vol. 1, 1957, p. 335.

60. Kezdi, R., Note on Soil Mechanics--Lecture Series, Princeton University, 1969.

61. Lambe, T. W., Soil Testing for Engineers, John Wiley and Sons, New York, 1951.

62. Lambe, T. W., "Methods of Estimating Settlement," Journal of the Soil Mechanics and Foundations Division, ASCE, Vol. 90, SM 4, 1964, pp. 61-87.

63. Lambe, T. W., "Stress Path Method," Journal of the Soil Mechanics and Foundations Division, ASCE, Vol. 93, SM 6, 1967, pp. 309-331.

64. Lambe, T. W. and Whitman, R. V., Soil Mechanics, John Wiley and Sons, Inc., New York, 1969, p. 419.

65. Lambe, T. W., "Predictions in Soil Engineering," Geotechnique, Vol. 23, 1973, pp. 151-202.

66. Ledbetter, R. H., "Pavement Response to Aircraft Dynamic Loads," Vol. III, TRS-75-11, U. S. Army Waterways Experiment Station, June 1976.

67. Lee, K. L. and Idriss, I. M., "Static Stresses by Linear and Nonlinear Methods," Journal of the Geotechnical Division, ASCE, Vol. 101, GT 9, September 1975, pp. 871-887.

68. Leonards, G. A., "Engineering Properties of Soils," Foundation Engineering, G. A. Leonards, editor, McGraw-Hill Book Co., Inc., New York, 1962.

69. Leonards, G. A., "Estimating Consolidation Settlements of Shallow Foundations on Overconsolidated Clay," Manual of Practice: Estimation of Consolidation Settlement, Special Report No. 163, Transportation Research Board, 1976, pp. 13-16.

70. Leonards, G. A. and Narain, J., "Flexibility of Clay and Cracking of Earth Dams," Journal of the Soil Mechanics and Foundations Division, ASCE, Vol. 89, SM 2, March 1963.

71. Martin, R. E., "Estimating Foundation Settlements in Residual Soils," Journal of the Geotechnical Engineering Division, ASCE, Vol. 103, GT 3, March 1977, pp. 197-213.

72. McMahan, T. F. and Yoder, E. J., "Design of a Pressure Sensitive Cell and Model Studies of Pressure in a Flexible Pavement Subgrade," Proceedings of Highway Research Board, Vol. 39, 1960, pp. 650-683.

73. Mesri, G. and Rokhsar, A., "Theory of Consolidation for Clays," Journal of the Geotechnical Engineering Division, ASCE, Vol. 100, GT 8, August 1974.

74. Meyerhof, G. G., "Building on Fill with Special Reference to the Settlement of a Large Factory," Structural Engineering, Vol. 29, No. 2, February 1951, pp. 46-57, and Discussion, Vol. 29, No. 11, November 1951, pp. 297-305.

75. Meyerhof, G. G., "Shallow Foundation," Journal of the Soil Mechanics and Foundations Division, ASCE, Vol. 91, SM 2, March 1965, pp. 21-31.

76. Meyerhof, G. G., "Ultimate Bearing Capacity of Footing on Sand Layer Overly Clay," Canadian Geotechnical Journal, Vol. 11, May 1974, pp. 223-229.

77. Mitchell, J. K., "In-Place Treatment of Foundation Soils," Journal of the Soil Mechanics and Foundations Division, ASCE, Vol. 96, SM 1, January 1970.

78. Mitchell, J. K. and Gardner, W. S., "Analysis of Load-Bearing Fills Over Soft Subsoils," Journal of the Soil Mechanics and Foundations Division, ASCE, Vol. 97, SM 11,

November 1971, pp. 1549-1571.

79. Moore, P. J. and Spencer, G. K., "Settlement of Building on Deep Compressible Soil," Journal of the Soil Mechanics and Foundations Division, ASCE, Vol. 95, SM 3, May 1969, pp. 769-790.

80. Morgan, J. R. and Holden, J. C., "Deflection Prediction on Prototype Pavements," Proceedings, Second International Conference on Structural Design of Asphalt Pavements, Ann Arbor, Michigan, 1967, pp. 707-718.

81. Morgenstern, N. R. and Phukan, A. L. T., "Stress and Displacement in a Homogeneous Non-Linear Foundation," Proceeding of the International Symposium in Rock Mechanics, Madrid, 1968, pp. 313-320.

82. Parry, R. H. G., "A Direct Method of Estimating Settlements in Sand from S.P.T. Values," Proceedings, Symposium on Interaction of Structure and Foundation, Midlands Soil Mechanics and Foundation Engineering Society, 1971, pp. 29-37.

83. Peattie, K. R., "Stress and Strain Factors for Three Layer Elastic System," Highway Research Board No. 342, 1962, pp. 215-253.

84. Peattie, K. R. and Sparrow, R. W., "The Fundamental Action of Earth Pressure Cells," Journal of Mechanics and Physics of Solids, Vol. 2, 1954, pp. 141-155.

85. Peck, R. B. and Bazaraa, A. R. S. S., Discussion of Paper by D'Appolonia, D. J., D'Appolonia, E. and Brisette, R. F. on "Settlement of Spread Footing on Sand," Journal of the Soil Mechanics and Foundations Division, ASCE, Vol. 95, SM 3, 1969, pp. 305-309.

86. Perloff, W. H. and Baron, W. B., Soil Mechanics, The Ronald Press Company, New York, 1976, p. 186.

87. Pile, K. C., "Correlation Between Actual and Predicted Settlements for a Large Test Footing," Proceedings, Second Australia-New Zealand Conference on Geomechanics, July 1975, pp. 297-301.

88. Poulos, H. G., "Stress and Displacements in an Elastic Layer Underlain by Rough Rigid Base," Geotechnique, Vol. 17, No. 4, December 1967, pp. 378-410.

89. Poulos, H. G. and Davis, E. H., Elastic Solutions for Soil and Rock Mechanics, John Wiley and Sons, Inc., New York, 1974.

90. Purushothamarai, P., Ramiah, B. K., and Rao, K. N. V., "Bearing Capacity of Strip Footings in Two Layered Cohesive-Friction Soils," Canadian Geotechnical Journal, Vol. 11, No. 1, February 1974, pp. 32-46.

91. Raymond, G. P., Townsend, D. L., and Lojkasek, M. J., "The Effect of Sampling on the Undrained Soil Properties of a Leda Soil," Canadian Geotechnical Journal, Vol. 8, 1971, pp. 546-557.

92. Raymond, G. P. and Wahls, H. E., "Estimating One-Dimensional Consolidation, Including Secondary Compression, Clay Loaded From Overconsolidated to Normally Consolidated State," Manual of Practice, Estimation of Consolidation Settlement, Special Report, No. 163, Transportation Research Board, 1976, pp. 14-23.

93. Reddy, A. S. and Srinivasan, R. J., "Bearing Capacity of Footing on Layered Clays," Journal of the Soil Mechanics and Foundations Division, ASCE, Vol. 93, SM 2, 1967, pp. 83-99.

94. Roark, J. R. and Young W. C., "Formulas for Stress and Strain," Fifth Edition, McGraw-Hill Book Company, 1975.

95. Rutledge, P. C., "Relation of Undisturbed Sampling to Laboratory Testing," Transaction, ASCE, Vol. 109, 1944.

96. Schiffman, R. L., Discussion on "Vertical Stress in Subgrade Beneath Statically Loaded Flexible Pavements," Highway Research Board, Bulletin No. 342, 1962, pp. 124-126.

97. Schmertmann, J. H., "Estimating the True Consolidation Behavior of Clay From Laboratory Test Results," Proceedings, ASCE, Vol. 79, Separate No. 311, 1953.

98. Schmertmann, J. H., "Static Cone to Compute Static Settlement Over Sand," Journal of the Soil Mechanics and Foundations Division, ASCE, Vol. 96, SM 3, May 1970, pp. 1011-1043.

99. Schmertmann, J. H., Hartman, J. P., and Brown, P. R., "Improved Strain Influence Factor Diagrams," Technical Note, Journal of the Geotechnical Engineering Division, ASCE, Vol. 104, GT 8, August 1978, pp. 1131-1136.

100. Scott, R. F., Principal of Soil Mechanics, Addison-Welsey Publishing Company, Reading, Mass., 1963.

101. Seed, H. B., Mitry, F. G., Monismith, C. L., and Chan,

C. K., "Prediction of Pavement Deflections from Laboratory Repeated Load Tests," Report No. TE 65-6, Department of Civil Engineering, University of California at Berkeley.

102. Selig, E. T., "A Review of Stress and Strain Measurement in Soil," Proceeding of the Symposium on Soil Structure Interaction, University of Arizona, 1964, pp. 172-186.

103. Selig, E. T., "Soil Strain Measurement Using Inductance Coil Method," Proceeding of the Symposium on Performance Criteria and Monitoring for Geotechnical Construction, ASTM, STP 584, 1975, pp. 141-158.

104. Selig, E. T. and Grangaard, O. H., "A New Technique for Soil Strain Measurement," Journal of Material Research and Standards, Vol. 10, No. 10, 1970, pp. 19-36.

105. Shanker, N. B., Ratnam, M. V., and Rao, A. S., "Three-Dimensional Consolidation of a Saturated Clay Under Model Footings," Soils and Foundation, Vol.14, No. 1, Tokyo, Japan, March 1974, pp. 88-92.

106. Simons, N. E., "Settlement Studies on Two Structures in Norway," Proceeding, Fourth International Conference on Soil Mechanics and Foundation Engineering, Vol. 1, 1957, pp. 431-436.

107. Simons, N. E., "General Report on Normally and Lightly Overconsolidated Cohesive Materials," Proceedings of the Conference on Settlement of Structures, British Geotechnical Society, April 1974, pp. 500-530.

108. Skempton, A. W. and Bjerrum, L., "A Contribution to the Settlement Analysis of Foundations on Saturated Clay," Geotechnique, Vol. 7, No. 4, December 1957, pp. 168-178.

109. Skempton, A. W., Peck, R. B., and McDonald, D. H., "Settlement Analysis of Six Structures in Chicago and London," Proceeding of Institute of Civil Engineering, Part 1, Vol. 4, No. 4, 1955, pp. 525-544.

110. Soderman, L. G. and Kim, Y. D., "Field and Laboratory Studies of Modulus of Elasticity of a Clay Till," Highway Research Record, No. 243, 1968.

111. Sowers, G. F., "Foundation for Marginal Sites," Proceedings of the Chicago Soil Mechanics Lecture Series, Illinois Institute of Technology, Chicago, Illinois, 1970, pp. 169-217

112. Sowers, G. F., "Analysis and Design of Lightly-Loaded Foundations," Proceedings of the Conference on Analysis and Design in Geotechnical Engineering, ASCE, Vol. 2, June 1974, pp. 49-78.

113. Sower, G. F. and Hedges, C. S., "Dynamic Cone for Shallow In-Situ Penetration Testing," Vane Shear and Cone Penetration Resistance Testing of In-Situ Soils, ASTM STP 399, 1966, pp. 29.

114. Sowers, G. B. and Sowers, G. F., Introductory Soil Mechanics and Foundation Engineering, Third Edition, The MacMillian Company, 1970, p. 338.

115. Sowers, F. G. and Vesic, A. S., "Vertical Stresses in Subgrade Beneath Statically Loaded Flexible Pavements," Highway Research Board, Bulletin No. 342, 1962, pp. 90-123.

116. Stuart, E., Miyaoka, Y., Skok, E. L., and Wenck, N. C., "Field Evaluation of an Asphalt Stablized Sand Pavement Design Using the Elastic Layered System," Proceedings of the Association of Asphalt Paving Technologists, February 1974.

117. Sutherland, H. B., General Report on Granular Materials, Proceedings of the Conference on Settlement of Structures, British Geotechnical Society, April 1974, pp. 473-499.

118. Tcheng, Y., "Foundations Superficielles en Milieu Stratifie," Proceeding of the Fourth International Conference on Soil Mechanics and Foundation Engineering, Vol. 1, 1957, pp. 449-452.

119. Terzaghi, K., "Undisturbed Clay Samples and Undisturbed Clays," Journal of Boston Society of Civil Engineers, Vol. 28, No. 3, 1941, pp. 211-232.

120. Terzaghi, K., Theoretical Soil Mechanics, John Wiley and Sons, Inc., New York, 1943, pp. 382-383.

121. Terzaghi, K. and Peck, R. B., Soil Mechanics in Engineering Practice, John Wiley and Sons, Inc., New York, 1967, p. 277.

122. Triandafilidis, G. E., "Soil Stress Gage Design and Evaluation," Journal of Testing and Evaluation, ASTM, Vol. 2/3, 1974, pp. 146-158.

123. Trollope, D. H., Lee, I. K., and Morris, J., "Stresses and Deformation in Two Layer Pavement Structures Under Slow Repeated Loading," Proceedings, Australian Road Research Board, Vol. 1, Part 2, 1962, pp. 693-721.

124. Turnbull, W. J., Maxwell, A. A., and Ahlvin, R. G., "Stress and Deflection in Homogeneous Soil Masses," Proceedings of the Fifth International Conference on

Soil Mechanics and Foundation Engineering, Vol. 2, p. 337.

125. U. S. Army Waterways Experiment Station, "Soil Pressure Cell Investigation," Technical Memorandum, No. 210-1, 1944.

126. U. S. Army Waterways Experiment Station, "Report No. 1, "Investigation of Pressures and Deflections for Flexible Pavements: Clayey Silt Test Section," Vicksburg, Mississippi, 1951.

127. U. S. Army Waterways Experiment Station, "Investigation of Pressures and Deflections for Flexible Pavements: Homogeneous Sand Test SEction," Technical Memorandum No. 3-323, 1954.

128. Vesic, A. S., "Analysis of Ultimate Loads of Shallow Foundations," Journal of the Soil Mechanics and Foundations Division, ASCE, SM 1, January 1973, pp. 45-70.

129. Vesic, A. S., "A Study of Bearing Capacity of Deep Foundations," Engineering Experiment Station, Georgia Institute of Technology, Report B-189, Final Report, 1967.

130. Vesic, A. S., "Bearing Capacity of Shallow Foundation," Chapter 3, Foundation Engineering Handbook, edited by Winterkorn, H. F. and Fang, H. Y., 1975, pp. 121-145.

131. Walter, D., Kriebel, A. R., and Kaplan, K., "URS Free-Field Soil-Stress Gage, Design, Construction and Evaluation," URS 758-6, Final Report to U. S. Department of Transportation, Washington, D. C., 1971.

132. Westergaard, H. M., "A Problem of Elasticity Suggested by a Problem in Soil Mechanics: A Soft Material Reinforced by Numerous Strong Horizontal Sheets," Contribution, Mechanics of Solids, S. Timoshenko, 60th Anniversary Volume, The Macmillan Company, New York, 1938.

133. Whiffin, A. C. and Lister, N. W., "The Application of Elastic Theory to Flexible Pavements," Proceedings of the First International Conference for Structural Design of Asphalt Pavements, Ann Arbor, Michigan, 1962, pp. 499-521.

134. Yamaguchi, H., "Practical Formula of Bearing Value for Two-Layer Ground," Proceeding of the Second Asian Conference on Soil Mechanics and Foundation Engineering, 1963, pp. 176-180.

135. Zeevaert, L., Foundation Engineering for Difficult Subsoil Conditions, Van Nostrand Reinhold Company, New York, 1973, p. 169.

VITA

Somboon Intraprasart was born on July 19, 1943, in Suphanburee, Thailand. He graduated from the Armed Forces Academy Preparatory School in 1963 and went on to finish his freshman year at the Chulachomklao Royal Military Academy where he ranked first in his class. He then attended The Citadel, the Military College of South Carolina, under the sponsorship of the Royal Thai Army and received his Bachelor of Science in Civil Engineering in 1969. Upon graduation, he was commissioned as a second lieutenant and became a lecturer in the Department of Civil Engineering at the Chulachomklao Royal Military Academy. He returned to the United States in 1972 to begin his graduate study at the Georgia Institute of Technology where he received his Master of Science in Civil Engineering in 1974 and continued to work for a Ph.D. until 1978.

His professional activities included membership in the Thai Society of Civil Engineers and the American Society of Civil Engineers. He is a registered civil engineer in Thailand.

He is married to former Karuna Titapavang, and they have no children.